Mol Neurobiol (2012) 46 (Suppl 1):S1–S99
DOI 10.1007/s12035-012-8319-0

Abstracts of the 2012 International Conference of Neurological Disorder, from Molecular Neurobiology to Clinical Therapy

Published online: 26 August 2012

Preface

The major neurological disorders such as Alzheimer's disease, Parkinson's disease and mental retardations as well as brain injuries such as stroke have become or shortly will become the leading cause of death of human beings. In the past 10 years, there has been a tremendous increase in the understanding of the cellular, molecular and genetic mechanisms of the diseases. Although many of these mechanisms have been exploited as the targets for drug development in the hope of the clinically effective therapies, to date, the fruition of these efforts remains limited.

The aim of this conference is to bring distinguished neuroscientists from overseas all over the world together with domestic researchers in the people of republic of China to discuss recent advances in both basic and clinical aspects of the diseases. For the purpose, the conference will consist of three keynote speeches (KS), one special presentation (SP) and twenty-seven symposium talks (ST). The keynote speeches are scheduled to be delivered by Professors Yuh-Nung Jan, and Lily Jan of the University of California at San Francisco; and Nancy IP of Hongkong University of Sciences and Technology. A special presentation will be given by Professor Nicolas Bazan of the Louisiana State University School Medicine at New Orleans. In this special presentation, Dr. Bazan will talk about the new mediators of neuronal protection that rescues brain function after stroke and in models of neurodegenerative diseases. Actually, this presentation is also a keynote lecture sponsored by Neuron Biotech Co. Ltd.. Needless to say, this conference will bring the best of the participants and to forester future collaborations among partners and to promote new discoveries in the diagnosis, treatment, and prevention of the major neurological disorders.

This conference is sponsored by Huazhong University of Science and Technology, Tongji Medical College and supported by National Natural Science Foundation and the Ministry of Science and Technology of the People's Republic of China, as well as the Editorial office of Molecular Neurobiology.

On behalf of the organization committee, I would like to express my deepest gratitude and warm welcome to participants from overseas, who will travel to this conference from all over the world. Wuhan's autumn is the best time of the year, and I wish you all pleasant stay in Wuhan, China.

Youming Lu, PhD
President
The 2012 International Conference of Neurological Disorders

International Conference of Neurological Disorder: From Molecular Neurobiology to Clinical Therapy

Sept. 26-29th, 2012, Wuhan, China

Program

Sept. 26 th, 2012
8AM–9PM, Registration

Sept. 27 th, 2012
8AM–6PM, Registration
8AM–8:30AM Open ceremony

Session 1: Chair: Yang Xiong-Li, Wang Jian-Zhi
8:30AM–9:10AM Jan YN KS-001
9:10AM–9:50AM Lily Jan KS-002
9:50AM–10:20AM Michael Salter ST-001
10:20AM–10:30AM Coffee break

Session 2: Chair: Duan Shu-Min, Zhu Ling-Qiang
10:30AM–11:10AM Nancy Ip KS-003
11:10AM–11:45AM James Woodgett ST-002
11:45AM–12:05PM Olympus Special Talk: Two photon imaging in Neuroscience
12:05AM–1:30PM Lunch

Session 3: Chair: Gao Tian-Ming, Wang Yi-Zheng
1:30PM–2:05PM Michael Tymianski ST-003
2:05PM–2:40PM Lo EH ST-004
2:40PM–3:10PM Ming Guo-Li ST-005
3:10PM–3:40PM Yan Ri-Qiang ST-006
3:40PM–4:10PM Zheng Hui ST-007
4:10PM–4:35PM Gao Tian-Ming ST-008
4:35PM–4:40PM Coffee break

Session 4:
Neuron Biotech Special Lecture, Chair: Lu You-Ming
4:40PM-5:20PM Bazan Nicolas SP-001

Session 5-1:
5:20PM–6:30PM Poster session PL001-051
Session 5-2:
5:20PM–6:30PM Satellite meeting by Proteintech Inc. SL-001

6:30PM Welcome Reception

Sept. 28 th, 2012
8AM–6PM, Registration

Session 6: Chair: Luo Jian-Hong, Li He
8:00AM–8:25AM Li Xiao-Jiang ST-009
8:25AM–8:50AM Zhang Xia ST-010
8:50AM–9:15AM Zhu Dong-Ya ST-011
9:15AM–9:40AM Wang Lu-Yang ST-012
9:40AM–9:50AM Coffee break

Session 7: Chair: Zhang Zhuo-Hua, Xu Hua-Xi
9:50AM–10:15AM Bazan Haydee ST-013
10:15AM–10:40AM Zhang Zhuo-Hua ST-014
10:40AM–11:05AM Li Rena ST-015
11:05AM–11:30AM Zhang Yun-Wu ST-016

Session 8:
11:30AM–12:10PM Special lecture
12:10PM–1:30PM Lunch

Session 9: Chair: Zhu Dong-Ya, Xu Zhi-Heng
1:30PM–1:55PM Zhou Zhuan ST-017
1:55PM–2:20PM Xu Zhi-Heng ST-018
2:20PM–2:45PM Zhao Ming-Gao ST-019
2:45PM–3:10PM Qiu Zi-Long ST-020
3:10PM–3:35PM Chen Xiao-Wei ST-021
3:35PM–4:00PM Liu Jing-Gen ST-022
4:00PM–4:10PM Coffee break
Session 10: Chair: Li Xiao-Ming, Tian Qing
4:10PM–4:35PM Li-Xiao-Ming ST-023
4:35PM–5:00PM Zhang Yan ST-024
5:00PM–5:25PM Liu Li ST-025
5:25PM–5:50PM Kang Li-Jun ST-026
5:50PM–6:15PM Li Xiang-Yao ST-027
6:15PM–6:30PM Closing ceremony
6:30PM Farewell Dinner

Sept. 29 th, 2012
(Clinical therapy part)
8:30AM–9:00AM Opening Ceremony of the Clinical Session

Session 11: Chair: Hu Bo
9:00AM–9:30AM Wang Yong-Jun
9:30AM–10:00AM Xie Peng
10:00AM–10:30AM Hu Xue-Qiang
10:30AM–10:50AM Coffee break
10:50AM–11:20AM Zeng Jin-Sheng
11:20AM–11:50AM Dong Qiang
12:00PM–1:30PM Lunch

Session 12: Chair: Hu Bo
1:30PM–2:00PM Zhou Dong
2:00PM–2:30PM Zhao Gang
2:30PM–3:00PM Xu An-Ding
3:00PM–3:20PM Coffee break
3:20PM–3:50PM Chen Kang-Ning
3:50PM–4:20PM Hu Bo
4:20PM–4:50PM Closing Ceremony

Abstracts – Oral

KS-001

Dendrite morphogenesis and neurological disorders

Yuh-Nung Jan

HHMI, UCSF
1550 4th Street, the Rock Hall, Room 484E
San Francisco, CA 94158
E-mail: yuhnung.jan@ucsf.edu

Dendrite arborization patterns are a hallmark of neuronal type and important determinants of neural circuit formation. Dendrite defects are associated with a variety of human neurological disorders. In the past decade, we have been using the dendritic arborization (da) neurons, a major subtype of multiple dendritic (MD) sensory neurons in the *Drosophila* PNS, as a model system for a genetic dissection of dendrite development in order to gain insights into how axons and dendrites are made differently, how a neuron acquires its neuronal type specific morphology, how the dendrites of different neurons are organized, how the size of a dendritic arbor is controlled, and how the pruning and remodeling of dendrites are regulated during development (reviewed in Jan and Jan, Nature Review Neuroscience, 2010). I will present our recent progress in uncovering some of the molecular mechanisms underlying dendrite development. I will also discuss the potential relevance of our studies to human neurological disorders.

KS-003

Title: Understanding receptor tyrosine kinase-dependent signaling in synaptic plasticity

Nancy Y. Ip

Division of Life Science, Molecular Neuroscience Center and State Key Laboratory of Molecular Neuroscience, The Hong Kong University of Science & Technology, Hong Kong, China
Email: boip@ust.hk

Experience-dependent remodeling of dendritic spines underlies learning and memory, while spine abnormalities have been associated with neurodegenerative diseases and psychiatric disorders. Elucidating the molecular mechanisms that control dendritic spine morphogenesis is therefore fundamental to our understanding of brain functions, and is pivotal for the identification of new molecular targets and drug development. Here I will describe how the interplay between distinct receptor tyrosine kinases (RTKs) and the serine/threonine kinase Cdk5 differentially regulates spine formation and elimination during synaptic plasticity. We found that while activation of the RTK TrkB stimulates its phosphorylation at Ser-478 in a Cdk5-dependent manner, the Ser-478 phosphorylation of TrkB regulates activity-dependent spine enlargement through enhancing the interaction of the receptor with the guanine nucleotide exchange factor (GEF) TIAM1. The TrkB knockin mice carrying the phospho-deficient mutation (S478A) display defective hippocampal long-term potentiation, a well-studied form of learning-related synaptic plasticity, as well as impaired spatial memory, therefore revealing an important role of Cdk5-mediated phosphorylation of TrkB in promoting spine growth during memory formation. On the other hand, we have also identified another RTK EphA4 as a major negative regulator of excitatory neurotransmission through retraction of dendritic spines, which involves signaling to actin cytoskeleton through the Cdk5-dependent phosphorylation of RhoGEF ephexin1. Together, these observations illustrate how Cdk5 differentially regulates spine remodeling through coupling to different RTKs. Given that impaired synaptic functions in the brain is associated with Alzheimer's disease, our findings raise the intriguing possibility that these RTKs and their associated signaling molecules are promising targets for developing novel treatments to alleviate the cognitive deficits of afflicted patients.

Acknowledgments: This work was supported in part by the Research Grants Council of Hong Kong SAR (HKUST 661109, 661309, 660810 and 661010) and the Innovation and Technology Fund for State Key Laboratory (ITCPT/17-9).

ST-001

Src upregulation of NMDA receptors: a common link in pain and schizophrenia

Michael W. Salter*

Program in Neurosciences & Mental Health
Hospital for Sick Children, Toronto, Canada, M5G 1X8
*Email: mike.salter@utoronto.ca

Regulation of the function of postsynaptic glutamate receptors is one of the principal mechanisms for producing alterations of synaptic efficacy in physiological and pathological processes in the CNS. At glutamatergic synapses, NMDA receptors (NMDARs) are upregulated by Src family tyrosine kinases which are opposed by the action of tyrosine phosphatases including STEP. Src kinase itself is a point through which multiple signaling cascades from converge to upregulate NMDA receptor activity. Src is anchored within the NMDA receptor complex by the adaptor protein ND2. This interaction is critical for holding Src in association with NMDARs when Src-mediated enhancement is normally required for triggering the synaptic potentiation that underlies learning and memory.

We have discovered that excessive Src-mediated enhancement of NMDAR activity in the dorsal horn of the spinal cord mediates the hypersensitivity underlying chronic pain. On the other hand, we have found that Src-mediated enhancement of NMDAR function is interrupted by signaling through the receptor-ligand pair, neuregulin 1(NRG1) -ErbB4 preventing NMDAR-dependent synaptic potentiation in the hippocampus and prefrontal cortex. Increased NRG1-ErbB4 signaling is genetically linked to schizophrenia, leading us to hypothesize that this excessive signaling suppresses NMDAR-dependent synaptic plasticity thereby producing positive symptoms of this disorder. Together our findings suggest that aberration of Src-mediated enhancement of NMDA receptor and pathological neuroplasticity is a unifying theme for several CNS disorders. Thus, normalizing Src enhancement of NMDARs is a novel therapeutic approach for CNS disorders, an approach without the deleterious consequences of directly blocking NMDARs.
Acknowledgments: Supported by CIHR, Krembil Fdn, ONF and HHMI.

ST-002

Determination of the effects of brain-specific inactivation of GSK-3 on behaviour and glucose metabolism in mouse models of human disease

Jim Woodgett*, Oksana Kaidanovich-Beilin, JohnRoder and Albert Wong[1]

Samuel Lunenfeld Research Institute and[1] Centre for Addiction and Mental Health, Toronto, Ontario, Canada
* Email: Woodgett@lunenfeld.ca

Glycogen synthase kinase-3 (GSK-3) is a protein kinase that lies downstream of several important signaling pathways and acts to suppress the functions of these systems. GSK-3 also plays several roles in brain development and neurological functions and has been implicated in depression, bipolar disorder, schizophrenia and anxiety. We have used conditional alleles of the two isoforms of GSK-3 to analyse the effect of selectively inactivating this protein kinase in the forebrain of mice. This has been achieved using a Tamoxifen-inducible Cre recombinase driven from the CamK-II promoter. We have tested the impact of deletion of both alleles of GSK-3 on mouse behavior, glucose metabolism and the effects of high fat diet. These experiments have revealed roles of forebrain GSK-3 in control of intermediary metabolism and behaviours. In addition, we have examined the impact of crossing GSK-3 mutant mice with other mouse models of neurological disease, such as DISC1. These and related data will be discussed.

Acknowledgments: This work was supported by the Canadian Institutes of Health Research MOP 74711

ST-003

Treatment of ischemic brain damage using PSD95 inhibitors

Michael Tymianski MD PhD FRCSC*

Toronto Western Hospital Research Institute, Toronto, ON, Canada M5T-2S8
* Email: mike.tymianski@uhn.ca

Stroke and traumatic brain injuries are disorders of major socioeconomic significance worldwide. However, presently, there are no pharmacological treatments to increase the resilience of the brain to ischemia or trauma.
This lecture will address the discovery and development of a new class of drugs, termed “PSD95 inhibitors” for the treatment of ischemic and traumatic brain injuries. PSD95 inhibitors uncouple postsynaptic density 95 protein from signaling molecules that effect brain damage, including NMDA receptor-mediated excitotoxicity. These agents reduce stroke and TBI damage in rats, and have been tested in primates in various models of brain ischemia. A Phase 1 and Phase 2 human clinical trial have been conducted, suggesting efficacy in reducing ischemic brain damage in humans.

Acknowledgments: This work was supported by funding from the Canadian Institutes of Health Research, the National Institute of Health, and the Canadian Stroke Network.

ST-004

Biphasic neurovascular responses in stroke injury and repair

Eng H. Lo, Kazuhide Hayakawa & Changhong Xing

Massachusetts General Hospital/ East Neuroprotection Research Lab, Bldg. 149, Rm. 2401 149 13th Street Charlestown, MA 2129
Email: lo@helix.mgh.harvard.edu

Abstract: The neurovascular unit provides a conceptual framework for investigating the pathophysiology of how brain cells die after stroke, brain injury, and neurodegeneration. Emerging data now suggest that this concept can be further extended. Cell-cell signaling between neuronal, glial and vascular elements in the brain not only mediates the mechanisms of acute injury. But integrated responses in these same elements may also be required for recovery as the entire neurovascular unit attempts to reorganize and remodel. These biphasic neurovascular responses involve coordinated interactions between both central as well as

peripheral cells. Understanding the common signals and substrates of this transition between acute injury and delayed repair in the neurovascular unit may reveal useful paradigms for augmenting neuronal, glial and vascular plasticity in damaged and diseased brain.

ST-005

Regulation of neuronal development by risk genes for mental disorders

Ju Young Kim, Eunchai Kang, Xin Duan, Jason Chiang, Zhexing Wen, Kimberly Christian, Hongjun Song and Guo-li Ming*
Institute for Cell Engineering; The Solomon H. Snyder Department of Neuroscience; Johns Hopkins University School of Medicine; Baltimore; MD USA. a, 210001.
* Email: gming1@jhmi.edu

Disrupted in schizophrenia 1 (DISC1) gene was initially identified in a Scottish family with schizophrenia and other major mental disorders, due to a balanced translocation that disrupt the DISC1 gene. DISC1 encodes a scaffold protein that is involved in the regulation of multiple processes of neurodevelopment both in early and adult neurogenesis. The signaling mechanisms of how DISC1 regulates neural development are still largely unknown. We have recently shown that, during adult neurogenesis, knockdown of DISC1 leads to multiple neuronal developmental deficits, including enlarged cell body, accelerated morphogenesis and maturation of newborn granule neurons in the dentate gyrus of hippocampus, and these actions of DISC1 is mainly mediated through the AKT/mTOR pathway. More recently, we have identified additional components in DISC1 signaling, from the extracellular cue to cytoplasmic pathways. Interesting, many of these molecules have been implicated in mental disorders, including schizophrenia and autism. We also have obtained independent evidence supporting interaction between these factors in increasing the risk for schizophrenia in different patient cohorts. Together, these studies reveal novel roles of mental disorder risk genes in neuronal development.

Acknowledgments: This work was supported by the National Institute of Health.

ST-006

The roles of BACE1 in Alzheimer's disease and other neurological dysfunctions

Riqiang Yan[1]

[1]Department of Neurosciences, Lerner Research Institute, Cleveland Clinic, Cleveland, OH 44195

BACE1, a type I transmembrane aspartyl protease, cleaves amyloid precursor protein (APP) at the β-secretase site. Following this cleavage, γ-secretase processes the membrane-bound APP C-terminal fragment to release amyloid peptides (Aβ). Since Aβ aggregation is the major component in amyloid plaques and excessive production of Aβ is linked to both familial and sporadic Alzheimer's disease (AD) pathogenesis, inhibition of BACE1 is widely pursued as an important target for AD therapy. A large volume of experimental results has shown that chemical inhibition of BACE1 in both mouse models and humans produces substantial inhibition of Aβ generation and amyloid deposition. Because of its promising potential applications in human AD treatment, it is imperative to understand the potential side effects associated with mechanistic inhibition of BACE1. To address this practical question, we have used BACE1-knockout mice to explore the physiological functions of BACE1. We demonstrate that, in BACE1-null mice, the process of myelination of both central and peripheral nerves is delayed and that myelin thickness is markedly reduced, indicating that genetic deletion of BACE1 causes hypomyelination during the developmental stage. In addition, axonally injured adult BACE1-null mice exhibit impaired remyelination. We have now found that a more severe phenotype in BACE1-null mice is the occurrence of spontaneous epileptic seizures. To explore the underlying molecular mechanisms associated with these phenotypes, we conducted various biochemical characterizations and identified cleavages of relevant BACE1 substrates, such as neuregulin and sodium channel proteins. Both in vitro and in vivo experiments have been performed to determine whether partial reducing BACE1 activity would affect the cleavage of these substrates, and provide guidance for chemical inhibition of BACE1 in human. Together, we conclude that BACE1 is an important molecule that plays multiples roles in various neurological processes.

ST-007

Deciphering the Role of the Amyloid Precursor Protein in Synaptic Regulation

Hui Zheng

Huffington Center on Aging, Baylor College of Medicine
Email: huiz@bcm.edu

Genetic and biochemical studies establish a central role of the amyloid precursor protein (APP) in Alzheimer's disease (AD): Genetic mutations and gene amplification of *APP* are linked to a subset of early onset of familial Alzheimer's disease (FAD), and APP processing generates β-amyloid (Aβ) peptides, which are the principal components of the amyloid plaque pathology. Although β-amyloid plaques are the hallmark of AD, synaptic dysfunction closely correlates

with cognitive impairment and is recognized as a causal event leading to AD pathogenesis. Since Aβ is naturally generated along with other products through APP processing, investigating the role of APP and its cleavage products in synaptic function and dysfunction is critically important in understanding AD pathogenesis. We seek to understand the pathophysiological functions of APP in neurons and synapses using *in vivo* mouse models and *in vitro* culture systems. Analysis of the *APP* knockout mice allows us to identify a functional role of APP in synaptic plasticity and learning and memory. Our investigation of mice deficient in *APP* and its homolog *APLP2* establishes an essential role of APP family protein in mediating cholinergic synaptic structure and neurotransmission in both peripheral neuromuscular synapse and central cholinergic neurons. By creating an *APP* conditional allele, we demonstrate that APP is required in both pre- and postsynaptic terminals; and that pre- and postsynaptic APP interact to mediate synaptic structure and function. These *in vivo* findings are supported by *in vitro* mixed-culture studies, which reveal that APP potently induces synaptogenesis, and that this activity requires both the APP extracellular and intracellular domains. Our studies identify APP as a novel synaptic adhesion molecule. We postulate that trans-synaptic APP interaction modulates its synaptic function, and that perturbed APP synaptic adhesion activity may contribute to synaptic dysfunction and AD pathogenesis.

ST-008

Glial control of depressive-like behaviors

Tian-Ming Gao

Department of Neurobiology, School of Basic Medical Sciences, Southern Medical University, Guangzhou 510515, China.
E-mail: tgao@fimmu.com

Abstract: Major depressive disorder (MDD) is a cause of disability that affects approximately 16% of the world's population, but little is known about the underlying biology. Evidence from animal, postmortem brain and imaging studies of depressed patients has implicated glial dysfunction in MDD pathophysiology. However, the molecular mechanism through which astrocytes modulate depressive behaviors is largely unknown. Here, we identified adenosine 5'-triphosphate (ATP) as a key factor involved in astrocyte modulation of depressive behavior expression in adult mice. ATP is deficient in the brains of mice after social defeated, and ATP administration produced a rapid antidepressant (AD)-like effect. Both a lack of IP_3R2 and transgenic blockage of vesicular gliotransmission caused a deficiency of astrocytic ATP release, which produced depressive-like behaviors that were rescued by ATP administration. Furthermore, genetically stimulating endogenous ATP release from astrocytes produced AD-like effects in a mouse model of depression. These results highlight astrocytic ATP release as a biological mechanism of MDD.

SP-001

Docosanoid Signaling in Neuroinflammation: New Mediators for Neuroprotection and Long Term Rescue

Nicolas G. Bazan, M.D., PhD.

Neuroscience Center of Excellence, Louisiana State University Health Sciences Center, School of Medicine, New Orleans, Louisiana, USA
Email: NBazan@lsuhsc.edu

The significance of the selective enrichment in omega-3 essential fatty acids (docosahexaenoyl –DHA- chains of membrane phospholipids, 22C and 6 double bonds) in the nervous system (eg. synaptic membranes, dendrites and photoreceptors) has remained, until recently, incompletely understood. While studying mechanisms of cell survival in neurodegenerations, we contributed to the discovery of a docosanoid synthesized from DHA by 15-lipoxygenase-1, which we dubbed neuroprotectin D1 (NPD1,10R,17S-dihydroxy-docosa-4Z,7Z,11E,13E,15E,19Z hexaenoic acid). This mediator is a docosanoid because it is derived from a 22C precursor (DHA), unlike eicosanoids, which are derived from the 20 C arachidonic acid family of essential fatty. We found that endogenous NPD1 biosynthesis is promptly induced in response to oxidative stress, protein misfolding/proteotoxicity, seizures , brain ischemia-reperfusion, and by neurotrophins. NPD1 is neuroprotective in these conditions. experimental brain damage, oxidative-stressed retinal pigment epithelial (RPE) cells, and in human brain cells exposed to amyloid-β peptide. Thus we envision NPD1 as a protective sentinel, one of the very first defenses activated when cell homeostasis is threatened by neurodegenerations. We provide here recent experimental examples that highlight the specificity and potency of NPD1, spanning beneficial bioactivity during events critical during the initiation and early progression of neurodegenerations:
1) We used epileptogenesis as a model to explore key mechanisms that sustain neuronal network integrity under adverse conditions. Using LC-MS/MS-based mediator lipidomic analysis we found that NPD1 increases during seizures in the hippocampus, and when we administered this docosanoid during pharmacologically–induced epileptogenesis it elicited a remarkable attenuation of pathological brain oscillations. This effect reflects modulatory bioactivity of aberrant neuronal networks that lead to spontaneous recurrent seizures. We used multi-microelectrode arrays in freely moving mice. Thus, docosanoid-mediated signaling rescues neuronal network disruptions.
2) Since protein misfolding and proteotoxic stress takes place in early stages of several neurodegenerative diseases

we have explored these events as a possible NPD1 target in cell culture models (human RPE cells and primary neuronal mix cultures). We have studied expansion of unstable translated CAG repeats that encode polyglutamine tracts that cause Spinocerebellar ataxia type 1 and Huntington's disease: that is Ataxin-1 Poly-Q and huntingtin Poly-Q. The expression of Ataxin-1 82Q or of huntingtin 72Q exerted a remarkable activation of endogenous NPD1 synthesis. Moreover we found that NPD1 attenuated proteotoxicity of both CAG reapeat containing proteins. NPD1 also decreased phospho-Ser -776 in Ataxin-1. We speculate that in agreement with our previous findings that NPD1 may work by increasing PP2A activity. Thus the lipid mediator may counteract PP2A inhibition, allowing the 82Q form to be de-phosphorylated and cleared or relocated into the spliceosome. The fact that Anp32 was proposed to have a stronger interaction with the expanded form rather than with the wild type Ataxin-1 makes this protein an excellent target candidate for NPD1 signaling. Thus in addition to the expansions in the poly-glutamine tract, AXH has an important role in the functionality of Ataxin-1. AXH, a self-folding domain present in Ataxin-1, is responsible for the protein-protein interactions between Ataxin-1 and other transcription factors, such as the capicua homolog CIC protein. The sequestration of the complex partners formed by Ataxin-1 by its inactive counterpart may be involved in the loss of function observed in neurodegenrations. Brother of Ataxin-1 (Boat), another member of the AXH domain-containing protein family, is an example of the proposed loss of function. Boat is an *in vivo* binding partner of Ataxin-1 that is also affected by the malfunction of Ataxin-1 82Q.. Thus the expression of AXH alone in our cells resulted in increased apoptosis. Furthermore, it aggravated the cytotoxicity induced by Ataxin-1 82Q . Unlike the sequestration scenario, in which the complexes are formed but are inactive, AXH induces toxicity in this case by increasing disassembly of the complex, thus promoting inactivation of its partners. NPD1 signaling promotes survival by modulating a set of genes that homeostatically control cell fate and regulate proteostasis. NPD1 reversed the toxicity of Ataxin-1 82Q as well as of Huntingtin 72Q in our cells (J. Calandria et al., J Biol Chem. 2012)

3) We found that NPD1 is drastically reduced in CA1 areas from Alzheimer's patients (Lukiw et al., J.Clin Inv. 2005). Therefore we have explored the significance of NPD1 in cellular models that recapitulate part of the Alzheimer's pathology. Human neurons and astrocytes challenged by amyloid-β or by overexpressing APPsw (double Swedish mutation that causes familial forms of the disease) show that NPD1 downregulates amyloidogenic processing of amyloid-β precursor protein, switches off pro-inflammatory gene expression (TNF-α, COX-2 and B-94-TNF-α inducible pro-inflammatory element), and promotes neural cell survival. Moreover, anti-amyloidogenic processing by NPD1 targets α- and β-secretases and PPARγ receptor activation (Y. Zhao et al. PLOsOne, 2011). Currently we are also using imaging MALDI/TOF-MS to further unravel the lipidome in specific brain regions. The availability of anti-apoptotic BCL-2 proteins is positively modulated by NPD1, whereas pro-apoptotic BCL-2 proteins are negatively regulated, as is microglial activation.

The cell survival cascade and the events that sustain neuronal network homeostatic integrity involves multiple checkpoints and signaling networks that include restoring proteostasis during protein misfolding/proteotoxicity. NPD1 regulation of targets upstream events of cell survival, neuroinflammatory signaling and transcription in turn promotes homeostatic regulation of synaptic and neural circuitry integrity.

(Supported by NIH: NINDS R01 NS046741, NEI R01 EY005121)

ST-009

Huntington disease pathology in transgenic animal models

Xiao-Jiang Li[1,2], Shihua Li[1]

[1]Department of Human Genetics, Emory University; Atlanta, GA USA,
[2]Institute of Genetics and Developmental Biology, Chinese Academy of Sciences, Beijing, China.
Email: xli2@emory.edu

Transgenic animal models are powerful tools for understanding the pathogenesis of human diseases. For investigating neurological disorders, transgenic mouse models have been more extensively used than other small animal models because the complexity of their central nerve system is relatively closer to that of human brains. Extensive studies of transgenic mice that model age-dependent neurodegenerative diseases such as Alzheimer (AD), Parkinson (PD), and Huntington (HD) diseases have provided important insight into the pathogenesis of these diseases and uncovered the common pathology mediated by misfolded proteins. However, the brains of transgenic mouse models of AD, PD, and HD do not show the striking neuronal loss or degeneration, which is an important pathological feature of these neurodegenerative diseases. By examining the brains of transgenic monkeys and pigs of HD, we observed axonal degeneration and apoptosis in their brains, which have not been found in transgenic HD mice. Also, the mutant HD proteins seem to mediate more severe phenotypes in transgenic monkey and pigs than in transgenic mice. These studies suggest that species difference is important for the nature of neuropathology caused by misfolded proteins in age-dependent neurodegenerative diseases. The studies also underscore the importance in establishing transgenic large animal models to study the pathogenesis of neurological disorders and to develop their therapeutics.

Acknowledgements: The work was supported by grants (NS041669, AG019206, NS045016, AG031153) from NIH.

ST-010

Glia and Memory

Xia Zhang*

University of Ottawa Institute of Mental Health Research at The Royal, 1145 Carling Ave, Ottawa, Canada K1Z7K4.
* Email: Xia.Zhang@theroyal.ca

Our recent study provides the first evidence that an acute system administration of the exogenous cannabinoid (exCB) HU210 or THC produces significant impairment effects on the performance of spatial working memory via an *in vivo* long-term depression (LTD) at the excitatory CA3-CA1 synapses in the hippocampus (Han et al., Cell 2012, 148: 1039-1050). This *in vivo* exCB-LTD required sequential activation of astroglial cells and postsynaptic NMDA receptor for induction and endocytosis of postsynaptic AMPA receptor for expression. More recently, we were surprised to observe that microglial-mediated chronic increase of brain concentrations of endogenous cannabinoids or endocannabinoids (eCB) was able to improve spatial reference memory in the mouse model of Alzheimer disease via an *in vivo* LTD at CA3-CA1 synapses. This *in vivo* eCB-LTD, which also required activation of postsynaptic NMDA receptor for induction and endocytosis of postsynaptic AMPA receptor for expression, did not significantly affect spatial working memory.

Acknowledgments: This work was supported by grants from the Canadian Institutes for Health Research, China-Canada Joint Research grant, and Natural Sciences and Engineering Research Council of Canada

ST-011

Neuroprotective agent with double targets in the rat model of ischemic stroke

Hai-Yin Wu, Ying Tang, Chun-Xia Luo, Dong-Ya Zhu*

Laboratory of Cerebrovascular Disease, Key Laboratory of Cardiovascular Disease and Molecular Intervention, Nanjing Medical University, Nanjing, China; 210029
*Email: dyzhu@njmu.edu.cn

Stroke is a major cause of death and the most frequent cause of acquired disability in adults. To date, the only approved treatment for ischemic stroke is intravenous tissue plasminogen activator. However, its efficacy is limited by a very narrow therapeutic time window of 3h and by reperfusion injury and potentially severe hemorrhagic complications because the drug is aimed at restoring cerebral blood flow rather than at preventing the actual mechanisms associated with neuronal cell death. Thus, the successful treatment of acute ischemic stroke remains one of the major challenges in clinical medicine. Free radical production contributes to the early ischemic response and the neuroinflammatory response to injury initiates the second wave of cell death following ischemic stroke. We investigated the synergistic effect of scavenging free radical and inhibiting pro-inflammatory mediator expression in the rat model of transient cerebral ischemia. Edaravone scavenged ·OH, NO· and $ONOO^-$ concentration-dependently. Borneol inhibited ischemia/reperfusion-induced TNF-α, iNOS, IL-1β and COX-2 expressions. The optimal proportion of edaravone to borneol was 4:1 for preventing transient cerebral ischemia. The combination of edaravone with borneol had significant synergistic effect, exhibited a therapeutic time window of 6 h and potent long-term effect, including improved elemental vital signs, sensorimotor functions and spatial cognition. We demonstrate a synergistic effect of scavenging free radical and inhibiting pro-inflammatory mediator expression and suggest a novel neuroprotective agent consisting of edaravone and borneol for treating ischemic stroke.

Acknowledgments: This work was supported by the National Natural Science Foundation of China (30971021, 81030023), National Basic Research Program of China (973 Program) (2011CB504404) and Natural Science Foundation of Jiangsu Province-Special Program (BK2011029).

ST-012

Coupling voltage-gated calcium channels to neurotransmitter release and neurological diseases

Lu-Yang Wang

Program in Neurosciences and Mental Health, SickKids Research Institute & Department of Physiology, University of Toronto; 555 University Avenue, Toronto, ON, Canada M5G 1X8
Email: luyang.wang@utoronto.ca

Background: Calcium influx through voltage-gated calcium channels (VGCCs) during action potentials (APs) plays critical roles in mediating neurotransmitter release and replenishment, and mutations in these channels have been implicated neurological diseases and degeneration such as familiar migraine, ataxia, absence seizure and epilepsy. However, subsynaptic mechanisms underlying deficits in neurotransmission and behavioral phenotypes remain elusive. We investigated such mechanisms by examining the Tottering Leaner ($tg^{la/la}$),

mouse, in which the C-terminal of α_{1A} subunit encoding P/Q-type VGCCs carries a spontaneous missense splicing mutation leading to its truncation, and consequentially impaired channel function and severe ataxia and seizure. Interestingly, the C-terminal of α_{1A} is thought to be necessary for physically tethering of these channels to synaptic vesicles (SVs) via synaptic proteins RIMs and RIM-BPs and hence transmitter release in central synapses (Kaeser et al., Cell, 2011).

Methods: Using the developing calyx of Held synapse in the mouse auditory brainstem as a model, we investigated whether and how the $tg^{la/la}$ mutation affects the targeting and biophysical properties of VGCCs in the nerve terminal and transmitter release by patch-clamp recordings of presynaptic Ca^{2+} currents (Pre-I_{Ca}) and/or excitatory postsynaptic currents (I_{EPSCs}) from principle neurons in brainstem slices from P8-P18 postnatal wild-type (WT) and $tg^{la/la}$ mutant mice. Subtype specific toxins, namely ω-ATX and ω-CTX, were applied to block P/Q- and N-type VGCCs at this synapse in order to assay contributions of each subtype to Pre-I_{Ca} and transmitter release in WT and $tg^{la/la}$ synapses.

Results: I_{EPSCs} were comparable between WT and $tg^{la/la}$ synapses before the onset of hearing (i.e.P11/12), after which significantly attenuated. Incidentally, transmitter release during this critical period of development is mediated by both N- and P/Q-type before P11/12 and exclusively mediated by P/Q-type afterwards in WT mice. In contrast to WT mice, both ω-CTX sensitive N-type and ω-ATX sensitive mutant P/Q-type VGCCs remained at the nerve terminal throughout P8-18, but continued presence of N-type failed to fully compensate for synaptic deficits, suggesting that mutant P/Q-type channels play a dominant negative role in mediating neurotransmitter release. Furthermore, after blocking N-type VGCCs with ω-CTX, presynaptic injection of slow calcium buffer EGTA did not block transmitter release mediated by mutant P/Q-type channels, indicating that the mutant channel in the absence of its C-terminal is capable of forming tight nanodomain couplings to SVs. By examining Pre-I_{Ca} and I_{EPSCs} relationships evoked by real and pseudo APs between WT and $tg^{la/la}$ synapses, we further demonstrated that synaptic deficits are likely accounted for by a combination of low open probability (Po) of mutant P/Q-type VGCCs and developmental AP narrowing.

Conclusions: Our observations suggest that mutant α_{1A} without the C-terminal can be targeted to occupy preferred release sites and tether SVs in the nanodomain modality for release, whereas N-type VGCCs cannot fully rescue the deficit in $tg^{la/la}$ synapses. We conclude that decreasing number of VGCCs activated per AP due to developmental AP narrowing, and intrinsic low Po of dysfunctional P/Q-type VGCCs ultimately converge to exacerbate the deficit in transmitter release, and potentially underlie neurological and behavioral phenotypes associated with $tg^{la/la}$ and other mutants of VGCCs.

Supported by CIHR, BWF and EJLB

Keywords: voltage-gated calcium channels; synaptic transmission; calyx of Held synapse; familiar migraine, ataxia, absence seizure and epilepsy

ST-013

Regeneration of corneal nerves in experimental refractive surgery

Haydee E.P. Bazan, PhD

Neuroscience Center of Excellence and Department of Ophthalmology, Louisiana State University Health Sciences Center, School of Medicine, New Orleans, Louisiana, USA. Email: HBazan1@lsuhsc.edu

The cornea is an avascular and transparent tissue localized on the surface of the eye that serves as a barrier to protect the eye and to transmit and refract light. This tissue is densely packed with sensory nerves that play an important role in maintaining a healthy cornea surface. Interruption of corneal innervations may cause altered epithelial morphology and function, and poor tear film production inducing dry eye and delayed wound healing. Several causes produce corneal nerve damage. Among the most prevalent are surgery to correct vision, herpes simplex virus infection, diabetes and epithelial basement membrane dystrophy.We have shown that rabbit corneas treated with pigment epithelial derived factor (PEDF) plus docosahexaenoic acid (DHA) after lamellar keratectomy increase nerve regeneration. Eight weeks after surgery the percentage of total sub epithelial nerves and calcitonin-gene-related peptide (CGRP) –positive nerve fibers were similar to normal corneas. Five weeks after surgery and treatment with PEDF plus DHA there is an increase in corneal sensitivity compared to vehicle treated animals. The treatment stimulates cornea wound healing and increases epithelial cell proliferation. Extraction of lipids from corneas treated with PEDF plus DHA show synthesis of neuroprotectin D1 (NPD1), a docosanoid derived from DHA by the action of 15-lipoxygenease. Synthesis of NPD1 occurs in the corneal epithelial cells and is blocked by 15-lipoxygeneaseinhibitors A group of rabbits was treated with NPD1 after refractive surgery in order to investigate if topical application of NPD1 stimulates the regeneration of functional nerves. NPD1 increased the percentage of βIII-tubulin nerves and CGRP-positive nerves in a similar manner as PEDF plus DHA. There was also significant increase in nerve sensitivity and tear secretion. The use of PEDF plus DHA, or its derivative NPD1, represents a novel therapeutic

approach for managing eye conditions that perturb corneal nerve regeneration.
(Supported by NIH-NEI grant EY019465).

References to our work

Cortina MS, He J, Li N, Bazan NG, **Bazan HEP**: PEDF plus DHA induces neuroprotectin D1 synthesis and corneal nerve regeneration after experimental surgery. *Invest Opthalmol Vis Sci* 51:804-810, 2010.
He J, **Bazan HEP**. Omega-3 fatty acids in dry eye and corneal regeneration after nerve refractive surgery. *Prostaglandins Leukot.Essent.Fatty Acids* 82:319-325, 2010.
He J, Bazan NG, **Bazan HEP**. Mapping the entire human corneal nerve architecture. *Exp Eye Res*, 91:513-523, 2010
Cortina MS, Bazan HEP. Docosahexaenoic acid, protectins and dry eye. *Curr Opin Nutr Metab Care* 14:132-137, 2011
Cortina MS, He J, Li N, Bazan NG, **Bazan HEP**. Recovery of corneal sensitivity, CGRP positive nerves and increased wound healing are induced by PEDF plus DHA after experimental surgery . *Arch Opthalmol*. 130(1):76-83, 2012.
He J, **Bazan HEP**. Mapping the nerve architecture of diabetic human corneas. *Ophthalmology (in press)*

ST-015

Endogenous estrogen levels in the brain determine responses to estrogen replacement therapy via regulation of BACE1 and NEP in female Alzheimer's transgenic mice

Ping He[1,2], Matthias Staufenbiel[3], Nobuhiro Harada[4], Yong Shen[2], Rena Li[1*]

[1]Center for Hormone Advanced Science and Education, [2]Center for Advanced Therapeutic Strategies for Brain Disorders, Roskamp Institute, Sarasota, FL 34243, USA, [3]Novartis Pharma Ltd., Nervous System Research, CH-4002 Basel, Switzerland, [4]School of Medicine, Fujita Health University, Aichi 470-1192, Japan
Email: rli@rfdn.org

Estrogens, including 17β-estradiol, have been found to improve memory and reduce risk of dementia, although conflicting results also been reported. Although dosage, duration and the form of estrogen all contribute to the controversial outcome of hormone replacement therapy, endogenous estrogen exposure throughout a life time is also associated with cognitive function in older women. Only recently, our published human brain studies showed a depletion of brain estrogen in women with Alzheimer's disease, while other studies have demonstrated cognitive impairment believed to be caused by inhibition of endogenous estrogen synthesis in females. To investigate whether a shortage of brain estrogen alters the sensitivity of response to estrogen replacement therapy, we have used genetic and surgical animal models to examine the response of estrogen treatment in Alzheimer's disease (AD) neuropathology. Our studies have shown that early treatment with 17β-estradiol (E2) or genistein (Gen) could reduce brain amyloid levels by increasing Aβ clearance in both APP23 mice with genetic aromatase deficiency (APP/Ar$^{+/-}$), and in APP23 mice with an ovariectomy (APP/OVX). However, only APP/Ar$^{+/-}$ mice showed a great reduction in brain amyloid plaque formation after E2 or Gen treatment along with downregulation of beta secretase (BACE1) mRNA and protein expression. Our results suggest that early and long-term usage of E2 and/or Gen may prevent AD pathologies in a manner dependant on endogenous estrogen levels in the brain in aging females.

Acknowledgements. This work was supported by grants from the Alzheimer's Association IIRG-07-59510, American Health Assistance Foundation Grant G2006-118, NIH R01AG032441-01, NIH R01AG025888.

ST-016

Roles of sorting nexin family proteins in neurodegeneration

Yonghao Zhao[1], Xin Wang[2], Yunshu Wang[1], Jiaye Yang[1], and Yun-wu Zhang[1]*

[1]Fujian Provincial Key Laboratory of Neurodegenerative Disease and Aging Research, College of Medicine, Xiamen University, Xiamen, Fujian 361005, PR China
[2]Neurodegenerative Disease Research Program, Sanford-Burnham Medical Research Institute, La Jolla, California 92037, USA
* Email: yunzhang@xmu.edu.cn

Dysregulated protein trafficking has been found to be associated with neurodegenerative diseases. Sorting nexins (SNXs) are a diverse group of cellular trafficking proteins that are unified by the presence of a phospholipid-binding (PX) motif. Some SNX members have been found to be involved in Alzheimer's disease (AD), one of the most common neurodegenerative diseases. However, the functional roles of other SNX proteins, especially their involvement in neurodegeneration, deserve further scrutiny. AD is initiated by overproduction/accumulation of β-amyloid (Aβ), which is generated from β-amyloid precursor protein (APP) through sequential cleavages by β-secretase (or β-site APP cleaving enzyme 1, BACE1) and γ-secretase. Herein, we find that one SNX member, SNX12, can interact with BACE1 and modulate BACE1 endocytosis, thus affecting Aβ generation. In addition, we find that another SNX member, SNX27, can interact with ionotropic glutamate receptors (NMDAR and AMPAR) and regulate their

sorting/trafficking to plasma membrane for recycling. Furthermore, we find that the level of SNX27 is decreased in Down Syndrome (DS) brains and demonstrate that SNX27 expression is indirectly regulated by miR-155, a chromosome 21-encoded microRNA. Together, our results suggest that SNXs are important for trafficking of proteins crucial for neurodegenerative diseases and alternations of SNXs may contribute to disease pathogenesis.

Acknowledgments: This study was supported by grants from the Alzheimer's Association, National Natural Science Foundation of China (30973150 and 81161120496), 973 Prophase Project (2010CB535004), Natural Science Foundation of Fujian Province of China (2009J06022), the Fundamental Research Funds for the Central Universities, and Fok Ying Tung Education Foundation.

ST-017

Cocaine modulates a vesicle pool for dopamine release in striatum *in vivo*

Pan-Li Zuo[1], Xin-Jiang Kang[1], Hua-Dong Xu[1], Bo Zhang[1], Li Zhou[1], Hai-Qiang Dou[1], Fei-Peng Zhu[1], Li-Na Liu[1], Shu Guo[1], Jin Lü[1], Qing Li[1], Shi-Rong Wang[1], Wei Yao[1], Howard Gu[2], Zhuan Zhou[1*]

[1]State Key Laboratory of Biomembrane Engineering and Center for Life Sciences, Institute of Molecular Medicine, Peking University, Beijing 100871, China; [2]Department of Pathology, ACM Medical Laboratory, Rochester, NY 14626, USA.
*Corresponding author: Zhuan Zhou
e-mail: zzhou@pku.edu.cn

Cocaine, an addictive drug, increases the apparent extracellular dopamine (DA) concentration (DA overflow) through the inhibition of the uptake activity of DA transporters (DAT). In addition, cocaine could also potentiate evoked DA release and thus contribute to the increased DA overflow. Using micro electrochemical carbon fiber electrodes, we have recently reported two kinetically distinct DA releasable vesicle pools, a fast releasable pool (FRP) and a prolonged releasable pool (PRP), in rat striatum *in vivo* (Wang et al, 2011, JNC, 119:342). Here we show that FRP and PRP exist also in mouse striatum *in vivo*. DA overflows in mouse stratum were readily evoked by electric field stimulation at Medial forebrain bundle (MFB) *in vivo* (Fig). Cocaine selectively enhanced the DA release from the FRP and the FRP replenishment. Using a cocaine-insensitive DAT mouse model, we revealed that the DAT was required for the cocaine-induced potentiation effect on FRP. D2 receptors, which are more sensitive to PRP, were not involved in the effect. Therefore, we conclude that cocaine preferentially increase the DA release from the FRP via DAT-mediated replenishment of the FRP in mouse striatum *in vivo*.

Acknowledgments: This work was supported by grants from the NSFC and MoST/"973" program

ST-018

Microcephaly Associated Gene *WDR62* is Essential for Proper Neurogenesis and Neuronal Migration During Cortex Development

Yaqing Wang, Dan Xu, Feng Zhang, Jason Xu, Yiming Sun, and Zhiheng Xu[1*]

[1]State Key Laboratory of Molecular Developmental Biology, Institute of Genetics and Developmental Biology, Chinese Academy of Sciences, Beijing, China 100101.
[*]Correspondence author: Zhiheng Xu (e-mail: zhxu@genetics.ac.cn).

Abstract Autosomal recessive primary microcephaly (MCPH) is a kind of neural developmental disorder. Patients with MCPH usually have significantly reduced brain size accompanied by mental retardation. WDR62, also known as MCPH2, has been found recently to be associated with the spindle pole and is mutated in different microcephaly families. We investigated the role of WDR62 in brain development and the potential pathological mechanism of WDR62 mutation in MCPH. We demonstrate that knockdown of WDR62 by RNA interference results in defects in the proliferation and/or differentiation of neural progenitor cells, neurogenesis and neuronal migration during cortical development. Interestingly, those defects can be rescued well by wild-type human WDR62 but not the five of the different mutants found in MCPH patients. Thus our findings provide an impetus to further explore the underlying pathogenesis of MCPH using murine animal model with knock-in of human WDR62 mutants.

ST-019

Abnormal neuronal dendritic development caused by astrocyte-released neutrophin-3 in a mouse model of Fragile X Syndrome

Qi Yang, Bin Feng, Kun Zhang, Ming-Gao Zhao *

Department of Pharmacology, School of Pharmacy, Fourth Military Medical University, 710032 Xi'an, China
*Email: minggao@fmmu.edu.cn

Fragile X syndrome (FXS) is a neurodevelopmental disorder caused by lack of fragile X mental retardation protein (FMRP) due to the mutation of the fragile X mental retardation 1 (*Fmr1*) gene. Recent studies suggest the role of astrocytes in neuronal growth. However, the mechanisms involved in the regulation process of astrocytes from FXS remain unclear. In this study, we found that astrocytes derived from a Fragile X model, the *Fmr1*-knockout (KO) mouse which lacks FMRP expression, inhibit the proper elaboration of dendritic processes of neurons *in vitro*. Furthermore, astrocytic conditioned medium (ACM) from KO astrocytes inhibits proper dendritic growth of both wild type (WT) and KO neurons. Inducing expression of FMRP by transfection of FMRP vectors in KO astrocytes restored dendritic morphology and levels of synaptic proteins. Further experiments revealed that KO ACM contained elevated levels of the neurotrophin-3 (NT-3). Addition of high concentration of exogenous NT-3 to culture medium reduced dendrites of neurons and synaptic protein levels, whereas knockdown of NT-3 expression in KO astrocytes by shRNAs normalized these measures. Finally, we demonstrated that excessive astrocyte-derived NT-3 in KO ACM exhibited elevated levels of two oxidative stress measures, MDA and ROS, and that knockdown of NT-3 partially restored levels to that seen in WT ACM. This study indicates that excessive NT-3 from astrocytes contributes to the neuronal developmental disorder of FXS and astrocytes could be a potential therapeutic target for FXS.

Acknowledgments: This work was supported by the National Natural Science Foundation of China (31070923)

ST-020

Molecular insights into autism spectrum disorders

Tianlin Cheng[1], Zhizhi Wang[2], Yan Zhang[1], Wenqing Xu[2], Zilong Qiu*

[1]Institute of Neuroscience, CAS,
[2]University of Washington, Seattle, WA
* corresponding author, zqiu@ion.ac.cn

Mutations in the X-linked gene Methyl-DNA binding protein 2 (MeCP2) are found in over 90% of patients with Rett syndrome, a severe form of autism spectrum disorders. It is known that MeCP2 binds to methylated DNA and represses gene transcription. Here we report that MeCP2 also regulates gene expression post-transcriptionally by suppressing nuclear microRNA processing. We found that MeCP2 binds directly to DiGeorge syndrome critical region 8 (DGCR8), a critical component of the microRNA processing complex, and disrupts its interaction with Drosha, another essential component of the processing complex. Protein targets of MeCP2-suppressed microRNAs include CREB and LIMK1, which play critical roles in brain development. Thus, control of microRNA processing via direct interaction with DGCR8 represents a novel mechanism of MeCP2 regulation of gene expression, and suggests new potential therapeutic targets of Rett syndrome.

Key Words: MeCP2, DGCR8, miRNA processing, development

ST-021

Cortical state-dependent calcium signaling in dendritic spines *in vivo*

Xiaowei Chen[1,2], Bert Sakmann[2], Arthur Konnerth[2]

[1]Brain Research Center, Third Military Medical University, Chongqing 400038, PR China
[2]Institute of Neuroscience, Technical University Munich, 80802 Munich, Germany
Email: shxiaow@yahoo.com

Cortical states are essential determinants of many cognitive processes, including sensory information processing, attention and memory consolidation. However, state-dependent signaling properties of single cortical synapses are unknown. Here, we use *in vivo* two-photon imaging to analyze calcium signals in dendritic spines during spontaneous up- and down-states in cortical neurons. We demonstrate that NMDA-R-dependent synaptic spine calcium signals are present in layer 2/3 mouse auditory cortical neurons during subthreshold up-states, but almost absent during down-states. Approximately 500 excitatory synapses are on average active during an up-state event. Importantly, we demonstrate that the same subset of spines that is reliably active during sensory stimulation is also reliably active during up-states., indicating that cortical up-states and sensory stimulation-evoked responses may be driven by highly overlapping sets of up-stream cortical neurons. Thus, spontaneously recurring up-states can evoke in these spines calcium signals that may underlie synaptic strength consolidation.

ST-022

Mechanism underlying amygdalar synaptic structure plasticity regulation of conditioned place aversion formation and long-term depression

Yao Liu, Chun Yu, Jing-Gen Liu*

State Key Laboratory of Drug Research, Shanghai Institute of Materia Medica, Shanghai Institutes for Biological Sciences, Chinese Academy of Sciences, Shanghai 201203, China
* Email: jgliu@mail.shcnc.ac.cn

Opiate addiction is the chronic relapsing disorder characterized by compulsive drug seeking and taking. Increasing evidence suggests that the maintenance of compulsive use of the drugs is substantially motivated by aversive affective memories associated with drug withdrawal in dependent subjects. However, the mechanisms underlying the formation of aversive memories remain unclear. We find that conditioned morphine withdrawal induces actin rearrangements and increases activity-regulated cytoskeletal-associated protein (Arc) expression in the amygdala and that blockade of actin rearrangements by intra-amygdala injections of latrunculin A, an inhibitor of actin polymerization, disrupts CPA behavior, indicating that actin polymerizations at amygdalar synapses are required for the formation of aversive memory associated with morphine withdrawal. We further demonstrate that actin polymerizations within the amygdala are essential for the enhancement of Arc/Arg3.1 expression at amygdalar synapses. Increased synaptic Arc/Arg3.1 expression contributed to induction of LTD in the amygdala and aversive memory formation by regulating synaptic AMPA receptor endocytosis, as blockade of AMPA receptor endocytosis prevented both LTD expression and aversive memory formation. This study provides first evidence that behavior training triggers Arc/Arg3.1 translocation at the synapses through actin polymerization and Arc/Arg3.1 contributes to synaptic depression and aversive memory formation by regulating synaptic AMPA receptor endocytosis. Therefore, our findings extend previous studies on the role of Arc/Arg3.1 in synaptic plasticity and memory by revealing how Arc/Arg3.1 is transported at active synapses in response to behavior training and that Arc/Arg3.1 is a crucial mediator for actin polymerization in regulating synaptic plasticity and memory. Our findings also underscore the unknown details how actin polymerizations mediate synaptic plasticity and memory. Moreover, as negative affective state induced by opiate withdrawal has long believed to enhance the incentive value of the drug, leading to persistent drug seeking and relapses, this study reveals the critical molecular events involved in the formation of aversive affective memory, providing new strategies for treating maladaptive neuroadaptations related to drug addiction.

Acknowledgments: This work was supported by the National Basic Research Program grant from the Ministry of Science and Technology of China (2009CB522005) and by the National Natural Science Foundation of China (81130087)

ST-023

The function of NRG1-ErbB4 signaling in the Fast-spiking interneurons

Ke-Xin Li, Jian-Ming Yang, and Xiao-Ming Li*

Department of Neurobiology; Key Laboratory of Medical Neurobiology of Ministry of Health of China; Zhejiang Province Key Laboratory of Neurobiology, Zhejiang University School of Medicine, Hangzhou, Zhejiang 310058, China.
* Email: Lixm@zju.edu.cn

Neuregulin1 (NRG1) and its receptor ERBB4 are putative susceptibility genes for the neurodevelopmental disease schizophrenia, yet their precise functions in the disorder are currently unknown. Primarily based on the cell-type specific expression of ErbB4 on parvalbumin-positive fast-spiking (FS) interneurons, NRG1-ErbB4 signaling is considered to play an important role in the development of GABAergic circuitry mediated by these interneurons. Here, we demonstrate that NRG1-ErbB4 signaling is dispensable for FS interneuron development in vivo. However, NRG1-ErbB4 signaling increases activity-dependent GABAergic transmission by regulating the intrinsic excitability of FS interneurons in adult brain. This effect was mediated by increasing the near threshold responsiveness and decreasing the voltage threshold for action potentials through Kv1.1, a voltage-gated potassium channel. These findings suggest that NRG1-ErbB4 signaling majorly target to FS interneuons and regulate their excitability in adult brain but dispensable for early development of FS interneuron.

Acknowledgments: This work was supported by the National Natural Science Foundation of China (91132714, 30970916 and 31070926) and the Major Research Program of the State Ministry of Science and Technology of China (2010CB912004).

ST-024

Tunneling nanotube and its implications in neurodegenerative diseases

Xiaqin Sun, Yan Zhang*

State Key Laboratory of Biomembrane and Membrane Biotechnology, College of Life Sciences, Peking University, Beijing, 100871, China
Email: yanzhang@pku.edu.cn

Tunneling nanotubes (TNTs) can be induced in rat hippocampal astrocytes and neurons with hydrogen peroxide or serum deprivation. Major cytoskeletal component of TNTs is F-actin. TNTs transfer cellular organelles including endoplasmic reticulum, mitochondria, Golgi, endosome. Interestingly, intracellular and extracellular amyloid β can be transferred by TNTs at a speed much faster than other organelles. When two populations of

cells are co-cultured, it is the stressed cells that always develop TNTs toward the healthy cells. p53 is important for TNT development. In addition, we find that among the genes activated by p53, epidermal growth factor receptor (EGFR) is also critical to TNT development. Akt, phosphoinositide 3-kinase, mTOR and M-Sec are involved in TNT induction. Our data suggest that TNTs might be a mechanism for cells to respond to insults and transfer cellular substances or energy to another cell. TNTs may play roles in neurodegeneration.

ST-025

The Novel Long non-coding RNA regulates *Drosophila* Locomotion

Meixia Li , Zhefeng Gong , Li Liu *

State Key Laboratory of Brain and Cognitive Science, Institute of Biophysics, Chinese Academy of Sciences, 15 Datun Road, Chaoyang District, Beijing, 100101, China.
Email: liuli@sun5.ibp.ac.cn

Movement disorders are defined as any neurological condition affecting the speed, frequency, fluency, or ease of motion. *Drosophila*, as one of the models for studying on movement disorders, provides opportunity to link between genes and mechanism in movement disorders. We found a novel long non-coding RNAs, expressed in the nervous system through the whole development stages in *Drosophila*, which could be involved in the regulation on the locomotion in adult *Drosophila*, and this effect was mediated by the the adjacent protein-coding gene. Our further experiments revealed the underlying molecular mechanism. These results provided insights to explore the pathogenesis of neurological diseases associated with movement disorders.

ST-026

Indentify the Mechano-Transduction Channels Underlying Touch and Pain Sensation in *C. elegans*

Zou Wenjuan, Lijun Kang*

Medical School, Zhejiang University, Hangzhou, China, 310058
* Email: kanglijun@zju.edu.cn

Mechano-transduction channels mediate several common sensory modalities such as hearing, touch, and pain. However, very little is known about the molecular identities of these channels in metazoans. Since it has been known that it is very difficult to answer this question in mammals, we thought to dissect this question in a popular genetic model organism *Caenorhabditis elegans*. We combined in vivo whole-cell recording and genetic approaches to explore mechano-receptor currents (MRCs) in the nematode *C.elegans*. Our results showed that TRP-4, a TRP subfamily channel, functions as a pore-forming subunit of a mechano-transduction channel in ciliated dopaminergic neurons CEP and PDE. Importantly, the short latency and rapid activation kinetics of TRP-4 currents are consistent with the view that this type of channels is gated by mechanical forces. This study raised the solidest evidence to support the notion that TRP channel can play a direct role in mechano-transduction. We also found epithelial Na^+ channel (ENaC) regulates harsh (painful) touch sensation in PVD neurons. Currently we are focusing on a mechano-receptor neuron OLQ. We found there are two distinct mechano-receptor channels present on a single OLQ neuron with different thresholds and kinetics. We are checking if other channels, such as TRPV, PIEZO, are severed as mechano-transduction channel in OLQ neuron. Thus *C.elegans* offers a valuable genetic model to indentify the molecular mechanisms underlying touch and pain sensation.

ST-027

Long-term imprecision of information coding in the anterior cingulate cortex of mice with chronic pain

Xiang-Yao Li[1,2], Kohai Koga[2],Tao Chen[2], Min Zhuo[1,2*]

[1]Center for Neuron and Disease, Frontier Institute of Science and Technology, Xi'an Jiaotong University, Xi'an 710054, China
[2]Department of Physiology, Faculty of Medicine, University of Toronto, 1 King's College Circle, Toronto, Ontario M5S 1A8, Canada
Correspondence should be addressed to Dr. Min Zhuo, Department of Physiology, University of Toronto, Faculty of Medicine, Medical Science Building, Room #3342, 1 King's College Circle, Toronto, Ontario M5S 1A8, Canada
Phone: 1-416-978-4018. Fax: 1-416-978-4940.
Email: min.zhuo@utoronto.ca

Background: Recent studies suggest that long-term potentiation (LTP) of excitatory synaptic transmission along the sensory pathway contributes to the maintenance of chronic pain. However, how the alterations of synaptic transmission under chronic pain affect information coding still kept unclear.
Methods: Whole-cell patch clamp recording, chronic pain animal model, computation.
Results: We found that CFA injection or nerve injury significantly increased the jitter of APs firing (bigger jitter

means less precision of action potentials) in the ACC. Blocking the synaptic transmission by a cocktail of CNQX, D-AP5 and picrotoxin removed the difference in temporal precision between normal and CFA-injected or nerve injury mice. CFA injection could not increase jitter in AC1 KO mice, bath application of Forskolin increased the Jitter of APs, suggesting that c-AMP signaling pathway contribute to the changed temporal precision of APs.
Conclusion: Our study provides the first evidence that chronic pain decreased the temporal precision of information processing by the enhancement of synaptic transmission.

SL-001

New Antibodies, New discovery— Diagnostic Tools for Neurological Disorder

Ping Lan

Proteintech Group, Inc., 2201 W. Campbell Park Dr. STE12, Chicago, IL 60612, USA, Tel: 1(888)4PTGLAB(1-888-478-4522) (toll free in USA) , Fax: 1 (312) 455-8408
Email: Proteintech@ptglab.com

In the field of neuroscience, many secrets still wait to be uncovered. And antibodies are powerful tools to uncover the secrets. In recent years, establishment of diagnostic method and progress in etiology and pathology for various neurological disorders, are closely related with application of new antibodies. Antibodies generated by whole proteins usually are better as it is the way nature intended. Those antibodies are more powerful for exploring the unknown world.
Proteintech Group makes the majority of antibodies using the whole proteins. Many scientists made great breakthrough in neurodegenerative disease and other fields with our antibodies, which include:
Neurodegenerative Disease: TDP43, FUS, C9ORF72, SMN2, PTN,SESN2 ,TMEM106B;
Neural Markers: GFAP, NEFH, NEFM;
Neuronal growth/Development: LIN28, ATF4,MEF2C;
Neuronal Signaling: Marcks, STIM1, DUSP6.
Proteintech Group,Inc. was established in 2001 in Chicago, U.S.A., with the mission to develop a wide spectrum of antibodies against all human proteins, known as the Human Antibody Project. So far a repertoire of 12,000 antibodies against 12,000 different human proteins has been produced. We strive to provide the research community with superior antibodies and first-class customer service. From antibody production to their arrival at your bench and beyond, we are there every step of the way.

Abstracts – Poster

PL-001

Computational Prediction of Epitope Clusters of P2X7 Receptor

Sen Liu*, Chaoqi Liu

*Corresponding author:Institute of Molecular Biology, Medical Science College, China Three Gorges University, Yichang 443002, China.
E-mail: pkustar@gmail.com

Background: Cell surface purine/pyrimidine nucleotide receptors, (P2 receptors) are membrane receptors that are expressed in nearly all cell types. The P2X7 receptor is selectively expressed in cell types in CNS (microglia and astrocytes), and in inflammation and immune system, including mast cells, monocytes, and lymphocytes. Therefore, P2X7 receptors are promising drug targets in relating diseases. We hope to find the specific epitopes for developing P2X7 receptor antibodies.
Methods: Firstly, the extracellular sequence of the human P2X7 receptor was used to predict the antigenic peptides using the "antigenic" program (EMBOSS). Secondly, the identified antigenic peptides were submitted to the NCBI blastp server, to see if the peptides are unique for the human P2X7 receptor. Unique peptides were chosen according to the returned E values. After that, a monomer 3D structural model was constructed for the extracellular domain in Modeller, using the homologous structure of the zebrafish P2X4 receptor (PDB ID: 3H9V), to see to what extent these unique peptides are exposed. Also, a trimmer structure model was constructed to see the unique peptides are still accessible.
Results: First, to find the continuous regions in the extracellular domain of the human P2X7 receptor, the antigenic prediction protocol in EMBOSS package was used to predict the antigenicity of different regions of the receptor from the primary sequence. The protein sequence used was the extra-cellular domain (residues 47-334) of the human P2X7 receptor. Overall, 15 peptides were found as promising antigenic peptides with antigenic scores above 1.0. Second, we set out to determine is these 15 peptides are specific enough for the P2X7 receptor. So the NCBI blastp was used for homology scanning of the 15 peptides against the human non-redundant protein sequence database. Of these 15 peptides, 7 peptides were found to be unique for the human P2X7 receptor. An peptide was determined to be unique if there were no homologous sequences found with E values higher than 0.01 when the E value of the P2X7 receptor is lower than 0.01. Next, the 7 unique antigenic peptides were

mapped onto the 3D model structure of the human P2X7 receptor (the extra-cellular domain), to see if they are well exposed so that they accessible by antibodies. From the monomer 3D structure, 6 of the 7 unique peptides were found to be highly exposed, and the other one is totally buried. Also, 3 peptides were found to have good secondary structures (α-helix or β-sheet). Because it's found that P2X receptors are in trimmers when active, so a trimmer model was also constructed from the monomer model. In the trimmer model, one peptide was found to be buried, and the other 5 peptides are still accessible.

Conclusion: The human P2X7 receptor is a promising drug target in many diseases, and a highly specific antibody against the receptor will be very useful for both antagonizing the receptor and identifying its expression level. Here, we identified a unique non-continuous epitope cluster for further developing antibodies against the extracellular domain of the human P2X7 receptor.

Keywords: P2 receptor; Conformational epitope; Epitope prediction; P2X7 antibody

Acknowledgements: This work was jointly supported by the National Natural Science Foundation of China (No. 21103098), the Key Discipline Construction Foundation of China Three Gorges University (No. 2011071001) and the Research Team Funding of Hubei Province (T201203).

PL-002

Ischemia/Reperfusion Induces Hyperphosphorylation of Tau in Rats Hippocampus via ER Stress

Liu Zan-Chao*,Zhao Zeng-Yi ,Li Rong,Yu Ji-Ning

*Corresponding author:The Shijiazhuang Second Hospital of Hebei Province, Shijiazhuang 050051, China.
Email: liuzanchao2007@yahoo.cn

Background: Alzheimer's Disease (AD) is the most common neurodegenerative disease, which accounts for 60% of adult dementia. Cognitive impairment and the degraded learning and memory ability are the main clinical symptoms of AD patients. AD is mainly characterized by the formation of numerous intracellular neurofibrillary tangles (NFTs) and extracellular senile plaques (SPs) in the brain, which of neurofibrillary tangles (NFTs) is mainly formed by hyperphosphorylated tau protein. Tau protein is a microtubule-associated protein, and when hyperphosphorylated it loses its nomal characteristics and functions in tubulin assembling and axonal transport, and so on. The amount of NFTs formed by hyperphosphorylated tau is closely positive correlated with the clinical dementia degree of AD patients. Phosphorylation of tau is regulated by protein kinase and phosphatase, in which glycogen synthase kinase-3β (GSK-3β) and protein phosphatase 2A (PP2A) are the most important protein kinase and phosphatase involved in AD-like hyperphosphorylation of tau.

Brain Ischemia/reperfusion is a frequent important pathophysiological process of brain injury. Some scholars have proposed "ischemia / reperfusion" hypothesis of AD and regard the reischemia/reperfusion as an important pathophysiological pathogenesis in the sporadic AD. However, the molecular mechanism of ischemia/reperfusion-induced AD remains unclear. Ischemia/reperfusion can cause cell stress response, such as endoplasmic reticulum stress (ER Stress). GRP78/Bip as an inherent molecular chaperone in the endoplasmic reticulum is the marker of ER stress. The increased ER stress and Bip expression were found in the AD brain. It is necessary to investigate that whether ischemia or ischemia/reperfusion can affect tau phosphorylation via the ER stress. ER stress can activate P38 and JNK, which are both important stress-induced kinase.

Methods: In this study to investigate the relationship between ischemia/reperfusion and the AD-like tau hyperphosphorylation, the SD rats were used to make the animal models of cerebral ischemia 20min and ischemia/reperfusion (1d, 3d, 5d) by bilateral carotid artery occlusion. The phosphorylation levels of tau protein, the expressions and activities of GSK-3β, PP2A catalytic subunit (PP2Ac), P38 and JNK were observed.

Results: The results showed that reperfusion after ischemia 20min induced significantly increased tau phosphorylation in hippocampus at the Ser396, Ser404, Ser198/199/202 sites and increased Bip expression after ischemia 20min and reperfusion (1d, 3d, 5d). The expressions of P38, JNK, GSK-3β, PP2Ac had no significant change after ischemia and ischemia/reperfusion. The increased levels of phosphorylated P38 (activated form) after ischemia and reperfusion, increased phosphorylation levels of GSK-3β-Tyr216 after ischemia and reperfusion and decrased phosphorylation levels at Ser9 after reperfused 3d and 5d, and increased phosphorylation levels at Tyr307 of PP2Ac after reperfusion were observed. JNK phosphorylation levels have no obvious alteration after ischemia and reperfusion. To furtherly clarify the key role of ER stress in the hyperphosphorylation of tau after ischemia/reperfusion, we used the inhibitor of ER stress, PBA, to treat the ischemia/reperfusion rat models and found that PBA could significantly reduce the expression of Bip and the phosphorylation of tau at Ser396, Ser198/199/202 phosphorylation sites.

Conclusion: These results confirmed that ischemia/reperfusion could cause ER stress, which induce hyperphosphorylation of tau via activating P38 and GSK-3β and inhibiting PP2A.

Keywords: ischemia/reperfusion, endoplasmic reticulum stress,tau,Alzheimer's Disease, PBA

PL-003

Chronic cerebral hypoperfusion downregulate expression of ADAR2 in hippocampus of rat

Zhao-hui Yao *,Gang-yan Zhu

*Corresponding author:Department of Gerontology, Renming Hospital, Wuhan University,Ziyang Road 99#, Wuhan, China, 430060.
Email: yaozhaohui2004@126.com

Background: As the old increasing, the cognition dysfunction disease is prevalent. Currently, it is well known that the cerebral blood flow decrease for the old because of poor cardiovascular function[1]. Moreover, the recent research show the cerebral hypoperfusion is common in Alzheimer's disease and mild cognition impairment[2]. So it is supposed that chronic cerebral hypoperfusion(CCH) maybe companies the pre-symptoms in cognition-related disease. ADAR2 is an editing enzyme of RNA of GluR2, which downregulate after acute cerebral ischemia to lead to calsium overload and excitable neurotoxic[3]. It is unknown that ADAR2 expression is affected by CCH.
Method: To explore this, we use permanent bilateral common carotid arteryocclusion(2VO) to reproduce the CCH animal model and study the learning and memory abilities by Morris water maze and expression of ADAR2 using Western blot, PCR, and immunohistochemistry.
Result: We found that CCH can impair the learning and memory abilities. Meanwhile, CCH downregulate ARAR2 and adar2 mRNA expression in hippocampus of rats, but not cortex. Moreover, we found activity of CREB, the upstream regulate element of ADAR2, also downregulate.
Conclusion: Therefore, we concluded that CCH can reduce the expression of ADAR2. The calcium overload induced by over-activated GluR2 maybe play critical in cognition impairment after CCH.
Keyword: chronic cerebral hypoperfusion; ADAR2; CREB

Acknowledgments: This work was supported by Grant Number 2011CDB524 from the Natural Science Foundation of Hubei Province.
[1]de la Torre JC. Cerebromicrovascular pathology in Alzheimer's disease compared to normal aging. Gerontology 1997; 43(1-2): 26-43.
[2]de la Torre JC. Vascular basis of Alzheimer's pathogenesis. Annals of the New York Academy of Sciences 2002; 977: 196-215.
[3]Peng PL, Zhong X, Tu W, et al.ADAR2-dependent RNA editing of AMPA receptor subunit GluR2 determines vulnerability of neurons in forebrain ischemia. Neuron 2006; 49(5): 719-33.

PL-004

Alpha-synuclein oligomerization occurs in manganese treated organotypic brain slice cultures

Bin Xu*, Sheng Wen Wu and Shen Mao Wang

*Corresponding author: Department of Environmental Health, School of Public Health, China Medical University, Shenyang, China, 110001.
Email: xubin@mail.cmu.edu.cn

Recent studies have shown that manganese (Mn), as one of the risk factors of Parkinson's disease (PD), can cause α-synuclein overexpression, but the α-synuclein oligomerization and its cytotoxicity are not mentioned. Understanding the exact molecular mechanisms of Mn neurotoxicity may play a critical role linking environmental neurotoxins to the pathogenesis of PD. In our study, brains of Wistar rats at postnatal days 3–4 were sliced in 300 μm thick sections on tissue slicer. Normally, 4–6 slices with intact basal ganglia cytoarchitecture were collected, transferred to cell culture inserts (pore size 0.4 μm), placed in 6-well culture dishes and fed with 1 mL culture medium consisting of 50% minimum essential medium, 24% horse serum and 25% HBSS, 1% penicillin-streptomycin. Cultures were maintained at 37 °C under room air+5% CO2. Cultured slices at 13-15 days in vitro were exposed to Mn (0, 25, 100, 400 μM). After 24 hours of treatment with Mn, brain slices were use for apoptosis assays, quantitative Real-Time PCR and western blotting analysis. In order to measure membrane-bound form and free cytosolic form of a-synuclein oligomers, membrane / cytosolic proteins were respectively extracted. Equal amounts of protein of each fraction were loaded onto 4-20% non-denaturing polyacrylamide gradient gel electrophoresis without boiling. Our results demonstrated that cell apoptosis rate was 2.59% in the control slices. In 25-400 μM Mn-treated slices, cell apoptosis rate respectively increased to 11.65%, 19.46% and 30.11%. At the same time, there were significant increase in expressions of a-synuclein mRNA and protein in a dose-dependent manner. With the increasing of Mn-treated levels, oligomers were significantly increased, especially on membrane-bound form. It indicated that α-synuclein oligomers were more likely to combination cell membranes and resulting in membrane damage. Therefore, our results demonstrated that Mn not only caused α-synuclein overexpression but also leaded to α-synuclein oligomerization, which would further result in nerve cell damage.

Acknowledgments: This work was supported by the National Natural Science Foundation of China (81102098).

References:

Guilarte TR (2010) Manganese and Parkinson's disease: a critical review and new findings. Environ Health Perspect 118: 1071-1080

Ohnishi M, Katsuki H, Unemura K, Izumi Y, Kume T, Takada-Takatori Y, Akaike A (2010) Heme oxygenase-1 contributes to pathology associated with thrombin-induced striatal and cortical injury in organotypic slice culture. Brain Res 1347: 170-178

Cai T, Yao T, Zheng G, Chen Y, Du K, Cao Y, Shen X, Chen J, Luo W (2010) Manganese induces the overexpression of alpha-synuclein in PC12 cells via ERK activation. Brain Res 1359: 201-207

Lee HJ, Choi C, Lee SJ (2002) Membrane-bound alpha-synuclein has a high aggregation propensity and the ability to seed the aggregation of the cytosolic form. J Biol Chem 277: 671-678

PL-005

Left-Right Asymmetrical Expression of KLF4 in the Hippocampal Formation of Normal and Depression Mice

Shuai Wang[1], Shuiping Han[2], Hui Qiao[3], Chang Xu[3], Chanyuan Wang[1], Shucheng An[3], Shaoli Cheng[4], and Lijun Zhao*[1]

*Corresponding author:
[1]Key Laboratory of Medicinal Plant Resources and Natural Pharmaceutical Chemistry, College of Life Sciences, Shaanxi Normal University, Xi'an, China;
[2]Department of Pathology, School of Medicine, Xi'an Jiaotong University, Xi'an, China;
[3]Department of Physiology, College of Life Sciences, Shaanxi Normal University, Xi'an, China;
[4]Morphological Experiment Centre, School of Medicine, Xi'an Jiaotong University, Xi'an, China.
Shuai Wang and Shuiping Han contributed equally to this work.
College of Life Sciences, Shaanxi Normal University,Xi'an, China.,710062

Kruppel-like factor-4 (KLF4) is a transcriptional repressor of axon growth of neurons, its expression can be triggered by glutamatergic stimulation and sensitize neurons to N-methyl-D-aspartate (NMDA)-induced caspase-3 activity. However, KLF4 expression in hippocampal formation and its role in depressive disorders remain largely unknown. In this study, we aimed to use immunehistochemistry to analyze KLF4 expression in the hippocampal formation in the development of depression. Firstly, we found that KLF4 is asymmetrically expressed in healthy mouse hippocampal formation with a dominant expression in the left side and significant low expression in the right. Then, we studied its expression in the hippocampal formation of chronic unpredictable mild stress (CUMS) mouse model of depression. We found KLF4 expression in the left hippocampal formation is not significantly altered, whereas is elevated in the right side. We also observed newly adult-born neurons in both left and right dentate gyrus (DG) and right CA2 sector of CUMS mice, these neurons were lack of KLF4 expression and showed GFAP negative but Nissl positive staining. In conclusion, our results suggest that KLF4 is asymmetrically expressed in mouse hippocampal formation and depressive stress can stimulate KLF4 expression in the right hippocampal formation and adult-born neurogenesis in DG and the right CA2 sector.

Keywords: CUMS; neurogenesis; Dentate Gyrus; CA2; mouse

PL-006

Neuroprotective effects of saponin from Panacis majoris rhizome against cerebral ischemia/reperfusion injury via scavenging overgeneration and accumulation of ROS and inducing nuclear translocation of Nrf2

Haibo He[1], Nianyu Huang[1], Mengqiong Shi[2]*, Wenyan Yang[2], Qiaoyin Zhang[1], Yanqiang Xiong[2]

[1]Hubei Key Laboratory of Natural Products Research and Development, China Three Gorges University;
[2]Medical Science College, China Three Gorges University, Yichang, China, 443002.
*Corresponding author
E-mail: shmq0212@126.com

Increasing evidences have showed that oxidative stress causes the overgeneration and accumulation of reactive oxygen species (ROS) are central to cerebral ischemia / reperfusion (I/R) injury, while nuclear factor erythroid 2-related factor 2 (Nrf2) which activates a defense system to combat oxidative stress is considered to be a multi-organ protector, and widely viewed as a mediator of neuroprotection. Saponin from Panacis majoris rhizome (SPM) has been reported to exhibit neuroprotective properties. However, its precise mechanism, particularly its antioxidation mechanism, remains elusive. In the present study, we investigated the neuroprotective effects of SPM on middle cerebral artery occlusion (MCAO)-induced cerebral I/R in mice and in vitro ischemic model of oxygen-

glucose deprivation followed by reperfusion (OGD/R) damage in primary mouse cortical neurons, based on these results, investigate the antioxidative mechanisms involved. In vivo, mice were pretreated with SPM (50, 100 and 200 mg/kg) or vehicle orally once daily for 7 consecutive days before MCAO was performed, and the neuroprotective effects of SPM were analyzed within 24h after I/R. SPM at doses of 50,100 and 200mg/kg could significantly reduced cerebral infarct area and ameliorated neurological functional deficits; At the same time, SPM significantly increased superoxide dismutase (SOD), catalase (CAT) and glutathione peroxidase (GPx) activities, decreased malondialdehyde (MDA) content in I/R brain tissues, enhancing endogenous antioxidant activity, and with the dose of SPM increasing, the aforesaid improvement became more and more strong. In vitro, pretreatment of SPM (25, 50 and 100 μg/mL) might remarkably protect primary mouse cortical neurons against lethal stimuli, increase cell viability, decrease the apoptosis rate, improve cell morphous, reduce intracellular ROS generation, improve SOD, GPx, CAT activities, decrease lactic acid, lactate dehydrogenase and MDA levels in OGD/R-induced primary mouse cortical neurons; Real-time PCR and Western blotting results showed SPM could upregulate SOD1-SOD3, CAT and GPx mRNA expressions and increase Nrf2 protein expressions in the nucleus, and there was dose-effect relationship among the three SPM pretreated groups. Our results demonstrate that SPM has a neuroprotective effect in cerebral I/R injury, which may involve scavenge overgeneration and accumulation of ROS and induce nuclear translocation of Nrf2. Therefore, the present study supports the notion that SPM may be a promising neuroprotective agent for the treatment of cerebral ischemia disease.

Keywords: Cerebral ischemia/reperfusion; Cortical neurons; Oxidative stress; Reactive oxygen species; Saponin from Panacis majoris rhizoma

Reference:

Loh KP, Huang SH, De Silva R, et al. Oxidative stress: apoptosis in neuronal injury[J]. Curr Alzheimer Res, 2006, 3 (4):327-337.

Li M, Zhang XJ, Cui LL, et al. The neuroprotection of oxymatrine in cerebral ischemia/reperfusion is related to nuclear factor erythroid 2-related factor 2 (Nrf2)-mediated antioxidant response: role of Nrf2 and hemeoxygenase-1 expression [J]. Biol. Pharm. Bull, 2011, 34(5) 595-601.

Qian Y, Guan T, Huang M, et al. Neuroprotection by the soy isoflavone, genistein, via inhibition of mitochondria-dependent apoptosis pathways and reactive oxygen induced-NF-κB activation in a cerebral ischemia mouse model [J]. Neurochem Int, 2012, 60 (8):759-767.

Zhao B, Chen Y, Sun X, et al. Phenolic alkaloids from Menispermum dauricum rhizome protect against brain ischemia injury via regulation of GLT-1, EAAC1 and ROS generation[J]. Molecules, 2012, 17(3):2725-2737.

Röhnert P, Schröder UH, Ziabreva I, et al. Insufficient endogenous redox buffer capacity may underlie neuronal vulnerability to cerebral ischemia and reperfusion [J]. J Neurosci Res, 2012, 90 (1):193-202.

PL-007

SIRT1 activation mitigates high glucose induced tau hyperphosphorylation and cognitive impairment

Lai-Ling Du*, Jia-Zhao Xie#, Xiang-Shu Cheng, Xia Jiang, Zhi-Wei Ma, Xin-Wen Zhou*

Department of Pathophysiology, Key Laboratory of Neurological Diseases of Education Committee of China, Tongji Medical College, Huazhong University of Science and Technology, Wuhan 430030, China. *Corresponding author. Email: dulailing@163.com; zhouxinwen@mail.hust.edu.cn

There is a high risk of onset Alzheimer's disease (AD) or AD like tau pathology in patients with diabetes mellitus or high glucose animal model. The reduction of protein level and activity of SIRT1 parallels with the accumulation of hyperphosphorylated tau in both of status. However, whether or how SIRT1 regulates tau phosphorylation and influences the progress of AD in high glucose condition is still elusive. Here we treated 3-months old rats with streptozotocin(STZ) via intracerebroventricular injection(3mg/kg, twice, with an interval of 48 h) to establish high glucose of brain in rat, meanwhile, after STZ treatment, rats were treated with resveratrol (SIRT1 specific activator) or vehicle via intraperitoneal injection for 8 weeks, Our data showed: ①The levels of phosphorylated tau and p-ERK1/2 were increased significantly, SIRT1's activity was blocked and cognition was impaired by western blot, the assay kit, or Morris water maze in STZ-treatment group when compared with control; ②The resvertrol, a specific activator of SIRT1, could attenuate STZ induced-tau hyperphosphorylation and cognitive impairment; ③STRT1and ERK1/2 interacted with each other, and ERK1/2 could be modified by acetylation. Taken together, our results demonstrate that SIRT1 can protect against tau hyperphosphorylation and cognitive impairment induced by high glucose via the deacetylation of ERK1/2.

Keywords: High glucose;tau;SIRT1;deacetylation

PL-008

Neurohypophyseal Neuregulin-1 (Nrg1) is a potential prolactin (PRL) modulating neuropeptide derived from the hypothalamus

Weijiang Zhao[1]*, Songguang Ren[2]

*Corresponding author:
[1]Center for Neuroscience, Shantou University Medical College, Shantou, Guangdong Province 515041, China.
[2]Department of Medicine, Cedars-Sinai Medical Center, Los Angeles, California, USA.
Email: neuromancn@yahoo.com.cn

Background: The binding of Neuregulin-1 (Nrg1) to the epidermal growth factor family of receptor tyrosine kinases (ErbB) regulates a broad spectrum of biological processes [1, 2, 3].We here investigated the expression and localization of Nrg1 in the hypothalamus-hypophyseal structures and its potential in modulating prolactin (PRL) secretion.
Method: Female Wistar-Furth rats were used. RT-PCR was employed to identify Nrg1 isoforms in the hypothalamus. Double immunofluorescence was used to examine the Nrg1 localization and Nrg1 expressing cells in the hypothalamus, as well as in the posterior and the intermediate pituitary. Western blotting was used to detect hypothalamic Nrg1 expression at the protein level. In addition, rat somatolactotroph prolactinoma GH3 cells were seeded overnight and treated with recombinant Nrg1α(rNrg1α) dosed from 0-10 nM for 4 time courses:10 minutes (min), 6 hours (h), 24 h and 48 h.Western blotting was utilized to determine the levels of phosphorylated ErbB-3 receptor.ErbB-3 receptor phosphorylation level was indexed by the ratio of phosho-ErbB-3 to D-glyceraldehyde-3-phosphate dehydrogenase (GAPDH).
Result: In this study, we demonstrate that type I, IIand III Nrg1 isoforms are expressed in the hypothalamus. In the periventricular neucleus (PEVN), Nrg1 was partially localized in the somatostatin positive cells, and co-localized with vasopressin in the supraoptic nucleus and the structures surrounding the vasculature in the pituitary stalk-median eminence region. Nrg1 was extensively distributed in the posterior pituitary, including in the neuronal fibers surrounding the vasculature and Herring bodies. In contrast, Nrg1 was not detected in the intermediate lobe. Western blotting revealed bands with the molecular weight at 45, 40, and 30 kDa in the hypothalamus, while only a 30 kDa band was detected in the posterior pituitary. rNrg1α induced a rapid and sustained ErbB-3 receptor phosphorylation in GH3 cells. Maximal phosphorylation of ErbB-3 receptor was achieved with 5 nM of rNrg1α and correlated with a significant increase in PRL but not growth hormone (GH) secretion into the conditioned culture medium at 24 h. Conclusion:Collectively, we conclude that hypothalamus-derived Nrg1 may function as a neurohypophyseal neuropeptide and exert multiple functions, including regulating PRL secretion in a paracrine pattern. Thus, our observation can partially underly the mechanisms for hypoprolactinemic and hyperprolactinemic pituitary dysfunctions.

Key words: Neuregulin-1 (Nrg1);hypothalamus;pituitary; prolactin (PRL)
References:
1.Zhao W, Shen Y, Ren S. Endogenous expression of Neuregulin-1 (Nrg1) as a potential modulator of prolactin (PRL) secretion in GH3 cells. Cell Tissue Res, 2011, 344:313–320.
2.Vlotides G, Siegel E, Donangelo I, Gutman S, Ren SG, Melmed S. Rat prolactinoma cell growth regulation by epidermal growth factor receptor ligands. Cancer Res, 2008, 68:6377–6386.
3.Vlotides G, Cooper O, Chen YH, Ren SG, Greenman Y, Melmed S. Neuregulin regulates prolactinoma gene expression. Cancer Res, 2009, 69:4209–4216.

Acknowledgements: We thank Dr. Kolja Wawrowsky from the medical department of Cedars-Sinai Medical Center for his assistance in immunofluorescence imaging. The work was partially supported by the National Natural Science Foundation of China (Project 81171138).
Correspondence to Weijiang Zhao: Center for Neuroscience, Shantou University Medical College, Shantou, Guangdong Province 515041, China
Phone number: 86-13794125386; Fax: 86-75488900236;
E-mail: neuromancn@yahoo.com.cn.

PL-009

Anxiolytic effects of estrogen receptor GPR30 activation by a selective agonist in female mice

Shui-bing Liu, Ming-gao Zhao*

*Corresponding author:NO.17 Changle West Road, Xi'an, Shaanxi.
Email: minggao@fmmu.edu.cn

Estrogen G-protein-coupled receptor 30 is reported to be a novel estrogen receptor uniquely localized to the membrane and endoplasmic reticulum. This receptor is widely distributed and has numerous physiologic functions in the central nervous system. Our study has found that GPR30 is highly expressed in GABAergic neurons in basal amygdala (BA) and lateral amygdala (LA). In addition, a significant increase of GPR30 expression in amygdala of mice with ovariohysterectomy (OVX) accompanied anxiety-like behavior induced by restraint stress. Patch-clamp recordings revealed that activation of GPR30 significantly increased GABAergic synaptic transmission in LA. LA local infusion of GPR30 agonist reversed stress-induced anxiety-like behaviors. Furthermore, western-blot analysis demonstrated that GPR30 agonist reversed the up-regulation of AMPA receptor GluR1 subunit and NR2A-containing NMDARs in amygdala of mice after

stress. These data demonstrate, for the first time, that estrogen releases anxiety, at least partly, through the activation of GPR30 in the LA.
Keywords: Anxiety; Estrogen; GPR30; Amygdala

Acknowledgments: This work was supported by the National Natural Science Foundation of China (31070923)

PL-010

The neuroprotective effect of ipriflavone against amyloid beta induced toxicity on human neuroblastoma SH-SY5Y cell

Zhimin Xiao[1, 3], Can Huang[1], Li Sun[1], Wei Hao[1], Jun-Jian Zhang[2] and Jian Huang[1, 4]*

[1]College of Life Sciences, Wuhan University, Wuhan, Hubei 430072, China
[2]Department of Neurology, Zhongnan Hospital, Wuhan University, Wuhan 430071, China
[3]Curent Address: China Initiative, Harvard University School of Public Health, Boston, MA, 02115, USA
[4]Correspondence to Dr. Jian Huang,
E-mail: jianhuang@whu.edu.cn

Alzheimer's disease (AD) is one of the most common forms of dementia among the aged. Excessive amyloid beta (Aβ), as a result of either increased production or decreased degradation, is proposed to play a crucial role in neuron death and the pathology of AD. Estrogenic compounds are proposed to relieve Aβ induced toxicity. Efforts have focused on structural modification of estrogenic compounds to engineer successful candidate therapeutics, but it's a long way for them to be translated to clinic. We identified the estrogen structure similar compound - ipriflavone (IP), an over-the-counter product in the United States used to treat osteoporosis, efficiently antagonized Aβ induced toxicity, which might be translated to clinic in the near future for the treatment of AD. In our study, we demonstrated that IP protects against Aβ-induced toxicity in the human neuroblastoma cell line SH-SY5Y at a very low concentration. At 0.1nM and 10nM, IP enhanced SH-SY5Y cell survival rate from 50% which caused by 30μM Aβ25-35 solo treatment to 65.7±0.6% and 71.5±2.0% respectively, while no significant cell proliferation was observed when IP was applied alone. IP also efficiently reduced Aβ25-35 induced ROS levels, which is 185% of untreated control, to 145% and 125% of control at 0.1nM and 10nM respectively. We also found that caspase-3 inhibition, PI3K and MAPK activation are involved in the neuroprotective effect of IP. IP at 10nM reduced the Aβ-induced elevation of caspase-3 activity from 1.8 fold to 1.2 fold. The addition of LY294002, a PI3K inhibitor, or PD98059, a MAPK inhibitor completely neutralized the neuroproetcive effect of 10nM IP treatment. As a compound being previously characterized, IP has great potential for its expedited clinical translation for AD therapeutics.
Keywords: Ipriflavone, neuroprotective effect, Aβ, Alz heimer's disease

Acknowledgments: This work was supported by the National Natural Science Foundation of China (30670647 and 30970914)

PL-011

Neuroglobin attenuates Alzheimer-like Tau hyperphosphorylation by inhibiting PKA signaling

Liming Chen[1]* and Fanli Kong[2]

[1]Department of Neurology of the First People's Hospital of Jingzhou (The First Affiliated Hospital of Yangtze University), Jingzhou 434000, People's Republic of China.
[2]Department of Pathophysiology, Key Laboratory of Neurological Diseases of Education Committee of China, Tongji Medical College, Huazhong University of Science and Technology, Wuhan, China. *Corresponding author.
E-mail: 51651286@qq.com

Alzheimer's disease (AD) is a neurodegenerative disease that depends on age. Neuroglobin (Ngb) is a new member of hemoglobin family, reported by T. Burmester in 2000.A close relation between gene of Ngb and AD was released by research on the analysis of single nucleotide polymorphism (SNP). We focus our job on the mechanism of hyperphosphorylation tau during the development of AD. It's been reported that there was a negative correlation between the level of hyperphosphorylation tau and the expression of Ngb in transgene mice of AD model by our lab reported in the beginning of 2011.PKA is an important intracellular kinase that contributes to the hyperphosphorylation of tau in AD patient. There is no any knowledge about the interaction between Ngb and PKA and its influence on tau.In this study,treat HEK293 cell, which is stably expressing tau, with proper concentration of Forskolin, and to establish a pathological model of hyperphosphorylation tau, transfect with PKA plasmid. After transfect with Ngb to this model, examine whether Ngb could function on hyperphosphorylation of tau, induced by the upregulation of PKA by immunoblotting, fluorescence imaging, and assay kit for detecting concentration of cAMP.Our data indicate that Ngb could make effect on the activity of PKA via reducing

the concentration of cAMP and interacting directly, thus influence on tau. Explore a new field on how Ngb function on intracellular pathway of kinase.
Keywords: Alzheimer's disease; neuroglobin; tau; phosphorylation; protein kinase A; cyclin AMP

PL-012

Pre-moxibustion improved Aβ induced spatial learning and memory deficit in rats

Yan-Jun Du*, Guo-Jie Sun, Li-Hong Kong, Qing Tian , Jun Ma, Yan-chun Wang

*Corresponding author: College of Acupuncture and Moxibustion, Hubei University of Chinese Medicine, Wuhan, China, 430061.
E-mail: duyanjuncn@yahoo.com.cn

Background: Alzheimer's disease (AD), the most common type of dementia in the aged population, is characterized by the formation of neurofibrillary tangles and senile plaques. The later is composed primarily of β-amyloid 40 (Aβ40) and 42(Aβ42). Clinically moxibustion, a natural treatment of Traditional Chinese Medicine, has been reported effective to prevent the developing of AD in China, but the mechanism is not fully understood. Therefore, we performed moxibustion on two acupoints, Baihui (DU20) and Shenshu (BL23), in AD model rats and studied the effect of moxibustion.
Method: Aβ42 was injected into the hippocampus of 12-month old SD rats. In moxibustion group the rats were utilized 48-days daily moxibustion on Baihui (DU20) and Shenshu (BL23) before operation and the moxibustion continued 14 days after operation by a moxa cone (diameter: 8 mm). After moxibustion the rats were put into Morris water maze and their learning and memory abilities were tested.
Result: Aβ injected rats showed obvious damage of learning and memory. Under the electron microscope, endoplasmic reticulum, mitochondria, microtubules and microfilament were observed. In Aβ injected rats, cytoplasm was obvious loose and bright and fewer mitochondria and ribosomes were observed. The nuclei were swollen or pyknic and the euchromatins decreased, while the heterochromatins increased and became dense to granules. By immunohistochemistry, we found the phosphorylation level of hippocampal tau was much higher in the model rats. Moxibustion of Baihui (DU20) and Shenshu (BL23) significantly revised the spatial learning and memory deficit of Aβ injected rats and the pathologic changes induced by Aβ injection.
Conclusion: All these data suggested that moxibustion is beneficial to prevent the toxicity of Aβ.
Keywords: Alzheimer's disease; moxibustion; pre-moxibustion

Acknowledgments: This work was supported by the National Natural Science Foundation of China(81173323, 30901925)

PL-013

An L-type calcium channel agonist, Bay K8644, extends the window of intervention against ischemic neuronal injury

Honghai Hua, Fengqin Hou, Shuji Li, Huacheng Yan, Xiong Cao, Pu Wang, Yingying Fang, Xinhong Zhu*, Tianming Gao*

*Corresponding author:Department of Neurobiology, School of Basic Medical Sciences; School of Traditional Chinese Medicine; Southern Medical University, Guangzhou 510515, China.
E-mail: zhuxh@fimmu.com

Our previous data indicate that the inhibition of L-type calcium channels (LTCCs) might be the cause of post-ischemic neuronal injury and that the activation of LTCCs can give rise to neuroprotection. In the present study, we aimed to profile the intervention window of Bay K8644, an LTCC agonist. Four-vessel occlusion and oxygen-glucose deprivation models were employed to mimic ischemia/reperfusion damage in vivo and in vitro. Neuronal injury was analyzed by Nissl and Fluoro-Jade B staining in vivo and Hoechst 33342 and propidium iodide staining in vitro. Behaviors were tested using the Morris water maze. The phosphorylation of P38, JNK and ERK was detected by Western blotting. Results showed that Bay K8644 administered as late as 24 hours after reperfusion prevented CA1 neurons from death and ameliorated the deficiencies in spatial learning performance induced by global ischemia. On OGD, Bay K8644 delivered from 1 to 12 hours after reoxygenation reduced neuronal death. The decrease in p-ERK1/2 that was observed at 1 hour after OGD could be reversed by Bay K8644 application. Furthermore, the effect of Bay K8644 was blocked by U0126 and MEKKD transfection. Our data demonstrated that Bay K8644 extends the window of intervention against ischemic neuronal injury in both in vivoand in vitromodels and ERK1/2 might mediate the neuroprotection by Bay K8644, suggesting that opening LTCCs might have a great potential to provide a novel avenue for developing neuroprotectants.

Keywords: Neuroprotection; L-type calcium channels; global ischemia; ERK1/2

PL-014

Effect of Cell Cycle Inhibitor Olomoucine on Astroglial Proliferation and Scar Formation After Focal Cerebral Infarction in Rats

Zhang Gui-bin[1]*, Tian Dai-shi[2], Xu Yun-lan[2], Xie Min-jie[2], Wang Wei[2]

[1]Department of Neurology, Xiangyang Hospital Affilitated to Hubei University of Medicine, Xiangyang 441000, Hubei,China;
[2]Department of Neurology, Tongji Hospital of Tongji Medical College, Huazhong, University of Science and Technology, Wuhan 430030, Hubei,China.
*Corresponding author.
Email: zgb1969@126.com

Background: Astrocytes become reactive following many types of CNS injuries. Excessive astrogliosis is detrimental and contributes to neuronal damage. We sought to determine whether inhibition of cell cycle could decrease the proliferation of astroglial cells and therefore reduce excessive gliosis and glial scar formation after focal ischemia.
Methods: Cerebral infarction model was induced by photothrombosis method. Rats were examined using MRI, and lesion volumes were estimated on day 3 post-infarction. The expression of glial fibrillary acidic protein (GFAP) and proliferating cell nuclear antigen (PCNA) was observed by immunofluorescence staining. Protein levels for GFAP, PCNA, CyclinA and CyclinB1 were determined by Western blot analysis from the ischemic and sham animals sacrificed at 3,7,30 days after operation.
Results: Cell cycle inhibitor olomoucine significantly suppressed GFAP and PCNA expression and reduced lesion volume after cerebral ischemia. In parallel studies, we found dense astroglial scar in boundary zone of vehicle-treated rats at 7 and 30 days.Olomoucine can markedly attenuate astroglial scar formation. Western blot analysis showed increased protein levels of GFAP, PCNA, CyclinA and CyclinB1 after ischemia, which was reduced by olomoucine treatment.
Conclusion: Our results suggested that astroglial activation, proliferation and subsequently astroglial scar formation could be partially inhibited by regulation of cell cycle.Cell cycle modulation thereby provides a potential promising strategy to treat cerebral ischemia.
Keywords: Proliferation;Astrocytic scar;Cell cycle;Cyclins; Cyclin dependent kinase;Olomoucine

PL-015

Saponins from Panax japonicus attenuate D-galactose-induced brain aging via enhancing the Nrf2 antioxidant signaling pathway

Wang ting*, Di guo-jie, Xiong zhang-e, Zhang chang-cheng, Yuan ding

*Corresponding author: Medical College of Three Gorges University, Yichang 443002, PR China.
Email: tingting0301@126.com

Aging is an inevitable process featured by intelligence decline, behavioral disorders and cognitive disability. Increasing evidence indicates that oxidative stress plays a key role in the senescent development.A promising strategy to combat oxidative stress is by means of the induction of endogenous antioxidant genes regulated by the transcription factor Nrf2 (nuclear transcription factor related to NF-E2), which is currently considered the master regulator of redox homeostasis. Panax japonicus, in which the saponins are proved to make up the active major constituents, is a medicinal plant widely used in folk and traditional medicine for its antioxidative activity. But effect of saponins from Panax japonicuson the treatment of brain aging as well as its underlying mechanism is still unknown. In this study, we have investigated the brain protective role of saponins from Panax japonicusand its activation of Nrf2 in D-galactose-induced brain aging in rats. Male SD rats weighing 220 to 250 g were subcutaneously injected with D-galactose (250mg/kg per day) and were treated daily with saponins from Panax japonicusby gavage until sacrificed at 8 weeks later for behavioral,pathological, and mechanism evaluation. We found that administration of saponins from Panax japonicus (1)ameliorated the D-gal induced learning and memory impairment in both open field test and Morris water maze; (2) attenuated morphologic abnormalities of neurons in hippocampus region; (3) inhibited reactive oxygen species (ROS) and lipid peroxides formation as well as enhancing SOD and GSH-Px activities in the serum and brain. (4) promoted the hippocampal Nrf2 nuclear translocation; (5) enhanced the expressions of Nrf2-dependent antioxidant enzyme genes such as HO-1, NQO-1 and SOD1 in hippocampus tissue. These results indicated that saponins from Panax japonicas had a potential protect role of brain aging induced by D-gal and its mechanism, at least in part, via modification of Nrf2 antioxidant pathway.
Keywords: saponins from Panax japonicus; brain aging; Nrf2 signaling

Acknowledgments: This work was supported by the National Natural Science Foundation of China (81100957) and

the Natural Science Foundation of Hubei Province, China (2010CDB10703).

PL-016

Fyn/NMDA signaling involves the regulation of CREB activity by GSK-3β

Xin Yang, Si-Ming Nie, Xiao-Mei Liao, Shao-Hui Wang*

*Corresponding author: College of Life Sciences, Central China Normal University, Wuhan 430079, Hubei, PR China.
Email: wsh2002505@163.com

GSK-3β is a ubiquitously expressed serine/threonine kinase involved in a variety of cellular processes. Activated GSK-3β attributes to the inhibition of the transcriptional factor CREB, and impairs the learning and memory of animals. But the actual mechanism is not clear. In this study, we increased the GSK-3β activity by treating N2a neuroblastoma cell with wortmannin or transfecting with WT-GSK-3β plasmid, then administrated PP2 (an inhibitor of the nonreceptor protein tyrosine kinaseFyn) for 1 h. Finally we detected the activities of GSK-3β, Fyn, PKA, CREB and the tyrosinephosphorylation level of NR2B and the level of pNR2B-PSD95 complex by Western blotting and Immunoprecipitation. Results showed that: (1) In N2a cells, the activity of Fyn decreased to 75% of the control level by treated different concentration of PP2 (2.5 μM, 5 μM, 10 μM). (2) Compared with the control, the activity of GSK-3β increased significantly by 2.5 μM, 5 μM, 10 μM wortmannin or transfecting with wtGSK-3β plasmid and wasn't affected by the treatment of PP2. (3) The overactivity of GSK-3β up-regulated the Fyn activity in N2a cells, and the Fyn activity recovered to normal after the N2a cells treated with 2.5 μM PP2 for 1h. (4) Compared with the control, the activated GSK-3β increased the level of pNR2B and the pNR2B-PSD95 complex, while inhibition of Fyn by PP2, the level of pNR2B and the pNR2B-PSD95 complex decreased dramatically. (5) The increase of GSK-3β activity inhibited the activity of PKA, while 2.5 μM PP2 could reversed this action. (6) The phosphorylation of CREB at Ser133, decreased a half to normal after GSK-3β activation, while 2.5 μM PP2 treatment could recover it. In a conclusion, with the GSK-3β-mediated stimulation of Fyn activity, the overproduced pNR2B, a substrate of Fyn and the pNR2B-PSD95 complex, could decrease PKA activity and then down-regulate the CREB activity. This study implied a new mechanism of the CREB activity regulated by GSK-3β, and offered some new evidences of treating some CNS disorders including Alzheimer's disease and Parkinson's disease.

Keywords: GSK-3β; Fyn; CREB

Acknowledgments: This work was supported by the National Natural Science Foundation of China (No. 30700208 and No.30800329) and CCNU project (No. 091301009 and No. CCNU10A0160).

PL-017

Protective effect of vitamin E on DEHP-induced cytotoxicity in N2a cells

Peng-Yan Zhang, Dong Wang, Shao-Hui Wang, Xiao-Mei Liao*

*Corresponding author:Hubei Key Lab of Genetic Regulation and Integrative Biology, College of Life Sciences, Central China Normal University, Wuhan, China, 430079. Email: liaodebox2003@yahoo.com.cn

Diethylhexyl phthalate (DEHP) is currently the most widely used plasticizer to increase the flexibility of polyvinyl chloride. It has been shown that DEHP can compete with estrogen to bind the estrogen receptors within the human and animal body and lead to dysfunction of estrogen. Abundant evidence indicated DEHP show several toxic changes in many organs including brain, reproductive organs, liver, kidney etc. Recently reports also showed that child's intelligence was negatively related withthe level of DEHP in body. However, the underlying mechanism is still unclear and further research is needed. In order to explore mechanism of cytotoxicity of DEHP,we treated N2a cells with DEHP for 24h, then the protective roles of different content of vitamin E (25,50,100 μM) administrated 1h before DEHP treatment were studied. Oxidative stress status was examined by MDA, SOD and ROS assay kits. Then the level of phosphorylated tau protein and the activities of upstream kinases were detected by Western blot. Finally, we explored the relationship between DEHP and memory-related synaptic proteins. Results showed that: (1)Compared with control group, the level of MDA and ROS increased ($P< 0.05$) and the activity of SOD significantly decreased ($P< 0.05$). Vitamin E could reverse oxidative stress of DEHP on N2a cells in a dose-dependent manner. (2) DEHP increased tau phosphorylation at Thr231 and Ser262 epitopes compared with control and Vitamin E pretreatment could attenuate tau phosphorylation. (3) Compared with the control group, DEHP treatment could up-regulated the level of regulator subunit of PKA and down-regulated the level of catalytic subunit of PKA ($P<0.05$). While, vitamin E pretreatment remarkably decreased the level of regulator subunit of PKA and increased the level of catalytic subunit of PKA ($P<0.05$). (4) DEHP could induce some memory-related proteins, such as PSD95, synaptophysin and p-CREB decreased significantly ($P<0.05$),

and Vitamin E pretreatment could reverse the effect of DEHP. These results suggested that DEHP could increase tau phosphorylation by its upstream kinase activation induced by oxidative stress, and then further attenuated the synthesis of memory related proteins, while Vitamin E pretreatment had a preventive role.Our study provides a scientific basis which improving quality of our life could keep us from contacting with DEHP products.
Keywords: DEHP;tau protein;CREB

Acknowledgments: This work was supported by the National Natural Science Foundation of China (No. 30700208 and No30800329) and CCNU project (No. 091301009 and No. CCNU10A0160).

PL-018

Glycogen synthase kinase-3β is essential for amyloid-β induced long-term potentiation inhibition in rat hippocampal slices

Cairong Li*, Fei Cai, Juan Li, Rong Li, Xinyuan Zhao

*Corresponding author: Department of medicine, Medical College, Hubei University of Science and Engineering, Xianning, China, 437100.
Email: xnlcr@163.com

Amyloid-β (Aβ) protein is one of the pathological features of Alzheimer's disease (AD), a neurodegenerative disease characterized by a progressive loss of memory and cognitive deficits. But the mechanisms of Aβ on long-term potentiation (LTP), a synaptic model for investigating the molecular and cellular basis of learning and memory, have remained unclearly. By using the rat hippocampal slices, we investigated whether glycogen synthase kinase-3β (GSK-3β), a serine-threonine kinase, is involved in the inhibited effects of Aβ on hippocampal LTP. Electrophysiological results indicated that Aβ25-35inhibited LTP without affecting basal synaptic transmission and PPF in the hippocampus. SB415286, lithium and kenpaullone, three inhibitors of GSK-3β, produced a complete block of Aβ25-35-induced LTP suppression. Combined treatment with PI3K activator also restored Aβ25-35-induced LTP inhibition and this protective effect was almost completely blocked by PI3K inhibitor (LY294002). Western blot showed that Aβ25-35 caused a decrease in the phosphorylation of GSK-3β ser9 and phosphorylation of Akt thr308. Pretreatment with SB415286 restored the reduction of phosphorylation of GSK-3β but did not reverse the decreased phosphorylation of Akt. Combined treatment with PI3K activator restored Aβ25-35-induced decrease of phosphorylation of Akt and GSK-3β, and these effects were blocked by LY294002. Collectively, these experiments demonstrate that PI3K-Akt-GSK-3β pathwayis involved in inhibited effect of Aβ25-35onhippocampal LTP.
Keywords: Alzheimer's disease; amyloid-β; glycogen synthase kinase-3β; long term potentiation

PL-019

Inactivation of PICK1 reduced memory consolidation of cocaine-conditioned reward

Fei Cai*, Cai-Rong Li, Bin Xia, Pan-Feng Wu and Xin Yuan

*Corresponding author:Hubei Province Key Laboratory on Cardiovascular, Cerebrovascular, and Metabolic Disorders, Hubei University of Science and Engineering, Xianning, China, 437100.
Email: xncf@163.com

Modulation of AMPAR trafficking has emerged as a key regulator of memory and may contribute to the rewarding behavior of cocaine. PICK1 interacts with GluR2 and GluR3 AMPAR subunits and regulates their trafficking. The aim of this study was to evaluate the effect of FSC231, a new special antagonist of PICK1, on memory consolidation of cocaine-conditioned reward. Mice were administered with cocaine intraperitoneally at a dose of 20 mg/kg on 8 consecutive days, and FSC231 was given at the end of each conditioning session. The behavior changes were tested by conditioned place preference (CPP) and Morriz Water Maze. The hippocampal protein expression of GluR2, GluR3 and PICK1 were detected by Western blot. The results showed that mice treated with FSC231 spent significantly less time in the cocaine-paired compartment in CPP test. The learning of the platform location, an index of short-term spatial working memory, was significantly increased in cocaine-treated mice and this increasing was restored by administration of FSC231. Western blot showed that FSC231 inhibited the protein expression of PICK1 and GluR2 in the hippocampus of cocaine-treated mice, but did not affect the expression of GluR3. The results suggest that modulation of AMPAR trafficking by PICK1 may be necessary for the development of pharmacotherapies for cocaine addiction.
Keywords: PICK1, cocaine;AMPA;FSC231; conditioned place preference

Acknowledgments: This work was supported by the National Natural Science Foundation of China (81000576) and the Foundation of Hubei Ministry of Education (Q20112801).

PL-020

L-carnitine improve the hippocampus neurons secreting IGF II by decreasing the p53 oxidation

Wang Xiang*, Dan Wanyin, Wang Liangpin, Xu Yiqin

*Corresponding author: Hangkong road number 13, Wuhan City, Hu Bei provience.
Email: wangxiang027@gmail.com

AD is characterized by the cholinergic neurons lost and defects in learning and memory. Scopolamine is common used to imitate AD pathological features and also cause an obvious oxidative stress. After given the L-carnitine in the abdominal, it can partly reverse learning and memory defects tested by Morris water maze and LTP in vivo. As a significant decrease in Glur1s845 we detect the IGF II mRNA and find that there is a notable decrease after giving the scopolamine and can be reversed by the L-carnitine. Because the P53 can decrease the IGF II gene expression and P53 protein can be oxidative we find that the oxidative P53 is critical for the IGF II gene expression. In addition, by using the MDA, T-SOD, MSH and MSH-PH as the oxidative marker we find that L-carnitine can totally antagonistic the oxidative stress induced by scopolamine. We conclude the L-carnitine decreases the oxidative P53 to improve the IGF II gene expression by decrease the oxidative stress to reverse the learning and memory lost induced by scopolamine.
Keywords: IGF II, Oxiative P53, Oxiative stress

PL-021

Increased Plasma Homosysteine Levels Precede Accumulation of Intracellular β-amyloid/β-amyloid Plaque Pathology and Cognitive Impairment in a Triple Transgenic Mouse Model of Alzheimer's Disease

Ming Ying[1]*, Jiazuan Nia and Xifei Yang[1]

[1]College of Life Sciences, Shenzhen University, Nanhai Ave 3688, Shenzhen 518060, China;
[2]Key Laboratory of Modern Toxicology of Shenzhen, Shenzhen Center for Disease Control and Prevention, No. 8, Longyuan Road, Nanshan District, Shenzhen, 518055, China.
*Corresponding author.
Email: yingming@szu.edu.cn

Alzheimer's disease (AD) is the most common form of neurodegenerative disease. Homocysteine (Hcy) has been shown to be a risk factor for AD onset; however, there are also some conflicting results. Here reported that the levels of Hcy were significantly increased in plasma of a triple transgenic mouse model of AD (3 x Tg-AD) harboring PS1M146V, APPSwe, and taup301L transgenes at an early age of 2 months, occurring concomitantly with intracellular β-amyloid accumulation, but before the onset of accumulation of intracellular β-amyloid/β-amyloid plaque formation and cognitive impartment. These data demonstrate that an elevation of plasma Hcy could be also an early biomarker as well as a risk factor for AD.
Keywords: Homocysteine; Alzheimer's disease (AD)

Acknowledgments: This work was supported by the National Natural Science Foundation of China (31070731) and the Science Foundation of Shenzhen university (200916)

PL-022

ICR01 Improves Cognitive Impairment in Triple-Transgenic Alzheimer's Disease Model Mice and Attenuates Amyloid β-induced Mitochondrial Bioenergetic Deficit

Zhen Hai-Yang[1], Huang Chun-Lin[2], Zhang Yu[2], Zhang Dong-Sheng[1], Deng Han[2], Ni Jia-Zan[1]*, He Xiao-Yang[2]*

[1]College of Life Science, Shenzhen Key Laboratory of Microbial Genetic Engineering, Shenzhen University, Shenzhen 518060, China.
[2]College of Life Science, Shenzhen Key Laboratory of Marine Bioresources and Ecology, Shenzhen 518060, China.
*Corresponding author.
Email: hexy2008@szu.edu.cn

Increasing evidence from clinical trials and studies on Alzheimer's disease (AD) animal models suggests mitochondrial bioenergetic deficit as a common early pathomechanism integrating in A accumulation and synaptic dysfunction. In the present study, we investigated the early intervention of ICR01, a neuroprovention flavonoid compound from Epimedium brevicornum Maxim, on learning and memory in young PS1m146V/APPswe/tauP301L triple-transgenic AD (3xTg AD) model mice. Two and four-month-old 3xTg-AD mice that have compromised mitochondrial capacity, synaptic dysfunction as well as cognitive deficit precede the hallmark pathological lesions of A plaque and neurofibrillary tangles, were given diet chow containing 80mg/kg/d of dose of ICR01 for 20 weeks. Compared with regular diet control treatment, ICR01 administration significantly improved learning and long-term spatial memory of 3xTg AD mouse. That earlier ICR01 taking from 2 moths age have more effective intervention on the cognitive decline in 3x TG

AD mice was evidenced with magnificent decrease of escaping latencies during water maze acquisition training and increase of percentage of time spent in target quadrate in space exploration test. Our primary data revealed that ICR01 treatment lowered A levels in brain homogenates and recovered the pyruvate dehydrogenase (PDH) protein disturbance in 3xTG AD mice. Further studies are ongoing to investigate the mechanism of ICR01 on regulating APP processing, mitochondrial A accumulation, and expression of key enzymes, including PDH, involving in oxidative phosphoralation/glycolysis in 3x TG AD mice. The research findings support the idea that ICR01 balance back mitochondrial bioenergetic dysfunction in AD pathogenesis and that these "disease specific" effects might be relevant for early interpretation and planning of future clinical trials.

Keywords: ICR01, Alzheimer's disease, early intervention,
*to whom correspondence should be addressed at

PL-023

SelM prevents the aggregation of Aβ by reducing ROS generation

Ping Chen[1,2], Xiaojie Ma[1], Qing Liu[1], Qiong Liu[1]*, Jiazuan Ni[1]*

[1] College of Life Sciences, Shenzhen University, Shenzhen, China, 518060;
[2] College of Optoelectronic Engineering, Shenzhen University, Shenzhen, China, 518060.
Email:wyf10071121@yahoo.com.cn

Background: Deficiency of selenium (an essential trace element in vivo) has been reported to be linked to cognitive impairment and Alzheimer's disease (AD)[1]. Selenium exerts its biological functions mainly through selenoproteins, which play important roles in maintaining the optimal brain functions via redox regulation[2]. Selenoprotein M (SelM) is highly expressed in human brain and may take part in antioxidation, neuroprotection and cytosolic calcium regulation [3].
Methods: SelM and its mutant (where the Sec-encoding TGA in the SelM gene was site-directedly changed to Cys-encoding TGC) were cloned, re-constructed, and over-expressed using the pSelExpressl vector and special culture condition. The levels of reactive oxygen species (ROS) in HEK293T cells transfected respectively with SelM and its mutant were measured via flow cytometry. Laser confocal fluorescence microscope was used to detect the change of oxidative stress and Aβ deposition.
Results: Sodium selenite at proper doses could increase the expression of full-length SelM and decrease the expression of truncated SelM in the gene-transfected HEK293T cells. The full-length SelM had stronger anti-oxidative function than the mutant. Transfection of SelM and its mutant into the cells decreased the aggregation rate of Aβfrom 57.9±5.5% to 22.3±2.6% and 26.3±2.1%, respectively, and recruited the intumescent mitochondriato normal state.
Conclusion: Full-length SelM or its Sec-to-Cys mutant can inhibit intracellular ROS generation, protect mitochondrial, and prevent Aβ aggregation. This study proposes a new mechanism for selenium in preventing AD in its early stage.
Keywords: Selenoprotein M (SelM); antioxidant; reactive oxygen species (ROS); Alzheimer's disease(AD)

Acknowledgments: This work was supported by the National Natural Science Foundation of China (31070731), the Natural Science Foundation of Guangdong Province (10151806001000023),and the Grants of Shenzhen Municipal Science and Technology Industry and Information Technology Commission Research (CXB201005240008A).
[1] Loef M, Schrauzer GN, Walach H. J Alzheimers Dis 2011, 26(1):81-104.
[2] Zhang S, Rocourt C, Cheng WH. Mech Ageing Dev 2010, 131(4):253-260.
[3] Reeves MA, Bellinger FP, Berry MJ. Antioxid Redox Signal 2010, 12(7):809-818.

PL-024

Selenoprotein R interacts directly with Aβ1-42

Chao Wang, Zhenyu Zeng, Qiong Liu*, Jiazuan Ni*

Changchun Institute of Applied Chemistry, Chinese Academy of Sciences, Changchun 130022; College of Life Sciences, Shenzhen University, Shenzhen, 518060; Graduate University of the Chinese Academy of Sciences, Chinese Academy of Sciences, Changchun, China, 130022.
*Corresponding author.
Email: raulw2003@163.com

Background: Selenium is an essential trace element for organisms, which mainly performs its biological functions in the form of selenoproteins. Selenoproteins belong to a family of proteins containing a special amino acid selenocysteine (Sec) that is encoded by a stop codon UGA. Selenoprotien R (SelR), also called methionine sulfoxide reductase B1 (MsrB1), can stereo-specifically catalyze the reduction of oxidized methionine residues in proteins. b-amyloid peptide (Ab) is formed through the cutting of APP by b-secretase and g-secretase in sequence. The aggregate of Abforms senile plaques, which is one of the important pathological features of AD.

Methods: The Sec-encoding TGA of SelR gene was site-directedly mutated to TGC coding for a cysteine residue. The interactions between SelR and Aβ1-42were tested by the rfluorescence resonance energy transfer technique (FRET) and co-immunoprecipitation assay (co-IP).
Results: The open reading frames of SelR mutant and Aβ were cloned and inserted into the plasmids to construct the recombinants pcMV-myc-SelR¢and pECFP-Aβ, respectively. Co-IP experiments were performed in two ways, using either anti-myc antibody for immunoprecipitation (IP) and anti-GFP antibody for Western blotting (WB), or anti-GFP antibody for IP and anti-myc antibody for WB. Both co-IP results demonstrated the interaction between SelR¢and Aβ. The interaction between SelR and Aβ1-42 was further verified by FRET using the method of acceptor photobleaching.
Conclusion: The interaction between SelR¢and Aβ was detected by both co-IP and FRET. As an antioxidant enzyme, SelR functions as an ROS inhibitor to prevent Abaggregation during the formation of AD in the brain.
Keywords: selenoprotein R; Aβ1-42; fluorescence resonance energy transfer; co-immunoprecipitation

Acknowledgments: This work was supported by the National Natural Science Foundation of China (31070731), the Natural Science Foundation of Guangdong Province (10151806001000023),and the Grants of Shenzhen Municipal Science and Technology Industry and Information Technology Commission Research (CXB201005240008A).

PL-025

Changes in hypoxia-induced mediator levels in rat hippocampus during chronic cerebral hypoperfusion

Ying Yang, Junjian Zhang*, Hui Liu, Jing Wang

*Corresponding author:Department of Neurology, Zhongnan Hospital, Wuhan University, Wuhan, China, 430071.
Email: yang.y573@163.com; wdsjkx@163.com

Hypoxia is the physiologic condition triggering the signaling pathway mediated by hypoxia-induced factor (HIF). The expression of HIF-1α and its down-stream genes, both pro-apoptotic and pro-survival, was reported to be up-regulated in ischemic stroke. Moreover, many studies have shown that the role of HIF-1α may be quite different between the early and late stage after cerebral ischemia. As chronic cerebral hypoperfusion is prevalent in demented patients, HIF-induced long-term effect is suggested to be an important factor in the development of dementia. In the present study, permanent bilateral common carotid arteries occlusion (2VO) was used to induce the model of chronic global cerebral hypoperfusion in rats. The expression of HIF-1α and the effect on the transcription of the down-stream genes were measured at different time points, including 0h(before 2VO), 12h, 24h, 3d, 7d, 14d, 28d, 42d, and 56d after 2VO. We found the HIF-1α protein level increased as early as 12h after operation, and remained on a high levelfor at least 56d. Interestingly, mRNA transcription of both proapoptotic (bNIP-3, Noxa, and Nix) and prosurvival genes (Vegf, Glut-1) were upregulated after 2VO, peaked at around 24h-3d, then declined slowly to the normal level afterwards. The results showed that the HIF-1α protein level increased consistently during chronic cerebral ischemia, meanwhile both pro-apoptotic and pro-survival down-stream genes were only up-regulated early after 2VO. The mismatch might attribute to the lack of protective effect of highly expressed HIF-1α level at the chronic stage.
Keywords: hypoxia-induced factor;chronic cerebral ischemia

Acknowledgments: This work was supported by the National Natural Science Foundation of China (81171029)

PL-26

Effects of AVP on AQP4 expression in primary cultured astrocytes

Jinghua Zhou* and Weihua Zhuang

*Corresponding author: Department of Neurology, The First College of Clinical Medical Science, China Three Gorges University, Yichang, Hubei 443003, China.
Email: toddshall@163.com

Vasopressin (AVP) facilitates water across the astrocyte membrane. In the brain, AQP4 mainly locates in astrocytic end-feet and ependymal cells, mediates transmembrane water movement in metabolism and plays an important role in maintaining brain homeostasis. Many studies showed that vasopressin can cause astrocyte swelling and exacerbate brain edema(Sarfaraz and Fraser, 1999).through activation of V1aR. Astrocyte extends specialized processes to perisynaptic and perivascular region to mediate the bidirectional flow of metabolic, ionic, and water between neuron and the blood stream, AQP4 knockout mice showed a remarkable reduction in brain edema(Manley et al., 2000).The water permeability of AQP4 in astrocyte can be rapidly regulated through proteinphosphorylation(Zelenina et al., 2002),but the long-term regulation of brain AQP4 is unclear. AQP4 might be long-termly regulated by AVP-activated V1aR in expression level. This study was designed to assess the effect of AVP on the expression of AQP4 in rat primary cultured astrocytes. Astrocytes were purified to >98 % by

passage from new-born rat cerebral cortex. Primarycultured astrocytes were incubated in culture medium containing 500 nM AVP or 500 nMV1areceptor (V1aR) antagonistfor 1, 6, 12,and 24 h, harvested for determination of AQP4 protein and AQP4 mRNA expression by immunohistochemical technique and reverse transcription polymerase chain reaction (RT-PCR). After addition of 500 nM AVP for 6 h, AQP4 proteins expression became to increase ($P<0.01$), the peak presented at 12 h ($P<0.01$), remained to 24 h ($P<0.01$). When astrocytes were treated with V1aR antagonist, AQP4 protein did not show higher expression than control at the above-mentioned time points ($P>0.05$).After treated with 500 nM AVP for 6 h, astrocytes showed increased expression of AQP4 mRNA ($P<0.01$), the peak was at 12 h ($P<0.01$), which lasted to 24 h ($P<0.05$). Under the condition of 500 nM V1aR antagonist being added, the AVP did not induce the higher AQP4 mRNA expression .The results suggest high level of AVP may induce overexpression of AQP4 mRNA and AQP4 protein by activation of V1aR, which may increases water permeability of astrocyte membrane, and makes astrocyte swell.

Keywords: arginine vasopressin; aquaporin-4; astrocyte

References:

Sarfaraz D., Fraser CL (1999) Effects of arginine vasopressin on cell volume regulation in brain astrocyte in culture. Am J Physiol 276:E596-601

Manley GT., Fujimura M., Ma T., Noshita N., Filiz F., Bollen AW., Chan P., Verkman AS(2000) Aquaporin-4 deletion in mice reduces brain edema after acute water intoxication and ischemic stroke. Nat Med 6:159-163

Zelenina M., Zelenin S., Bondar AA., Brismar H., Aperia A(2002) Water permeability of aquaporin-4 is decreased by protein kinase C and dopamine.Am J Physiol Renal Physiol

PL-027

Neurotoxicity of Silica Nanoparticles: Brain Localization, Alzheimer's Disease-like Pathology and Spatial Memory Impairment

Xifei Yang, Hongbing Cheng, Chun'e He, Wen-Xu Hong, Desheng Wu, Xinfeng Huang, Zhixiong Zhuang and Jianjun Liu*

*Corresponding author: Key Laboratory of Modern Toxicology of Shenzhen, Shenzhen Center for Disease Control and Prevention, Shenzhen, China, 518055.
Email: junii8@126.com

With the rapid development of nanotechnology, nanomaterials are widely used in modern industry and life, especially in the filed of environmental protection. Silica nanoparticles (SiNPs) are among the most produced nanomaterials and have been formulated for cellular and for non-viral gene delivery in the central nerve system (CNS). However, whether SiNPs can enter the brain and their potential toxic effects on the brain remain poorly understood. In this study, the Sprague Dawley (SD) rats were treated with 15-nm SiNPs at doses of 0.625 mg/kg·bw and 2.5 mg/kg·bw by intranasal instillation. SiNPs administration was performed every other day and lasted for 2, 4 and 8 weeks, respectively. The localization of SiNPs in the brain was analyzed by transmission electron microcopy (TEM). The potential neurotoxicity of SiNPs, the effects on Alzheimer's disease (AD) pathologies and spatial learning and memory in the rats were evaluated by using the techniques including immunohistochemistry (IHC), Western-blot analysis and Morris water maze test. TEM analysis reveals that that SiNPs by intranasal instillation enter the brain and are widely distributed in olfactory bulb, hippocampus and cortex of the rat brain. SiNPs promote the release of pro-inflammatory cytokines, TNF-α, IL-1β and IL-6, in the olfactory bulb, hippocampus and cortex of the brain, and activate astrocyte cells as evidenced by increased expression of glial fibrillary acidic protein (GFAP) and morphological alterations of activated form in the brain. SiNPs induce oxidative stress as suggested by decrease in the total antioxidant capacity and increase in the levels of malondialdehyde (MDA) in the olfactory bulb, hippocampus and cortex of the brain. In addition, SiNPs is found to induce plaque-like AD pathology in the olfactory bulb, hippocampus and cortex of the brain. ELISA analysis reveals that SiNPs significantly increase the production of β-amyloid 1-40/42 (Aβ1-40/1-42) with concurrent up-regulation of amyloid precursor protein (APP), indicating that the up-regulation of APP likely contribute to Aβ over-production in the brain. Western-blot analysis shows that phosphorylation of tau at Ser 262, Ser 396 and Ser 404 is significantly increased, and that phosphorylated glycogen synthase kinase (GSK)-3β at Ser 9 (inactive form) and phosphorylated catalytic subunit of protein phosphatase-2A (PP-2Ac) are significantly decreased in olfactory bulb, hippocampus and cortex of the brain. The levels of cyclin-dependent kinase 5 (Cdk-5) and its co-activators p25/p35 are not significantly changed in either region of the brain. Activated GSK-3β and inactivated PP-2A may be responsible for increased phosphorylation of tau caused by SiNPs in the brain. Furthermore, Morris water maze test reveals that exposure to SiNPs impairs spatial memory but not spatial learning abilities of the rats. In conclusion, our findings provide evidence demonstrating that SiNPs by intranasal instillation canenter the brain of the rats,

characterized by a wide distribution in various brain regions, and that exposure to SiNPs induces neurotoxicity, AD-like pathology and spatial memory impairment in the rats. These data suggest that the application of SiNPs might cause neurotoxicity, increase the risk of developing AD pathology and cognitive deficit.
Keywords: Alzheimer's disease

Acknowledgements: This work was supported by NSFC (the National Natural Science Foundation of China) [81102154] and the Upgrade Scheme of Shenzhen Municipal Key Laboratory [CXB201005260068A].

PL-028

Study of Immunoglobulin G Gene Expression in Various Regions of Rat Brain Subject to Acute Immobilization Stress

Sheng Wang, Yun Wang, Guowei Huang, Tao Huang, Jiang Gu*

*Corresponding author: 22 Xinling Road, Shantou, China, 515041.
Email: shengwang.diamond@gmail.com

Immunoglobulin G was recently found to be synthesized in neurons of the brain, hippocampus showing higher expression level. To determine whether IgG has any function in hippocampus, we established IgG expression in rat hippocampal neurons by immunohistochemistry, immunofluorescence, in situ hybridization and laser microdissection-assisted single cell RT-PCR on tissue sections. Elevation of IgG expression in hippocampus was observed in an acute immobilization stress model of rat, no change was observed in cortex and thalamus. Further, elevation of IgG was unique without other neural protein up regulation. Based on these findings, we speculate that hippocampal IgG may be responsive to adverse circumstances such as stress in a unique manner. The finding of increased IgG expression in hippocampus with stress responses may provide possibilities for developing antidepressant medication.
Keywords: IgG;acute stress;hippocampus

Acknowledgements: This work was supported by the National Natural Science Foundation of China (81102280)

PL-029

Non-acetylated tau represses the expression of synaptic protein in N2a cells

Hui Tang, Ling-qiang Zhu*

*Corresponding author: Tongji Medical College, Huazhong University of Science and Technology, Wuhan, P. R. China.
Email: zhulq1979@yahoo.cn

Microtubule associated protein tau can be chemically modified in several forms, such as phosphorylation, glycosylation, sumoylation, ubiquitination, truncation as well as acetylation. Papers about the impact of acetylated tau on synapse are few compared with other modification forms. Our results shows that when introduce non-acetylated tau into N2a cells for 48h, synaptic proteins such as psd93 and synI are decreased 20% and 40% respectively. Which implies us that acetylated tau has a role in synapse formation.
Keywords: acetylated tau;post translational modification; synapse

PL-030

Estrogen receptor β decreases the level of tau phosphorylation through inactivate GSK-3β

Yansi-Xiong, Jian-Zhi Wang Ling-Qiang Zhu*

*Corresponding author: Department of Pathophysiology, Tongji Medical College, Huazhong University of Science and Technology, Wuhan 430030, PR China.
Email: zhulq@mail.hust.edu.cn

Alzheimer disease is the most common form of dementia, characterized by loss of neurons and synapses in the cerebral cortex and certain subcortical regions. Both amyloid plaques and neurofibrillary tangles are clearly visible by microscopy in brains of those affected by AD. It is reported that aggregates of hyperphosphorylated microtubule-associated protein tau is the major component of neurofibrillary tangles. Estrogen Replacement Therapy (ERT) has been found to both reduce the risk of developing AD and slow its progression in many studies. Women who receive ERT perform better on cognitive tasks than untreated women, which suggests that estrogen lessens the severity of AD. Estrogen receptors are activated by the hormone estrogen (17β-estradiol), and classified into two groups: estrogen receptor α(ERα)and estrogen receptor β (ERβ). It is reported that ERβ knock out mice mainly impairs memory, but ERα knock out mice mainly causes reproductive dysfunction. In the brain, ERβ mRNA expression was found in high levels in the cognitive related region, whereas ERα mRNA expression was found in high levels in the reproductive related region. This suggested that ERβ may play an important role in cognition and may provide us with treatment to AD.

While how ERβ affect the tau phosphorylation is not clear.
We transfected HEK293/tau cell line with pEGFP-ERβ plasmid to overexpress it, found the level of pS396, pS404, and pT231 decreased compared to the vector group, indicate that ERβ activation can rescue the pathological changes in the AD-like cell model. Moreover, we found the activity of GSK-3β detected by pospho-Tyr216 was decreased compared to the vector group. After administrating ERβ non-specific inhibitor ICI182780 to the transfected ERβ cells, the decreased phosphorylated tau was reversed compared to the DMSO group. In addition, the activity of GSK-3β was increased, indicating ERβ decreases the level of tau phosphorylation through inactivating GSK-3β.
Keywords: cellculture; transfection; western blot; immunofluorescent; immunoprecipitation

PL-031

Erythropoietin Ameliorates Spatial Memory Deficits Induced by β Amyloid 1-42 in Rats

Li Wang[1]*, Yipei Li[1], Junjie Shang[2], Gaoshang Chai[3], Li Jin[2]

*Corresponding author.
[1]Henan Medical College for Staff and Workers, Zhengzhou China 450003;
[2]Department of Pathophysiology, Zhengzhou University, Zhengzhou China 450052;
[3]Department of Pathophysiology, Key Laboratory of Neurological Diseases of Chinese Ministry of Education, Tongji Medical College, Huazhong University of Science and Technology, Wuhan, 430030. P.R.China.
Email: kyk02@126.com

In recent years, a large number of experimental studies confirmed that the functional erythropoietin (EPO) and its receptor are expressed in neurons and glial cells, so we suppose it may be a cytokine with multiple functions, especially in the treatment of Alzheimer diseases (AD). In the present study, acute AD rats models were constructed by stereo-orient-microamount injeceting condensed Aβ1-42 into rats' hippocampus. We found that supplement of EPO by peritoneal injection for 2 weeks in rats could ameliorate the Aβ1-42-induced memory deficits, increase the density of the dendritic spines, accompany with upregulation of synapsin I and PSD95 protein levels. Moreover, EPO enhanced the expression of several anti-apoptosis associated proteins including XIAP and Bcl-XL in rat hippocampus. These results suggest that EPO could ameliorate Aβ1-42-induced spatial memory deficits through modulation of memory-associated proteins, upregulation the density of the dendritic spines and inhibition neuronal apoptosis of hippocampal neurons. The findings above provide experimental evidences for further understanding of the exact neuroprotective mechanism of EPO in the prevention and treatment of AD.
Keywords: Erythropoietin; Alzheimer diseases; Synapsin I; Spatial Memory

PL-032

Effects of Erythropoietin on the Cognitive Function of Alzheimer's Disease-Like Rats

Yipei Li[1], Li Wang[1]*, Gaoshang Chai[2], Junjie Shang[3]

*Corresponding author.
[1]Henan Medical College for Staff and Workers, Zhengzhou China 450003;
[2]De-partment of Pathophysiology, Key Laboratory of Neurological Diseases of Chinese Ministry of Education, Tongji Medical College, Huazhong University of Science and Technology, Wuhan, 430030. P. R. China.
[3]Department of Pathophysiology, Zhengzhou University, Zhengzhou China 450052.
Email: kyk02@126.com

Recent studies have shown that erythropoietin (EPO) may inhibit apoptosis of neuron and promote its anti-oxidant ability. Meanwhile, EPO can keep the structure and function of cerebral vessels normality. However, the effects of EPO on Alzheimer disease-like (AD) cognitive function is not reported. In this study, we employed AD-like model induced by injeceting condensed β-amyliod 42 (Aβ42) (10μg) into hippocampus to investigate the roles of EPO in rats. We found that supplement of EPO by peritoneal injection for 2 weeks could improve the Aβ42-induced memory deficits remarkably, with attenuation of the injury of chondriosome and synapse. Supplement of EPO almost abolished the Aβ42-induced hippocampal apoptosis due to the upregulation of Bcl-2, nerve growth factor (NGF) and downregulation of Bax. Supplementation of EPO could significantly attenuate hydroxy radical, malondialdehyde (MDA) and enhance the activity of antioxidase (GSH-PH, SOD) in hippocampus. Our data suggests that EPO could be a candidate for arresting Aβ42-induced AD-like memory deficits.
Keywords: Erythropoietin; Mitochondria; Apoptosis; Oxidative Stress

Acknowledgements: This work was supported by the Medical Science Technology Key Project Foundation of Henan (200903117)

PL-033

The effects of ubiquitination and phosphorylation modification of tau protein on the biological function of tau and CREB phosphorylation after the inhibition of proteasome

Min Xie, Qi-Chang Ke, Zhi-Min Lu, Ying Pan, Xiao-Mei Liao*

*Corresponding author: 152 LuoYu Road, Wuhan, China. Email: mmtmrxm@sina.com

Tau protein is a substrate of the proteasome and its degradation is proteasome- dependent, additionally, the normal turnover of the tau protein is catalyzed by the proteasomal pathway. In many cases of tauopathies, hyperphosphorylated tau has been identified and tau protein may lose its normal functions. In our study, in order to explore the effects of protesome inhibition on tau modification (ubiquitination and hyperphosphorylation), microtubule-binding function and sequence effects on CREB we have generated a cellular model of tau pathology using different concentration proteasome inhibitor MG132 (0, 2, 4, 6 μM) treated N2a cells for 24 hours to drive the formation of hyperphosphorylated tau which loss of the normal function. Cycloheximide (CHX) was used to inhibit protein synthesis. The level of ubiquitination of tau protein was analyzed by the immunoprecipitation of ubiquitin and tau-5; the levels of phosphorylated tau protein were detected by western blotting. To determine whether MG-132 alters the interaction of tau with tubulin in the microtubules (MTs) of intact cells, the MT-binding assay was performed and taxol was used to stabilize microtubules. The coordinated regulation of the kinases and phosphatases controls the phosphorylation state of tau protein we used western blotting to detect the activities of kinases and phosphatase of tau protein. We demonstrated the inhibition of proteasome activity caused (1) the levels of ubiquitination protein increased and the interaction of tau and ubiquitin increased compared to the control ($P<0.05$); (2) compared to the control many epitops of tau were hyperphosphorylated include Ser396, Ser262, Thr205, and Thr231($P<0.05$); (3) compared to the control ubiquitination and hyperphosphorylation modification of tau protein decreased microtubule-binding ability of tau protein tested by the tau-microtubule binding assay ($P<0.05$); (4) compared to the control the activities of kinases PKB increased while the activity of PKA decreased; the phosphatase PP2A level decreased ($P<0.05$); (5) because the activity of PKA decreased, the level of phosphorylation of CREB weakened compared to the control ($P<0.05$).These results suggested because of the inhibition of proteasome, the polyubiquitins protein and immunoprecipitation of tau protein and ubiquitin enhanced compared to control indicated that tau was modified with polyubiquitins and are targeting proteins for degradation by the ubiquitin- proteasome system (UPS). The result also showed that phosphorylated CREB level reduced which coincided with decreased PKA activity decreased. Our results demonstrated that the impairment of proteasome activity caused the degradation disorder of aberrant tau protein and dysfunction of microtubule-binding ability of tau protein through resulted in the imbalance of the kinases and phosphatases. In addition, polyubiquitins protein degradation disorder may cause the aggregation within the cell and ultimately affect the normal function of neurons. And this imbalance may also reduce the expression of memory-related protein (e.g. CREB) and affect the plasticity of the nervous system.

Keywords: tau; proteasome; ubiquitination; hyperphosphorylation

PL-034

Activation of Brain Sonic Hedgehog Pathway Inhibits Cerebral Damage and Enhances Vasogenesis Following Ischemic Stroke

Yuan-peng Xia, Bo Hu*

*Corresponding author: Department of Neurology, Union Hospital, Tongji Medical College, Huazhong University of Science and Technology, Wuhan, 430022, China. Email: doctor_xiawang@163.com

Functional recovery following stroke damage involves several aspects of the tissue repairing such as endothelial cell growth and neurovascular regeneration, but its underlying cellular and molecular mechanisms remain unclear. The main efforts of our present study focused on a novel strategy for enhancing neurovascular regeneration in stroke damage via activation of Hedgehog (Hh) signaling pathway.Recombinant human Shh protein (rHu Shh) or PBS was injected into cerebral ventricle immediately after Rat permanent middle cerebral artery occlusion (MCAO) surgery. For evaluating its protective effect, neurological deficits and infarct volume were examined at day 1 after MCAO. For testing its role in cerebral recovery, cerebral blood flow (CBF), microvascular density and angiogenesis were separately measured at day 1, 3 and 7. The expression of Shh downstream genes (Patched1 and Gli-1)and angiogenetic factors (VEGF, Ang-1 and Ang-2)were determined at protein and/or mRNA levels.We found 1) Shh alleviated MCAO-induced brain damage, which were associated with Patched1 and Gli-1 up-regulation. 2) Shh preserved the CBF and microvascular density in peri-infarct area at day 1. 3)

Shh increased the angiogenesis in peri-infarct area at later days following MCAO, which was accompanied with up-regulation of Ang-1 and VEGF expression. These data demonstrate that brain administration of Shh protein is able to facilitate stroke-induced angiogenesis and promotes the functional recovery in stroke damage.
Keywords: Shh; PMCAO; angiogenesis

Acknowledgments: This work was supported by grants from the Program of National Natural Science Foundation of China (81070938), Program for New Century Excellent Talents in University (NCET-10-0406) and the Fundamental Research Funds for the Central Universities (HUST 2010JC028).

PL-035

The effect of corilagin on the expression of TLR2, TLR3 and TLR9 in herpes simplex virus encephalitis

YuanJin Guo, Na Wang,Yuanwu Mei*

*Corresponding author: Department of Neurology, Union Hospital of Tongji Medical College, Huazhong University of Science &Technology, Wuhan China, 430022.
Email: sophiaguo1028@yahoo.com.cn

Recent studies have shown that corilagin have therapeutical effects in herpes simplex virus encephalitis (HSE), but the pharmacological mechanisms were not fully elucidated. Toll-like receptor (TLR) plays an important role in the immune response to virus. So, in our study, a total number of 48 Balb/c mice were equally divided into three groups (saline, infection, corilagin). The HSE animal model was carried out through intracranial injection of herpes simplex virus 1 (HSV-1) in infection and corilagin groups. The saline group mice were injected with saline. Before HSV-1 infection, the corilagin group had been given corilagin for two days. Mice neurological scores were assessed daily. The HSV-1 infection was confirmed by real-time polymerase chain reaction (RT-PCR). The morphological change in mice brain was detected through pathological slices, the expression change of TLR2, TLR3 and TLR9 through Western blotting. We found that the clinical symptoms appeared on the third day after HSV-1 injection, including body weight loss, listlessness, piloerection, etc., which reached the peak on the fifth day. Pathology showed obviously edema, abundant perivascular lymphocytic infiltration and neural cell degeneration/necrosis in HSV-1 infection group, which was attenuated by corilagin. The expression of TLR2, TLR3 and TLR9 all decreased slightly in the infection group vs. saline group, and then increased in the corilagin group vs. infection group. Additionally, the HSV-1 titers decreased significantly in the brain of corilagin group compared with the infection group. In conclusion, the up-regulation of TLR2, TLR3 and TLR9 possibly mediated the effects of corilagin on attenuating pathological damage, decreasing virus titers, and improving living conditions.
Keywords: herpes simplex virus encephalitis corilagin

Acknowledgments: This work was supported by the National Natural Science Foundation of China (81100894)
References:
[1] Chen Y, Chen C. Corilagin prevents tert-butyl hydroperoxide-induced oxidative stress injury incultured N9 murine microglia cells. Neurochem Int. 2011. 59(2): 290-6.
[2] Guo YJ, Zhao L, Li XF, et al. Effect of Corilagin on anti-inflammation in HSV-1 encephalitis and HSV-1 infectedmicroglias. Eur J Pharmacol. 2010. 635(1-3): 79-86.
[3] Guo YJ, Zhao L, Li XF, et al. Effect of Corilagin on anti-inflammation in HSV-1 encephalitis and HSV-1 infectedmicroglias. Eur J Pharmacol. 2010. 635(1-3): 79-86.

PL-036

Passive rehabilitation training improves the learning and memory function of rats with cerebral infarction by inhibiting neuron cell apoptosis

Man Li , Yuan Fang*, Hu Bo*

*Corresponding author: Department of Neurology, Union Hospital, Tongji Medical College, Huazhong University of Science and Technology, Wuhan, China, 430032.
Email: fangyuan28@hotmail.com; hubo@mail.hust.edu.cn

Previous studies have shown that passive rehabilitation training, which is conducted in limbs of rats early after suffering from cerebral infarction, can effectively promote the recovery of motor function.However, some recent studies have shown that the brain damage is aggravated when passive movement of limbs isimplemented immediately in rats after cerebral infarction.In our study, two hundred SD rats are randomly divided into four groups: normal group, sham-operated group, model group and passive rehabilitation training treated group, each group is divided into five sub-groups according to different time of postoperative treatment:6 h, 12 h, 24 h, 48 h and 72 h.The model group and treated group are sutured to cerebral infarction model established by left middle cerebral artery occlusion (MCAO/R). Each sub-group of treated group is treated with passive rehabilitation training according to their individual time of postoperative treatment, while all the other groups including

sub-groups are treated at the same time with sham passive rehabilitation training. Treatment lasts for 14d. After treatment, the Morris water navigation task is applied to examine samples' spatial learning and memory. In infarcted area, the expression of Caspase-3 is assayed by immunohistochemical treatment, and real-time fluorescent quantitative PCR is used to measure the expression of Bcl-2 mRNA.Our results demonstrate that passive rehabilitation training is able to significantly improve the recovery of learning and memory function of rats with cerebral infarction, increase the expression level of Bcl-2mRNA and decrease the expression of Caspase-3. It plays an important role in protecting nerve cells and recovering neural function.The best time window is presumably to be 24h after perfusion treatment to ischemia.

Keywords: Cerebral infarction; Passive rehabilitation training; Escape latency;Bcl-2; Caspase-3

PL-037

Fasudil reduces the risk of hemorrhagic transformation in severe ischemic stroke: an experimental study in rat

Quan-Wei He1, Ming Huang1, Sheng-Cai Chen, Ling Mao, Yong Wang, Jian-Yong Li, Yan Huang, Ya-Nan Li, Yuan-Wu Mei, Bo Hu*

*Corresponding author: Department of Neurology, Union Hospital, Tongji Medical College, Huazhong University of Science and Technology, Wuhan, 430022, China.
Email: hubo@mail.hust.edu.cn

Patients suffering massive cerebral ischemic stroke are under great risk of hemorrhagic transformation (HT), and once it happens, the treatment of cerebral stroke fall into dilemma and the patients have worse outcome. Fasudil, a Rho kinase (ROCK) inhibitor, would prevent the risk of HT in massive cerebral ischemic stroke. To test the hypothesis, we adopted an experimental stroke model in rat. Rat subjected to permanent middle cerebral artery occlusion (MCAO) were treated with fasudil or not, and the effects were assessed by histological and biological measures. The results demonstrated that rat suffering severe ischemic stroke existed higher risk of HT than suffering moderate ischemic stroke, and cerebral ROCK activity in rat suffering severe ischemic stroke was higher than suffering moderate ischemic stroke. Rat suffering severe ischemic stroke with treatment of fasudil existed less quantity of hemorrhage and lower risk of HT than with none-treatment of fasudil. Moreover, with the treatment of fasudil, rat suffering severe ischemic stroke also showed less damage in blood brain barrier (BBB). To investigate the mechanism of fasudil's beneficial effects further, we also performed an in vitrostudy. And we found that fasudil could protect cerebral microvascular endothelial cells against oxygen glucose deprivation, and reduce the release of matrix metalloproteinase-2, 9. In brief, our results demonstrated that fasudil could reduce the risk of HT in rat with severe ischemic stroke by protecting BBB.

Keywords: fasudil, middle cerebral artery occlusion, hemorrhagic infarction, blood brain barrier, metalloproteinase

PL-038

Exendin-4 improved rat cortical neuron survival under oxygen/glucose deprivation through PKA pathway

Meng-Die Wang, Yan Huang, Ling Mao, Yuan-Peng Xia, Yuan-Wu Mei, and Bo Hu*

*Corresponding author: Department of Neurology, Union Hospital, Tongji Medical College, Huazhong University of Science and Technology, Jiefang Avenue, Wuhan 430022, P. R. China.
Email: hubo@mail.hust.edu.cn

Background and Objective: Exendin-4(Ex-4), a high-affinity GLP-1R agonist, is the first incretin mimetic to be approved by the FDA. Previous studies have shown that Ex-4 may also possess neurotrophic and neuroprotective functions. Nevertheless, little is known about their role in brain ischemia. Whether Ex-4 can protect neurons against brain ischemia warrants further study, but it has been confirmed that Ex-4 treatment reduces infarct size and improves outcome in MCAO. In this study, we studied the effects of Ex-4 on ER-related cortical neuron apoptosis in an in vitro ischemia model [by oxygen/glucose deprivation (OGD), cultured rat cortical neurons], and evaluated the potential of using Ex-4 as a neuroprotective agent for the treatment of stroke.

Methods: Primary cortical neurons were taken from neonatal Sprague-Dawley male rats and randomly divided into control group, OGD group and Ex-4 group. Real-time PCR and ELISA were performed to establish the existence of active GLP-1R. Flow cytometry assay were used to analyze the anti-apoptotic capability of Ex-4. GRP78 and CHOP mRNAs were detected by real-time PCR. Both immunofluorescence and immunoblotting were used to monitor the alternation of GRP78 and CHOP protein levels. To further understand the potential signaling events involved in survival-promoting effects elicited by Ex-4, H89 (protein kinase A inhibitor), LY294002 (PI3K inhibitor) or U0126 (MEK1/2 inhibitor) were also added to the cells.

Results: Active GLP-1Rs were detected in cultured primary cerebral cortical. OGD effectively decreased survival rate, promoted apoptosis, up-regulated the expressions of GRP78 and CHOP. The relative survival rate increased with the dosage of Ex-4 ranging from 0.2 to 0.8 μg/ml and pretreatment with H89 blocked this protection. The apoptosis rate was also reduced by Ex-4. The level of GRP78 was up-regulated substantially with time following Ex-4 treatment. This improvement was significantly higher than untreated cells. Protein level of CHOP in cortical neurons increased progressively after OGD and treatment with Ex-4 further elevated the level 4 and 8 h after OGD and then substantially decreased the level 12 h after OGD. Ex-4-regulated GRP78 and CHOP expressions after OGD were changed by both H89 and LY294002 but not by U0126. PKA expression was up-regulatedby Ex-4 in the presence or absence of OGD.
Conclusion: The results indicated that Ex-4 protected neurons against OGD in by inhibiting apoptosis via modulation of the UPR through PKA pathway and may be used as a novel therapeutic alternative for stroke.
Keywords: Exendin-4; oxygen/glucose deprivation; endoplasmic reticulum stress; unfolded protein response; neurons

PL-039

Neuroprotective effects of Exendin-4 on apoptosis after focal cerebral ischemia/reperfusion injury in rats

Yong Wang, Meng-Die Wang, Yan Huang, and Bo Hu*

*Corresponding author: Department of Neurology, Union Hospital, Tongji Medical College, Huazhong University of Science and Technology, Jiefang Avenue, Wuhan 430022, P. R. China.
Email: hubo@mail.hust.edu.cn

Researches over the past decade have proved solid proof that GLP-1s play important roles in the CNS, such as modulation of satiety, improvement of memory and learning, defence against insults. Nevertheless, little is known about their role in brain ischemia. Whether exendin-4, a high-affinity GLP-1R agonist, mediated protectiveaction is also applicable to brain ischemia still needs to be elucidated. In the present study, we investigated the potential protect effects of Exendin-4 extract on brain ischemia-induced apoptosis and the possible underlying mechanisms were investigated. At 20 min after right lateral ventricle administration of Exendin-4 or vehicle (PBS), adult male Sprague-Dawley rats were subjected to left middle cerebral artery occlusion (MCAO). We analyzed the expression of GLP-1 receptor. Brains were harvested at 1d, 3d and 7d after reperfusion for assays of infarct volume, neurological scores and neuronal apoptosis, real-time PCR and Western blot analysis for bcl-2, Bax levels. To further understand the potential signaling events involved in survival-promoting effects elicited by Exendin-4, Rp-cAMPS (protein kinase A inhibitor), wortmannin (PI3K inhibitor) or U0126 (MEK1/2 inhibitor) were also used and PKA expression was later assayed with Western blot analysis.Exendin-4 significantly reduced infarct volume, decreased apoptosis cell number, and ameliorated the neurological outcome. The Exendin-4 also increased the level of Bcl-2, but decreased Bax expression in the brain tissue. In addition, we found that the anti-apoptotic effect of Exendin-4 was blocked by chemical inhibition of PKA, but not by a PI3K or MEK1/2 inhibitor. Finally, PKA expressionwas up-regulatedby Exendin-4 in the presence or absence of I/R. These results indicate that in rat exposed to I/R insult, Exendin-4 protects cells from apoptosis, at least in part through the PKA pathway.
Keywords: Exendin-4; ischemia/reperfusion; apoptosis; rat

PL-040

Evaluation of Early Stroke Risk after Transient Ischemic Attacks with extra- and intracranial arterial stenosis

Zhang Lin-hong*, Zhan Pei-yan, Xu Wu-ping, Jing Ping

*Corresponding author: Department of Neurology, Wuhan Central Hospital, China.
Email: zhanglinhong05@sina.com

Recently, transient ischemic attack (TIA) as a predictor of stroke has been highly concerned, its research hotspots focus on how could early identify the subgroup of patients at higher risk of stroke. Severe intra or extracranial artery stenosis/ occlusion were independent risk factors of stroke occurrence in TIA patients. Here, by using the digital subtract angiography (DSA) technique, we detect the cerebral artery stenosis for the patients with noncardioembolic TIA and high risk stroke, and investigate the correlation between the early recurrent stroke and cerebral artery stenosis. The included criteria: (1)18~80 yrs, (2) admission in the hospital within 48h from the onset of symptoms, (3)clinical feature with focal motor weakness and/or speech disturbance, (4) finished DSA check within 5 d after admission, (5) signed informed consent voluntarily. Exclusion criteria: (1) TIA cause by heart disease, (2) clinical manifestations of pure abnormal feeling, dizziness and athletic symptoms. According to the standard, the group includes 88 male cases and 66

female cases. In the 88 patients, "criminal" vessels in 80 cases (90.9 %), including 69 cases with anterior circulation vessels stenosis/occlusion, 11 cases with posterior circulation vessels stenosis, 37 cases with intracranial artery stenosis/occlusion, 43 cases with extracranial artery stenosis/occlusion. The incidence of extracranial artery stenosis/occlusion is more than intracranial artery stenosis/occlusion. Acute ischemic stroke occurred after TIA in majority of patients (66.7%) with detection of artery stenosis ≥70% and less than 70% of artery stenosis had a low incidence of stroke (33.3%). In 8 cases without artery stenosis, only one case occurred stroke. The incidence of stroke and death at 7d, 30d and 90d after TIA: Stroke had occurred in 17 patients within 7 d of the index TIA, including 2 cases of death, 25 strokes occurred in 30 d, ≥50% of stroke occurred with 7 days after TIA. In 88 patients, the incidence of stroke or death within 7d,30d and 90d were respectively 19.3%, 28.4%, 37.5%. The incidence of death within 90d was 2.3%, which all occurred within 7d, which due to serious basal artery stenosis and brainstem infarction. The vascular etiology of TIA patients attribute to non-heart disease were investigated by DSA, the results was showed that 90.9 % (80/88) of patient with different degree of stenosis/occlusion of intra or extracranial artery, in which the degree of lesions stenosis was ≥70% and occlusion were about 59.1%, severe artery stenosis (>70%) was obviously higher than the <70% group among patients occurred stroke. The present results showed that most early strokes occur after TIAs with focal motor weakness and/or speech disturbance, especially associated with severe intra or extracranial artery stenosis/occlusion. These high-risk individuals should receive aggressive medical management, on occasion, performing endovascular intervention.

Keywords: TIAs, DSA, Arterial stenosis

PL-041

Endothelial precursor cells migrate to ischemic brain and take part in angiogenesis after stroke

Shengcai Chen[1], Ming Huang[1], Ling Mao and Bo Hu*

*Corresponding author: Department of Neurology, Union Hospital, Tongji Medical College, Huazhong University of Science and Technology, Wuhan 430022, P. R. China. Email: hubo@mail.hust.edu.cn

Angiogenesis plays a crucial role in recovery from ischemic stroke. In patients with ischemic stroke, the number of circulating endothelial progenitor cells (EPCs) increases as compared to at-risk control subjects. However, whether the circulating EPCs migrate to the ischemic brain and take part in angiogenesis remains unknown. In the present study we first demonstrated that the number of EPCs in peripheral blood increased in the rat model of middle cerebral artery occlusion (MCAO). To assess the role of increased circulating EPCs in angiogenesis, bone marrow cells expressing green fluorescent protein (GFP) were extracted from C57BL/6-TgN (ACTbEGFP) 1Osb mice, and transplanted into C57BL/6J mice through tail vein. 10 days after EPCs transplantation, the recipient mice were subjected to MCAO. EPCs surface markers CD34, CD133, and VEGFR2 in peripheral blood and ischemic brain tissue were monitored by immunofluorescent and flow cytometry. The EPCs expressing GFP were found in newly formed blood vessels in the ischemic brain. The transplanted EPCs were first found in the newly formed blood vessels 1d after MCAO, increased over time, and stay constant as long as 7 days. Collectively, our results indicate that EPCs from peripheral blood migrate to ischemic brain, and take part in angiogenesis after ischemic stroke.

Keywords: Endothelial precursor cells (EPCs), migration, angiogenesis, stroke

PL-042

Zinc supplementation does not improve learning and memory in chronic stressed mice

Jian-yong Li, Yu Jin, Fang Dong, Yang Yang, Rong Liu*

*Corresponding author: Department of Pathophysiology, Tongji Medical College, Huazhong University of Science and Technology.
Email: tjmuljy@163.com

The divalent cation zinc is an essential element, having both universal and specified functions throughout the body. In the mammalian telencephalon, zinc plays important roles in neurotransmission, modulating receptor function and second messenger systems. Strong evidences have shown that supplementation of zinc could improve the brain development in children; however, it is unknown whether zinc supplementation also benefits learning and memory in children under stress condition, which is common in normal life. In the present study, mice supplemented with zinc were exposed to chronic stress, the learning and memory ability was tested. Weaned ICR male mice (21 days) were supplemented with zinc (66.2 mg/L ZnSO4.7H2O in drinking water, equivalent to 10mg zinc daily intake for children) for 3 months, and then half of the mice were treated with chronic restraint stress for 2 h/20 days. At the end of the stress, a series of behavioral tests were explored to detect the learning and memory abilities. After that,

mice were sacrificed and the hippocampus isolated for western blotting. The open field test, novel object recognition test, and water Morris maze results showed that zinc supplementation can improve both short and long memory, but under chronic stress, such improvement was not observed. Compared with control mice, the zinc supplemented stressed mice showed decreased NMDA-NR2A, increased PKAβ and GSK3β levels, which may underlying the compromised behavior performance. The detailed relationship between such protein changes and behaviors needs to be further investigated.
Keywords: zinc supplementation; learning and memory; chronic restraint stress; NMDA receptor

PL-043

The Efficacy and Adverse Reaction of Bleeding of Clopidogrel plus Aspirin as Compared to Aspirin alone after Stroke or TIA: A meta-analysis about the prevention of stroke

Yan Huang, Bo Hu*

*Corresponding author: Department of Neurology, Union Hospital, Tongji Medical College, Huazhong University of Science and Technology, Jiefang Avenue, Wuhan 430022, P. R. China.
Email: baobaoxiong0401@163.com

Recent studies have shown that the combination use of clopidogrel and aspirin is more effective than monotherapy of aspirin. This meta-analysis determined the efficacy and adverse reaction of bleeding of these two protocols after stroke or TIA in the prevention of stroke. We analyzed the incidences of stroke, bleeding and severe bleeding. All randomized controlled trials comparing the effects of aspirin plus clopidogrel and aspirin plus placebo (or aspirin alone) on patients with the history of transient ischemia attack or ischemic stroke were included. 7 papers (including 6 original RCTs) involved 5572 patients were treated by either clopidogrel plus aspirin therapy or aspirin alone and evaluated the efficacy and the adverse reaction of bleeding (including 5550 patients) and severe bleeding (including 5345 patients) of the treatments. Our analysis showed that clopidogrel plus aspirin was more effective than aspirin alone for preventing the recurrence of stroke ($p=0.01$). As to the adverse reaction of bleeding, the incidence of bleeding was significantly higher in treatment group of clopidogrel plus aspirin than in aspirin-alone group ($p<0.00001$). No significant difference was found in severe bleeding between the treatment group and control ($p=0.20$). The combined use of aspirin and clopidogrel is more effective than aspirin alone for patients with previous transient ischemia stroke or stroke for the prevention of stroke, with risk of bleeding being higher. No statistical difference was found in severe bleeding between the two treatment protocols.
Keywords: Stroke, TIA (transient ischemic attack), Secondary prevention of stroke, Clopidogrel, Aspirin, Bleeding

Acknowledgments: This work was supported by grants from the Program of National Natural Science Foundation of China (No.81070938).

PL-044

Baicalein protects dopaminergic neurons by inhibiting aberrant cell cycle re-entry in Parkinson disease models in vitro and in vivo

Zhentao Zhang[1]*, Ling Mao[2], Hongcai Wang[2], Fengli Lan[2], Nian Xiong[2], Zhaohui Zhang[1], Xuebing Cao[2], Tao Wang[2]

*Corresponding author:
[1]Department of Neurology, Renmin Hospital of Wuhan University, Wuhan, 430060, China
[2]Department of Neurology, Union Hospital, Tongji Medical College, Huazhong University of Science and Technology, Wuhan 430022, P. R. China.
Email: zhangzhentao104@yahoo.com.cn

Parkinson disease (PD) is characterized by progressive loss of dopaminergic neurons in substantia nigra. Our understanding of cell events underlying neuronal death remains fragmentary. For this reason, no cure is available for this devastating disease. Our previous results show that aberrant cell cycle re-entry plays a critical role in neuronal death. Here we report that baicalein, a natural flavone glucuronide which has inhibitory effects on cell cycle progression, protected dopaminergic neurons against 1-methyl-4-phenyl-1,2,3,6-tetrahydropyridine (MPTP) toxicity by inhibiting cell cycle re-entry both in vitro and in vivo. In a cellular model, when primary cerebellar granule neurons were exposed to dopaminergic neurotoxin 1-methyl-4-phenylpyridine (MPP+), the postmitotic neurons re-entered into an abolished cell cycle, which resulted in neuronal apoptosis. Pretreatment with baicalein enhanced cell viability by inhibiting neurons from re-entering into the cell cycle. In the MPTP-induced mouse model of PD, The motor deficiency was ameliorated by 1-month treatment with baicalein. Baicalein inhibited substantia dopaminergic neuronal loss by 25%, and striatal dopamine loss by 32%. Cell cycle re-entry of postmitotic dopaminergic neurons was also inhibited by baicalein. Baicalein did not affect the body weight or complete blood count of the mice. Our results indicate that baicalein is a potential neuroprotective medicine in the treatment of PD.

Keywords: baicalein, cell cycle, dopaminergic neurons, Parkinson disease

Acknowledgments: This work was supported by the National Natural Science Foundation of China (81100958, 81101905)

PL-045

Pretreatment of 17β-estradiol prevents sublethal Aβ1-42 induced down-regulation of CREB phosphorylation in PC12 cells

Ying-Su[1], Yan-Xing Chen[1], Xiao-Qin Run, Hai-Bing Xiao, Wei Zhang, Zhou Sun, Yu-Dong Liu, Tao Wang, Sheng-Gang Sun, Zhi-Hou Liang*

*Corresponding author: Union Hospital, Tongji Medical college, Huazhong University of Science and Technology, 1277, Jiefang Avenue, Wuhan, China.
Email: suying0110@126.com

It is widely accepted that cAMP response element binding protein (CREB) is the core component in the process of learning and memory which is undermined in patients of Alzheimer's Disease (AD). Besides, epidemiological investigation indicates the declining memory is correlated with the lower estrogen level in AD patients. However, the effect of estrogen on CREB activity in AD is poorly known. In this study, we investigated the effect of 17β-estradiol pretreatment on the phosphorylation level of both CREB and the kinases associated with CREB activation in cells exposed to a sublethal concentration of Aβ1-42. We demonstrated the protection against Aβ1-42-induced changes of CREB by pretreatment of 17β-estradiol. 17β-estradiol pretreatment prevented Aβ1-42 induced down-regulation of CREB phosphorylation at Ser133 (CREB pS133). Furthermore, a transient (8 hours) up-regulation of the inhibitory GSK-3β phosphorylation at Ser9 (GSK-3β pS9) was detected in sublethal Aβ1-42 treated cells with pretreatment of 17β-estradiol, and this effect of 17β-estradiol was abrogated by AKT inhibitor LY294002. It suggests the inactivation of GSK-3β may be involved in the mechanism underlying the neuroprotection provided by 17β-estradiol pretreatment.
Keywords: estrogen; amyloid beta; CREB

PL-046

Intratumoral injection of recombinant lentivirus mediated Annexin A10 inhibits the growth of HepG2 xenografts in nude mice

Zhenzhen Hu, Qingmei Zhao, Xiaodong Peng1, Junhe Li , Xiaojun Zhong,Jianping Xiong*

*Corresponding author: Department of Oncology, The First Affiliated Hospital of Nanchang University, Nanchang, China. 330006a.
Email: pxddhbb@163.com

Recent studies have shown that ANNEXIN A10 (ANXA10), a member of annexin family, is potentially associated with hepatocellular carcinoma , ANXA10 overexpression inhibits proliferation and promotes apoptosis of hepatocellular carcinoma cell line HepG2 in vitro.But the efficient of ANXA10 in HepG2 in vivo is not mentioned.In our study, we construct and confirme Recombinant lentivirus expressing human ANXA10 and GFP, Lenti-PGC-Fu-ANXA10. A total of 24 female BALB/c-nu/nu nude mice aged 6-8 weeks was randomly assigned into 3 groups (experimental group,negative control group and blank control group).Xenografts in right subcutaneously in nude mice were established.-When the tumor diameter up to 0.3-0.5cm, Lenti-PGC-Fu-ANXA10 and lentivirus were intratumorally injected with 2×107TU (100ul) respectively in subcutaneous xenograft in experimental group and negative control group.Equal PBS were intratumorally injected in blank control group.Repeated injection 3h later.Tumor size was measured every 3 days.Nude mices were sacrificed and tumor samples removed after 3weeks. TUNEL (TdT-mediated biotinylated-dUTP nick end labing method) staining were used to determine apoptosis and apoptosis index were measured. The expression of ANXA10, MMP-9and VEGF in tumor samples was detected by RT-PCR and immunohistochemistry.The growth rate of subcutaneous significantly decreased in experimental group.The size and weight of tumor xenograft in experimental group were significantly lesser than those in negative control group and blank control group(for volume, $F=19.13$,$P<0.01$;for weight,$F=46.91$,$P<0.01$).In experimental group, the expression of ANXA10 was higher than the other two groups ($P<0.05$) and the expression of VEGF and MMP-9 was lower than the other two groups ($P<0.05$).Apoptosis index in experimental group (27.87±1.20)% was significantly higher than negative control group (3.47±0.72)% and blank control group(3.38±0.77%)%,($P<0.05$).Our results demonstrate that overexpression of ANXA10 gene dramatically inhibit the growth of tumor and the expression of MMP-9 and VEGF in human hepatocellular carcinoma cell line HepG2 and induce cell apoptosis in vivo.The overexpression of ANXA10 in HepG2 xenografts maybe inhibit the growth of human hepatocellular carcinoma cell line HepG2 and induce cell apoptosis by inhibiting the expression of MMP-9 and VEGF
Keywords: Lentiviruses; Annexin A10; Matrix metalloproteinase-9; Vascular endothelial growth factor

PL-047

Management of dementia,a nonmotor feature of Parkinson disease

Chen Xiaolu*

*Corresponding author: Tongji Medical College.
Email: 391058847@qq.com

Parkinson disease (PD) is an age-related neurodegenerative disorder with four cardinal clinical motor features: resting, tremor, rigidity, bradykinesia and gait dysfunction. However, the nonmotor, nondopaminergic features of PD, including neuropsychiatic problems, autonomic dysfunction, pain and sensory disturbances, mood disorders, sleep impairment and dementia are also common present in all stages. An intinsic nonmotor feature of PD is dementia which occurs at a time rate four to six tmes greater in patients with PD than in age matched controls without PD. So there is a crucial need for better strategies for preventing and managing cognitive decline. Risk factors for dementia in PD include early impairment in executive functions, age, and severity of PD motor features and it has been proposed that patients with PD have a subcortical dementia with preferential involvement of thought processing, decision making, attention,construction, visuospatial performance, memory and verbal fluency with relative sparing of language and social behavior.Formal neuropsychiatric evaluations may be required to recognize and define cognitive impairment in an individual patient with PD, particularly in the early stages of the disease and the MMSE is a simple means of assessing cognitive impairment.Trials of the cholinesterase inhibitors donepezil (Aricept) and rivastigmine(Exelon) have been carried out in demented patients with Parkinson. As metabolic disorders, dehydration, sedative and anxiolytic medications, depression and antiparkinsonian medications can all aggravate cognitive function in a patient with PD and should be actively addressed and treated.For demented patients that cannot be satisfactorily controlled with medicationgs, the needs of the caregiver and nursing home placement may have to be considered.
Keywords: Parkinson disease; Nonmotor feature; Dementia; Cognitive impairment; Cholinesterase inhibitors; Rivastigmine

PL-048

Intravenous gamma globulin combined with methylprednisolone in treatment of nervous system demyelination

Gong Dao-kai*

*Corresponding author: Jingzhou Central Hospital.
Email: 411898881@qq.com

Objective To study the effects of intravenousgamma globulin combined with methylprednisolone in the treatment of nervous system demyelinating effect. Methods in our hospital from 2010 March to 2012 March during inpatient treatment for 80 cases of patients with nervous system demyelination, were randomly divided into experimental groupand control group. The control group using high-dose methylprednisolone treatment, the experimental group based on the combined use of large doses of IVIg treatment of shock. Comparison of two groups of patients, cerebrospinal fluid abnormalities and neural function defect score difference. Result After the end of treatment, the experimental group total effective rate was 85%, 57.5% in the control group, the difference has statistical significance. Compared with the control group, the experimental group of cerebrospinal fluid abnormalities to recover faster, neural function defect score decreased faster, more obvious. Conclusion In thenervous system demyelination inpatients with intravenous gamma globulin combined with methylprednisolone in treatment, can rapidly, effectively control the disease, and is worth further clinical application.
Keywords: Nervous system demyelination; Gamma globulin; Methylprednisolone; Curative effect

PL-049

Activation of CREB reverses aging-related decline of neurogenesis in hippocampus

Xiaoxi Wang and Youming Lu*

*Corresponding author: Key Laboratory of Neurological Disease, Ministry of Education, China, Department of Pathophysiology, Tongji Medical College, Huazhong University of Science and Technology, Wuhan, 430030, China.
Email: tjmcwxx@sina.com

Adult neurogenesis in the hippocampal dentate gyrus plays an important role in learning and memory and decreases during aging. But the underlying mechanism is not well studied. In our study, we found that overexpression of cAMP-response-element-binding protein (CREB) by injection of constitutively active CREB virus (VP16-CREB) at the old dentate gyrus can induce expression of brain derived neurotrophic factor (BDNF) and in turn increase the number of new neurons and mice overexpressing CREB have better performance in MWM. Expression of small interfering RNA (siRNA) targeting the BDNF gene blocked CREB induced neurogenesis. Environmental enrichment active endogenous CREB and then increased the protein level of BDNF and generated functional granule neurons in the aged dentate gyrus. We also downregulated CREB by injection of dominantly negative mutated CREB virus (CREBA133),

and the results showed that CREBA133blocked environmental stimulation of neurogenesis. Moreover, expression of biologically active BDNF rescued the CREBA133 inhibition of neurogenesis. Thus, CREB induction of BDNF expression is both the necessary and sufficient conditions for continuation of functional neurogenesis in the dentate gyrus during aging.
Keywords: Neurogenesis; CREB; BDNF; Environmental Enrichment

PL-050

Tau-DAPK1 signaling in synaptic spine damage

Lei Pei, Xiaoxi Wang, Kunpeng Zhao, Ruojian Wen, Na Wei, Honglin Yan, Shan Wang, Lan Wang, Dan Liu, Youming Lu*

*Corresponding author: Key Laboratory of Neurological Disease, Ministry of Education, China, Department of Pathophysiology, Tongji Medical College, Huazhong University of Science and Technology, Wuhan, 430030, China.
Email: neurolei@gmail.com

Tau proteins, maintain neuronal morphology and dendritic processes, mislocalize to dendritic spines and cause abnormal remodeling of synaptic plasticity, which may contribute to the brain damage induced by transient cerebral ischemia. Recent study has shown that DAPK1 can be activated and considered as a primary mediator in brain damage of stroke, but it is still unknown whether activated DAPK1 can interact with tau and cause abnormal remodeling of synaptic spines and networks in stroke damage. In this study, we demonstrated the role of Tau-DAPK1 interaction in synaptic spine damage and dysfunction after cerebral ischemic stroke. Tau, DAPK1 and eGFP mutant mice were used and subjected to middle cerebral artery occlusion (MCAO) surgery to generate focal cerebral ischemia. Real-time PCR combined Western blot analysis to exam DAPK1 and tau expression. Enzymatic assay was performed to analysis DAPK1 activity. Co-immunoprecipitation was conducted to investigate Tau-DAPK1 interaction. Two-photon imaging with electrophysiological recording system was applied to observe the morphology and function of cortical synaptic spines. Our results demonstrate that, 1) Normal tau is required for neuronal survival and structural plasticity in stroke; 2) DAPK1 activation (pS306 dephosphorylation) mediates abnormal remodeling of synaptic spines and networks; 3) DAPK1 interacts with tau and abnormally regulates tau, resulting in abnormal remodeling of synaptic networks in stroke damage. Our work reveals specific tau-directed kinase regulator DAPK1, which promotes brain damage by interrupting the remodeling of synaptic spines from ischemic insults, may be a target for developing potential therapy for ischemic stroke in the future.
Keywords: Tau, DAPK1, Synaptic spine damage, Cerebral ischemic stroke

Acknowledgments: This work was supported by the National Natural Science Foundation of China (Grant 81130079 YL).

PL-051

Rosiglitazone Rescues Soluble Amyloid Oligomer-induced Impairment of Synaptic Development and Plasticity in Rats

Shujun Xu*, Guilan Liu, Xiaoming Bao, Jie Wu, Micha

*Corresponding author:Medical School, Ningbo University.
Email: xushujun@nbu.edu.cn

Recent evidence indicates that rosiglitazone, a potent agonist of peroxisome proliferator-activated receptor gamma (PPARγ), can prevent or attenuate neurodegeneration in Alzheimer's Disease (AD), but the underlying mechanisms remain to be fully elucidated. In this study, we examined the effects of soluble amyloid-β protein (Aβ) oligomers and rosiglitazone on the synaptic development and synaptic plasticity in rat hippocampal slices using live cell imaging and electrophysiological recording. We found that the incubation of hippocampal cultures with Aβ42 oligomers (500 nM) for 3 h hrs significantly decreased dendritic filopodia and spine density. Pretreatment with rosiglitazone (0.5-5 μM) for 24 hrs rescued the Aβ42-induced loss of dendritic filopodia and spines in a dose-dependent manner. However, neither Aβ42oligomers nor rosiglitazone has significant effect on the velocity and length of dendritic filopodia. The beneficial effect of rosiglitazone was abolished by the PPARγ-specific antagonist, GW9622. Electrophysiological recording showed that acute exposure of slices with 500 nM Aβ42 oligomers for 40 min impaired high frequency stimulation-induced hippocampal long term potentiation (LTP) in dentate gyrus region. Interestingly, pre-incubation of hippocampal slices with rosiglitazone significantly rescued the Aβ42-induced LTP deficit, which depended on rosiglitazone concentrations (1-5 μM) and pretreated period (1-5 hrs). In conclusion, our data suggest that rosiglitazone rescues Aβ42oligomers-induced synaptic

function impairment through the PPARγ-dependent pathway in a concentration and time dependent manner. This study provides novel insights into the mechanisms for the beneficial effect of rosiglitzone in AD patients.

Keywords: Aβ, Alzheimer's Disease, synaptic development, synapse plasticity, PPARγ, rosiglitazone, GW9622

Articles

AR-001

Astrocyte-derived sonic hedgehog contributes to angiogenesis in brain microvascular endothelial cells after oxygen glucose deprivation via RhoA/ROCK pathway

Quan-Wei He*, Yuan-Peng Xia*, Sheng-Cai Chen, Yong Wang, Ling Mao, Ming Huang, Yan Huang, Ya-Nan Li, Yuan Gao, Yuan-Wu Mei, Bo Hu

Department of Neurology, Union Hospital, Tongji Medical College, Huazhong University of Science and Technology, Wuhan, 430022, China.
*These authors contributed equally to this project.
Correspondence should be addressed to Dr. Bo Hu, Department of Neurology, Union Hospital, Tongji Medical College, Huazhong University of Science and Technology, Wuhan, 430022, China.
E-mail: hubo@mail.hust.edu.cn

Running title: *Astrocyte-derived Sonic Hedgehog Contributes to Cerebral Angiogenesis after Ischemia*

Abstract
Human adult brain possesses intriguing plasticity, including neurogenesis and angiogenesis, which may both be mediated by the activated sonic hedgehog (Shh). By employing a co-culture system, brain microvescular endothelial cells (BMECs) co-cultured with astrocytes, and an *in vitro* model, oxygen glucose deprivation (OGD), we tested the hypothesis that Shh secreted by OGD activated astrocytes promotes cerebral angiogenesis following ischemia. The results of this study demonstrated that Shh was mainly secreted by astrocytes and the secretion was significantly up-regulated after OGD. The tube formation in BMECs co-cultured with astrocytes was significantly enhanced, but cyclopamine, an Shh antagonist, reversed the change. Furthermore, silencing Ras homolog gene family, member A (RhoA) of BMECs by RNAi and blocking RhoA kinase (ROCK) by Y27632, a specific antagonist of ROCK, suppressed the up-regulation of tube formation after OGD. These findings suggested that activated astrocyte-derived Shh stimulated RhoA/ROCK pathway in BMECs after OGD, and the activation of RhoA/ROCK signaling cascade was involved in the tube formation after OGD.

Keywords: Tube formation; Oxygen glucose deprivation; Sonic hedgehog; RhoA; Brain microvascular endothelial cells

Introduction

Human adult brain is surprisingly plastic after stroke or injury [1]. Following stroke, neuroblasts proliferate and migrate from the sub-ventricular zone to the damaged regions, and then differentiate, a process called neurogenesis. Apart from neurogenesis, the recovering brain also experiences angiogenesis, and both are critical events contributing to survival and rehabilitation. Recently, inducing angiogenesis has been used as a therapeutic strategy for stroke and this gives rise to a new concept of "neurovascular unit", which now has been generally accepted [2]. According to the notion, cell-cell signaling between the neuronal, glial and brain endothelial cells mediates angiogenesis after stroke. Although astrocytes are the most abundant glial cells in the brain and mounting evidence revealed that they are involved in the retinal angiogenesis during development or under pathological conditions, the role of mature astrocytes in cerebral angiogenesis after stroke not fully understood.

Shh, a glycoprotein has both morphogenic and mitogenic properties and is a well-established angiogenic factor in individual development and tissue repair[3]. Traditionally, it has been believed that Shh is an indirect angiogenic factor that can up-regulate two other families of angiogenic growth factors, i.e., vascular endothelial growth factor and angiopoietins-1 and -2 via a canonical signaling pathway. However, previous studies revealed that exogenous Shh directly worked on peripheral endothelial cell tube formation under physiological conditions [4]. Immediately after these investigations, researchers found that RhoA/ROCK was involved in Shh-mediated the tube formation of peripheral vascular endothelial cells: Shh stimulates heterotrimeric G (i) protein and the small GTPase RhoA, and then results in the activation of Rho-dependent kinase (ROCK), and consequently mediates the formation of actin stress fibers, which is essential for the tube formation[5]. Recently, we have demonstrated Shh could protect neurons and astrocytes against oxidative stress, and can be secreted by astrocytes under oxidative stress [6-8]. These findings suggested that endogenous Shh may also function as an angiogenic factor after ischemia. However, the role of Shh in cerebral angiogenesis after ischemia has not been fully understood yet, especially in BMECs and under pathological conditions. In this study, we used an OGD model and a co-culture system of BMECs with astrocytes) to see if astrocyte-derived Shh directly mediates cerebral angiogenesis in vitro.

Materials and methods All studies were approved by the Animal Care Committee of Tongji Medical Collage of Huazhong University of Science and Technology, Wuhan, China.

Culture of Primary Rat Brain Microvascular Endothelial Cells (BMECs) Cerebral microvascular endothelial cells were isolated from rats from SD rats (n=4, 3–5 weeks of age), according to published protocols[9]. Briefly, rats were swabbed, sacrificed and then their brains were collected and removed of white matter, brain stem, surface vessels and leptomeninges with care. The isolated cerebral cortices were put into ice-cold PBS, minced into small pieces and then homogenized. The homogenates were centrifuged at 500 g for 5 min (4°C). The pellet was re-suspended in 20% BSA and centrifuged at 1000 g for 20 min (4°C). The microvessels in the lower layer were transferred to a new tube and washed once with PBS. The microvessel pellets were digested by using 0.1% collagenase II/dispase and 1000 U/ml DNase I at 37°C for 1 h. After centrifugation at 500 g for 5 min (4°C), the microvessel pellets were re-suspended in 10 ml M131 medium supplemented with microvascular growth supplement (MGS), 100 U/ml penicillin and 100 U/ml streptomycin. The cell suspension was seeded into a 75 cm2 flask, and 3-6 passage BMECs were used. BMECs were incubated at 37° Cin humidified 5% CO_2/95% air.

Culture of primary cortical astrocytes Cortical astrocytes were harvested from the brain of 1-day-old rats by following a previously reported method with some modifications[10]. Briefly, cerebral cortices were isolated, cleaned of white matter and meninges, minced, and digested with trypsin (0.25 mg/mL) and DNase (0.1 mg/mL) for 20 min at 37 °C. The dissociated cells were diluted with growth medium (high glucose Dulbecco's modified Eagle's medium (DMEM) supplemented with 10% FBS and 1% penicillin/streptomycin), seeded onto poly-L-lysine pre-coated 75 cm^2 plastic flasks at a density of 2×10^5 cells/cm^2, and maintained in a humidified 5% CO_2 incubator at 37 °C. After 14 days, the flasks were sealed and gently shaken at 260 rpm for 18 h to remove the loosely adherent oligodendrocytes and microglial cells from the monolayer of astrocytes. The remaining cells were identified morphologically by glial fibrillary acidic protein (GFAP) immunohistochemical staining. Over 95% of the cells were found to be GFAP-positive. The density of confluent astrocytes was ~1×10^5 cells/cm^2.

Oxygen Glucose Deprivation and Reperfusion Cells were exposed to OGD for 2, 4, 6 h and the oxygen and glucose supple was resumed 24 h late in accordance with a previous report with some modifications [11]. In brief, the culture medium was replaced with a hypoxic medium previously saturated for 20 min with 95% N_2 and 5% CO_2 and containing NaCl 116 mM, KCl 5.4 mM, $MgSO_4$ 0.8 mM, $NaHCO_3$ 26.2 mM, $NaH2PO_4$ 1 mM, $CaCl_2$ 1.8 mM, glycine 0.01 mM. Hypoxic conditions were maintained by using a hypoxia chamber (temperature 37°C, atmosphere 95% N2 and 5% CO_2). Re-oxygenation was achieved by returning to normoxic conditions (37°C in a humidified 5% CO_2 atmosphere).

Co-culture of Astrocytes and BMECs Co-culture model was established by employing a previously reported method with some modifications[12]. Briefly, confluent astrocytes and BMECs were trypsinized, re-suspended, and adjusted to 5×10^5 cells/ml. Astrocytes were plated onto the transwell inserts (corning costar, 3.0 μm) at 1×10^5 cells per insert, while equal amount of BMECs were plated onto 24-well plates. Medium was changed every 3 days until processed for further experiments.

Immunofluorescent Staining After fixation in 4% paraformaldehyde solution and permeabilization by 0.2% Triton X-100 in PBS, cells were kept in 5% PBS-diluted normal horse serum for 30 min to block non-specific binding. Cells were then incubated separately with rabbit anti-VWF (Abcam, 1:100), rabbit anti-CD31 (Abcam, 1:100), rabbit anti-ZO-1 (Abcam, 1:100) antibodies overnight, and finally incubated with fluorescein isothiocyanate (FITC)-labeled goat anti-rabbit antibody and tetramethyl rhodamine isothiocyanate (TRITC)-labeled mouse anti-rabbit antibody, and then DAPI. Cells were examined for immunofluorescent staining under a confocal microscope (Olympus, USA).

ELISA 100 μL medium was collected from the culture of BMECs alone, co-culture of BMECs and astrocytes treated with cyclopamine (Cyc) or the co-culture without Cyc treatment and detected for Shh levels by using a rat-specific Shh ELISA kit (USCNK Lifesciences, China) in accordance with the instructions.

Observation of Tube formation Basement membrane matrix (Matrigel, BD Biosciences) was thawed at 4°C, and 300 μl was used to coat each well of a 24-well plate. The plate was incubated for 30 minutes at 37°C to polymerize the Matrigel. BMECs (5×10^4 cells/100 μl) were suspended in M131 containing MGS, plated into a Matrigel-coated well and incubated for 24 hours at 37°C. Tube length was quantitatively determined at 40× magnifications from pictures captured. Each sample was examined in 3 randomly selected fields and the examination was repeated 3 times.

Proliferation Assay Cell proliferation was observed by using immunofluorescent staining with a proliferation marker Ki-67 (rabbit anti-Ki-67, Abcam, 1:100) as aforementioned. The Ki-67-positive cells were counted at 200× magnifications from the pictures captured. Each sample was observed in 3 randomly chosen fields and the observation was repeated 3 times

Wound Healing Assay Cells (5×105 per well) were seeded into 24-well plates and allowed to adhere for 24 h. Confluent monolayer cells were scratched by using a 200 μl pipette tip and then washed 3 times with 1×PBS to clear cell debris and suspension cells. Fresh serum-free medium was added, and the cells were allowed to heal for 24 h. Photographs were taken at the same site 0, 24 h after the injury. The healing of the wounds was assessed by measuring the wound gap.

Immunoblotting Cells were harvested and lysed in lysis buffer (50 mM Tris-HCl, 150 mM NaCl, 1% Nonidet P-40, 0.5% sodium deoxycholate, 0.1% SDS, and 1 mM phenylmethylsulfonyl fluoride). A Bio-Rad protein assay kit was used to determine protein concentrations, with bovine serum albumin (BSA) acting as a reference. Samples containing 30 μg of protein were put on 10% SDS-polyacrylamide gels and electrophoretically transferred to nitrocellulose membranes. Membranes were incubated with specific primary antibodies, rabbit anti-RhoA antibody (Abcam, 1:200), rabbit anti-ROCK antibody (Abcam, 1:200), rabbit anti-β-actin antibody (Abcam, 1:2000), and then incubated with horseradish peroxidase-conjugated secondary antibody (Sigma 1:10000). Proteins were visualized with a Super Signal West Pico chemiluminescence kit (Thermo Scientific, USA).

Quantitative Real-time Reverse Transcriptase-polymerase Chain Reaction (RT-PCR) RNA was isolated from 3×105 cells by RNA STAT-60 kit (TEL-TEST Electronics Labs Inc, Austin, TX, USA) according to the manufacturer's instructions. Total RNA was reversely transcribed with a Taqman cDNA Synthesis Kit (Applied Biosystems, Foster City, CA, USA) and amplified by using a Taqman 7500 (Applied Biosystems). Primer and probe sequences are: forward 5'-GCA GGT AGA GTT GGC TTT ATG-3' and reverse 5'-GCT TCA TTT TGG CTA ACT CCC-3' for RhoA; forward 5'-TGG ACC TTT CGG ATT CAA CTA-3' and reverse 5'-TGC TGC TCA CCA CAA CAT ACT-3' for RhoA; forward 5'-TGG AAT CCT GTG GCA TCC ATG AAA C-3'and reverse 5'-TAA AAC GCAGCT CAG TAA CAG TCC G-3' for β-actin. The relative expression of each mRNA was calculated by the comparative threshold cycle (CT) method and normalized to β-actin expression.

siRNA Transfection Lentivirus was commercially obtained and titration was performed according to the directions of the manufacturer (Genechem, China). siRNA-mediated knockdown of RhoA (GenBank accession number NM_057132) was achieved by transfection of the virus, by using a siRNA oligonucleotides kit (siRNA1, siRNA2 or siRNA3), into BMECs in accordance to the kit instruction. A commercial procured non-targeting siRNA from the same corporation was used as negative control. The incorporation of siRNAs into BMECs was verified by fluorescence microscopy. RhoA expression in siRNA-transfected BMECs was detected by Western blotting using the rabbit-anti RhoA antibody (1:200) and RT-PCR.

Statistical Analysis Student's t-test was used to determine statistical significance. All P values were derived from at least 3 independent experiments. A value of $P<0.05$ was accepted as statistically significant.

Results

Enhancing Effect of Shh Secreted by Activated Astrocytes on Capillary-like Tube Formation in BMECs after OGD

Cells isolated from cerebral microvessels formed a confluent monolayer and exhibited cobblestone pattern (Fig1A). More than 95% of these cells were labeled with vWF (Fig. 1B), CD31 (Fig. 1C) and ZO-1 (Fig. 1D). We compared the levels of Shh in brain microvascular endothelial cells (BMECs), astrocytes and neurons after OGD. Results showed that 2, 4, 6-h OGD increased the levels of Shh in both BMECs (1.61±0.11-folds, 4.30±0.77-folds, 2.57±0.42-folds of normal control, $P=0.139$, $P<0.001$, $P<0.01$ vs. normal control, respectively, Fig. 1E) and astrocytes (1.97±0.18-folds, 5.57±0.93-folds, 9.88±1.92-folds of normal control, $P=0.301$, $P<0.001$, $P<0.001$ vs. normal control, respectively, Fig. 1F), but decreased the levels in neurons (0.71±0.08-folds, 0.51±0.03-folds, 0.49±0.04-folds of normal control, $P<0.001$, $P<0.001$, $P<0.001$ vs. normal control respectively, Fig. 1G).To examine whether Shh, a soluble protein, secreted by astrocytes after stroke promotes angiogenesis, we performed a capillary-like tube formation assay in vitro. Co-culture of BMECs with astrocytes 4 h after OGD significantly increased the tube formation compared with culture of BMECs alone after OGD and co-culture of BMECs with normally incubated astrocytes (5.18±0.26-folds vs. 2.43±0.12-folds, or 5.18±0.26-folds vs. 2.75±0.14-folds, $P<0.001$, $P<0.001$ vs. None group or normal group respectively, Fig. 1H-J, Fig. 1L), while co-culture of BMECs with normally incubated astrocytes did not significantly increase the tube formation (2.75±0.14-folds vs. 2.43±0.12-folds, $P=0.0528$, Fig. 1H, Fig. 1I, and Fig. 1L). Cyclopamine, an Shh antagonist, significantly attenuated capillary-like tube formation after OGD (2.85±0.15-folds vs. 5.18±0.26-folds, $P<0.001$, Fig. 1J, Fig. 1K, and Fig. 1L). Moreover, ELISA showed that Shh in the supernatant collected from the co-culture of BMECs with astrocytes after OGD was higher than that collected from the co-culture of BMECs after OGD with normally incubated astrocytes, and Shh in the latter was higher than that collected from the culture of BMECs alone after OGD (17.21±2.84-folds vs. 3.47±0.55-folds vs. 3.47±0.19-folds, $P<0.001$, $P<0.001$, respectively, Fig. 1M).

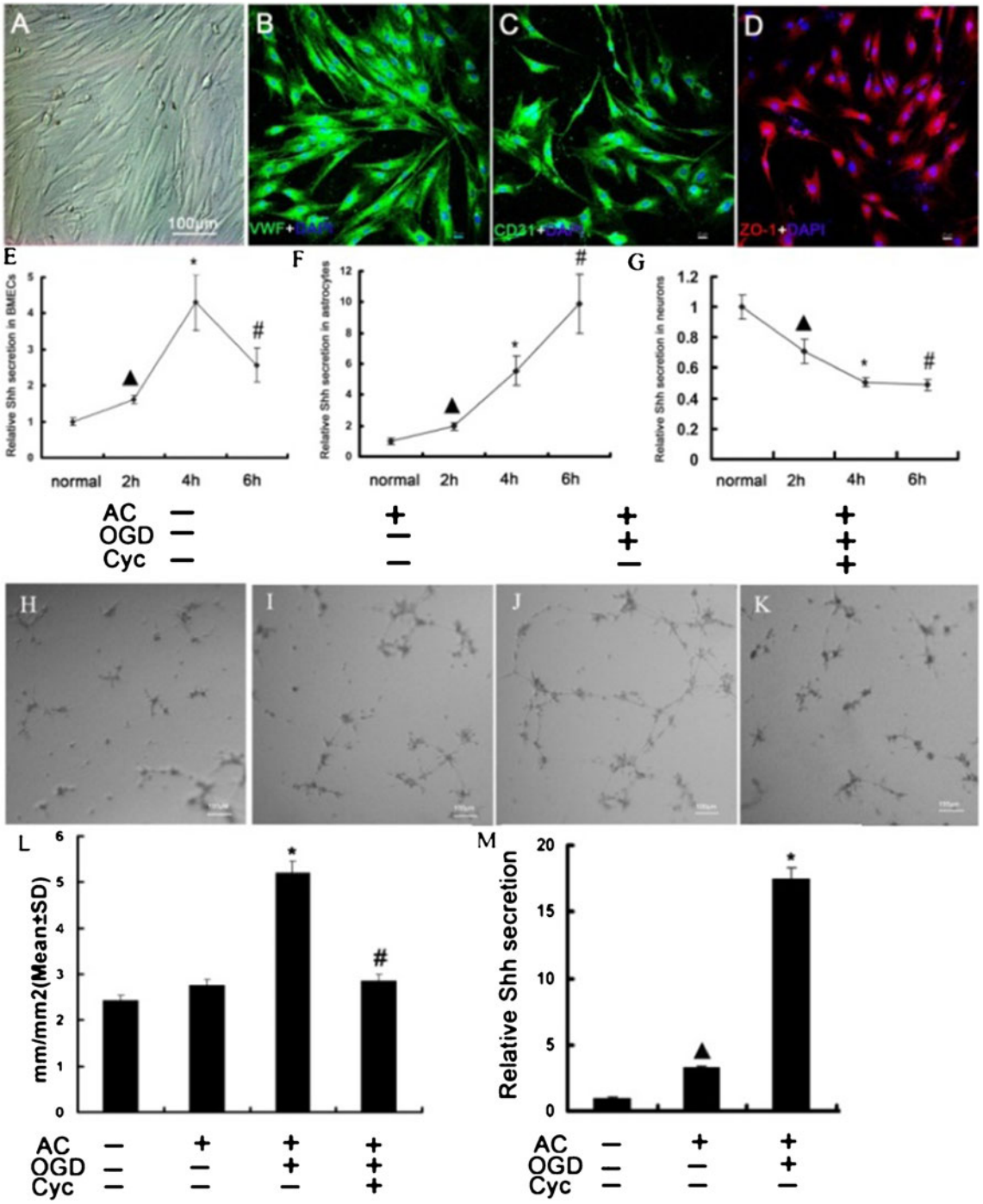

Fig. 1 Enhancing Effect of Shh Secreted by Activated Astrocytes on Capillary-like Tube Formation in BMECs after OGD. **1A-D** Cells isolated from cerebral microvessels formed a confluent monolayer and exhibited cobblestone morphology, and immunofluorescent staining showed that these cells were VWF- (green), CD31- (green) and ZO-1-positive (red). Bar=100μm for 1A, Bar=25μm for 1B, 1C, 1D. Brain microvascular endothelial cells (BMECs), astrocytes and neurons were treated oxygen glucose deprivation (OGD) for 2 h, 4 h, 6 h, and then re-perfused for 24 h. The medium was collected and the concentration of Shh in the medium was examined by ELISA. **1E-G** After 2-, 4-, 6-h OGD and 24-h reperfusion, the Shh secreted by BMECs, astrocytes and neurons were increased as compared with normally cultured BMECs, and the Shh secreted by BMECs after 6-h OGD and reperfusion was lower than that by BMECs after 4-h OGD and 24-h reperfusion. **1H-K** The representative pictures of tuber formation in BMECs cultured alone after 4- h OGD (control group), BMECs co-cultured with astrocytes after 4-h OGD (none group), and BMECs co-cultured with astrocytes after 4-h OGD (OGD group) and BMECs co-cultured with astrocytes after 4-h OGD, and treated with cyclopamine (Cyc group). **1L** Capillary-like tubes were microscopically observed. Fields of vision were randomly selected and pictures were captured and quantitatively detected by using Image J software package. Data were expressed as mean±SD (n=3), *P<0.05 *vs.* none group, $^{\#}P<0.05$ *vs.* OGD group. Bar=100μm. **1M** The media were collected and then the concentrations of Shh were detected by a commercially available ELISA kit. Data were expressed as mean±SD (n=3), $^{\blacktriangle}P<0.05$ *vs.* control group, $^{*}P<0.05$ *vs.* none group, $^{\#}P<0.05$ *vs.* OGD group

Promoting Effect of Shh Secreted by Activated Astrocytes on the Proliferation and Migration of BMECs after OGD

To examine whether Shh secreted by activated astrocytes could promote proliferation and migration of BMECs, which are the key steps of cerebral angiogenesis, we performed immunofluorescent staining with Ki-67, a mark of cellular proliferation, and wound healing assay respectively. Co-culture of BMECs after OGD with normally cultured astrocytes significantly increased the number of Ki67-positive BMECs compared with BMECs alone after OGD group (14.92±2.37% vs. 7.54±0.69%, P< 0.001, Fig. 2A, Fig. 2B and Fig. 2M). When BMECs were co-cultured with astrocytes after OGD, the number of Ki67-positive BMECs was further increased compared with BMECs after OGD co-cultured with normally incubated astrocytes (37.89± 0.87% vs. 14.92±2.37%, P<0.001, Fig. 2B, Fig. 2C and Fig. 2M), while cyclopamine decreased the number of Ki67-positive BMECs significantly (37.89±0.87% vs.25.92±1.85%, P< 0.001, Fig. 2C, Fig. 2D and Fig. 2M). Wound healing assay showed the similar results: The relative migration distance of BMECs after OGD co-cultured with normally incubated astrocytes was significantly increased as compared with BMECs cultured alone after OGD (1.38±0.21-folds vs.1.00±0.22-folds, P<0. 05, Fig. 2E, Fig. 2F, Fig. 2I, Fig. 2J and Fig. 2N). When BMECs were co-cultured with astrocytes after OGD, the relative migration distance further increased as compared BMECs after OGD co-cultured with normally incubated astrocytes (1.98± 0.40-folds vs. 1.38±0.21-folds, P<0. 005, Fig. 2F, Fig. 2G, Fig. 2J, Fig. 2K and Fig. 2N), and cyclopamine also decreased the relative migration distance (0.93±0.10-folds vs. 1.98±0.40-folds, P=0. 00163, Fig. 2G, Fig. 2H, Fig. 2K, Fig. 2L, Fig. 2N).

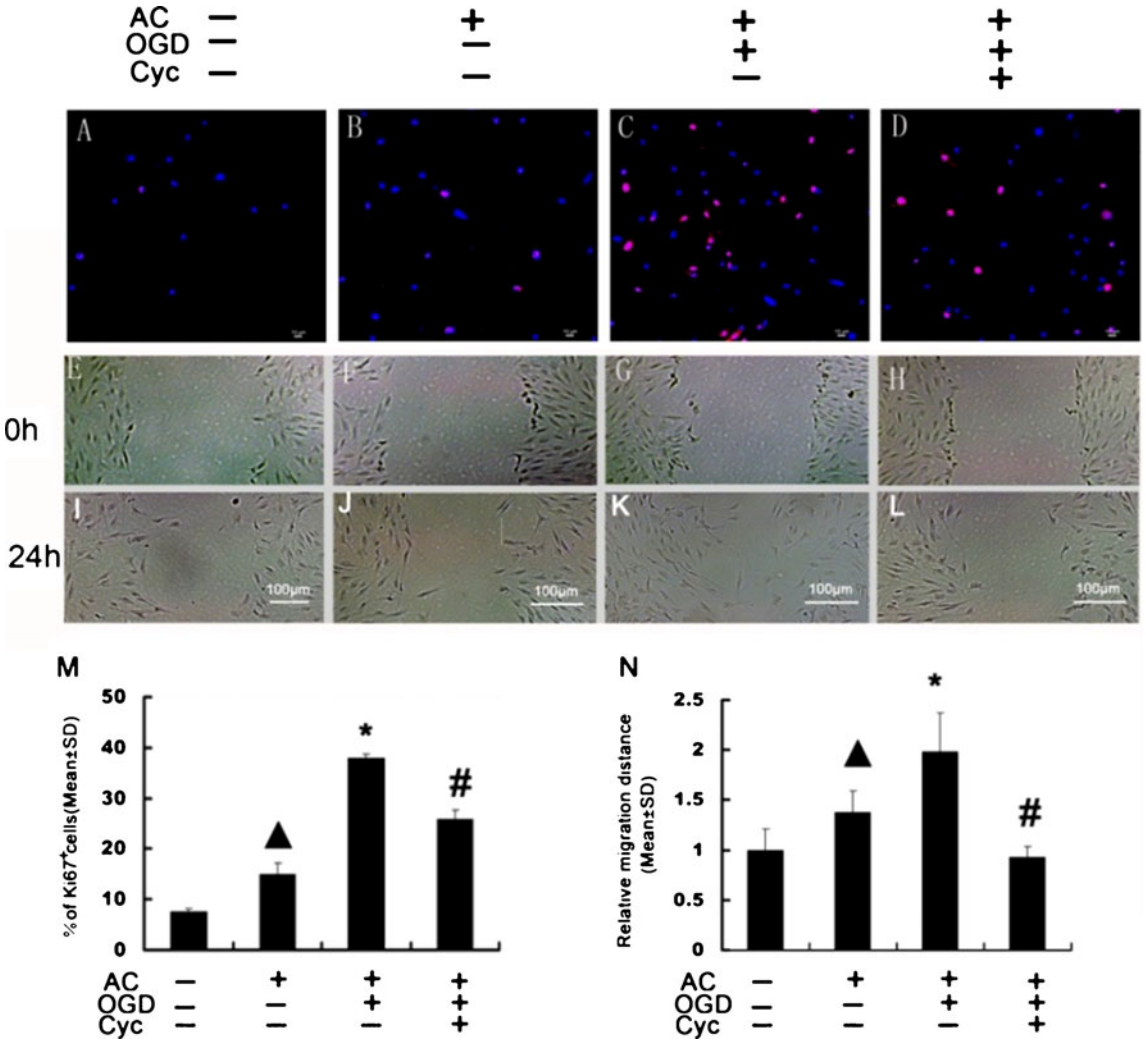

Fig. 2 Promoting Effect of Shh Secreted by Activated Astrocytes on the Proliferation and Migration of BMECs after OGD. **2A-D** the representative pictures of proliferation in the aforementioned 4 groups (control group, none group, OGD group and Cyc group). **2M** Fields of vision were randomly selected, and pictures were captured and quantitatively detected. The Ki-67-positive cells (red) were counted (n=3). Data were expressed as mean±SD (n=3), ▲P<0.05 *vs.* none group, *P<0.05 *vs.* none group, #P<0.05 *vs.* the OGD group. Bar=10μm. **2E-L** the representative pictures of migration in the aforementioned 4 groups (control group, none group, OGD group and Cyc group). **2N** Fields of vision were randomly selected, and pictures were then captured and quantitatively detected. The relative migration distances were detected by the Image J software package (n=3). Data were expressed as mean±SD(n=3), ▲P<0.05 *vs.* control group, *P< 0.05 *vs.* none group, #P<0.05 *vs.* OGD group. Bar=100μm

Activation of RhoA / ROCK Pathway by astrocytes-derived Shh in BMECs after OGD RhoA/ROCK pathway, essential to cellular proliferation and migration, is involved in angiogenesis. To examine whether astrocytes-derived Shh can activate RhoA/ROCK pathway in BMECs, we detected the key molecules by Western blotting and RT-PCR. It was found that the expression of RhoA (Fig. 3A, Fig. 3B and Fig. 3E), ROCK (Fig. 3A, Fig. 3D and Fig. 3F) protein and mRNA in BMECs co-cultured with astrocytes after OGD was up-regulated as compared with BMECs cultured alone after OGD and BMECs after OGD co-cultured with normally incubated astrocytes, while the expression of RhoA, ROCK protein and mRNA was significantly down-regulated by treating BMECs with cyclopamine. Moreover, astrocytes-derived Shh is also involved in the phosphorylation of RhoA. This study showed that the expression of GTP-RhoA was much higher in BMECs co-cultured with astrocytes after OGD than in BMECs cultured alone after OGD and in BMECs after OGD co-cultured with normally incubated astrocytes, and cyclopamine reversed this change (Fig. 3A, Fig. 3C).

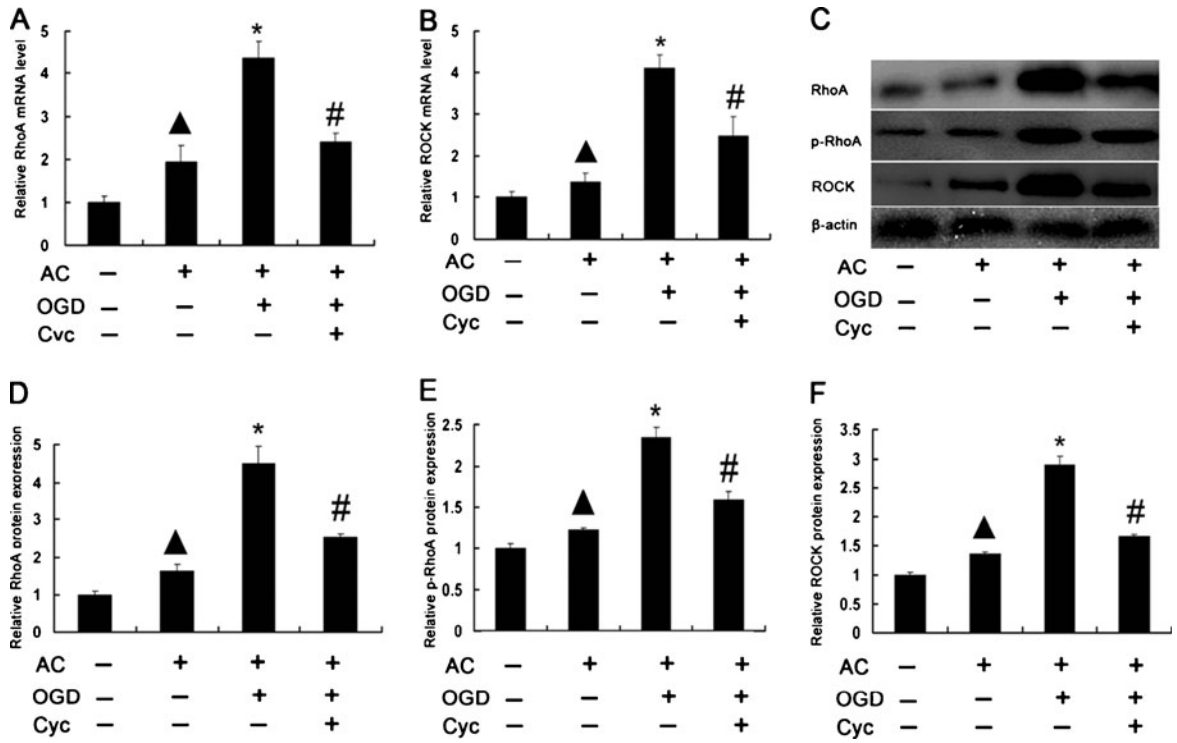

Fig. 3 Activation of RhoA / ROCK Pathway by astrocytes-derived Shh in BMECs after OGD. **3A** Cells were collected from the aforementioned 4 groups (control group, none group, OGD group and Cyc group) and cells were immediately lysed in RIPA buffer and exposed to microwave for 5 s, and then Laemmli buffer was added and samples were detected for total RhoA (RhoA), phospho-RhoA (P-RhoA), and ROCK by using Western blotting, and β-actin was used as an internal control. **3B-D** The RhoA, P-RhoA and ROCK were densitometrically determined by using Image J software, and normalized against β-actin. The values obtained from control group were taken as 1. The results were expressed as mean±SEM (n=3), $^{\blacktriangle}P<0.05$ *vs.* none group, $^{*}P<0.05$ *vs.* none group, $^{\#}P<0.05$ *vs.* OGD group.3E-F RhoA and ROCK gene expression was detected by RT-PCR. The values obtained from the control group was taken as 1. The results were expressed as mean±SEM (n=3), $^{\blacktriangle}P<0.05$ *vs.* control group, $^{*}P<0.05$ *vs.* none group, $^{\#}P<0.05$ *vs.* OGD group

RhoA / ROCK Pathway-mediated Promoting Effect of activated astrocytes on Tube Formation, Proliferation and Migration of BMECs after OGD The tube formation of BMECs treated with Y27632, a specific inhibitor of ROCK, and co-cultured with astrocytes after OGD was decreased as compared with non-treated BMECs (5.54±0.28 *vs.* 2.74±0.14, $P<0.001$, Fig. 4A-C). The treatment with Y27632 also decreased the number of Ki-67-positive BMECs (37.21±3.36% *vs.*29.05±1.10%, $P<0.01$, Fig. 4D-F) and migration distance (100±11.2% *vs.*45.31±8.60%, $P<0.01$, Fig. 6G-K) when compared with their non-treated counterparts. RNA interference by transfection with lentivirus showed that, after RNAi, both RhoA mRNA and protein expression was decreased significantly (Fig. 5A-C). The tube formation of BMECs in the siRNA group was significantly decreased compared with the vector group (5.55±0.28 vs. 1.85±0.09, P<0.01, Fig. 5D-F). siRNA also decreased Ki-67-positive BMECs (37.56±2.17% vs.23.83±2.75%, P<0.01, Fig. 5G-I) and migration distance

(100±4.79% vs.32.37±6.86%, P<0.001, Fig. 7J-N) compared with the vector group.

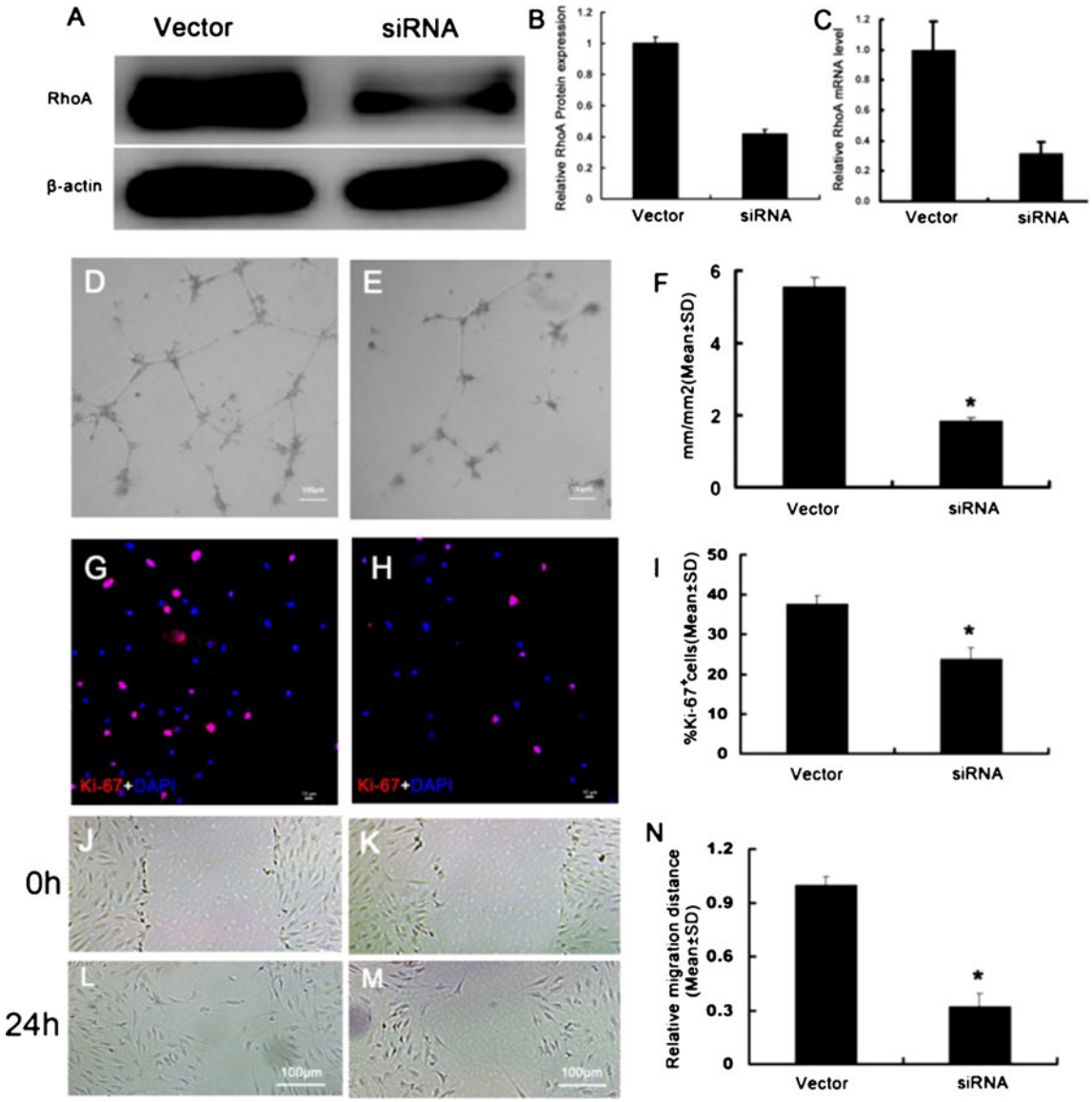

Fig. 4 Increase of tuber formation, proliferation and migration of BMECs Induced by activated astrocytes after OGD is mediated by RhoA. **4A-B** the RhoA protein expression in BMECs transfered with non-targeting siRNA and co-cultured with astrocytes after 4-h OGD (vector group) and in BMECs transfered with targeting siRNA and co-cultured with astrocytes after 4-h OGD (siRNA group) (n=3). 4C the RhoA mRNA levels in BMECs transferred with non-targeting siRNA and co-cultured with astrocytes after 4 hours OGD (vector group) and BMECs transferred with targeting siRNA and co-cultured with astrocytes after 4- h OGD (siRNA group) (n=3).**4D**, **4E** the representative pictures of tube formation in BMECs transferred with non-targeting siRNA and co-cultured with astrocytes after 4- h OGD (vector group) and BMECs transferred with targeting siRNA and co-cultured with astrocytes after 4-h OGD (siRNA group). **4F** Capillary-like tubes were observed by microscopy, random fields of vision were selected, and pictures were captured and quantified by Image J software. Data were expressed as mean±SD (n=3), **P*<0.05 versus the vector group. **4G**,**4H** the representative pictures of proliferation of BMECs transfered non-targeting siRNA and co-cultured with astrocytes after 4 hours OGD (vector group) and BMECs transfered targeting siRNA and co-cultured with astrocytes after 4 hours OGD (siRNA group). **4I** Fields of vision were randomly selected, pictures were captured and quantified. The number of Ki-67 positive cells (red) was counted (n=3). Data represent the mean±SD (n=3), **P*<0.05 versus the vector group. Bar=10μm. **4J-M** the representative pictures of migration of BMECs transfered non-targeting siRNA and co-cultured with astrocytes after 4 hours OGD (vector group) and BMECs transfered targeting siRNA and co-cultured with astrocytes after 4 hours OGD (siRNA group). **4N** Fields of vision were randomly selected, pictures were captured and quantified. The relative migration distances were detected by image J software (n=3). Data were expressed as mean±SD (n=3), **P*<0.05 *vs.* the vector group. Bar=100μm

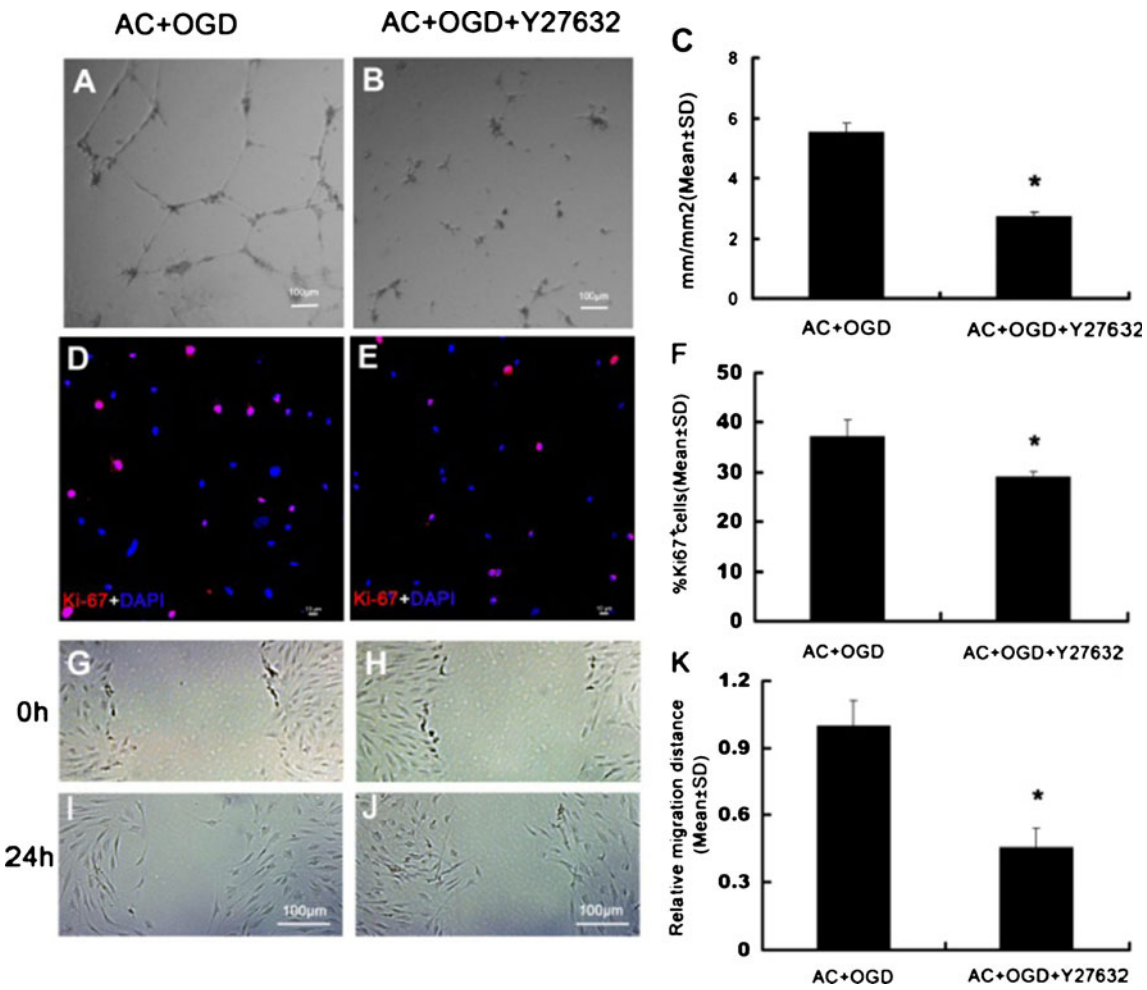

Fig. 5 Increase of tuber formation, proliferation and migration of BMECs Induced by activated astrocytes after OGD Is Rho Kinase Dependent. **5A**, **5B** the representative pictures of tube formation of BMECs co-cultured with astrocytes after 4 hours OGD (OGD group), or BMECs co-cultured with astrocytes after 4 h OGD, added Y27632 (Y27632 group). **5C** Capillary-like tubes were observed by microscopy, fields of vision were randomly selected, and pictures were captured and quantitatively detected by Image J software. Data were expressed as mean±SD (n=3), **P*<0.05 *vs.* the OGD group. **5D**, **5E** the representative pictures of proliferation of BMECs co-cultured with astrocytes after 4 hours OGD (OGD group), or BMECs co-cultured with astrocytes after 4 h OGD, added Y27632 (Y27632 group). **5F** Fields of vision were randomly selected, and pictures were captured and quantitatively detected. The number of Ki-67-positive cells (red) was counted (n=3). Data were expressed as mean±SD (n=3), **P*<0.05 *vs.* the OGD group. Bar=10μm. **5G-J** the representative pictures of migration of BMECs co-cultured with astrocytes after 4 hours OGD (OGD group), or BMECs co-cultured with astrocytes after 4 hours OGD and added Y27632 (Y27632 group).**5K** Fields of vision were randomly selected, and pictures were captured and quantitatively detected. The relative migration distances were detected by image J software (n=3). Data were expressed as mean±SD (n=3), **P*<0.05 *vs.* the OGD group. Bar=100μm

Discussion

The present study demonstrated that, after ischemia, astrocytes-derived Shh could directly promote cerebral angiogenesis *in vitro* via Rho/ROCK pathway. Shh, as a mitogen and morphogen, is involved in cell proliferation, migration in a variety of cells in the development and after tissue injury. However, whether Shh takes part in the ischemia-induced cerebral angiogenesis remains unclear. Our findings exhibited that Shh in culture medium was up-regulated after OGD and the Shh expression in astrocytes was substantially higher than in BMECs. These results are consistent with those reported by a previous study [13], which showed that the expression of Shh mRNA was elevated after 16-hour exposure to hypoxia, and astrocytes contained much more Shh mRNA than neurons. In this study, the time of exposure to OGD was much shorter than the time of hypoxic exposure reported by Sims *et al*. Another *in vivo* study also yielded similar results that Shh in the brain was up-regulated after trauma. Previous studies by us and other researchers also suggested, after ischemia, Shh is secreted in large quantity and astrocytes, rather than BMECs or neurons, may be the principal source[6,7]. The increased expression of Shh may result from the transcription of more Shh genes, as supported by a previous study which demonstrated that hypoxia-induced Shh mRNA expression might be

mediated by HIF-1. However, it is unclear what causes the up-regulation of Shh after ischemia.

It is well known that astrocytes are reactive and play a crucial role in retinal angiogenesis during development or under pathological conditions. Previous studies have revealed that, in brain, astrocytes-conditioned medium could induce mitogenesis in BMECs and astrocytes-derived epoxyeicosatrienoic acids could regulate cerebral angiogenesis [14]. This study suggested that astrocytes may also play a crucial role in cerebral angiogenesis after ischemia by secreting glycoprotein Shh. Moreover, cyclopamine, a special Shh antagonist, could significantly reverse the increased angiogenesis induced by activated astrocytes, indicating that Shh may participate in astrocytes-mediated angiogenesis. In this study, we found that endogenous Shh is involved in astrocytes-mediated tube formation after OGD. However, it is of note that cyclopamine treatment could not completely reverse the increased angiogenesis induced by activated astrocytes, suggesting that some other angiogenic factors secreted by astrocytes or released by other mechanisms may also contribute to the change after OGD.

Furthermore, mounting evidence has showed that RhoA/ROCK pathway is essential to angiogenesis of endothelial cells. RhoA/ROCK pathway is involved in VEGF-induced angiogenesis, and fasudil, a ROCK inhibitor, suppresses the angiogenesis [15]. RhoA/ROCK is also involved in tumor angiogenesis and HA1077, another ROCK inhibitor, inhibits glioma-induced angiogenesis [16]. Previous studies also demonstrated that Shh signaling is transducted by RhoA/ROCK. In view of this, we examined the role of RhoA/ROCK pathway in the tube formation induced by astrocyte-derived Shh, and the results suggested that RhoA/ROCK cascade participates in endogenous Shh-induced angiogenesis after ischemia. Astrocytes after OGD-induced up-regulation of angiogenesis is significantly reversed by down-regulating RhoA by RNA interference or by treatment with Y27632, a special ROCK antagonist, and the finding were coincident with those reported by Renault *et al* [4]and Chinchillas *et al* [17]. However, two notions have to be stressed: The first is that the signal transduction pathway of Shh concerning angiogenesis is quite complicated. Apart from the canonical pathway, Shh may also activate the phosphoinositide kinase 3 (PI3K)/Akt pathway[7] and RhoA/ROCK pathway. Moreover, Shh induces expression of chicken ovalbumin upstream promoter transcription factor II (COUP TFII) in mouse embryonic carcinoma cells and extracellular signal-regulated kinases 1/2 (ERK 1/2) and protein kinase C (PKC) in fibroblasts. Second, the cross-talk between the Shh-related signal transduction pathways is quite common. For instance, PI3K/Akt may also mediate Shh/RhoA/ROCK signal cascade [18].

This study demonstrated that astrocytes-derived Shh can also directly function as an angiogenic factor after ischemia/OGD, which, at the same time, serves as an indirect angiogenic factor by controlling two families of angiogenic factors, i.e., VEGF and angiopoietin. Furthermore, our data also showed that Shh also promoted the proliferation and migration in BMECs via RhoA/ROCK pathway. Similar results were also reported by previous documents that RhoA/ROCK rather than Gli, is essential to Shh-induced fibroblast migration and cytoskeletal rearrangement.

To sum up, this study, by using an *in vitro* OGD model and a co-culture system of BMECs and astrocytes, provided the evidence that astrocytes-derived Shh is required for cerebral angiogenesis after ischemia. RhoA/ROCK pathway, not Gli, activated by astrocytes-derived Shh, directly induces post-ischemia cerebral angiogenesis. Astrocytes may be a promising target for stroke therapy, and Shh/RhoA signal pathway may be a novel alternative to induce angiogenesis.

Acknowledgements

This work was supported by grants 81070938 from the Program of National Natural Science Foundation of China (to BH), grant 81101905 from the Program of National Natural Science Foundation of China (to LM), New Century Excellent Talents in University NCET-10-0406 (to BH) and the Fundamental Research Funds for the Central Universities, HUST No.2010JC028 (to BH).

References

1. Liepert J, Bauder H, Wolfgang HR, Miltner WH, Taub E, et al. (2000) Treatment-induced cortical reorganization after stroke in humans. Stroke 31: 1210-1216.
2. Sa-Pereira I, Brites D, Brito MA (2012) Neurovascular unit: a focus on pericytes. Mol Neurobiol 45: 327-347.
3. He H, Zhang H, Li B, Li G, Wang Z (2010) Blockade of the sonic hedgehog signalling pathway inhibits choroidal neovascularization in a laser-induced rat model. J Huazhong Univ Sci Technolog Med Sci 30: 659-665.
4. Renault MA, Roncalli J, Tongers J, Thorne T, Klyachko E, et al. (2010) Sonic hedgehog induces angiogenesis via Rho kinase-dependent signaling in endothelial cells. J Mol Cell Cardiol 49: 490-498.
5. Polizio AH, Chinchilla P, Chen X, Kim S, Manning DR, et al. (2011) Heterotrimeric Gi proteins link Hedgehog signaling to activation of Rho small GTPases to promote fibroblast migration. J Biol Chem 286: 19589-19596.
6. Dai RL, Zhu SY, Xia YP, Mao L, Mei YW, et al. (2011) Sonic hedgehog protects cortical neurons against oxidative stress. Neurochem Res 36: 67-75.
7. Xia YP, Dai RL, Li YN, Mao L, Xue YM, et al. (2012) The protective effect of sonic hedgehog is mediated by the propidium iodide 3-kinase/AKT/Bcl-2 pathway in cultured rat astrocytes under oxidative stress. Neuroscience 209: 1-11.
8. Zhou Y, Dai R, Mao L, Xia Y, Yao Y, et al. (2010) Activation of Sonic hedgehog signaling pathway in S-type neuroblastoma cell lines. J Huazhong Univ Sci Technolog Med Sci 30: 271-277.

9. Diglio CA, Grammas P, Giacomelli F, Wiener J (1982) Primary culture of rat cerebral microvascular endothelial cells. Isolation, growth, and characterization. Lab Invest 46: 554-563.
10. McCarthy KD, de Vellis J (1980) Preparation of separate astroglial and oligodendroglial cell cultures from rat cerebral tissue. J Cell Biol 85: 890-902.
11. Allen C, Srivastava K, Bayraktutan U (2010) Small GTPase RhoA and its effector rho kinase mediate oxygen glucose deprivation-evoked in vitro cerebral barrier dysfunction. Stroke 41: 2056-2063.
12. Kim JA, Tran ND, Wang SJ, Fisher MJ (2003) Astrocyte regulation of human brain capillary endothelial fibrinolysis. Thromb Res 112: 159-165.
13. Sims JR, Lee SW, Topalkara K, Qiu J, Xu J, et al. (2009) Sonic hedgehog regulates ischemia/hypoxia-induced neural progenitor proliferation. Stroke 40: 3618-3626.
14. Zhang C, Harder DR (2002) Cerebral capillary endothelial cell mitogenesis and morphogenesis induced by astrocytic epoxyeicosatrienoic Acid. Stroke 33: 2957-2964.
15. Washida N, Wakino S, Tonozuka Y, Homma K, Tokuyama H, et al. (2011) Rho-kinase inhibition ameliorates peritoneal fibrosis and angiogenesis in a rat model of peritoneal sclerosis. Nephrol Dial Transplant 26: 2770-2779.
16. Nakabayashi H, Shimizu K (2011) HA1077, a Rho kinase inhibitor, suppresses glioma-induced angiogenesis by targeting the Rho-ROCK and the mitogen-activated protein kinase kinase/extracellular signal-regulated kinase (MEK/ERK) signal pathways. Cancer Sci 102: 393-399.
17. Chinchilla P, Xiao L, Kazanietz MG, Riobo NA (2010) Hedgehog proteins activate pro-angiogenic responses in endothelial cells through non-canonical signaling pathways. Cell Cycle 9: 570-579.
18. Polizio AH, Chinchilla P, Chen X, Manning DR, Riobo NA (2011) Sonic Hedgehog activates the GTPases Rac1 and RhoA in a Gli-independent manner through coupling of smoothened to Gi proteins. Sci Signal 4: pt7.

AR-002

Sonic hedgehog (Shh) Regulates the Expression of Angiogenic Growth Factors in Oxygen-Glucose-Deprived Astrocytes by Mediating the Nuclear Receptor NR2F2

Yanan Li*, Yuanpeng Xia*, Yong Wang, Lin Mao, Yuan Gao, Quanwei He, Ming Huang, Shengcai Chen, Bo Hu[△]
Department of Neurology, Union Hospital, Tongji Medical College, Huazhong University of Science and Technology, Wuhan, 430022, China.

*These authors contributed equally to this project.

[△]Correspondence should be addressed to Dr. Bo Hu, Department of Neurology, Union Hospital, Tongji Medical College, Huazhong University of Science and Technology, Wuhan, 430022, China.
E-mail: hubo@mail.hust.edu.cn

Running title: *Regulative Role of Sonic Hedgehog Signaling*

Abstract
Sonic Hedgehog (Shh) has been found to regulate the angiogenic growth factor such as VEGF, Ang-1 and Ang-2 during ischemic insults, but the underlying mechanism is not fully understood. In this study, we employed oxygen-glucose deprivate (OGD) in astrocytes to mimic the ischemia *in vitro*. We found that OGD could induce the expression of VEGF, Ang-1 and Ang-2, with the expression of Shh signaling components increased. Moreover, inhibiting the Shh signaling pathway with 5EI, a specific antibody, could decrease the expression of VEGF, Ang-1 and Ang-2. Moreover, administration of exogenous Shh could induce the expression of VEGF, Ang-1 and Ang-2 in astrocytes. The results of silencing Gli-1 or NR2F2, exhibited that exogenous Shh could regulate the expression of VEGF, Ang-1 and Ang-2 in astrocytes by activating the NR2F2, but not the Gli-1. These results suggested that Shh could regulate the angiogenic growth factor after ischemic insults in astrocytes, and the regulation was partially mediated by the NR2F2.
Keywords: sonic hedgehog (Shh), angiogenic growth factors, astrocytes, NR2F2

Introduction The morphogen sonic hedgehog (Shh) is a well-known indirect angiogenic factor, which up-regulates a wide array of angiogenic cytokines, angiopoietins-1, 2 (Ang-1, 2) and vascular endothelial growth factor (VEGF) and is involved in angiogenesis during embryogenesis and after ischemic insults [1, 2]. Moreover, Shh was found to be transiently up-regulated during the early phase of ischemic brain [3]. Our previous studies with rat model of MCAO also showed that Shh was up-regulated in response to oxidative stress and could promote functional recovery of brain after ischemia by enhancing expression of angiogenic growth factors, VEGF, angiopoietins (Angs) (data not shown).
Several studies revealed that Shh signaling may play a role in development and functionality of astrocytes [4]. Moreover, evidence has demonstrated that astrocytes were

capable of secreting VEGF, ang-1 and ang-2 after ischemia [5]. Our previous studies also found that Shh was mainly secreted by astrocytes under oxidative stress [4]. However, the exact mechanism by which Shh works in astrocytes under ischemic insults remains poorly understood. Thus, in this study, we employed an *in vitro* model of oxygen-glucose deprivation (OGD), to mimic the ischemic insults on astrocytes, with an attempt to explore the mechanisms of Shh regulating the expression of VEGF, Ang-1 and Ang-2.

Shh, as a secreted protein, could be activated during development and organ injury. In the canonical signaling pathway, Shh binds to Patched-1 (Ptc1) and then activates the transcriptional factors of Gli family and thereby regulates the expression of target genes [6, 7]. However, Pola *et al* have found that the Gli response elements were not present in VEGF or Shh promoter regions [8]. On the other hand, a Shh response element was identified in the NR2F2 promoter, which was different from Gli [9]. Therefore, in this study, we investigated the promoting effect of Shh on the expression of angiogenic growth factors via Gli or NR2F2.

NR2F2 is essential to neurogenesis and may be a major angiogenesis regulator under the tumor microenvironment. Disruption of NR2F2 in mice might lead to defects in angiogenesis and cardiovascular disorders, and eventually death at early embryonic stage [10, 11]. Moreover, NR2F2 is necessary for the induction of gliogenesis in neural stem/progenitor cells [12]. Therefore, we are led to postulate that NR2F2 might be involved in Shh-induced expression of angiogenic factors.

In the present study, we conducted a series of experiments *in vitro* to examine the possible direct angiogenic effects of Shh, to see if that NR2F2 mediates Shh-induced angiogenesis by up-regulating the expression of downstream target genes such as VEGF, Ang-1 and Ang-2.

Materials and Methods

Primary astrocytes culture Astrocytes for primary culture were taken from the brain tissue of Sprague-Dawley rats as previously described [4]. Briefly, dissociated cerebral cortices from 1-day-old embryos were minced and digested with trypsin (0.25 mg/mL) and DNase (0.1 mg /mL) for 20 min at 37 °C. The growth medium (high glucose Dulbecco's modified Eagle's medium (DMEM) supplemented with 10% FBS and 1% penicillin/streptomycin) was added into the cells, plated onto poly-L-lysine-coated 75 cm^2 plastic flasks at a density of 2×10^5 cells/cm^2, and stored in an incubator in 5% humidified CO_2 at 37 °C. After 14 days, the flasks were sealed and gently shaken at 260 rpm in order to remove the loosely adhered oligodendrocytes and microglial cells from the monolayer of astrocytes. The remaining cells were identified morphologically under a light microscope and by using immunohistochemical staining with glial fibrillary acidic protein (GFAP). Ninety-five percent of the cells were found to be GFAP-positive. The density of confluent astrocytes was ~1×10^5 cells/cm^2.

Drug treatment Astrocytes were incubated in a serum-free medium for 3 h before exposure to medium containing exogenous recombinant Shh (0.5 ng/ mL, 0.3 μg/mL, 3 μg/mL and 30 μg/mL dissolved in PBS, Curis, Cambridge, MA). Shh was employed to activate the Shh signaling pathway. A specific inhibitor of the Shh signaling pathway, 5EI (20 μM, LC Laboratories, USA), dissolved in ethanol, was used to block Shh signaling pathway. Astrocytes were treated with Shh (3 μg /ml) or 5E1 (10 μg /ml) and then were exposed to OGD for different times.

Oxygen Glucose Deprivation (OGD) Cells were exposed to OGD for 4, 8, and 12 h according to a previously reported technique with some modifications [13]. Briefly, the culture medium was replaced with a hypoxic medium previously saturated for 20 min with 95% N_2 and 5% CO_2 and containing 116 mM NaCl, 5.4 mM KCl, 0.8 mM MgSO4, 26.2 mM $NaHCO_3$, 1 mM NaH2PO4, 1.8 mM $CaCl_2$, 0.01 mM glycine. OGD conditions were maintained by using a hypoxia chamber (temperature 37°C, atmosphere 95% N_2 and 5% CO_2).

siRNA Transfection Lentivirus was commercially obtained and titration was performed by following kit instructions (Genechem, China). siRNA-mediated knockdown of Gli-1 and NR2F2 (GenBank accession number NM_057132) was attained by transfecting an siRNA into astrocytes by using oligonucleotides kit (siRNA1, siRNA2 or siRNA3) in accordance to the instructions. A commercially procured non-targeting siRNA from the same corporation was used as negative control. The incorporation of siRNAs into astrocytes was verified by fluorescence microscopy. Gli-1 and NR2F2 expression in siRNA-transfected astrocytes was detected by Western blotting and RT-PCR.

Quantitative Real-time Reverse Transcriptase-polymerase Chain Reaction (RT-PCR) RNA was isolated from 3×10^5 cells by RNA STAT-60 (TEL-TEST Electronics Labs Inc, Austin, TX, USA) according to the manufacturer's instructions. Total RNA was reversely transcribed by using a Taqman cDNA synthesis kit (Applied Biosystems, Foster City, CA, USA) and was amplified with a Taqman 7500 (Applied Biosystems, Foster City, CA, USA). Primer and probe sequences

are listed in Table1. The relative expression of each mRNA was calculated by using the comparative threshold cycle (CT) method and normalized to β-actin expression.

Immunoblot analysis Astrocytes were incubated in lysis buffer (50 mM Tris-HCl, 150 mM NaCl, 1% Nonidet P-40, 0.5% sodium deoxycholate, 0.1% SDS, and 1 mM phenylmethylsulfonyl fluoride) at 37 °C for 1 h before the experiment. A Bio-Rad protein assay kit was used to determine protein concentrations, with bovine serum albumin (BSA) acting as a reference. Samples containing 30 μg of protein were subjected to 12% SDS-polyacrylamide gel electrophoresis. Blots were transferred to nitrocellulose, blocked for 1 h at 21°C and incubated with primary antibody (rabbit anti-Ang-1 antibody (Santa Cruz, 1:200), rabbit anti-Ang-2 antibody (Santa Cruz, 1:200), rabbit anti-VEGF antibody (Santa Cruz, 1:200), rabbit anti-NR2F2 antibody (abcom, 1:1000), rabbit anti-β-actin antibody (Santa Cruz, 1:500) overnight at 4°C. Afterwards, membranes were incubated with horseradish peroxidase-conjugated secondary antibody (ICN Pharmaceuticals, 1:2000).

Data analysis For all the experiments, data were expressed as the mean±SD. Statistical analyses were performed by using Statistical Package for the Social Sciences (SPSS 13.0, USA). The two-tailed Student's *t*-test or One-way ANOVA followed by *post hoc* Fisher's LSD multiple comparison test was employed for significance assessment. A $P<0.05$ was considered to be statistically significant.

Results

Promoting effect of OGD on the expression of VEGF and Ang-2 in astrocytes Both real-time RT-PCR and Western blotting showed that, after OGD for different time periods, the mRNA level of VEGF and Ang-2 was substantially increased in a time-dependent manner as compared to the control group (Fig. 1A, 1C, 1D). The expression level of Ang-1 did not change significantly (Fig. 1B, 1D).

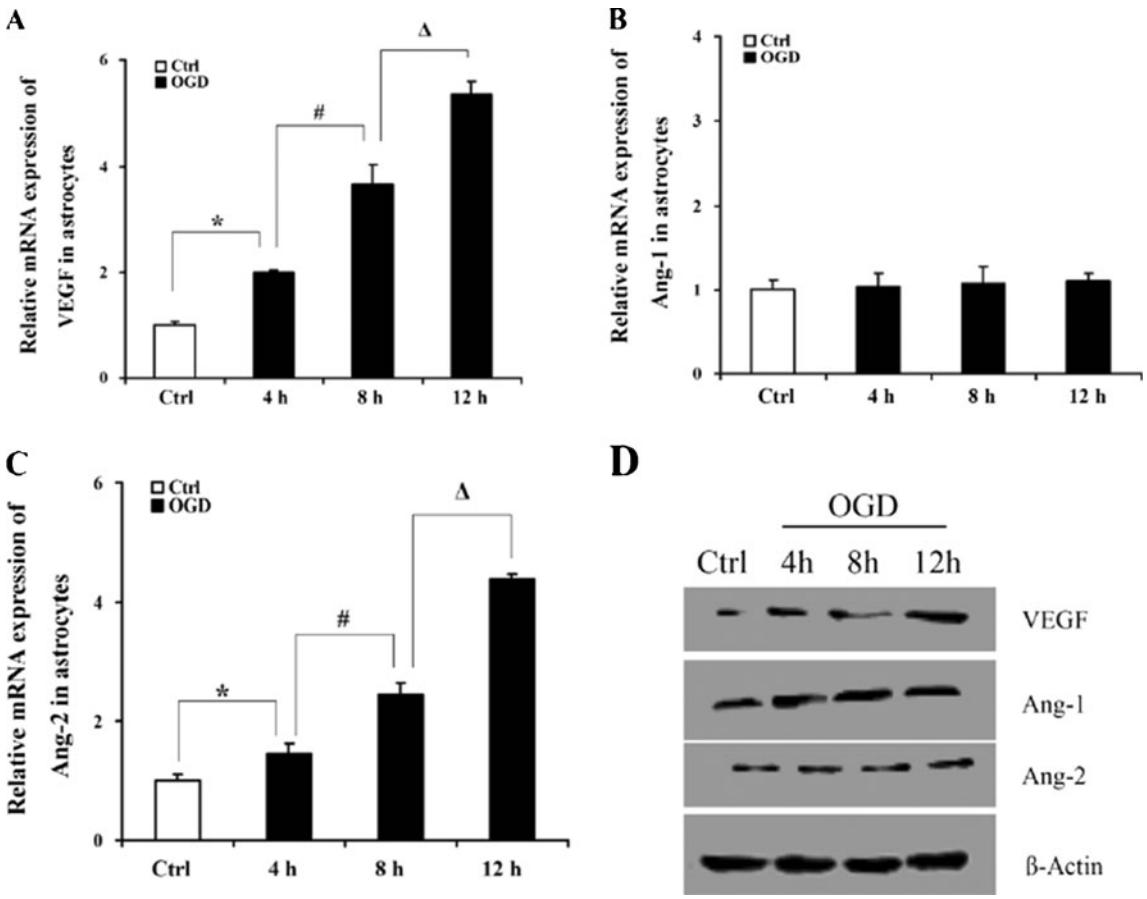

Fig. 1 OGD promotes the expression of VEGF and Ang-2 in astrocytes (**A-C**) The mRNA levels of VEGF, Ang-1 and Ang-2 were detected 4-12 hours following OGD. $N=4$, $^{*\#\square}$ $P<0.05$ *vs* controls. (**D**) The protein levels of VEGF, Ang-1 and Ang-2 were determined by Western blotting

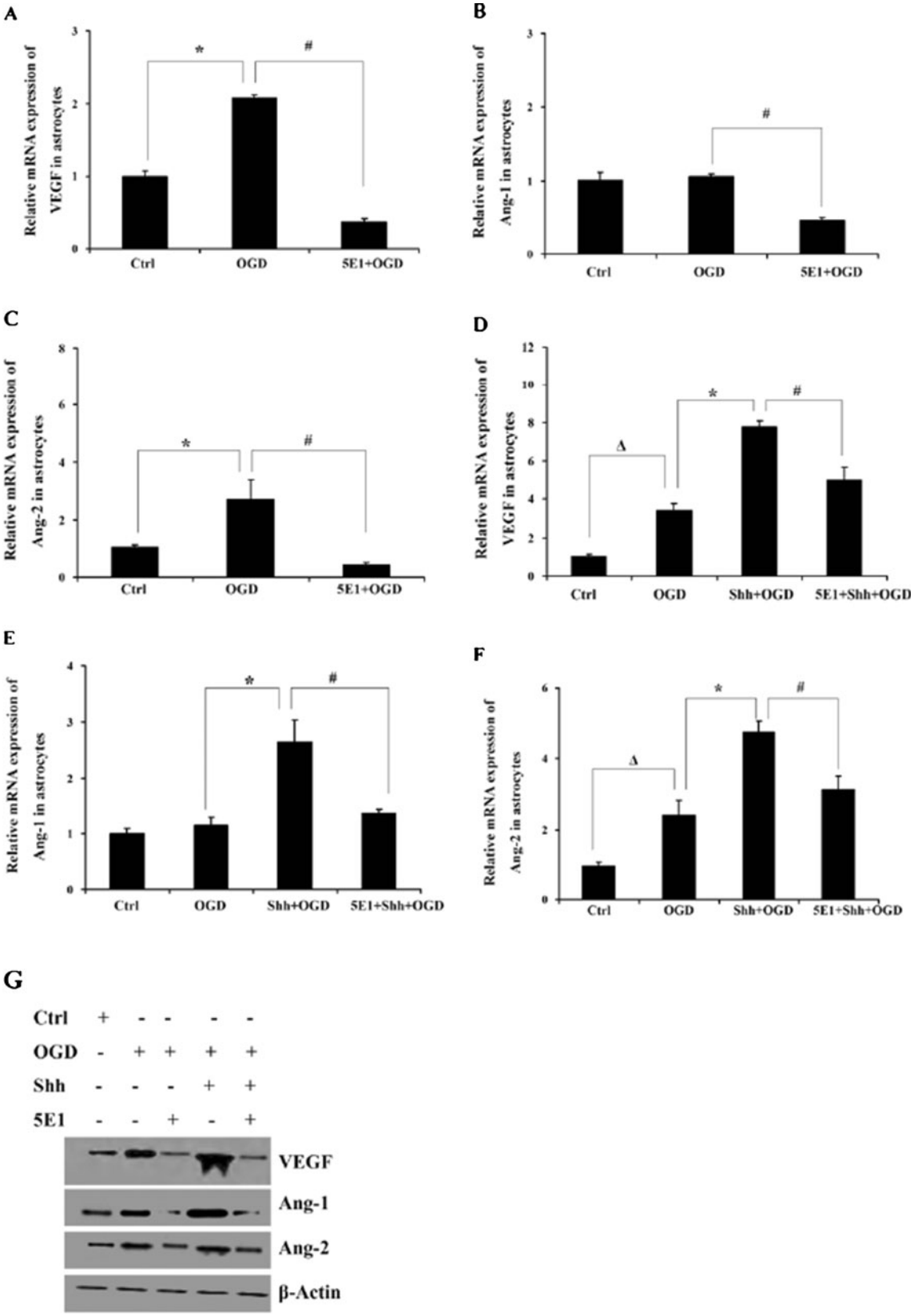

Fig. 2 Shh increase the expression of VEGF, Ang-1 and Ang-2 in astrocytes subjected to OGD insults (**A**-**C**) Astrocytes were treated with 5E1 (10 μg /ml) and then exposed to OGD. 5E1 (10 μg /ml) significantly reduced the expression of VEGF, Ang-1 and Ang-1.$^{*\#}$ $P<0.05$ *vs.* OGD group. (**D**-**G**) Astrocytes were treated with Shh (3 μg /ml) or 5E1 (10 μg / ml) and then were exposed to OGD for 12 h. Shh increased the expression of VEGF, Ang-1 and Ang-2 ($^{\Delta *}P<0.05$ vs. OGD group) and 5E1 significantly blocked the effect of Shh. $^{\#}$ $P<0.05$ vs. OGD+Shh group

The enhancing effect of Shh in the expression of VEGF, Ang-1 and Ang-2 in astrocytes subjected to OGD Real-time RT-PCR exhibited that, with OGD damage delivered at 12 h, the mRNA level of VEGF was significantly increased in astrocytes as compared with normal cultured astrocytes (Fig. 1A), but no significant difference was found in the mRNA level of Ang-1 between the OGD-treated astrocytes and normally-cultured astrocytes (Fig. 1B). Shh significantly increased the mRNA level of VEGF, Ang-1 and Ang-2 in astrocytes when compared with non-treated OGD groups. 5E1, a specific antibody against Shh, could partially reverse the effect of Shh (Fig. 2D-2F). Moreover, 5E1 significantly decreased the mRNA level of VEGF, Ang-1 and Ang-2 in normally-cultured astrocytes when compared with OGD groups (Fig. 2A-2C). The protein expression of VEGF, Ang-1 and Ang-2 in astrocytes subjected to different groups was also detected by western blotting (Fig. 2G).

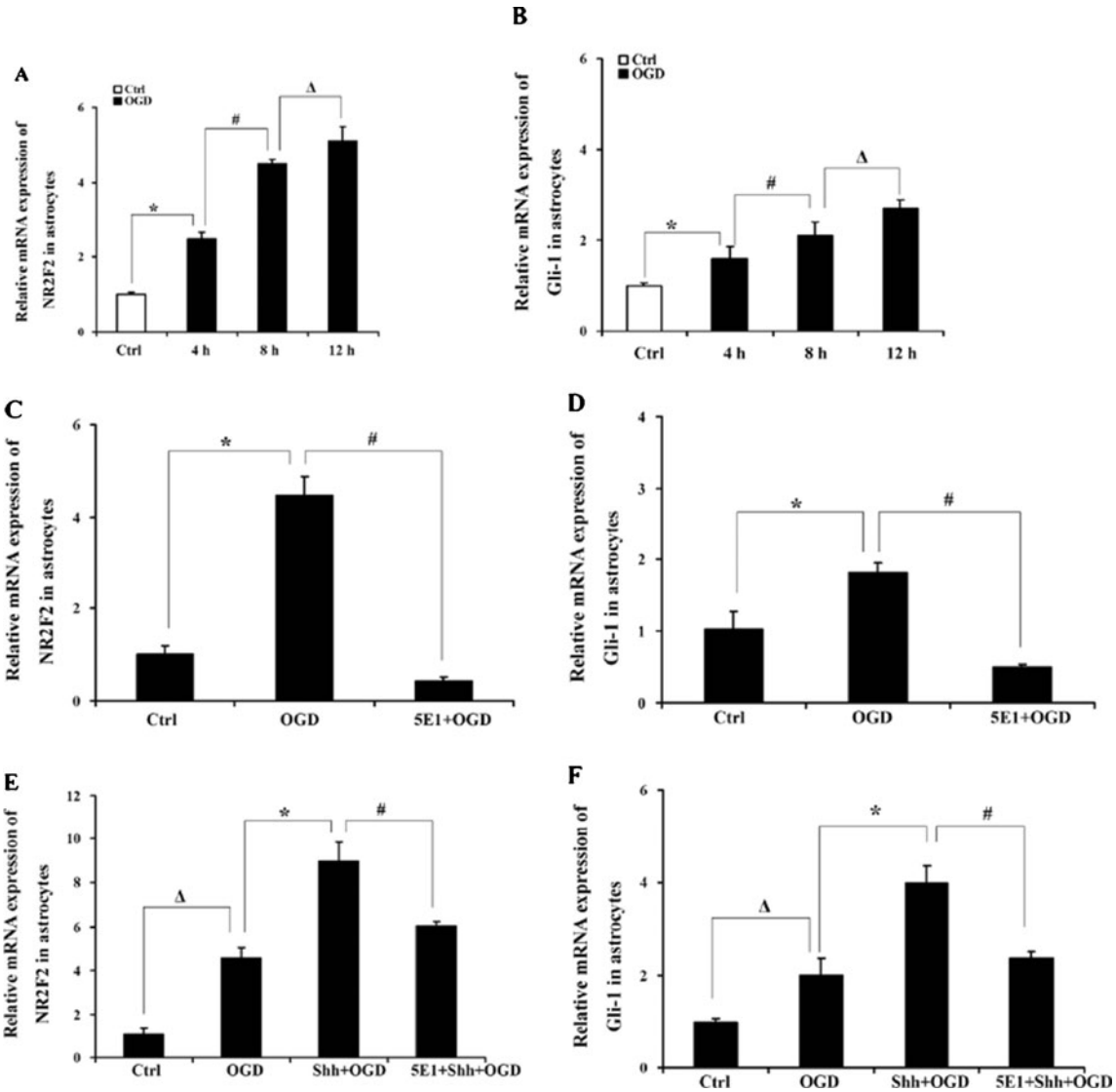

Fig. 3 NR2F2 and Gli-1 are activated in model of OGD and Shh increase the expression of NR2F2 and Gli-1 (**A-B**) The real-time RT-PCR results demonstrate that the expression of NR2F2 and Gli-1 was increased following OGD for 4-12 hours. $^{*}P<0.05$ *vs.* control, $^{\#\Delta}P<0.05$ *vs.* 12 hours group. (**C-D**) Exogenous 5E1 decreased the NR2F2 and Gli-1 effect after 12-h OGD $^{*\#}P<0.05$ *vs.* OGD group. (**E-F**) Shh significantly up-regulated the expression of NR2F2 and Gli-1. In contrast, 5E1 markedly decreased the mRNA and protein levels of NR2F2 and Gli-1. $^{\Delta *}P<0.05$ *vs.* OGD group, $^{\#}P<0.05$ *vs.* OGD+ Shh group

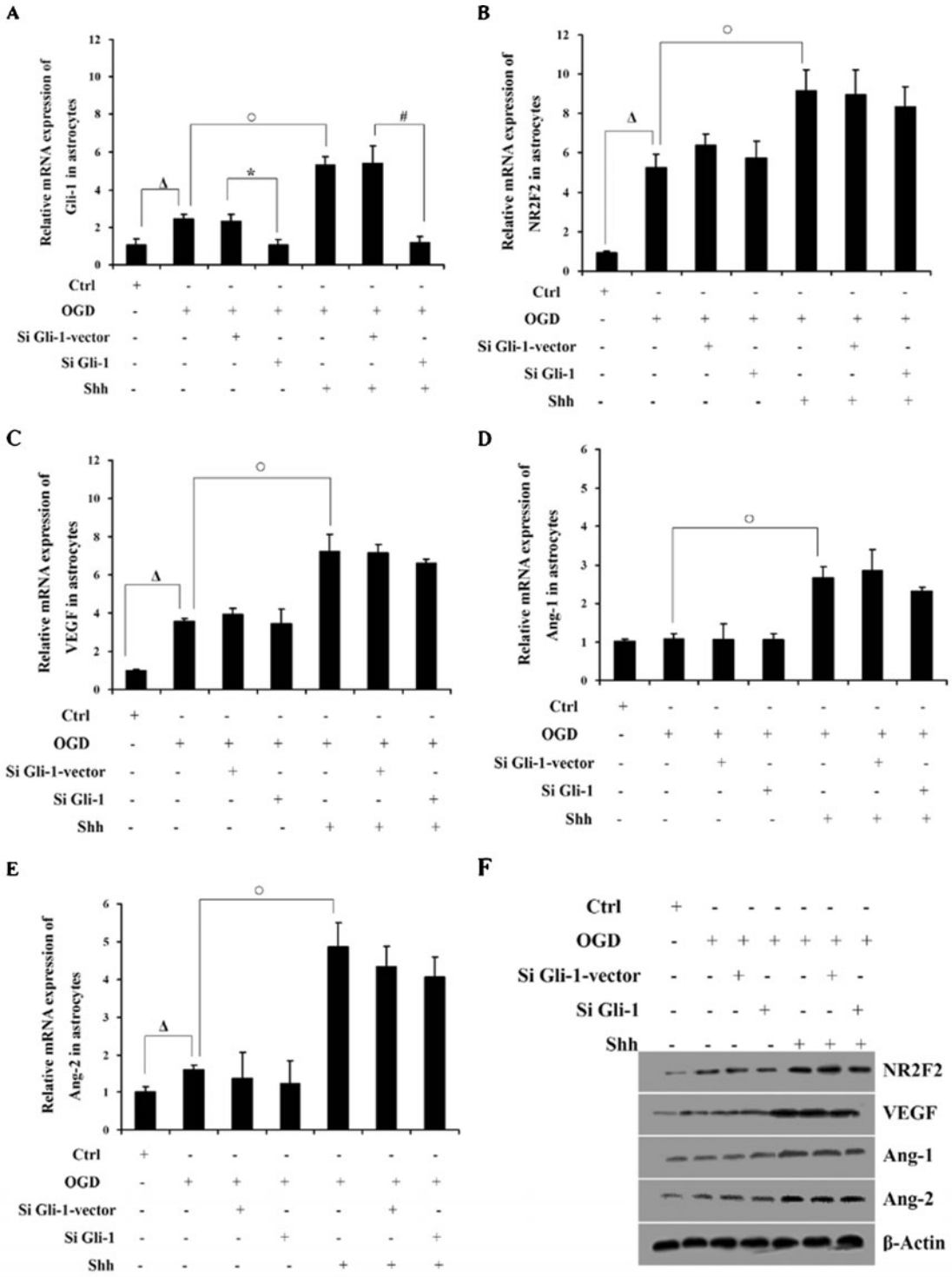

Fig. 4 Gli-1 is not required for Shh to induce the expression of VEGF, Ang-1 and Ang-2 in astrocytes under OGD insults (**A**-**E**) Gli-1-knockout astrocytes were treated with Shh and then subjected to OGD insults for 12 h. The mRNA expression of Gli-1, NR2F2, VEGF, Ang-1 and Ang-2 were determined by real-time RT-PCR. (**F**) Astrocytes were transfected with GFP siRNA, Gli-1 siRNA and then subjected to OGD for 12 h, and the NR2F2, VEGF, Ang-1 and Ang-2 protein expression was analyzed by Western blotting, with β-actin serving as internal control. Each value was obtained from 3 independent experiments. $^{\#}P<0.05$ *vs.* OGD+Shh+si-Gli-1 group. $^{\Delta}P<0.05$ *vs.* Control group. $^{\circ}P<0.05$ *vs.*OGD+Shh group. $^{*}P<0.05$ *vs.* OGD+si-Gli-1 group

Activation of NR2F2 and Gli-1 and up-regulating effect of Shh on the expression of NR2F2 and Gli-1 in model of OGD To explore how Shh up-regulates the expression of VEGF, Ang-1 and Ang-2 in astrocytes, we detected two related key signaling molecules: NR2F2 and Gli-1. In OGD astrocytes, compared to the control group, mRNA level and protein expression of NR2F2 and Gli-1 were substantially increased in a time-dependent manner (Fig. 3A-3B). Shh significantly increased the mRNA level of NR2F2 and Gli-1 in astrocytes when compared with OGD groups (Fig. 3E-3F). 5E1, a specific antibody against Shh, decreased the mRNA level and protein expression of NR2F2 and Gli-1 (Fig. 3C-3D).

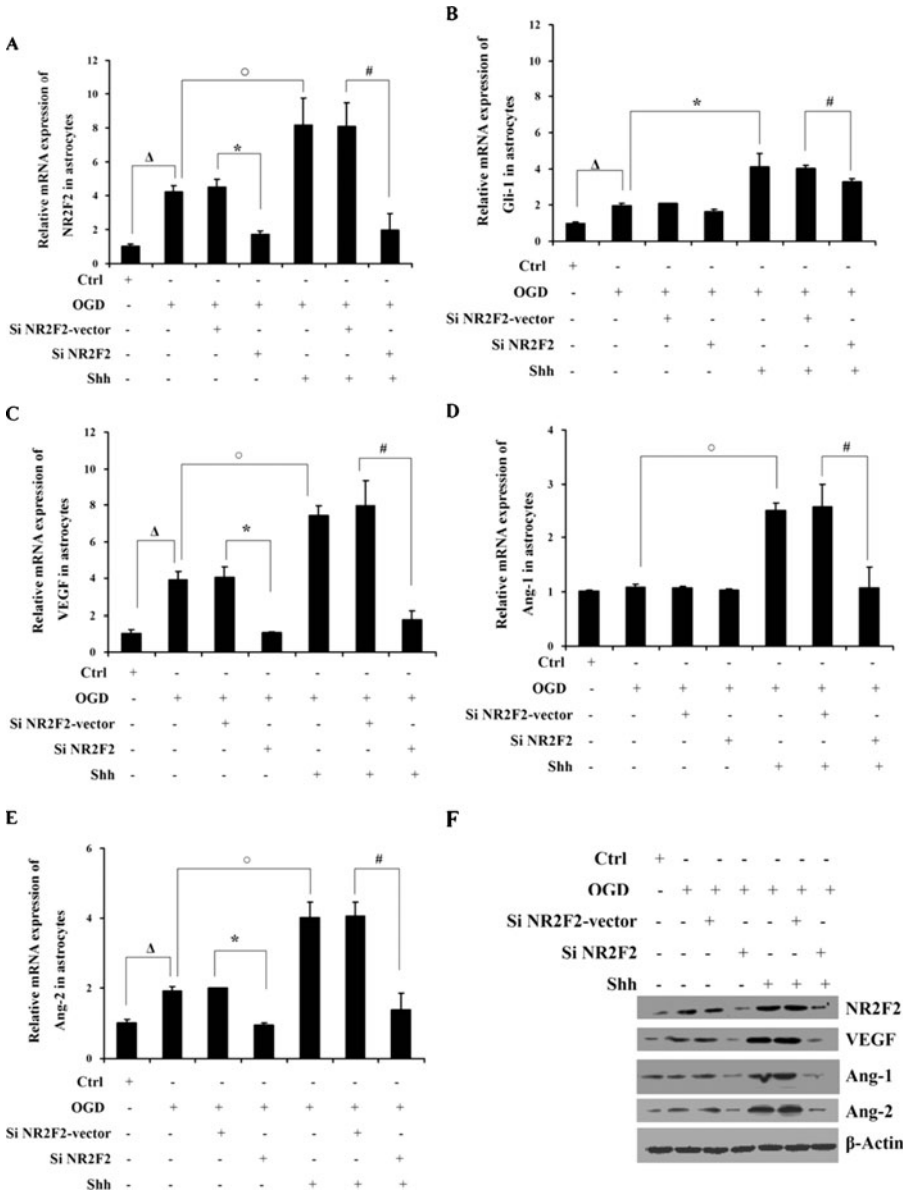

Fig. 5 NR2F2 is required for Shh to induce the expression of VEGF, Ang-1 and Ang-2 in astrocytes under OGD insults (**A**-**E**) NR2F2-knockout astrocytes were treated with Shh and then subjected to OGD insults for 12 h. The mRNA expression of Gli-1, NR2F2, VEGF, Ang-1 and Ang-2 were determined by real-time RT-PCR. (**F**) Astrocytes were transfected with GFP siRNA, NR2F2 siRNA and then subjected to OGD for 12 h, and the NR2F2, VEGF, Ang-1 and Ang-2 protein expression was analyzed by Western blotting, with β-actin serving as internal control. Each value was obtained from 3 independent experiments. $^{\#}P<0.05$ *vs.* OGD+Shh+si-NR2F2 group. $^{\Delta}P<0.05$ *vs.* Control group. $^{\circ}P<0.05$ *vs.*OGD+Shh group. $^{*}P<0.05$ *vs.* OGD+si-NR2F2 group

Gli-1-independent regulation of VEGF, Ang-1 and Ang-2 expression by Shh in astrocytes To examine whether the Shh regulates the VEGF, Ang-1 and Ang-2 expression in astrocytes via Gli-1, we constructed four Gli-1 siRNA-expressing retroviral constructs targeting different regions of the Gli1-coding sequence, and chose the most efficient sequence. Retroviruses produced from the constructs were able to lower the level of Gli-1 by about 80 %-90 % in astrocytes. Fig. 4A shows that the mRNA level of Gli-1 was decreased in Gli-1-silenced astrocytes subjected to OGD insults, and administration of Shh could not reverse the decreased expression of Gli-1. RT-PCR showed that the mRNA level of NR2F2, VEGF, Ang-1 and Ang-2 in Gli-1-silenced astrocytes was not significantly decreased when compared with the normal astrocytes subjected to OGD insults for 12 h (Fig. 4B-4E). Moreover, Shh could significantly increase the mRNA expression of NR2F2, VEGF Ang-1 and Ang-2 in Gli-1-silenced astrocytes (Fig. 4B-4E). The examination of protein expression of NR2F2, VEGF, Ang-1 and Ang-2 proteins by Western blotting yielded similar results (Fig. 4F).

NR2F2 essential to Shh-induced expression of VEGF, Ang-1 and Ang-2 in astrocytes subjected to OGD insults If NR2F2 is a downstream mediator of hedgehog signaling in angiogenesis, reduction of NR2F2 could prevent Shh from elevating the expression of VEGF, Ang-1 and Ang-2 in astrocytes. We tested this assumption by using the aforementioned retroviral siRNA delivery system. Four NR2F2 siRNA-expressing retroviral constructs targeting different regions of the NR2F2-coding sequence were constructed, and the most efficient sequence was chosen. Retroviruses produced from the constructs were able to decrease the level of NR2F2 by about 65%-70% in astrocytes (Fig. 5A). In astrocytes with reduced NR2F2, the mRNA levels of VEGF, Ang-1 and Ang-2 were significantly decreased as compared to the control group subjected to OGD. Nevertheless, administration of Shh did not reverse the elevated mRNA levels of VEGF, Ang-1 and Ang-2 in NR2F2-silenced astrocytes (Fig. 5B-5E). The detection of protein expression of NR2F2, VEGF, Ang-1 and Ang-2 in astrocytes of different groups by Western blotting yielded similar results (Fig. 5F).

Discussion

The major finding of the present study is that Shh enhances the expression of VEGF, Ang-1 and Ang-2 via NR2F2, a non-canonical factor, but not the Gli-1, a canonical one.

Until recently, ischemic injury is traditionally viewed from an axiomatic perspective of neuronal loss. However, because of the function of astrocytes, the "gliocentric view" of ischemic injury believes that pharmacological interventions targeting the functional integrity of astrocytes may be a viable strategy for neuroprotection [14]. Moreover, astrocytes secreting VEGF and Ang-1, 2 were reported to be important in the control of essential steps of vascular remodeling in the central nervous system [5]. Our previous study found that Shh was mainly secreted by astrocytes under oxidative stress and after OGD (data not shown). In the present study, we employed the OGD model of astrocytes to mimic the ischemic injury *in vitro* and found that OGD could enhance the expression of VEGF, Ang-1, 2 at different time points.

Our study demonstrated that the expression of angiogenic growth factor including VEGF, Ang-1 and Ang-2 was up-regulated in astrocytes after OGD insults. Accompanying with the increased expression of VEGF, Ang-1 and Ang-2, the expression of Shh signaling pathway components was also up-regulated in OGD astrocytes. After treatment with 5E1, a Shh-specific antibody, the expression of VEGF, Ang-1 and Ang-2 was decreased. These findings suggest that activated Shh signaling pathway might be associated with the enhanced expression of VEGF, Ang-1 and Ang-2 in astrocytes after OGD.

Previous studies found that embryonic Shh could regulate the expression of VEGF, Ang-1 and Ang-2 in postnatal ischemic injury [2]. Our findings demonstrated that exogenous Shh treatment also increased the VEGF, Ang-1 and Ang-2 expression. It is traditionally believed that Shh, work by interacting with the receptor Patched1 and thus activating the transcription factors Gli-1. Although to date, Gli-1 and Patched1 expressions are detected in virtually all cell types, the pathway is also involved in the regulation of other target genes, such as NR2F2 during floor plate development [6, 7, 9]. In this study, we found that OGD could up-regulate the expression of NR2F2 and Gli-1 by activating Shh signaling pathway in astrocytes. However, after using siRNA to down-regulate Gli in a model of OGD, Shh still induced VEGF, Ang-1 and Ang-2, suggesting that Gli-1 is not essential in Shh accommodating angiogenic factors. Moreover, the finding was coincident with that reported by a previous study, which demonstrated that Gli response elements are absent in the VEGF promoter region [8].

NR2F2 is a member of the steroid/thyroid hormone receptor superfamily and is necessary for the induction

of gliogenesis in NSPCs [12]. Moreover, in CNS development, NR2F2 may be another target of nuclear transcript factor Shh [9]. Nevertheless, recent studies found that NR2F2 directly up-regulated the transcription of angiopoietin-1 in pericytes and tumor cells and thereby enhanced angiogenesis [10]. NR2F2 also independently controlled vessel sprouting by directly regulating VEGFR-1 expression in vascular endothelial cells [15]. In this study, we found that Shh could up-regulate the expression of NR2F2 and silencing NR2F2 could significantly inhibit Shh-induced VEGF, Ang-1 and Ang-2 expression, whereas silencing Gli-1 did not inhibit these effects. Therefore, we are led to believe that Shh/NR2F2 pathway, rather than Gli-1, is important for the up-regulation of the expression of VEGF, Ang-1, 2 in astrocytes after OGD.

In summary, this study showed that the up-regulation of expression of angiogenic growth factor by Shh might be mediated by the nuclear transcript factor NR2F2 in ischemic astrocytes, rather than Gli-1, suggesting that Shh/ NR2F2 may serve as a new target for angiogenic therapy.

Acknowledgments

This work was supported by grants from the Program of National Natural Science Foundation of China (81070938), Program for New Century Excellent Talents in University (NCET-10-0406) and the Fundamental Research Funds for the Central Universities (HUST 2010JC028).

References

1. Lee, S.W., M.A. Moskowitz, and J.R. Sims, *Sonic hedgehog inversely regulates the expression of angiopoietin-1 and angiopoietin-2 in fibroblasts.* International journal of molecular medicine, 2007. 19 (3): p. 445.
2. Pola, R., et al., *The morphogen Sonic hedgehog is an indirect angiogenic agent upregulating two families of angiogenic growth factors.* Nat Med, 2001. 7(6): p. 706-11.
3. Sims, J.R., S.W. Lee, and J. Qiu, *Sonic Hedgehog Regulates Ischemia/Hypoxia-induced Neural Progenitor Proliferation.* Stroke; a journal of cerebral circulation, 2009. 40(11): p. 3618.
4. Xia, Y.P., et al., *The protective effect of sonic hedgehog is mediated by the propidium iodide 3-kinase/AKT/BCL-2 pathway in cultured rat astrocytes under oxidative stress.* Neuroscience, 2012.
5. Hermann, D.M. and M. Chopp, *Promoting brain remodelling and plasticity for stroke recovery: therapeutic promise and potential pitfalls of clinical translation.* The Lancet Neurology, 2012. 11(4): p. 369-380.
6. Zhou, Y., et al., *Activation of sonic hedgehog signaling pathway in S-type neuroblastoma cell lines.* Journal of Huazhong University of Science and Technology–Medical Sciences–, 2010. 30(3): p. 271-277.
7. He, H., et al., *Blockade of the sonic hedgehog signalling pathway inhibits choroidal neovascularization in a laser-induced rat model.* Journal of Huazhong University of Science and Technology–Medical Sciences–, 2010. 30(5): p. 659-665.
8. Pola, R., et al., *Postnatal recapitulation of embryonic hedgehog pathway in response to skeletal muscle ischemia.* Circulation, 2003. 108(4): p. 479.
9. Krishnan, V., et al., *Mediation of Sonic hedgehog-induced expression of COUP-TFII by a protein phosphatase.* Science (New York, NY), 1997. 278 (5345): p. 1947.
10. Qin, J., et al., *COUP-TFII regulates tumor growth and metastasis by modulating tumor angiogenesis.* Proceedings of the National Academy of Sciences, 2010. 107 (8): p. 3687-3692.
11. Pereira, F.A., et al., *The orphan nuclear receptor COUP-TFII is required for angiogenesis and heart development.* Genes & development, 1999. 13(8): p. 1037-1049.
12. Naka, H., et al., *Requirement for COUP-TFI and II in the temporal specification of neural stem cells in CNS development.* Nature neuroscience, 2008. 11(9): p. 1014-1023.
13. Du, H., et al., *Vascular endothelial growth factor signaling implicated in neuroprotective effects of placental growth factor in an in vitro ischemic model.* Brain research, 2010. 1357: p. 1-8.
14. Takano, T., et al., *Astrocytes and ischemic injury.* Stroke; a journal of cerebral circulation, 2009. 40(3 Suppl): p. S8.
15. Qin, J., et al., *Nuclear Receptor COUP-TFII Controls Pancreatic Islet Tumor Angiogenesis by Regulating VEGF/VEGFR-2 Signaling.* Cancer research, 2010. 70(21): p. 8812.

AR-003

Estrogen Deficit Induced Spatial Learning and Memory Deficit in Rats and Revised by PPT

Concise title: PPT revised ovariectomy-induced cognitive deficits

Na Qu[1,2], Qi Zhang[1,2], Lei Wang[1,2], Ling-Qiang Zhu[1], Qing Tian[1,*]

[1]Department of Pathology and Pathophysiology, Key Laboratory of Neurological Disease of National Education Ministry and Hubei Province, Tongji Medical College, Huazhong University of Science and Technology, Wuhan 430030, China
[2]Department of Neurology, Liyuan Hospital, Huazhong University of Science and Technology, Wuhan 430077, China
* Correspondence and reprint requests should be addressed to:
Dr. Qing Tian
Department of Pathophysiology, Tongji Medical College
Huazhong University of Science and Technology
13 Hangkong Road, Wuhan 430030, China
Tel: 86-27-83693883
Fax: 86-27-83693883
Email: tianq@mail.hust.edu.cn

Abstract
Decreasing estrogen level is reported as a risk factor of developing cognitive impairment in postmenopausal women. Ovariectomy is known as "surgical menopause" with low levels of estrogen in female rodents. In the brain, estrogen exerts neuroprotective effects through its receptors, estrogen receptor α (ERα) and β (ERβ). In this study, the bilaterally ovariectomized rats showed obvious cognitive deficits in Morris water maze. In the hippocampus, the significant loss of neurons and synaptic proteins were observed with the decreasing ERα, but not ERβ. Then, 8-week daily supplement of propylpyrazole triol (PPT, 1mg/kg/day), an agonist of ERα, was utilized and was found improved cognitive ability of ovariectomized rats. PPT supplement up-regulated the level of hippocampal ERα and also rescued ovariectomy-induced neuron loss by keeping the level of BCLxl. Furthermore, ovariectomy-induced down-regulated levels of synaptic proteins (synapsin I, NR2A and GluR1) and tau hyperphosphorylation at pT231 and pS404 sites were revised by PPT. These data shown the important role of ERα in cognitive impairment and that PPT might be an effective treatment to improve cognitive impairment after estrogen deficit.
Keywords: estrogen deficit, ovariectomy, estrogen receptor α, cognitive impairment

Introduction
The neuroprotective effects of estrogens have been widely demonstrated in Alzheimer-like pathology, such as tau hyperphosphorylation, β-amyloid toxicity, oxidative stress, mitochondrial failure, synapse damage and so on [1, 2]. Estrogen deficit may be involved in cognition impairment. For instance, menopausal women are reported to be more vulnerable to neurodegeneration in age-related congnitive decline [3]. Clinically, women in premenopause who accepted bilateral ovariectomy surgeries to treat or prevent ovarian diseases will enter menopause-like period, which is also known as "surgical menopause" [4]. The reported risks and adverse effects of "surgical menopause" include cognitive impairment [5]. To prevent the negative effects of menopause, the estrogen replace treatment was applied. However, as the mechanism of estrogen was unclear, it was not always effective to ovariectomy-induced cognitive impairment [6].
In brain, estrogen receptor α and β (ERα and ERβ) were generally expressed in a similar distribution. ERα was the predominant subtype in the hippocampus, preoptic area, and most of the hypothalamus, meanwhile ERβ was primarily localized in the olfactory bulb, cerebral cortex and septum [7, 8]. Accumulated data mentioned that ERα and ERβ involving in the formation of learning and memory [9, 10]. From now on, the action of estrogen receptor is involved in ovariectomy-induced cognitive impairment needs further investigation.
In this study, the bilateral ovariectomized rats showed cognitive impairment in Morris water maze with obvious neuron loss and synaptic proteins loss in hippocampus. The expression of ERα in hippocampus, but not ERβ, was found decreasing with low serum

estradiol level. Then, we used PPT, an agonist of ERα, to treat the ovariectomized rats and found PPT treatment improved cognitive ability of ovariectomized rats and rescued ovariectomy-induced neuron loss and synaptic protein loss and revised hyperphosphorylated tau in hippocampus. These results mentioned a new strategy to prevent ovariectomy-induced cognition deficit.

Methods and Materials

Animals and treatment 3-month-old female Sprague-Dawley (SD) rats were allowed free access to food and water and maintained at constant temperature (25± 2°C). The rats were 250-280g and supplied by Experimental Animal Central of Tongji Medical College, Huazhong University of Science and Technology. All efforts were made to minimize animal suffering and to reduce the number of rats used. All experimental procedures in this research have been approved by the Animal Care and Use Committee of Huazhong University of Science and Technology.

The rats were divided into four groups, namely sham operation group (Sham), ovariectomized group (Ovx) Vehicle group and PPT group. The ovariectomized rats were operated as previously [4] and Sham rats received the same incisions and sutures, but the ovaries were palpated instead of removed. In PPT treated group the ovariectomized rats have received chronic treatment (8-week daily subcutaneous injection of PPT, 1mg/kg/day) and the rats in vehicle group received equal volume of solvent (50%DMSO/50% Dulbecco's PBS) by daily subcutaneous injection. In the 7th week after operation the rats began 7-day training in the Morris water maze. The learning ability of rats was evaluated on the last day in the 7th week, and then they had a 6-day rest. On the last day in the 8th week, the memory was tested in the maze and the body weight and uterus weight were assayed.

Morris water maze Rats tested in the water-maze were extensively handled (2 min every day). Before each experiment (2 hours), the rats were brought to the site to allow them to be acclimatized. The temperature of the room and water was kept at 26±2 °C. The water in the pool was made opaque with ink to hide the escape platform. A computer with the water-maze software then processed the tracking information. The submerged platform (2 cm under the water) was located at a fixed position throughout training. A training session consisted of 3 trials altogether (one trial per quadrant) with a 30 seconds interval, lasting for 7 days. The first quadrant was included as the first trial everyday. On each trial, the rat started from one of the middle of the quadrant facing the wall of the pool and the trial ended when it climbed the platform. The rats were not allowed to search for the platform more than 60 seconds, after which they were guided to the platform. The rats were allowed 6-day rest before memory test on the last day of the 8th week. For the learning and memory testing, we chose the first quadrant as the testing area and the swimming pathways and latencies of testing were recorded.

Serum estradiol assay Serum was prepared by centrifuging blood at 10,000×g for 10 min and collecting the supernatant solution. The serum was stored frozen at -80°C until use and determined by using an estradiol assay kit (Cayman Chemical Co, Inc. USA).

Western blotting The rats were sacrificed by 6% chloral hydrate (0.06ml/kg) and the hippocampus was immediately removed from the brain and homogenized at 4°C using a Teflon glass homogenizer in 50mM Tris-HCl (pH 7.4), 150mM NaCl, 10mM NaF, 1mM Na_3VO_4, 10mM β-mercaptoethanol, 5mM EDTA, 2mM benzamidine, 1.0 mM phenylmethylsulfonyl fluoride, 5 μg/ml leupeptin, 5μg/ml aprotinin, and 2μg/ml pepstatin. The homogenate was mixed in 2:1 (v/v) ratio with lysis buffer containing 200mM Tris-HCl (pH 7.6), 8% SDS, 40% glycerol and boiled for 10 min in a water bath, stored at -80°C for Western blotting analysis. The concentration of protein in the extracts was measured using a BCA kit according to manufacturer's instruction Pierce Chemical Company (Rockford, IL, USA). The protein were separated by 10% Sodium Dodecyl Sulfate Polyacrylamide gel Electrophoresis (SDS-PAGE) and transferred to nitrocellulose membranes. The membranes were blocked with 2% nonfat milk dissolved in TBS (50 mM Tris-HCl, pH 7.6, 150mM NaCl) for 1 hour and probed with primary antibodies ERα (1:500, Abcam), ERβ (1:500, SataCruz), DM1A (1:1000, Sigma), BCLxl (1:1000, Abcam), synapsin I (1:1000 Abcam) GluR1 (1:1000,Millipore), NR2A (1:1000, Abcam) pT231 (1:1000, Biosource) pS396 (1:1000, Biosource) Tau46 (1:1000, Sigma). Then the blots were incubated with anti-rabbit or anti-mouse IgG conjugated to IRDye™ (800CW) (1:10000) for 1 h at room temperature and visualized using the Odyssey Infrared Imaging System (Licor biosciences, Lincoln, NE, USA). Band intensity was measured as the sum optical density and expressed is as a level relative to each control.

Nissl Staining For Nissl staining studies, brains were removed and post-fixed in perfusate overnight and then cut into 30μm sections with a vibratome (Leica, Nussloch, Germany; S100, TPI). The sections of rat brain were collected consecutively in PBS for Nissl staining. Selected slices were stained in 0.1% toluidine blue solution for 20 minutes. The slices were then quickly rinsed in distilled water and differentiated in 95% ethyl alcohol for 15 minutes. The images were observed using a microscope (Nikon Eclipse 90i, Japan). The images were analyzed with Image-Pro Plus 4.5 system (Media Cybernetics, Inc. USA).

Statistical Analysis Statistical analysis was performed using SPSS 12.0 statistical software (SPSS Inc., Chicago, Illinois, USA). Data are expressed as means±S.E.M. Differences among four groups were tested with the one-way analysis of variance (ANOVA) procedure followed by Student-Newman-Keules test was used to determine the different means among groups. The differences between groups were tested with two-sample *t* tests. A p value <0.05 was considered significant.

Results

Ovariectomy induced spatial learning and memory deficit in rats

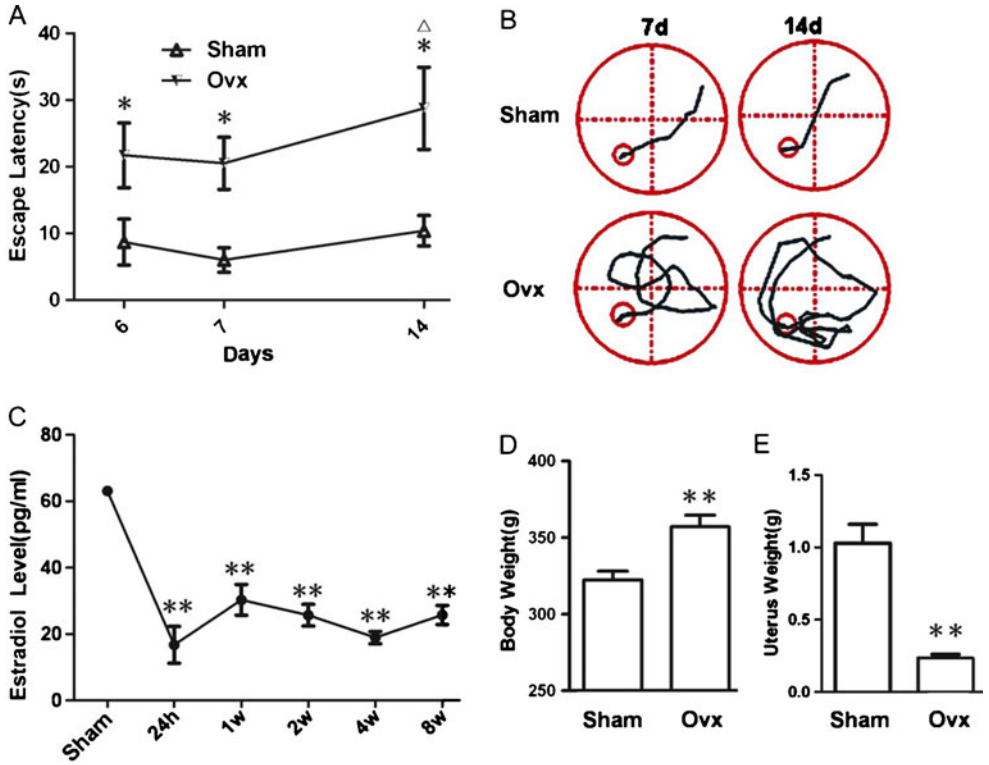

Fig. 1 Ovariectomy induced cognitive deficits in Morris water maze with low serum estradiol level in SD rats. The spatial learning ability of ovariectomized rats (Ovx) and sham operated rats (Sham) was tested in the 7th week and their memory was tested in the last day of the 8th week after operation. Escape latency (time used to find the platform) (**A**) and swimming tracks (**B**) were measured (n=12/group). The serum estradiol levels of rats at 24 h and 1, 2, 4 and 8 weeks after operation (**C**), body weight (**D**) and uterus weight (**E**) at 8 weeks after operation were detected (n=12/group). Data were presented as means±SEM. * p<0.05, ** p<0.01 *vs.* Sham; ▵ p<0.05 *vs.* the latency of the last day in learning. From Morris water maze results which were tested in the 7th week after operation and the memory was tested in the last day of the 8th week. It was found that the ovariectomized rats took longer time to find the hidden platform on the 6th and 7th day of the learning period (Fig.1 **A**). In the memory test, the latency of ovariectomized rats to find the platform was much longer than the latency themselves has taken on the 7th day of the learning (Fig.1 **A**). The increased latency in ovariectomized rats was due to their cognitive impairment rather than physical weakness as demonstrated by their swimming path (Fig.1 **B**). The Sham rats in the memory test found the hidden platform as quickly and directly as they performed on the 7th day of the learning (Fig.1 **A**, **B**). Then, we found ovariectomy induced estradiol decreasing at five different time points after operation (Fig.1 **C**). The serum estradiol level of Sham rats was 63.9 ±1.4pg/ml and it significantly decreased to 16.8±3.5pg/ml at 24h after ovariectomy. Till 8 weeks after ovariectomy the lower estradiol level still remained (Fig.1 **C**). We also found the ovariectomy induced body weight increased 357± 7.5g (Fig.1 **D**) and decreased uterine weight 0.2±0.03g (Fig.1 **E**)

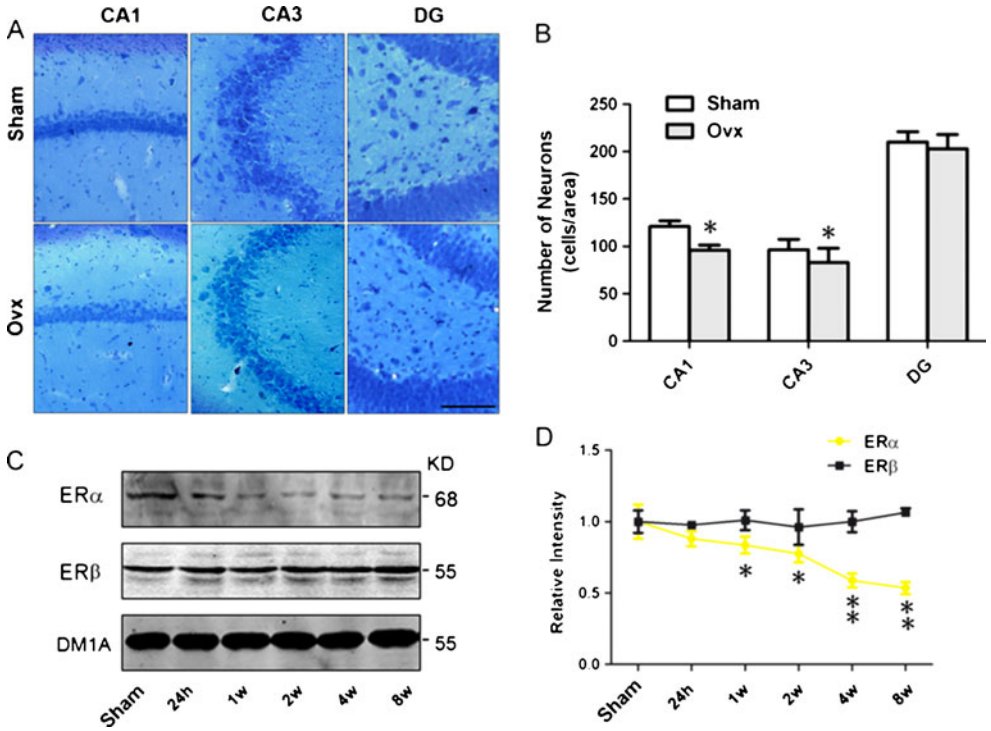

Fig. 2 Hippocampal neuron loss and decreased expression of ERα was induced by ovariectomy. The number of neuron was shown by Nissl staining (**A**) and neuron counting (**B**) (n=3/group, Scale bars=100μm). The expressions of ERα and ERβ in hippocampus at 24 h and 1, 2, 4 and 8 weeks after operation were detected by Western blot (**C**) and quantitatively analyzed (**D**) (n=6/group). Data were presented as means±SEM. * $p<0.05$, ** $p<0.01$ *vs.* Sham at the same time point

Ovariectomy induced neuron loss with decreased ERα in the brain Previous studies demonstrated that estrogen protects neuron from all kinds of brain damage such as ischemia [11-14]. Therefore, we detected the number of neuron by Nissl staining after ovariectomy. We found that the numbers of neuron in hippocampal CA1 and CA3 regions were significantly reduced in ovariectomized rats and in DG region was remained (Fig. 2 A, B). We did not found any alterations of the neuron in cortex (Data not shown). To know the effect of estrogen receptor in hippocampus, we tested it by Western blot and found that ERα in hippocampus was declined (Fig. 2 C, D). However, there is no alternation in the expression of ERβ (Fig.2 C, D). These data indicated ERα was sensitive than ERβ when estrogen deficits in hippocampus.

PPT revised ovariectomy-induced spatial cognitive deficit in rats To confirm the effect of hippocampal ERα in ovariectomy-induced cognitive impairment, we used PPT, a special ligand for ERα, to treat the rats (1mg/kg/day). After 8-week daily PPT treatment (Fig.3 A), the latency for ovariectomized rats to find the hinden platform was much shorter than that of the ovariectomized rats accepted vehicle (Fig.3 B). In the memory test, the latency of ovariectomized rats with

PPT showed no significantly difference with the latency themselves has taken on the 7th day of learning (Fig.3 B). PPT treated ovariectomized rats in the memory test found the hidden platform as quickly and directly as they performed on the last day of the learning (Fig.3 C). And the serum estradiol level in PPT treated ovariectomized rats was 43.3 ±7.3 pg/ml (Fig. 3 D), and vehicle treated group was 30.2±2.3 pg/ml (Fig. 3 D). Compared with the vehicle treated rats, PPT treated rats maintained uterine weight 1.0±0.13 g (Fig.3 E) and decreased body weight 324±7.1 g (Fig.3 F).

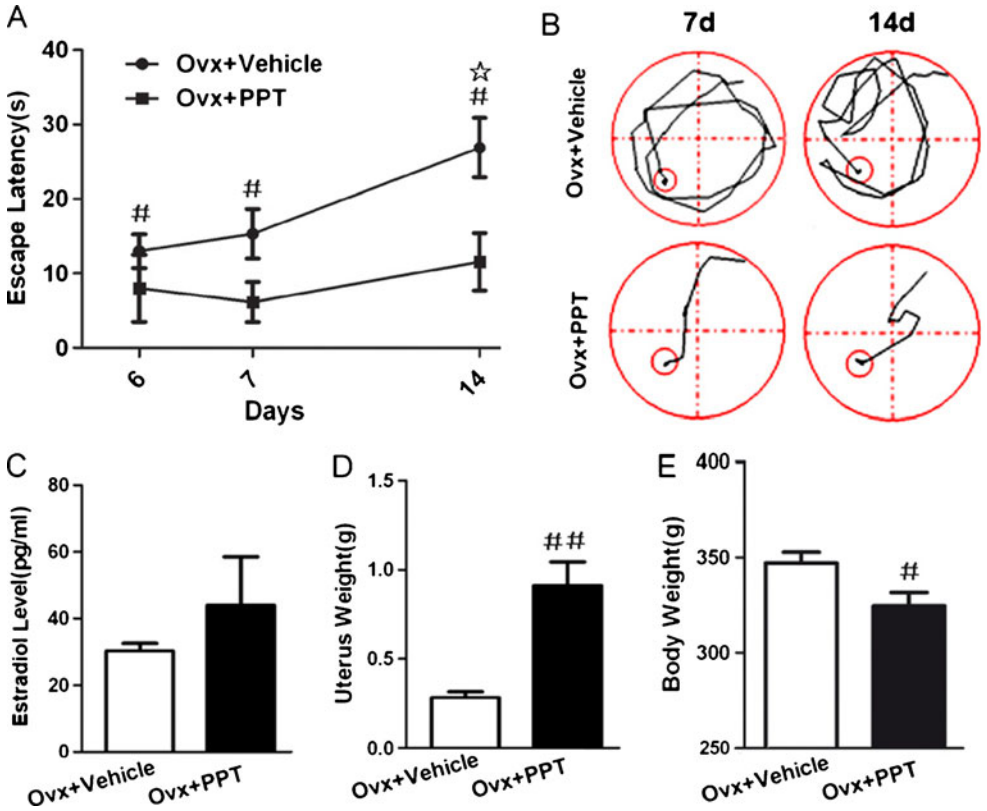

Fig. 3 Effect of PPT on cognitive ability of ovariectomized rats. Escape latency (time used to find the platform) (**A**) and swimming tracks (**B**) were measured (n=12/group). The serum estradiol level (**C**), uterus weight (**D**) and body weight (**E**) at 8 weeks after operation were detected (n=12/group). Data were presented as means±SEM. # $p<0.05$, ## $p<0.01$ *vs.*Ovx+Vehicle; ☆$p<0.05$ *vs.* the latency of the last day in learning

PPT revised neuron loss and hippocampal ERα level

To explore the effect of PPT on neuron and ERα expression, we assayed the number of neuron and hippocampal ERα level after PPT treatment. We found the number of neuron in CA1 and CA3 regions were significantly increased compared with vehicle treated group by Nissl staining (Fig. 4 A,

B). And ERα was obviously up-regulated compared with vehicle treated group (Fig. 4 C, D). Moreover PPT treatment rescued the ovariectomy-induced decreased Bclxl protein, a key anti-apoptosis factor (Fig.4 C E). These data mentioned that the protection of ERα to the survival of neuron after ovariectomy.

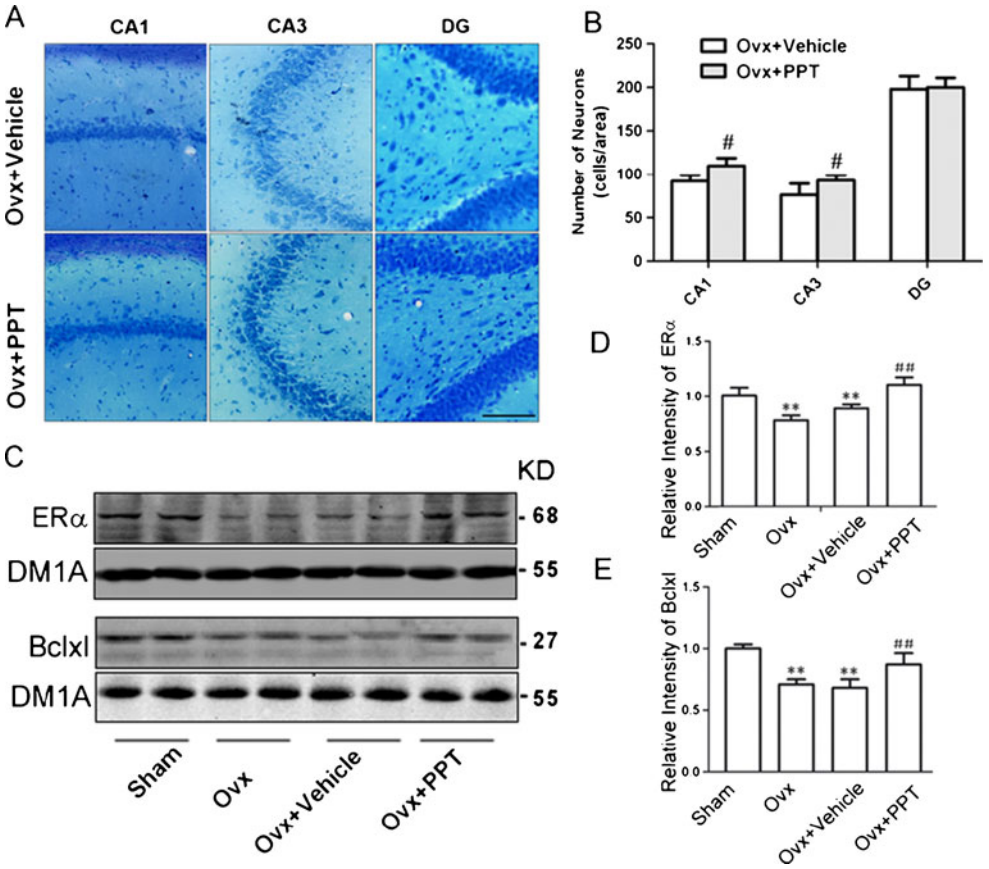

Fig. 4 Effect of PPT on the number of neuron and expression of ERα in hippocampus. The number of neuron was shown by Nissl staining (**A**) and neuron counting (**B**) (n=3/group, Scale bars= 100μm). The expression of ERα in hippocampus after operation were detected by Western blot (**C**) and quantitatively analyzed (**D**) (n=6/group). The expression of the anti-apoptosis protein BCLxl was tested by Western blot (**C**) and quantitatively analyzed (**E**) (n=6/group).Data were presented as means±SEM. * $p<0.05$, ** $p<0.01$ *vs.* Sham; # $p<0.05$, ## $p<0.01$ *vs.* Ovx+Vehicle

PPT revised ovariectomy-induced synapse loss and tau hyperphosphorylation in hippocampus Previous research demonstrated that estrogen involve in synaptic communications. And the synaptic protein in hippocampus is basis in the formation of learning and memory. Therefore, we studied the synapse damage after ovariectomy and the effect of PPT. In this study, we found that the synapsin I, one important presynapsic protein, was decreased after ovariectomy. N-Methyl D-Aspartate receptor 2A (NR2A) and glutamate receptor 1 (GluR1), the important postsynapsic proteins which are reported be involved in estrogen enhanced synaptic transmission were found decreased also and these synaptic proteins were revised by PPT treatment (Fig.5 A, B). In addition, estrogen plays an important role in the phosphorylation of tau, which impacts the formation of learning and memory [15]. Accumulated data reported that ovariectomy induced tau hyperphosphorylation is one of the pathological mechanisms in synapse damage. From our study, Western blotting analyses indicated that tau hyperphosphorylated at pT231 and pS396 sites after ovariectomy (Fig. 5 C, D). These results suggested that PPT

treatment is effective way to delay the synapse damage after ovariectomy.

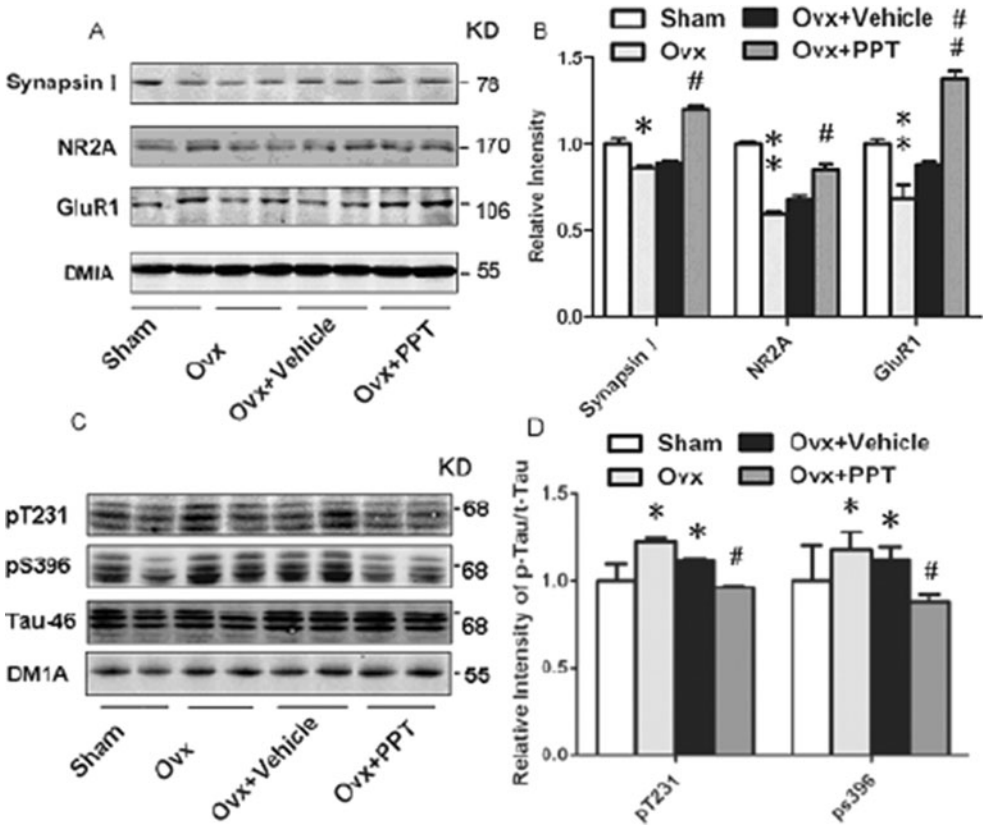

Fig. 5 Effect of PPT on synaptic proteins and tau hyperphosphorylation in hippocampus.The expression of synapsinI, NR2A and GluR1 in hippocampus after operation were detected by Western blotting (**A**) and quantitatively analyzed (**B**) (n=6/group). The phosphorylation levels of pT231, Ser396 and Tau-46 in hippocampus were also detected by Western blot (**C**) and quantitatively analyzed (**D**) (n=6/group). The relative phosphorylation levels were normalized against the level of Tau-46(total-Tau). Their relative phosphorylation levels (active form) were calculated against those of Sham rats. Data were presented as means±SEM. * $p<0.05$, ** $p<0.01$ *vs.* Sham; # $p<0.05$, ## $p<0.01$ *vs.* Ovx+Vehicle

Discussion

Estrogen has been reported to have a neuroprotective effect in many neurodegenerative diseases and improve cognitive ability [5, 6]. Due to complex of estrogen the diverse and some times opposite effects in basic and clinic research that result from the use different estrogenic compounds or given via different delivery routes to women of different ages and health status, estrogen replace treatment is limited. The popular hypothesis "critical period" discusses completely opposite results about estrogen replace treatment [12]. It suggests that estrogen replace treatment initiated early, around the time of menopause and continued for several years has an enduring neuroprotective effect on cognitive functioning 2-3 decades later, which if initiated late, might cause more harm than good [12-14]. Many previous studies mention that long term estrogen deprivation (LTED) alters the ability of subsequent estrogen replace treatment to have an effect on cognition. However, only a small number of studies have investigated the effect of the estrogen receptor in long term estrogen deprivation.

The biological effects of estrogen are mediated by two known isoforms of the estrogen receptor ERα and ERβ. Accumulating reports suggest that estrogen exerts its neuroprotective action through ERα-mediated mechanisms. And estrogen stimulated glutamatergic synapse formation in the developing hippocampus through an ERα dependent mechanism. However, ERβ was reported to have the ability to regulate hippocampal synaptic plasticity and improve hippocampus-dependent cognition, while its agonist had the capability to modulate synaptic structure and related proteins. Furthermore, the agonist of ERα and ERβ was

reported to have an effect at different times in neurodegenerative diseases. ERα agonist has an anti-inflammatory effect and is involved in neuroprotection at the onset and throughout the disease course in the multiple sclerosis. ERβ agonist has no effect at disease onset but promot recovery during the chronic phase of the disease.In this study, the alternation of estrogen receptors at five different time points after ovariectomy was tested. We found that except for hippocampal ERβ, serum estradiol levels and expression of hippocampal ERα were significantly reduced at 8 weeks after ovariectomy. Therefore, we chose the observing time point was the 8th week after ovariectomy. After 8 weeks of ovariectomy, the rat displayed obvious spatial learning and memory deficit in the Morris water maze along with neurons and synaptic protein loss. Recently, the noticeable decrease of ERα and not ERβ in the hippocampal CA1 at 10 weeks after ovariectomy in rats was reported by Brann et al [9, 10]. These results mentioned that ERα could be a switch target to affect cognitive ability after ovariectomy. Therefore, in our studies we treated PPT, an agonist for ERα which displays 400-fold more binding affinity for ERα than ERβ in ovariectomized rats after 2 hours of operation for 8 weeks. It was found to keep the expression of hippocampal ERα and reinstated ovariectomy-induced neurons loss in CA1 and CA3 regions. All these studies indicate that decreased ERα is critical for ovariectomy-induced hippocampus related cognition.

Previous research conclude that estrogen up-regulated immunoreactivity for the largest NMDA receptor subunit and PPT was shown as estrogen to modulate both hippocampal NMDA receptors and AMPA receptors in ovariectomized rats and increase the number of hippocampal neuron. In comparison, the ERβ agonist; 2,3-bis (4-hydroxyphenyl) -propionitrile (DPN), was not regulated glutamatergic receptor which displayed 100-fold more affinity for ERβ than ERα and was inactive on ERα transcriptional activity. While, some researches reported that estrogen can trigger many intracellular signaling cascades. Such as the activation of MAPK and phosphatidylinositol 3-kinase (PI3K)/Akt pathways, induction of ion channel fluxes and G-protein-coupled receptor-mediated second messenger generation. In addition, accumulate evidence has demonstrated that abnormally hyperphosphorylated microtubule-associated protein tau, which aggregates into paired helical filaments, is the main protein component of neurofibrillary tangles. The known phosphorylation sites are on pT231 and Ser396/Ser404 motifs which can be abonormal phosphorylated in AD brain [15]. And estrogen could improve the formation of tau protein to impact synapse plasticity. Moreover estrogen activates CaMK IIα, ERK and Akt and contributes to the formation of long-term potentiation (LTP) in mouse hippocampus through ERα. Therefore, we tested the possible synaptic mechanism of ERα in ovariectomy-induced cognitive impairment. The results showed that level of Tau phosphorylation was up-regulated after ovariectomy. And PPT treatment rescued the levels of presynaptic protein synapsin I and the postsynaptic proteins, NR2A and GluR1, and reduced abnormal Tau hyperphosphorylation. These results indicate that ERα play important role in estrogen-participated synaptic function and the formation of learning and memory.

In summary, we observed that ovariectomized rats display apparent cognitive impairment in Morris water maze as well as loss of neurons and synaptic proteins. Along with the serum estradiol level was declined, the expression of ERα in the hippocampus, but not ERβ decreased from one week after the ovariectomy was performed. Prompt PPT treatment improved spatial learning and memory ability of ovariectomized rats and rescued ovariectomy-induced neurons loss, synaptic proteins loss and tau hyperphosphorylation. Present results provide support for an important role ERα plays in the neuroprotection and indicate prompt ERα rescue is important for hippocampal depended cognition after ovariectomy.

Acknowledgments This work was supported by grants from the Natural Science Foundation of China (30971008, 30971204, 30971478,30871035).

Reference

1. Correia, SC, Santos, RX, Cardoso, S, Carvalho, C, et al. (2010) Effects of estrogen in the brain: is it a neuroprotective agent in Alzheimer's disease? Curr Aging Sci 3(2): 113-126.
2. Walf, AA, Paris, JJ, Rhodes, ME, Simpkins, JW, et al. (2011) Divergent mechanisms for trophic actions of estrogens in the brain and peripheral tissues. Brain Res 1379: 119-136.
3. Rocca, WA, Grossardt, BR, Shuster, LT (2010) Oophorectomy, menopause, estrogen, and cognitive aging: the timing hypothesis. Neurodegener Dis 7(1-3): 163-166.
4. Stout Steele, M, Bennett, RA (2011) Clinical Technique: Dorsal Ovariectomy in Rodents. J EXOT PET MED 20(3): 222-226.
5. Rocca, WA, Bower, JH, Maraganore, DM, Ahlskog, JE, et al. (2007) Increased risk of cognitive impairment or dementia in women who underwent oophorectomy before menopause. Neurology 69(11): 1074-1083.
6. Shuster, LT, Gostout, BS, Grossardt, BR, Rocca, WA (2008) Prophylactic oophorectomy in premenopausal women and long-term health. Menopause Int 14(3): 111-116.
7. Mitra, SW, Hoskin, E, Yudkovitz, J, Pear, L, et al. (2003) Immunolocalization of estrogen receptor beta in the mouse brain: comparison with estrogen receptor alpha. Endocrinology 144(5): 2055-2067.
8. Shughrue, PJ, Lane, MV, Merchenthaler, I (1997) Comparative distribution of estrogen receptor-alpha and -

beta mRNA in the rat central nervous system. J Comp Neurol 388(4): 507-525.
9. Zhang, QG, Han, D, Wang, RM, Dong, Y, et al. (2011) C terminus of Hsc70-interacting protein (CHIP)-mediated degradation of hippocampal estrogen receptor-alpha and the critical period hypothesis of estrogen neuroprotection. Proc Natl Acad Sci USA 108(35): E617-E624.
10. Zhang, QG, Raz, L, Wang, R, Han, D, et al. (2009) Estrogen attenuates ischemic oxidative damage via an estrogen receptor alpha-mediated inhibition of NADPH oxidase activation. J Neurosci 29(44): 13823-13836.
11. Pompili, A, Arnone, B, Gasbarri, A (2012) Estrogens and memory in physiological and neuropathological conditions. PSYCHONEUROENDOCRINO (Epub ahead of print).
12. Sherwin, BB, Henry, JF (2008) Brain aging modulates the neuroprotective effects of estrogen on selective aspects of cognition in women: a critical review. Front Neuroendocrinol 29(1): 88-113.
13. Sherwin, BB (2009) Estrogen therapy: is time of initiation critical for neuroprotection? Nature Rev Endocr 5 (11): 620-627.
14. Suzuki, S, Brown, CM, Dela, CC, Yang, E, et al. (2007) Timing of estrogen therapy after ovariectomy dictates the efficacy of its neuroprotective and antiinflammatory actions. Proc Natl Acad Sci USA 104(14): 6013-6018.
15. Wang JZ, Liu F (2008) Microtubule-associated protein tau in development, degeneration and protection of neurons. Prog Neurobiol 85(2):148-75.

AR-004

A systematic analysis of genomic changes in Tg2576 mice

Lu Tan[a], XiongWang[a], Zhong-FeiNi[a], XiumingZhu[d], Wei Wu[e], Ling-Qiang Zhu[a,c], Dan Liu[b,c,*]

[a]Department of Pathophysiology, Tongji Medical College, Huazhong University of Science and Technology, Wuhan, PR China

[b]Department of Genetics, Tongji Medical College, Huazhong University of Science and Technology, Wuhan, PR China

[c]Key Laboratory of Neurological Diseases of Education Ministry of China, Tongji Medical College, Huazhong University of Science and Technology, Wuhan, PR China

[d]Department of Computer Science, University of Texas at Austin, TX, USA

[e]Department of Pediatrics, Tongji Hospital, Tongji Medical College, Huazhong University of Science and Technology, Wuhan, PR China

*Corresponding author: Dr. Ling-Qiang Zhu, E-mail: zhulq@mail.hust.edu.cn or Dr. Dan Liu, E-mail: liudan_echo@mail.hust.edu.cn

Tel.: +86 2783692625; Fax: +86 27 83693883

Abstract The purpose of this study is to investigate gene expression related to Alzheimer's disease (AD) based on published microarray data on Tg2576 mice. A hierarchical Cluster analysis and Gene Ontology was performed to group genes on the basis of gene product characteristics and annotation data. Genes with prominent alteration are clustering in apoptosis and axon guidance pathways. Combined with the literatures, we proposed that the mitochondrial mediated apoptosis pathway might be crucial for neuronal loss and the axon guidance factors dysfunction might induce the synaptic disorder in AD. Furthermore, we applied Positional Gene Enrichment (PGE) analysis and Gene Set Enrichment analysis (GSEA) and found identified regulation of transcription of AD genes might be important in the pathogenesis of this disease.

Keywords: Gene ontology analysis, cluster, chromosome, Alzheimer's disease

AD is the most prevalent neurodegenerative disorder that characterized with the presence of extracellular amyloid plaques and intracellular neurofibrillary tangles (NFT), neuronal loss, memory and cognitive decline (Suh and Checler 2002). In 2006, there are 26.6 million sufferers worldwide and, that is predicted to affect 1 in 85 people globally by 2050(Brookmeyer et al. 2007). Unfortunately, the clear mechanisms of AD are not be elucidated and there are still no effective therapeutic strategies.

Nowadays, it is widely recognized that Aβ, the major component of amyloid plaques, might be the primary criminal for AD so that a lot of transgenic mice with severe Aβ deposition and memory deficits had been generated to investigate the possible underlying pathogenesis of AD by overexpressing mutated β-amyloid precursor protein (APP)(Lehman et al. 2003). Among them, Tg2576 mouse that overexpressed the APPsw protein, the 695 amino acid form of human APP containing the K690N/M671L FAD mutation, under the influence of a PrP promoter was widely used in the past 16 years(Hsiao et al. 1996). The "Swedish" APP mutation affects the β-secretase cleavage site of the Aβ domain, leading to increased brain production of both $A\beta_{1\text{-}40}$ and $A\beta_{1\text{-}42}$. In this mouse, Aβ is increased significantly at 2-3 months and rapidly increased in about 7 months with amyloid plaques beginning at 9-12 months. Tg2576 mice also show behavioral disorders, including reduced spontaneous alternation performance in Y-maze and increased escape latency in the Morris Water Maze, making them suitable for examining the relationship between Aβ and memory(Suh and Checler 2002).

The pathogenesis of AD is complicated and it might be caused by variation in a large number of genes/proteins

and disruption of their anfractuous interactions rather than single gene/protein. Several studies including some microarray analysis had been performed in Tg2576 mice and hundreds of differentially expressed genes were identified, in particular, regarding changes in plasticity-related genes(Dickey et al. 2003). However, few studies had focused on the co-expression patterns of associated pathways with the core genes and transcription factors. To understand those questions, we applied systematic biology approaches with published microarray data and revealed (1) Aβoverload induced neuronal apoptosis mainly through mitochondrial mediated apoptotic pathway; (2) lots of genes important in axon guidance are misregulated in Tg2576 mice and might be responsible for the synaptic degeneration; (3) disturbance of some transcriptional factors (TF) and TF-binding motifs might participate in inflammatory process.

Materials and Methods

Published microarray data from Stein TD's article can be obtained from Gene Expression Omnibus (GEO) data base with an accession No. GSE1556(Stein et al. 2004). Gene Ontology (GO) analysis, Positional Gene Enrichment (PGE) analysis and Gene Set Enrichment analysis (GSEA) were performed as previously (De Preter et al. 2008; Mootha et al. 2003; Subramanian et al. 2005).

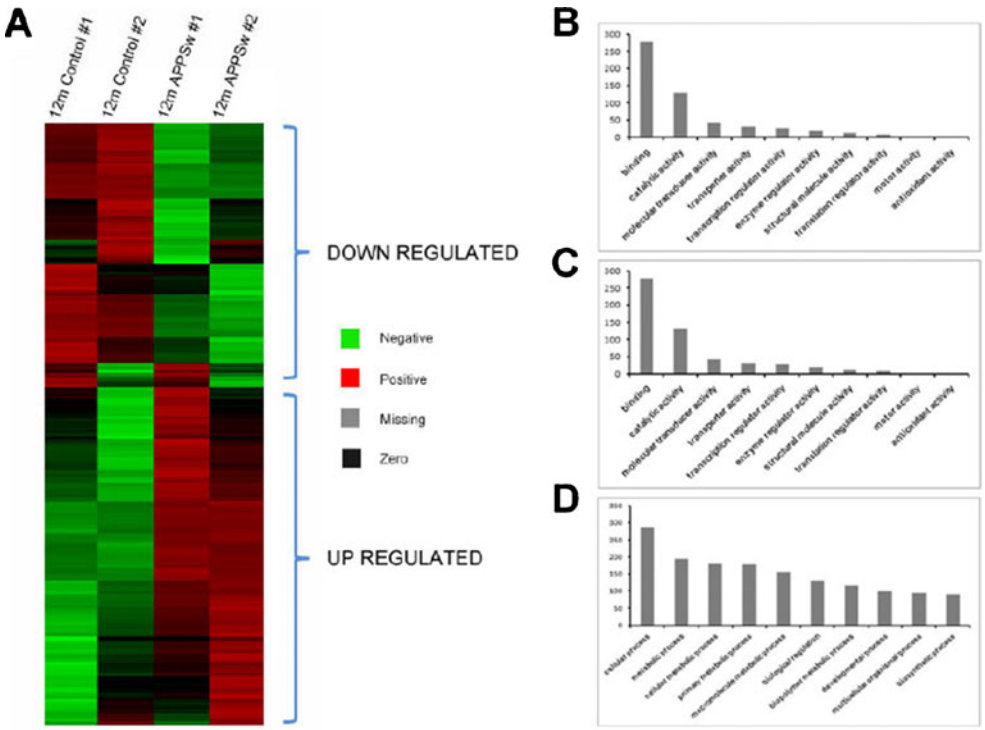

Fig. 1 (**A**) Heatmap of 676 genes differentially expressed in the tg2576 Mice. Each line in the heatmap represents a gene upregulated (red) or downregulated (green) expression. No change in expression is indicated in black. (**B**, **C**, **D**) GO annotation with Molecular Function, Cellular Component and Biological Process categories respectively

Clustering by Significant and Differential Expression

Comparative analysis of whole genome expression between Tg2576 and wild type mice identified 676 differentially expressed genes (±1.2-fold expression difference and *P* value is less than 0.05) and 408 were up-regulated (within a range of 1.2 to 16-fold change), and only 268 were down-regulated (range between -1.2 to -9-fold change) (Fig. 1A). Among these genes, the expression profile included many important genes that crucial in AD as previously described, such as presenilin1, apolopoprotein E, caspase 3, GSK-3β, calmodulin.

Tg2576 mice at 12 month exhibited severe memory deficit, neuron loss and synaptic dysfunction, we then annotated the differentially expressed 676 genes by assigning them to Molecular Function, Cellular Component and Biological Process, three categories as designated by the Gene Ontology (GO) database (http://www.geneontology.org/). In each category, we further classed the differentiated genes into subgroups and the top ten genes in every category are listed as Fig. 1 respectively. 369 of the 676 genes were matched to Molecular Function categories. 380 genes were matched

to Cellular Component categories and 350 genes were matched to Biological Process categories. However, this annotation still didn't provide the detailed functions of those genes due to the overlap in some high level of terms. For example, lots of genes overlapped in the higher level termed "metabolic process" and "cellular process" might be also crucial in the lower level term of "regulation of transcription". But due to the plenty of genes were gathered in the higher level of terms, we can't find the term of "regulation of transcription" in the top ten lists. In order to avoid this redundancy in different GO terms, we further employed default DAVID (The Database for Annotation, Visualization and Integrated Discovery) parameters for meaningful functional annotation clustering analysis(Huang et al. 2009a; Huang et al. 2009b). We found that the most enriched clusters revealed functions are:"developmental process", "protein localization" and "apoptosis" (Table 1). We then focused on the apoptosis signals and the axon guidance signals for these might play important roles in the neuronal loss and synaptic dysfunction of AD.

Table 1 The Top 10 Annotation Clusters Identified by the DAVID Functional Annotation Clustering Tool

Annotation cluster	Representative annotation terms	Enrichment score
1	Embryonic development	2.27
2	Protein localization / transport	2.16
3	Regulation of apoptosis / cell death	2
4	Pattern specification process	1.79
5	Negative regulation of transcription	1.75
6	Positive regulation of transcription	1.67
7	Inositol / polyol metabolic process	1.64
8	Epithelium development	1.62
9	Response to hormone / insulin stimulus	1.55
10	Reproductive process	1.53

The genes were analyzed by the Functional Annotation Clustering Tool. The top 10 annotation clusters are ordered by group enrichment score. The representative biology terms associated with the top 10 annotation clusters are manually selected, showing a much clearer and non-redundant view of the annotation terms associated with the study.

Alteration of genes involved in apoptosis signaling Apoptosis is implicated in both acute and chronic neurological disorders. It is mediated by two typical pathways: the intrinsic or mitochondrial pathway and the extrinsic or cell surface death receptor pathway. In this mouse, a total of 28 genes are related to apoptosis, and most of them are involved in the mitochondrial pathway (Fig. 2A). There are 18 transcripts implicated in mitochondria-dependent apoptosis including PTEN, CD27, VDR and MAL. PTEN is expressed in most neurons and localized in both cytoplasm and nucleus, and PTEN deficiency in neurons led to synaptic disorder. As a pro-apoptotic protein, PTEN accumulated gradually in the mitochondria accompanied with a translocation of Bax to mitochondria in apoptosis(Zhu et al. 2006). CD27-binding protein (siva) mediates apoptotic cell death via caspase-8 by interacting with its cognate receptor, CD27 to mediate mitochondrial membrane permeability, and to release the pro-apoptotic molecules, cytochrome C and apoptosis-inducing factor (AIF) (Hase et al. 2002). Vitamin D_3, acts through the nuclear vitamin D_3 receptor (VDR), inducing apoptosis by disruption of mitochondrial function, which is associated with Bax translocation to mitochondria, cytochrome C release, and production of reactive oxygen species (Narvaez and Welsh 2001). MAL may induce apoptosis via a direct interaction with mitochondria and lead to the release of cytochrome C into the cytosol (Kohler et al. 1999). We also found some genes that participate in apoptosis pathway activated by ER stress, such as DDIT3, also known as C/EBP homologous protein (CHOP), the first identified protein that mediates ER stress-induced apoptosis. It is to be noted that overexpression of CHOP leads to translocation of Bax from the cytosol to the mitochondria. CHOP-mediated apoptosis pathway is finally transmitted to the mitochondria. Several studies indicated that mutations in presenilin-1, which increased the production of β-amyloid, led to increase CHOP protein(Oyadomari and Mori 2004). It has been reported that Aβ is a potent mitochondrial poison, inhibiting key mitochondrial enzymes in the brain of AD patients. Based on the previous studies and our analysis, we suggested that mitochondrial dysfunction and subsequent neuronal apoptosis should been regarded as a potential mechanism in the pathogenesis of AD.

Changes of genes encoding axon guidance Our network analysis also points to the involvement of molecules regulating axon guidance, which might associate with loss of synaptic communication (Figure 2B). Brain function is based on precise neuronal-network formation during development, which is largely controlled by many axon-guidance molecules. The axon-guidance pathway consists of four major classes of ligands (ephrin, netrin, semaphorin and slit proteins) and their respective receptors (e.g. eph, DCC and UNC, neuropilin and plexin, and ROBO proteins) coupled with several downstream signaling proteins (e.g. Nck1, RhoA, Gi, and Fyn proteins). The expression levels of several genes implicated in these four axon guidance

pathways are significantly changed in Tg2576 mice and were marked with red star in Figure 2B.

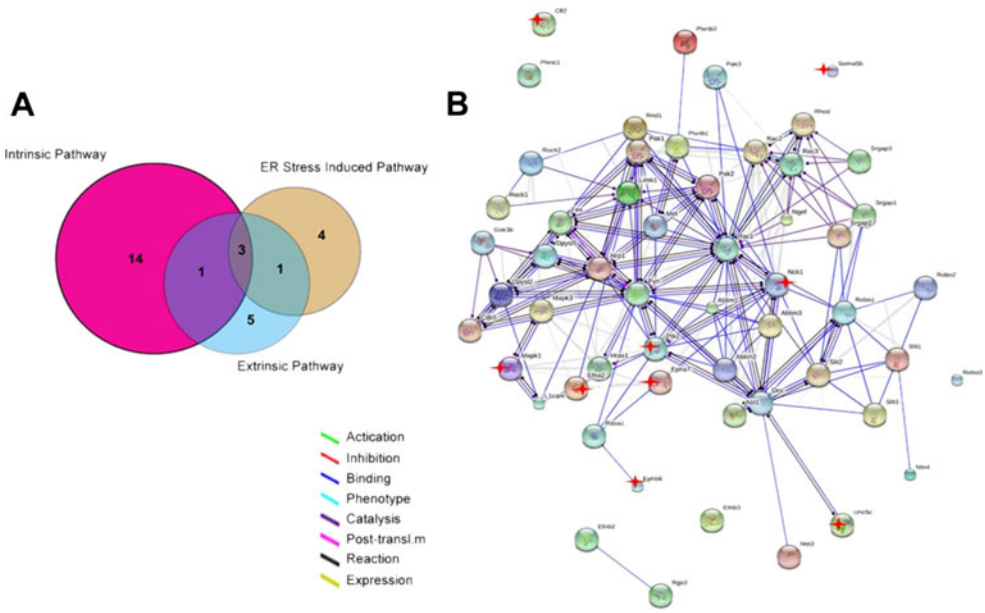

Fig. 2 (**A**) Venn diagram comparison of intrinsic, extrinsic and ER stress induced apoptosis pathway interactions identified in this study. (**B**) Graphic representation of a network consisting of predicted axon guidance pathway with differentially expressed genes

Receptor tyrosine kinases of the Eph family binding to ephrin ligands are important in development, especially in mediating axon guidance events that shape the formation of precise neuronal connections. In the developing CNS, EphB–ephrinB binding regulates cell migration, axon guidance and synaptogenesis, while in the adult brain it regulates memory-related functions, including synaptic plasticity and long-term potentiation(Sloniowski and Ethell 2012). In addition, a recent study had revealed that the expression level of EphB2 is downregulated in AD animal model and overexpression of EphB2 could rescue the cognitive defects (Cisse et al. 2011). Ephrin also stimulates multiple signal pathways that involved in modulating the dynamic cytoskeletal rearrangements required during cellular remodeling, such as migration and neurite outgrowth. Interestingly, Nck1, known as actin cytoskeleton regulators, the direct target of EphAs from our network, has been reported to function as downstream of several axon guidance receptors including ROBO, DCC and the Eph receptor tyrosine kinases (RTKs)(Mohamed et al. 2012), whereas Nck indirectly interact with EphBs. Both Nck1 and PTK2 interact with Fyn, one of the hubs in the network that involved in the synaptic and behavioral deficits associated with Aβ deposition. Fyn depletion reduced the synaptotoxicity in hAPP mice while Fyn overexpression exacerbated cell death in hAPP transgenic mice (Chin et al. 2005). Furthermore, Fyn and focal adhesion kinase (FAK), known as PTK2, are essential mediators in Netrin signaling. Suppression of Fyn or FAK impairs neurite outgrowth and cell migration. Both of FAK and Fyn are overexpressed in AD brains and participating in Aβ-induced tyrosine phosphorylation of Tau (Williamson et al. 2002). On the other hand, Aβ binds to integrin and activates FAK, inducing the reactivation of the cell cycle and cell death ultimately (Frasca et al. 2008). Together, these chemical signals provide a series of attraction and repulsion cues that direct axons to their targets. In summary, targeting these chemical signals might be beneficial in AD.

AD-Related Chromosomal Distribution of Differentially Expressed Genes We further identified whether the differentially expressed genes are significantly enriched in particular chromosomal and within specific chromosomal regions by applying positional gene enrichment (PGE) analysis to map the genes that are higher expressed in Tg2576 mice (De Preter et al. 2008). We defined the “enriched region” as clustering with at least three genes and FDR P-value is less than 0.05 and a total of 16 regions were found (Table 2). The most significant regions that had clusters of at least 6 genes, were found in chromosomes 3, 4, 6, 11, 15, and 18 (Fig. 3). One particular cluster on chromosome 3 (n=10 genes) included ADAR (adenosine deaminase, RNA specific), which encodes RNA-editing enzyme, is responsible for conversion of A-to-I in double-stranded (ds) RNA. This kind of alterations in A-to-I editing has been implicated in physiological and neuropsychiatric disorders including schizophrenia, Alzheimer's disease, Huntington's disease and depression with suicide(Mehler and Mattick 2006).Interestingly, among the genes localized in

chromosomal 4, 50% of genes of interests are in the clustered region are associated with transcription regulation, including LEDGF/p75 (a transcriptional co-activator involved in neuro-epithelial stem cell differentiation and neurogenesis), transducin-like enhancer protein 1 (inhibits NF-kappa-B-regulated gene expression) and zinc finger protein 37.

Table 2 Chromosomal Regions Significantly Enriched

Chr	Coordinates	Corrected P value	% Genes detected per region
15	78,229,695-79,158,583	1.38E-02	19
4	3,476,418-3,870670	1.38E-02	44
3	88,128,982-89,866366	1.38E-02	14
2	27,7422,05-28,477,511	1.44E-02	36
6	83,085,881-85,401,262	1.51E-02	18
3	95,792,724-98,663,717	1.77E-02	13
18	32,282,783-35,750,460	1.77E-02	15
15	10,107,410-12,114,218	1.77E-02	25
19	45,822,226-46,470,228	1.77E-02	22
10	126,459,388-126-733,340	1.87E-02	21
11	94,189,315-96-146,639	2.42E-02	11
2	25,207,810-26,063,709	2.44E-02	12
19	3,896,052-4,156,711	2.44E-02	16
17	44,632,936-46,384,944	2.80E-02	14
14	13,205,077-21,475,717	3.26E-02	10
4	61,850,577-86,257,928	3.28E-02	9

Chr, chromosome.Significant results had a minimum clustering of three genes within each region (FDR, P-value<0.05).

Regulatory elements and transcription factors of co-regulated genes Computational analysis of promoters of co-expressed genes can provide additional evidence for the regulation of a gene set by specific TFs. By using Gene Set Enrichment Analysis (GSEA), we searched for significantly over-represented TF promoter binding motifs in their promoter regions among differentially up-regulated genes (Table 3). Of note, multiple gene sets could be assigned to the same TF, including paired box gene 4, GABPA/GABPB2 and NFAT/NFATC. Consistent with the result, several previous studies suggested serum response factor (SRF) and myocardin (MYOCD), two interacting transcription factors that are overexpressed in AD, can block Aβ clearance(Bell et al. 2009). NFAT, a nuclear factor of activated T cells in immune/inflammatory signaling, was also found in the regulation of Ca^{2+} homeostasis, neuronal viability, and Aβproduction (Abdul et al. 2010). These finding reinforce the importance of these motifs associated with AD.

Moreover, we found some interesting TF-binding motifs such as retinotopic acid receptor (RAR)-related orphan receptor alpha (RORA). It exerted both neuroprotective and anti-inflammatory functions in neuronal and glial cells by increasing the expression of antioxidant proteins making them less sensitive to apoptotic stimuli. Epidemiological genetic analysis implicated this gene in several neurodegenerative diseases including: depression, age-related macular degeneration, and Parkinson's disease. And it has also been suggested as a candidate for pleiotropic association between fractional anisotropy (FA) and gray matter (GM) thickness in a neuroimaging study from AD patient (Kochunov et al. 2011).

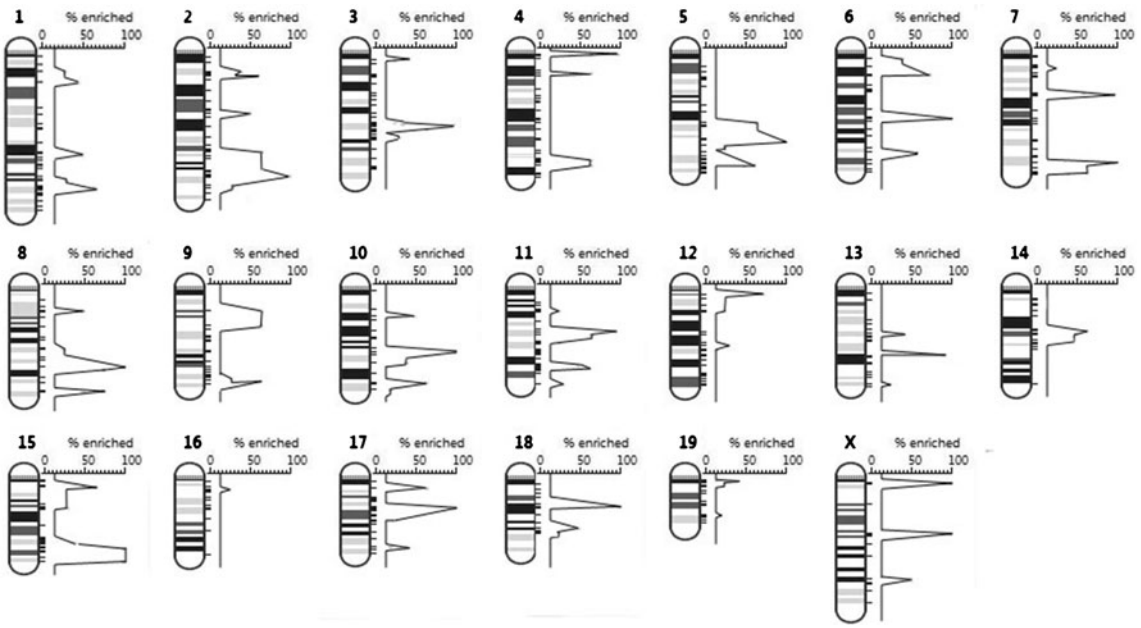

Fig. 3 Karyotype density map of all significantly enriched chromosomal regions. Peaks reflect significant chromosomal clusters, P<0.05. See Table 2 for associated *P* values

Table 3 Occurrence of Transcription Factor-Binding sites Detected by GSEA Analysis

Transcription factor-binding site	Gene set name	SIZE	NES
PAX2: paired box gene 2	V$PAX_Q6	118	1.4
NR6A1: nuclear receptor subfamily 6, group A, member 1	V$GNCF_01	28	1.3
GABPA/GABPB2	V$GABP_B	103	1.3
	MGGAAGTG_V $GABP_B	325	1.1
RORA: RAR-related orphan receptor A	V$RORA2_01	62	1.2
NFAT/NFATC	V$NFAT_Q4_01	114	1.2
	V$NFAT_Q6	112	1.2
LHX3: LIM homeobox 3	YTAATTAA_V $LHX3_01	68	1.2
TITF1: thyroid transcription factor 1	V$TITF1_Q3	109	1.2
FOXI1: forkhead box I1	V$HFH3_01	93	1.2
SRF: serum response factor	CCAWWNAAGG_V $SRF_Q4	44	1.2
NKX2-5: NK2 transcription factor related	V$NKX25_01	55	1.1
NR3C1: nuclear receptor subfamily 3, group C	V$GRE_C	54	1.1
PAX4: paired box gene 4	V$PAX4_04	97	1.1
	V$PAX4_02	103	1.0
CEBPA: CCAAT/enhancer binding protein (C/EBP), alpha	V$CEBP_C	98	1.1
CART1: cartilage paired-class homeoprotein 1	V$CART1_01	80	1.1
OLF1/OR5I1	V$OLF1_01	122	1.1
FOXJ2: forkhead box J2	V$FOXJ2_02	99	11
CUTL1: cut-like 1, CCAAT dis placement protein	V$CDP_02	51	1.1
KLF12: Kruppel-like factor 12	V$AP2REP_01	73	1.1
STAT5A: signal transducer and activator of transcription 5A	V$STAT5A_04	88	1.1
SRY: sex determining region Y	V$SRY_02	110	1.0
CRX: cone-rod homeobox	V$CRX_Q4	118	1.0

Gene set name, Gene sets that contain genes that share a TF-binding site as defined in the TRANSFAC database; size, number of genes in gene set; NES, normalized enrichment score

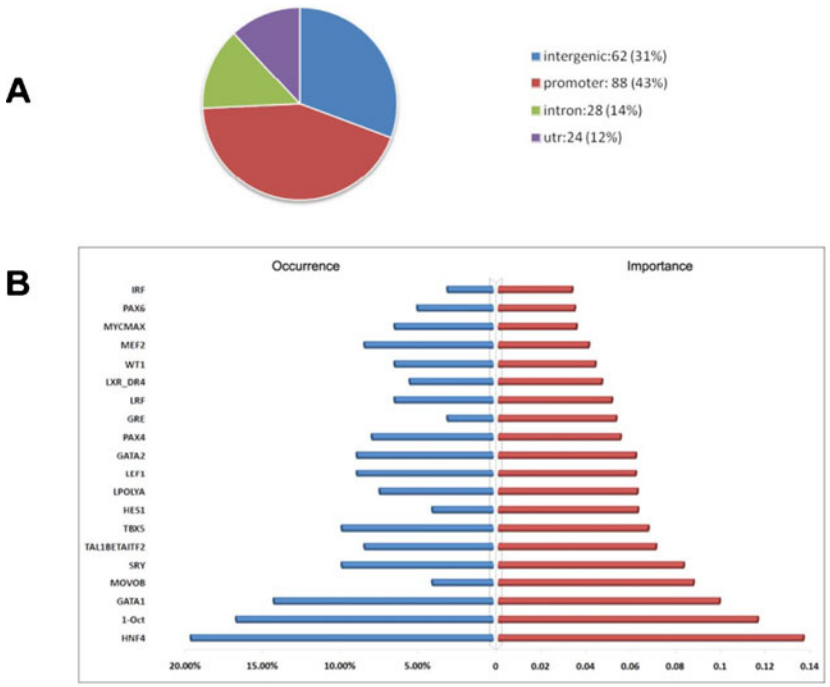

Fig. 4 (**A**) Predicted distant regulatory elements identified using DiRE analysis. (**B**) "Occurrence" describes the percentage of candidate regulatory elements containing a conserved binding site for a particular TF. "Importance" is defined as the product of the TF response element occurrence and its assigned weight

Next, we used comparative genomic tool Distant Regulatory Elements of co-regulated genes (DiRE) to predict distant regulatory elements within the promoters of those genes based on their inter-species conservation and their transcription factor binding sites (Gotea and Ovcharenko 2008). When the analysis was extended to promoters and the most conserved Evolutionary Conserved Regions (ECRs), the majority of which were distributed to

promoters (43%), we also predict regulatory elements within intergenic regions (31%), introns (14%) and UTRs (12%) (Fig. 4A). This indicates the genes we interested might be regulated not only through classically positioned upstream promoters, but also by nonclassical proximal and distal regulatory elements. The candidate TFs with the highest occurrence and importance that bind to these regulatory elements presented in Figure 4B. The identification of paired box family members (PAX4) and SOX (SRY-like box) gene family members (SRY), which were detected by GSEA analysis (Table 3), further strengthens our hypothesis that TFs play a significant role in the response of overexpression APPsw.

Conclusion Numerous studies identified that Aβ play a significant role in the onset and progression of AD. Aβcould induce apoptosis and impair synaptic connection by disturbing the function of mitochondria, which is the prominent contributor to the alterations of intracellular Ca^{2+} signaling and source of ROS. Understanding the downstream of mitochondrial apoptosis pathway may uncover potential therapeutic targets for AD. It is of noted that evidence also suggests transcription as a significant functional group in their analysis of gene expression profiles. Modulators of inflammatory process and neuronal Ca^{2+} signaling, which were impaired by some disturbance of transcriptional factors (TF) and TF-binding motifs, may be potential therapeutic targets for AD.

Acknowledgements This work was supported in parts by the National Natural Science Foundation of China (30971478, 91132725), the New Century Excellent Talent of Education Ministry (NCET-10-0421), the Ministry of Science and Technology of China (2011DFG33250), Fundamental Research Funds for the Central Universities, HUST (2012QN134), and the New Investigator Research Grant of Alzheimer's Association (NIRG-11-205737).

References:

Abdul, H.M., Furman, J.L., Sama, M.A., Mathis, D.M., Norris, C.M. (2010). NFATs and Alzheimer's Disease. Mol Cell Pharmacol 2, 7-14

Bell, R.D., et al. (2009). SRF and myocardin regulate LRP-mediated amyloid-beta clearance in brain vascular cells. Nat. Cell Biol. 11, 143-53 doi:10.1038/ncb1819

Brookmeyer, R., Johnson, E., Ziegler-Graham, K., Arrighi, H.M. (2007). Forecasting the global burden of Alzheimer's disease. Alzheimers Dement 3, 186-91 doi:10.1016/j.jalz.2007.04.381

Chin, J., et al. (2005). Fyn kinase induces synaptic and cognitive impairments in a transgenic mouse model of Alzheimer's disease. J. Neurosci. 25, 9694-703 doi:10.1523/JNEUROSCI.2980-05.2005

Cisse, M., et al. (2011). Reversing EphB2 depletion rescues cognitive functions in Alzheimer model. Nature 469, 47-52 doi:10.1038/nature09635

De Preter, K., Barriot, R., Speleman, F., Vandesompele, J., Moreau, Y. (2008). Positional gene enrichment analysis of gene sets for high-resolution identification of overrepresented chromosomal regions. Nucleic Acids Res. 36, e43 doi:10.1093/nar/gkn114

Dickey, C.A., Loring, J.F., Montgomery, J., Gordon, M.N., Eastman, P.S., Morgan, D. (2003). Selectively reduced expression of synaptic plasticity-related genes in amyloid precursor protein+presenilin-1 transgenic mice. J. Neurosci. 23, 5219-26

Frasca, G., Carbonaro, V., Merlo, S., Copani, A., Sortino, M.A. (2008). Integrins mediate beta-amyloid-induced cell-cycle activation and neuronal death. J. Neurosci. Res. 86, 350-5 doi:10.1002/jnr.21487

Gotea, V., Ovcharenko, I. (2008). DiRE: identifying distant regulatory elements of co-expressed genes. Nucleic Acids Res. 36, W133-9 doi:10.1093/nar/gkn300

Hase, H., Kanno, Y., Kojima, H., Morimoto, C., Okumura, K., Kobata, T. (2002). CD27 and CD40 inhibit p53-independent mitochondrial pathways in apoptosis of B cells induced by B cell receptor ligation. J. Biol. Chem. 277, 46950-8 doi:10.1074/jbc.M209050200

Hsiao, K., et al. (1996). Correlative memory deficits, Abeta elevation, and amyloid plaques in transgenic mice. Science 274, 99-102

Huang, D.W., Sherman, B.T., Lempicki, R.A. (2009a). Systematic and integrative analysis of large gene lists using DAVID bioinformatics resources. Nat Protoc 4, 44-57 doi:10.1038/nprot.2008.211

Huang, D.W., Sherman, B.T., Lempicki, R.A. (2009b). Bioinformatics enrichment tools: paths toward the comprehensive functional analysis of large gene lists. Nucleic Acids Res. 37, 1-13 doi:10.1093/nar/gkn923

Kochunov, P., et al. (2011). Genetic analysis of cortical thickness and fractional anisotropy of water diffusion in the brain. Front Neurosci 5, 120 doi:10.3389/fnins.2011.00120

Kohler, C., Hakansson, A., Svanborg, C., Orrenius, S., Zhivotovsky, B. (1999). Protease activation in apoptosis induced by MAL. Exp. Cell Res. 249, 260-8 doi:10.1006/excr.1999.4472

Lehman, E.J., Kulnane, L.S., Lamb, B.T. (2003). Alterations in beta-amyloid production and deposition in brain regions of two transgenic models. Neurobiol. Aging 24, 645-53

Mehler, M.F., Mattick, J.S. (2006). Non-coding RNAs in the nervous system. J Physiol 575, 333-41 doi:10.1113/jphysiol.2006.113191

Mohamed, A.M., Boudreau, J.R., Yu, F.P., Liu, J., Chin-Sang, I.D. (2012). The Caenorhabditis elegans Eph receptor activates NCK and N-WASP, and inhibits Ena/VASP to regulate growth cone dynamics during axon guidance. PLoS Genet 8, e1002513 doi:10.1371/journal.pgen.1002513

Mootha, V.K., et al. (2003). PGC-1alpha-responsive genes involved in oxidative phosphorylation are coordinately downregulated in human diabetes. Nat. Genet. 34, 267-73 doi:10.1038/ng1180
Narvaez, C.J., Welsh, J. (2001). Role of mitochondria and caspases in vitamin D-mediated apoptosis of MCF-7 breast cancer cells. J. Biol. Chem. 276, 9101-7 doi:10.1074/jbc.M006876200
Oyadomari, S., Mori, M. (2004). Roles of CHOP/GADD153 in endoplasmic reticulum stress. Cell Death Differ. 11, 381-9 doi:10.1038/sj.cdd.4401373
Sloniowski, S., Ethell, I.M. (2012). Looking forward to EphB signaling in synapses. Semin. Cell Dev. Biol. 23, 75-82 doi:10.1016/j.semcdb.2011.10.020
Stein, T.D., Anders, N.J., DeCarli, C., Chan, S.L., Mattson, M.P., Johnson, J.A. (2004). Neutralization of transthyretin reverses the neuroprotective effects of secreted amyloid precursor protein (APP) in APPSW mice resulting in tau phosphorylation and loss of hippocampal neurons: support for the amyloid hypothesis. J. Neurosci. 24, 7707-17 doi:10.1523/JNEUROSCI.2211-04.2004
Subramanian, A., et al. (2005). Gene set enrichment analysis: a knowledge-based approach for interpreting genome-wide expression profiles. Proc Natl Acad Sci U S A 102, 15545-50 doi:10.1073/pnas.0506580102
Suh, Y.H., Checler, F. (2002). Amyloid precursor protein, presenilins, and alpha-synuclein: molecular pathogenesis and pharmacological applications in Alzheimer's disease. Pharmacol. Rev. 54, 469-525
Williamson, R., et al. (2002). Rapid tyrosine phosphorylation of neuronal proteins including tau and focal adhesion kinase in response to amyloid-beta peptide exposure: involvement of Src family protein kinases. J. Neurosci. 22, 10-20
Zhu, Y., Hoell, P., Ahlemeyer, B., Krieglstein, J. (2006). PTEN: a crucial mediator of mitochondria-dependent apoptosis. Apoptosis 11, 197-207 doi:10.1007/s10495-006-3714-5

AR-005

Study of multiple genes introduced-neural stem cells transplantation to treat aganglionic megacolon mice

Yong Xiao[1,6], Jingbo Chen[2,6], Nianfeng Sun[3,6], Qingliang Meng[1], Jintong Ji[1], Shugguang Huang[5], Xinwei Wang[1], Huijuan Jin[4,*], Xiaogang Shu[1,*], Guobin Wang[1,*]

[1]Departments of Gastrointestinal Surgery, Union Hospital, Tongji Meddical College, Huazhong University of Science and Technology, 1277 Jiefang Avenue, Wuhan Hubei 430022, P.R China
[2]Departments of Gastrointestinal Surgery, Shandong Provincial Qianfoshan Hospital. The city of Jinan by ten Road No. 16766, Shandong Province, 250014, P.R China
[3]Departments of Vascular Surgery, Jinan Central Hospital. No.105 Jiefang Road, 250013, P.R China
[4]Departments of the First College of Clinical Medical Science, China, Three Gorges University
[5]Departments of General Surgery, Wuhan Medical Health Center for Women and Children,Jiangan District, 100th Road, Hong Kong. Wuhan Hubei 430016, P.R China
[6]These authors contributed to this work.
*Correspondence: jinhuijuan1983@163.com, sxg678@yahoo.com, wgb@whuh.com

Abstract
To explore a potential methodology for treating aganglinonic megacolon, neural stem cells (NSCs) expressing engineered endothelin receptor type B (EDNRB) and glial cell-derived neurotrophic factor (GDNF) genes were transplanted into the aganglinonic megacolon mice. After transplantation, the regeneration of neurons in the colon tissue was observed and expression levels of differentiation related genes were determined. Primary culture of NSCs were obtained from the cortex of postnatal mouse brain and infected with recombinant adenovirus expressing EDNRB and GDNF genes. The mouse model of aganglionic megacolon was developed by treating the colon tissue with 0.5% Benzalkonium Chloride (BAC) to selectively remove the myenteric nerve plexus that resemble the pathological changes in human congenital megacolon. The NSCs stably expressing the EDNRB and GDNF genes were transplanted into the benzalkonium chloride (BAC)-induced mouse aganglionic colon. Survival and differentiation of the implanted stem cells were assessed after transplantation. Results showed that the EDNRB and GDNF genes were able to be expressed in primary culture of NSCs by adenovirus infection. One week after implantation, grafted NSCs survived and differentiated into neurons. Compared to the controls, elevated expression of EDNRB and GDNF was determined in BAC-induced aganglionic megacolon mice with partially improved intestinal function. Those founding indicated that the genes transfected into NSCs were expressed in vivo after transplantation. Also, this study provided favorable support for the therapeutic potential of multiple gene modified NSC transplantation to treat Hirschsprung's disease, a congenital disorder of the colon in which ganglion cells are absent.
Keywords: Hirschsprung's disease; Neural stem cells; EDNRB gene; GDNF gene

Materials and Methods

Materials Experimental Animals:New-born Kunming mice (male or female, average body weigh 1.5g±0.2g) and adult 8-week old male Kunming mice (average body weigh 29g± 1.8g) were purchased from animal core of Tongji Medical College (Wuhan, China). (Batch No: SYXK (E) 2004-0028). Major reagents:Diethyl pyrocarbonate, agarose, low

melting point agarose DMEM/F12 (1:1) (Sigma-Aldrich, St Louis, MO, USA), B27 Supplement (Invitrogen, Grand Island, NY, USA), EGF and βFGF (PeproTech, UK), 50% benzalkonium chloride (BAC) (Sigma, Fluka , Switzerland), Nestin polyclonal antibody (Boster, Wuhan, China), NSE monoclonal antibody (Abcam, Cambridge, MA, USA), GFAP monoclonal antibody (Sigma-Aldrich, St Louis, MO, USA), SABC-FITC, SABC-CY3 kit (Boster, Wuhan, China), SABC and DAB kit (Boster, Wuhan, China), IRES expression vector pIRES (Clontech, Mountain View, CA, USA), HEK 293 cell, E.coli DH5α were stored by our lab, M-MLV reverse transcriptase, Taq DNA polymerase (Roach, Indianapolis, IN, USA), RNAase inhibitor and dNTPs (Promega, Madison, WI, USA), T4 DNA ligase, endonuclease XbaI, KpnI, DNA marker DL 2000, Purigene DNA extraction kit (Takara, Dalian, China), diethyl pyrocarbonate, agarose and low melting point agarose (Sigma-Aldrich, St Louis, MO, USA), Trizol (Gibco, Grand Island, NY, USA). Primer design: upstream and downstream primers were designed based on sequence from Gene Bank and literature report, and synthesized by Shanghai bioengineering company.

Methods 1.Construction and identification of recombinant adenovirus vector with mouse GDNF and EDNRB gene

Construction of multiple-gene expression adenovirus vector The mouse GDNF and EDNRB cDNAs were derived from mouse brain and heart respectively by reverse transcription-polymerase chain reaction (RT-PCR). The primers for amplifying GDNF were: Primer-F: 5′ GCTCGGTACC GACTCTAAGATGAAGTTA 3′ and Primer-R: 5′ GGAGTCTAGAGGGTCAGATACATCCACAC 3′. Sequences of restriction endonuclease sites of KpnI and XbaI were added to the 5' end of forward and reverse primers respectively. The primers for amplifying EDNRB were Primer-F: 5′ CCGCTGTCTGGCATTCTC 3′ and Primer-R: 5′ GCCGTGCTGAAGTGCTGA 3′. EcoII and BamHI restriction sites were added to the 5' end of forward and reverse primers respectively. The PCR products of GDNF was subcloned into KpnI and XbaI multiple clone sites, followed by subcloning the PCR products EDNRB gene into EcoII and BamHI multiple clone sites of pAdTrack-CMV vector. An IRES sequence from pIRES vector was subcloned between GDNF and EDNRB gene by inserting into XbaI and EcoII sites of pAdTrack-CMV. The new constructed plasmid was named as pAdTrack-CMV-GE and was sequenced by Shanghai Bioengineering Company.

Preparation of Ad-GE recombinant adenovirus and measurement of virus titer AdEasier1 cells and EcoliDH5-α electroporated competent cells were prepared with 10% pre-cold sterile glycerol. The pAdTrack-CMV-GE plasmid was linearized by digestion with PmeI restriction enzyme. 1μg linear pAdTrack-CMV-GE was mixed with 20μl AdEasier1 and co-transformed into competent cells by electroporation at setting of 2,500 V, 200 Ω and 25μF. Transformed cells were selected by Kanamycin (50mg/L) resistance on LB solid agar plates. Fifteen colonies were randomly selected after incubation for 16 hours and plasmids were extracted from these clones. Positive plasmids with similar size of pAdEasy1 were further transformed into Ecoli DH5α competent cells by electroporation at the same setting that has used above. Recombinant adenoviral plasmids were extracted from clones grown on the plates and identified by Pad endonuclease digestion. The confirmed plasmid was named as pAD-GE and purified for transfection. Twenty-four hours prior to transfection, the 293 cells were seeded onto a 60mm cell culture plate at 2×106 cells per well until grown 60-80% of confluence. 4 μg of linearized pAD-GE plasmid digested by PacI endonuclease was transfected into 293 cells by Lipofectamine 2000 reagent according to the manufacture's instruction. Fresh FBS medium (100ml/L) was replaced at 24 hour after transfection. GFP fluorescence was observed at three days post transfection with fluorescence microscope. Seven days after transfection, 293 cells were collected and repeated freeze-thaw lysis for four times. After centrifugation, supernatant was collected. Virus expansion was achieved by infecting more 293 cells with the supernatant. After five days, infected 293 cells were collected and centrifuge at 1,500 rpm for 7 minutes. The supernatant was discarded and the pellets were washed with 2ml PBS per dish, followed by four repeated freeze-thaw cycles. The infection and collection steps were repeated one more time as described above. The final PBS supernatant was collected and the adenovirus was purified from the virus re-suspension by CsCL density-gradient ultracentrifugation. To calculate the virus titers, 293 cells were seeded at density of 5×105 per well onto a 6-well plate and infected with a series of virus dilutions. 72 hours later, the Ad-GE virus titers (expression forming unit/liter efu/L) were calculated based on the numbers of GFP positive cells observed.

2.NSCs primary culture and gene transfection

Mouse NSCs were obtained and cultured as described in literature. SABC immunohistochemistry staining against Nestin was performed to assess pre-differentiation status of neurospheres. Glial fibrillary acidic protein (GFAP) and Neuron specific enolase (NSE) are markers for astrocytes and neuron respectively, and were stained by IHC to examine the multiple potent of NSCs. NSCs were infected by adenovirus as described in jetPEITM In vitro transfection protocols. GFP fluorescence was dynamically observed at 24 to 72 hours after infection. At 48 hours after transfection, the average number of positive cells was calculated from 10 random fields under 100x objects. The average number multiplied by 50 is the positive cell number per well in a

24-well plate. Transfection efficiency was examined by FACstar flow cytometry at 24, 48 and 72 hours after infection. Three samples were tested from each group and 10,000 cells per sample were enumerated. The calculation formula of positive transfection rate was: efficiency (GFP positive cell ratio)=percentage of GFP positive cells (M1 region) – percentage of GFP negative cells (M1 region), and GFP positive cell region is designated M1 region based on the negative control of untransfected cells. The gene expression levels were examined at 24, 48 and 72 hours after transfection.

Primer design: Internal reference β-Actin 443bp Tm 52.6°C
Forward :5′- GGGAAATCGTGCGTGA-3′
Reverse :5′- CTGGAAGGTGGACAGTGAG-3′
EDNRB 208bp Tm 53.1°C
Forward :5′- ACAAGCACGATCCGTAGT-3′
Reverse :5′- ACGCCACCCACTAAGACC-3′
GDNF 240bp Tm 54.6°C
Forward :5′-TGGTCTATTTGTTCGCCG-3′
Reverse :5′-GGATGTCGTGGCTGTCTG-3′

3.Construction and identification of Mouse model of aganglionic megacolon

Ninety male Kunming mice of 8-week old were randomly divided into 3 groups: (1) BAC group (n=30), of which colonic serosa was treated with 0.5% BAC as denervation reagent. (2) NS group (n=30), received saline instead of a denervation reagent and (3) Normal control group (n=30), which has no treatment. For BAC treated group, mice were operated under anesthesia and 0.5 % BAC was applied onto the serous layer of colon descendens for 15 minutes. In NS group normal saline was applied instead of BAC. The behavior, diet and bowel movements were observed daily after surgery. 4 mice of each group were sacrificed at 2, 7, 14 and 28 days after surgery. The treated section of descending colon was obtained. After flushing intestinal lumen with saline, the tissues were examined for pathological changes, including the numbers of mysenteric neurons, mucous membrane, submuscous layer and muscle layer. To enumerate neurons, each treated colon segment was continuously cut into 200 slices of 5 μm thickness. Every 5 consecutive slices were combined as one group and total 40 groups were measured. The number of neurons was counted only from the first slice of each group and the sum of 40 groups was represented as the total neurons in a 1 mm of enteric plexuses of colon. Immuhistochemistry staining for NF-200 were performed to examine the removal of enteric plexuses. RT-PCR assay was performed to examine the mRNA expression level of NF-200 (Neurofilaments-200), GFAP (Glial fibrillary acidic protein), ChAT (Anti- Choline Acetyltransferase) and nNOS (neuronal nitric oxide synthase). Primers for RT-PCR were:

Internal reference β-actin 443bp
Forward :5′- GGGAAATCGTGCGTGA-3′
Reverse :5′- CTGGAAGGTGGACAGTGAG-3′
NF-200 215bp
Forward :5′- TTCAGCCAGACTACCTCCC-3′
Reverse :5′- CGCTGCGGATTAACAACC-3′
GFAP 188bp
Forward :5′- TTGTCCTTCTCGCGGTAC-3′
Reverse :5′- GTGGTATCGGTCTAAGTTTGC-3′
ChAT 159bp
Forward :5′- AAAATGGCGTCCAACGAG -3′
Reverse :5′- CAGGCATACCAGGCAGAT -3′
nNOS 102bp
Forward : 5′- ACAACCTCGCTACTATTCCA - 3′
Reverse : 5′- CCTTCTCCATCTCGGGTA - 3′

4.Survival, differentiation and gene expression of NSCs transplanted in the colonic wall of megacolon mice

NSCs transplantation Two weeks after denervation surgery, the mice survived from BAC group were randomly divided into two groups. (1) NSCs group (n=30) which received NSCs treatment and (2) NS group (n=30) which received saline treatment. NSCs introduced with EDNRB and GDNF genes were centrifuged and resuspended in PBS at a density of 1×10^6/100μl. A total of 200 μl NSC suspensions were injected into the denervated colon at 4 different sites using a 50 μl microinjector. After injection, the needle was hold in the same position for 5 minutes to distribute the cells suspension and prevent leakage. The sites of injection were labeled with 8-0 suture. In NS group, saline was injected instead of NSCs.

Survival and differentiation of NSCs *in vivo* The Biological features, behavior, diet and bowel movements were examined after transplantation surgery. At 7, 14, 21 and 28 days after surgery respectively, 2 mice were sacrificed from each group. Colons were harvested and frozen sections were prepared. GFP fluorescence was observed using fluorescence microscope to examine the survival of NSCs. NSE and GFAP expression in the frozen tissue sections were examined by immunofluorescence staining to determine the differentiation of transplanted NSCs. At the same time, number of neurons was counted used the same method as described above.

Examine the mRNA levels of ChAT, nNOS, GDNF and EDNRB genes by RT-PCR Two mice of each group were randomly selected and sacrificed at 28 days after transplantation. Segment of colon treated with NSCs or saline was harvested and cleaned. Mucous membrane and submuscous layer were carefully removed and the muscle layer was kept at -70 freezer and subjected to RT-PCR assay to detect the mRNA expression level of target genes. The method used and the primer design were described as above.

Statistical Analysis Data were analyzed using SPSS 13.0 (IBM SPSS Data Collection, Armonk, New York, US) and presented as mean±S.E.M. T test was used to compare the two different groups and difference between three or more groups were analyzed using a one-way ANOVA followed by the Newman-Keuls or Dunnett's *post-hoc* tests. *P*-values less than the 0.01 were considered statistically significant.

Results 1. Identification of pAdTrack CMV-GE by restriction endonuclease digestion

The recombinant plasmid pAd-GE was confirmed by restriction endonuclease digestion and agarose gel electrophoresis. The size of DNA fragments after digestion was the same as the size of GDNF and EDNRB genes, which matched with the DNA marker.(Fig 1a,b)

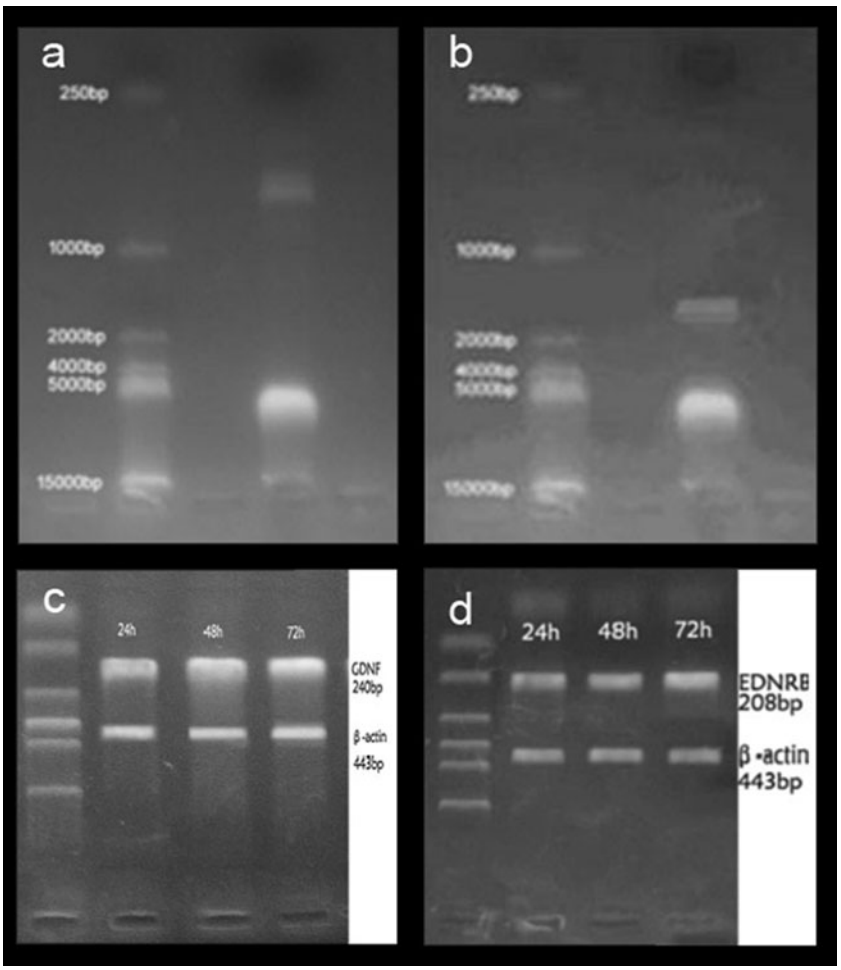

Fig. 1 Electrophoresis of pAdTrack CMV-GE by restriction endonuclease digestion and the expression levels of GDNF and EDNRB gene after transfection.The size of DNA fragments after digestion was the same as the size of GDNF and EDNRB genes, which matched with the DNA marker(a,b). The gene expression levels were examined at 24, 48 and 72 hours after transfection.Result showed that mRNA expression of these two genes can be detected as early as 24 hours after infection and reached to the maximum expression at 48 to 72 hours and declined gradually after 72 hours(c,d)

2.Primary culture of NSCs and transfection with recombinant adenovirus

GFP fluorescence was observed in small amount of NSCs at 24 hour after transfection with Ad-GE adenovirus. The intensity of fluorescence was strong and fluorescence was distributed in the neurospheres in circular or oval shape. The intensity of fluorescence reached the peak level at 48 hours after infection and the number of positive cells markedly increased. Cellular toxicity resulted from transfection was observed, including the appearance of less prominent projection on GFP positive cells, irregular shapes accompanied by distributed green granules and moderate number of cell deaths. However, the number of GFP positive cells can reach to 2.42×10^5 per well. Expression of reporter gene GFP suggested successful package of adenovirus particles.

Flow cytometry analysis showed that the efficiency of viral transfection was 15.36%, 24.67% and 25.73% at 24h, 48h and 72h respectively, and 0.45% for the control group.

Total RNA was extracted form NSCs at 24h, 48h, 72h and 96h after Ad-GE infection respectively. RT-PCR was

performed to examine the expression levels of GDNF and EDNRB gene. Result showed that mRNA expression of these two genes can be detected as early as 24 hours after infection and reached to the maximum expression at 48 to 72 hours and declined gradually after 72 hours.(Fig 1c,d)

3.Construction of mouse model of aganglionic megacolon

Histological measurement Histological measurement was performed at 2, 7, 14 and 28 day after surgery. Results showed that no morphological change was observed. The colons of sham and NS group of mice showed normal structures of mucous membrane, submuscous layer and muscle layers with normal distribution of myenteric neurons. In BAC group, mononuclear cell aggregates can be observed in serosa layer and muscle layers at 2 and 7 days after surgery. The structure of smooth muscle was close to normal at day 2 after surgery. Disordered and hypertrophy of smooth muscle structure appeared at 7 day after surgery. (Fig2)The number of myenteric neurons in BAC group mice has a significant decrease compared with sham and NS groups ($p<0.01$) at all of the time points measured after surgery. As early as 2 day after surgery, the number of myenteric neurons declined to 1/5 of the number in NS group, which is statistically significant compared to the other 3 time points. At 7, 14, 28 days after surgery, the reduced levels of neuron left were less than 10% of the number in normal group, and remained consistent with no marked difference between each time point.(Table1)

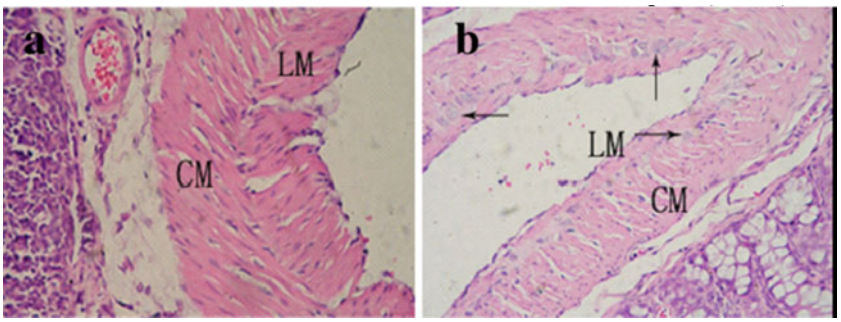

Fig. 2 HE staining was performed at 7 day after surgery. The tissues were examined for pathological changes, including the numbers of mysenteric neurons, mucous membrane, submuscous layer and muscle layer. BAC group showed myenteric nerve plexus absent and a smooth muscle layer with normal structure.-Mononuclear cell aggregates can be observed in serosa layer(a). NS group showed normal myenteric nerve plexus shown by the arrowhead(b)

Table 1 Number of myenteric plexus neurones at different time points after surgery (counts/mm)

(counts/mm)	Number of myenteric plexus neurons		
Postoperative days (d)	Normal group	NS group	BAC group
2	534.00±22.03	511.75±23.41	106.50±5.26●▲
7	533.50±39.61	520.25±14.43	38.50±8.23●▲
14	532.00±19.18	545.25±46.49	33.50±7.00●▲
28	523.00±39.41	531.75±30.77	28.50±6.19●▲

Normal group-Normal control, No treatment group; NS group-NS treatment group; BAC group-BAC treatment group; ●Compared with normal group $p<0.01$; ▲Compared with NS group $p<0.01$.

mRNA expression levels of NF-200, GFAP, ChAT and nNOS by RT-PCR

RT-PCR assay was used to examine the mRNA expression levels of NF-200, GFAP, ChAT and nNOS of each group at 14 days after surgery. Compared to Sham and NS control groups, BAC treatment led to a significant decrease of mRNA expression of NF-200, GFAP, ChAT and nNOS genes ($p<0.01$). The decreased mRNA expression in NF-200 and GFAP suggested a smaller number of neurons present in myenteric nerve plexus. The reduced mRNA expression of ChAT and nNOS suggested an impaired function of cholinergic neurons and nitrergic neurons which regulate the constriction and relaxation of smooth muscle, and consequently, the dysfunctional mobility of local intestinal segment.(Table2)

Table 2 The mRNA expression levels of NF-200, GFAP, ChAT and nNOS genes at 14 days after sugery

Group	NF-200	GFAP	ChAT	nNOS
Normal group	0.96±0.11	1.05±0.11	0.94±0.12	1.04±0.11
NS group	0.92±0.08	0.94±0.11	1.02±0.11	1.00±0.12
BAC group	0.18±0.04●▲	0.20±0.03●▲	0.15±0.02●▲	0.14±0.02●▲

Normal group-Normal control, No treatment group; NS group-NS treatment group; BAC group-BAC treatment group; ●Compared with normal group $p<0.01$; ▲Compared with NS group $p<0.01$.

4.Survival, differentiation and gene expression of transplanted NSCs in aganglionic megacolon mice

Survival and differentiation of transplanted NSCs At 7 days after transplantation, green fluorescence can be observed under UV light at muscle layer of colon wall in NSCs group. Immunofluorescence assay showed positive Nestin signal at NSCs transplanted colon segment but little NSE and GFAP positive cells. Results indicated that the NSCs can survive in myenteric microenvironment at 7 days after transplantation but no differentiation occurred yet. No positive signal was observed in NS group. At 21 days after NSCs transplantation, cells with green fluorescence were still present. Immunofluorescence assay showed no Nestion positive cells. Most are NSE positive cells and a small portion of cells were expressing GFAP, which suggested that by now NSCs have differentiated mostly into neurons and some differentiated into neurogliocytes.(Fig3) Compared to NSCs treatment group, only small portion of NSE positive cells can be detected in NS group.

mRNA expression levels of ChAT, nNOS, GDNF and EDNRB by RT-PCR RT-PCR assay was used to examine the mRNA expression levels of genes in NS and NSCs groups. At 28 days after transplantation surgery, relative expression level of ChAT in NS group was 0.27±0.03 compared to 0.53±0.04 at NSCs group ($P<0.01$). The relative expression level of nNOS in NS group was 0.17±0.03 compared to 0.4±0.04 at NSCs group ($P<0.01$).(Table3) The increased expression of ChAT and nNOS mRNAs suggested that the transplanted NSCs differentiated into functional cholinergic neuron and nNOS positive neurons which regulate the bowel movement function. RT-PCR results also show an elevated expression of GDNF and EDNRB mRNAs which suggested the genes introduced into NSCs can be effectively expressed in vivo after transplantation.

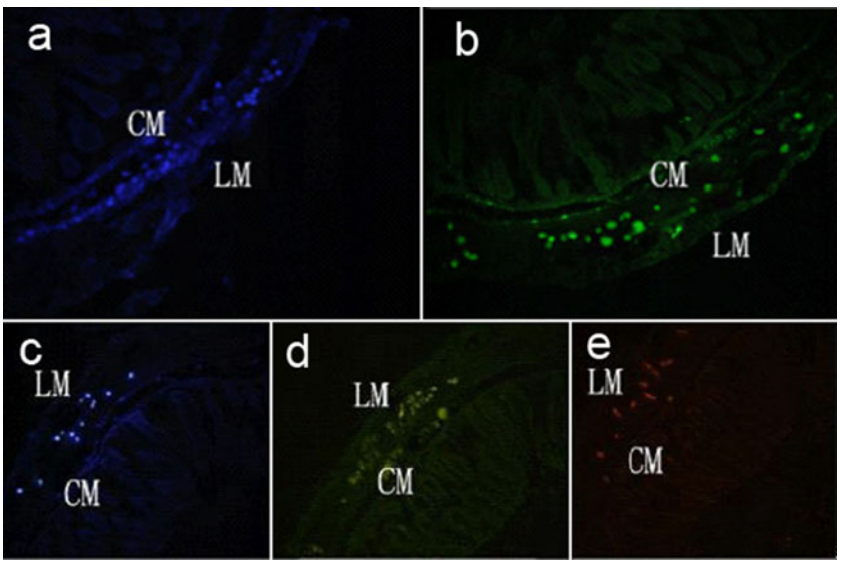

Fig. 3 After NSCs transplantation, fluorescence microscopy observed the muscle layer of colon wall in NSCs group. At 7 days, Hoechst3343 labeled NSCs can be observed under UV light at muscle layer of colon wall (a). Immunofluorescence assay showed positive Nestin signal at NSCs transplanted colon segment but little NSE and GFAP positive cells(b). However, at 21 days, Hoechst3343 labeled NSCs were still present(c), NSE expression determined by immunohistofluorescence staining, FITC-labeled(d) and GFAP expression, CY3-labeled(e)

Table 3 Relative mRNA expression levels of ChAT, nNOS, GDNF and EDNRB at 28days after transplantation

	ChAT	nNOS	GDNF	EDNRB
NS group	0.27±0.03	0.17±0.03	0.29±0.03	0.14±0.06
NSCs group	0.53± 0.04▲	0.40± 0.04▲	0.43± 0.05▲	0.57± 0.04▲

Compared with NS group $p<0.01$

Discussion

The enteric nervous system (ENS) is embedded in the lining of the gastrointestinal system (including pancreas and gallbladder) that consisted of neuron, neural transmitter, proteins and their supportive cells. The major neurons of the ENS come from myenteric nerve plexuses and submucosal nerve plexuses. The major function of ENS includes the control of motility and regulation of fluid exchange and local blood flow. The ENS originates from neural crest cells

that colonize the gut during intra-uterine life. [1]After colonizing, neural crest-derived cells within the gut wall then migrate, propagate and differentiate into glial cells plus many different types of neurons, and generate the most complex part of the peripheral nervous system under the control of microenvironmental changes from gut. Hirschsprung disease is a disorder of the gut which is caused by the failure of the neural crest cells to migrate properly during fetal development of the intestine and the lack of normal functional neurons in myenteric nerve plexus as a consequence. Currently, surgery is the major therapeutic option; however, there are several concerns such as various complications and large wound resulted from surgical section of affected intestinal segment. More importantly, the long-term outcome after surgery is still uncertain.

Neural stem cells (NSCs) are the self-renewing, multipotent cells that generate the main phenotypes of the nervous system. The major function of NSCs serves as reservoir of the cellular backup to repair the nerve system damage and replenish neuron cells lost due to normal death. The characteristic of NSCs including: 1) the ability of self-renewing and proliferation through symmetric and asymmetric divisions. Symmetric division is the basis for the self-propagation of NSCs, and asymmetric divisions provide an identical progeny cells to itself and another intermediate neural progenitor cell. Thus NSCs are self-replenished with potent for further differentiation. 2) The ability of multi-directional differentiation. NSCs can be induced under varied induction conditions to differentiate into specialized cells such as neurons, astrocytes or oligodendrocytes.[2] 3) the ability of migration and well tissue compatibility. During the developing process of CNS in human and mammalian, NSCs migrate along the developmental lines and undergo regeneration and differentiation at distinct locations. The transplanted NSCs have the same capability of migration. These NSCs tend to be attracted toward the injured neuron cells that release the neural signals and differentiate into specialized cells [3]. 4) Low immunogenicity. NSCs are undifferentiated progenitor cells which do not express any mature neurocyte antigen. The low immunogenicity of NSCs would rarely elicit graft rejection after transplantation which favors their survival.[4] Because these key features, NSCs transplantation to treat CNS neurodegeneration disease and spinal cord injury has become a hot spot in neuroscience research field and achieved some affirmative experimental results. Such as Glioblastoma Multiforme [5]

There is relatively little research on treating the enteric nervous system disease with NSCs. Ranch U etal[6] has reported that NSCs derived from intestine of fetus or neonate has the ability to differentiate into neural precursor-cell for neurons and neuroglia cells. Richard M etal [7] showed that after mouse neural precursor-cells were transplanted into aganglionic mouse fetus, the precursor-cells could migrate and differentiate into functional neurons and restore the ability of regulating the construction rate of colon. Furthermore, Micci MA etal[8] transplanted NSCs into pylorus of gastroparesis mice (nNOS_/_ mice) and examine the gastric empting and pylorus function. They found that after transplantation NSCs could differentiate into nNOS positive neurons, and the gastric emptying function was remarkably restored.

Base on the previous research, we designed experiments to study the therapeutic potential of treating aganglionic megacolon mice by transplantation of NSCs that have been introduced with both GDNF and EDNRB genes by adenovirus infection. Findings of our study would establish a fundamental principle for the treatment of the human Hirschsprung's disease with stem cell therapy. In this study, we have shown a successful isolation and culture of the NSCs by Neurosphere methods, and NSCs were identified by positive Nestin IHC staining. Those NSCs can be induced by FBS to differentiate into neurons, astrocytes or oligodendrocytes. Also, we also successfully constructed an aganglionic megacolon mouse model by selectively denervating the myenteric nerve plexuses with 0.5% BAC. This model is valuable in the study of NSCs treatment of aganglionic megacolon.

In our study, we used microinjection technique to deliver the NSCs at multiple sites into the muscle layer of denervated segment of colon wall. Histology examination showed no obvious inflammatory response in the area around injection site, which suggested the low immunogenicity of NSCs. After 7 days of NSCs transplantation surgery, Nestin positive cells can be detected that indicates the survival of transplanted NSCs within colon wall. Meanwhile, the negative staining of NSE and GFAP at 7 days suggested that those NSCs have not been differentiated yet. At 21 days after transplantation, no Nestion positive cells were present and the majority of cells were NSE positive with a small portion of GRAP positive cells. Those finding indicated that most NSCs have been differentiated into neurons and to a less extent, glial cells. The expression pattern of NSCs *in vivo* was different from our *in vitro* study. We found that in vitro NSCs would differentiate more to astrocytes than to neurons with a ratio of less than 20%. The reason of this difference is unknown, but it may be closely related to the local cytokines secretion and the different microenvironment for the cells. Therefore, we assume that colon walls of this mouse model may provide the favorable microenvironment for the differentiation of NSCs mostly into neuron rather than

glial cells. To validate this, definitely further investigation of the *in vivo* differentiation mechanism of NSCs is required. Neural glial cells differentiated from some NSCs could secrete nutrition factors, which provide nutritional supplements to support the growth of neurons and integration with host cells. Thus, neural glial cells might also be important for restoring bowel function.

The fates of transplanted NSCs could be: 1) cell death at the transplantation sites because of the different environments between in vitro and in vivo. 2) transplanted cells maintain in G0 phase with no proliferation or differentiation. 3) Cells successfully survive and differentiate into functional neurons and glial cells to repair the injured myenterice nerve plexus. In this study, we injected the NSCs with microinjector at a tilted angle with carefully controlled depth to minimize the traumatic damage to the colon wall. Also, we held the needle in situ for 5 more minutes after a slow injection to prevent the leakage of the NSCs. The NSCs was transfected with vector carrying GFP gene and the survival of these NSCs within colon wall was observed with GFP fluorescence. However, no Nestin positive cell was found at day 21 post transplantation, which indicated no continuous propagation of these NSCs within colon wall. Immunofluorescence assay showed the NSE and GFAP positive cell, which reveals that NSCs differentiated into neurons and neural glial cells in vivo. RT-PCR results showed the mRNA expression levels of ChAT and nNOS after NSCs transplantation was significantly higher than NS group, which suggests the regeneration of cholinergic neuron and nNOS neuron that may contribute to the repairing of the myenteric nerve plexus and restoration of the intestinal motility. The elevated expression of GDNF and EDNRB mRNA from NSCs transplantation group suggested that the genes introduced into NSCs can be expressed efficiently in vivo. This study establishes a fundamental basis for future study of multiple gene introduced stem cell therapy for congenital megacolon.

Nonetheless, the research of NSCs therapy for intestinal neuromuscular disorders is still at initial phase and there are many questions to be investigated such as: 1) the best resource of NSCs, of embryonic stem cell, mesenchymal stem cell, NSCs originated from CNS or neural crest stem cells, which is the best cellular donor? 2) whether the NSCs after transplantation in vivo could maintain its biological features as in vitro culture? 3) the detailed cellular mechanisms of the proliferation, differentiation and migration of the NSCs after transplantation, and long term outcome of NSCs transplantation.

In conclusion, we successfully constructed the recombinant adenovirus containing GDNF and EDNRB genes and transfected NSCs in primary culture. By using 0.5%BAC treatment, we developed the aganglionic megacolon mouse model which resembles the pathohistological changes seen in congenital megacolon. After transplantation of NSCs into the colon wall of aganglionic megacolon mice, we found out that the NSCs could survive and differentiate into neurons and neural glial cells within the colonic microenvironment. Most importantly, differentiated NSCs were able to repair the damaged myenteric nerve plexuses and partially restore the intestinal function. Meanwhile, expression of the target genes was detected by RT-PCR. Experimental data of this study support the therapeutic potential of multiple gene transfected neural stem cell therapy as a novel remedy for human Hirschsprung's disease.

Reference

1. Grundy D, Schemann M (2007) Enteric nervous system. Curr Opin Gastroenterol.23:121-126
2. Temple S (2001) The development of neural stem cells. Nature1414:112-117
3. Amar AP, Zlokovic BV, Apuzzo ML (2003) Endovascular restorative neurosurgery: a novel concept for molecular and cellular therapy of the nervous system. Neurosurgery 52:402-412
4. Modo M, Rezaie P, Heuschling P et al (2002) Transplantation of neural stem cells in a rat model of stroke: assessment of short-term graft survival and acute host immunological response. Brain Res 958:70-82
5. Gonzalez-Gomez P, Sanchez P, Mira H (2011) MicroRNAs Regulators of Neural Stem Cell-Related Pathways in Glioblastoma Multiforme. Mol Neurobiol 44:235-249
6. Rauch U, Hänsgen A, Hagl C, et al (2006) Isolation and cultivation of neuronal precursor cells from the developing human enteric nervous system as a tool for cell therapy in dysganglionosis. Int J Colorectal Dis 21:554-559.
7. Lindley RM, Hawcutt DB, Connell MG, et al (2008) Human and mouse enteric nervous system neurosphere transplants regulate the function of aganglionic embryonic distal colon. Jul 135:205-216
8. Micci MA, Kahrig KM, Simmons RS, et al (2005) Neural stem cell transplantation in the stomach rescues gastric function in neuronal nitric oxide synthase-deficient mice. Gastroenterology 129:1817-1824

AR-006

The application value of multi-b stretched-exponential model DWI in grading of cerebral gliomas

Wei Xiong[1,4], Weiming Xu[2,4], Qingliang Meng[3,4], Jing-jing Jiang[1], Ling-yun Zhao[1], Shun Zhang[1], Yuan-yuan Qin[1], He Wang[1], Xiaogang Shu[3,*], Wen-zhen Zhu[1,*]

[1]Department of Radiology, Tongji Hospital, Tongji Medical College, Huazhong University of Science and Technology, 1095 Jie Fang Da Dao, Wuhan, 430030, P.R.China
[2]Departments of Neurology Surgery, Union Hospital, Tongji Meddical College, Huazhong University of Science and Technology, 1277 Jiefang Avenue, Wuhan Hubei 430022, P.R China.
[3]Departments of Gastrointestinal Surgery, Union Hospital, Tongji Meddical College, Huazhong University of Science and Technology,1277 Jiefang Avenue,Wuhan Hubei 430022, P.R China.
[4]These authors contributed to this work.
*Correspondence: sxg678@yahoo.com, zhuwenzhen@hotmail.com

Abstract

Purpose Traditional mono-exponential model diffusion weighted imaging (DWI) has been appllied in assessing glioma characterization, preoperative diagnosis and early assessment of the effectiveness of therapy. However, the signal intensity attenuation of brain water does not follow monoexponential decay and will deviate from straightness when b-factor exceeds 1000 s/mm^2. A more accurate description of signal attenuation with high b-value over wide b-value range requires more complex biophysical models. The purpose of this study was to evaluate the application value of multi-b stretched- exponential model DWI in grading of gliomas.

Methods Fifty-nine patients with primary cerebral gliomas underwent traditional DWI and multi-b value DWI, ADC maps were created by applying the mono-exponential model using b-values of 0 and 1000 s/mm^2; DDC and α maps were created by applying the stretched-exponential model using b-values of 0, 1000, 2000, and 3000 s/mm^2, before any treatment was started. ADC, DCC and α value of tumors in grade II, III and IV group were measured and analyzed with One-way ANOVA, respectively.

Results Mean DDC had significant difference between any two groups of grade II, III, and IV gliomas ($P<0.05$),and much more higher in low-grade group than those of high-grade group. Mean α and ADC had significant differences between grade II and III or IV group ($P<0.05$) and no significant difference between grade III and IV group ($P>0.05$). Statistical analysis demonstrated a threshold value of 1.033×10^{-3}mm^2/s for DDC to provide sensitivity and specificity of 92.6, and 95.0%, respectively, in differentiating low- from high-grade gliomas. DDC has a strongly positive correlation with ADC in the solid part of tumors ($R=0.8493$; $P<0.001$).

Conclusion The multi-b stretched exponential model DWI provides a more accurate estimate in the preoperative grading of gliomas than the traditional mono-exponential model DWI. DDC can be a new imaging marker to differentiate the grade of gliomas and evaluate the effectiveness of therapy.

Keywords Glioma, DWI, Stretched-exponential, Intravoxel water diffusion heterogeneity, Multi-b value DWI

Introduction

Gliomas are the most common primary neoplasms of the brain, varying histologically from low grade (Grade I-II) to high grade (Grade III- IV) (1). Magnetic resonance imaging (MRI) plays an important role in the detection and evaluation of brain tumors (2). However, conventional MRI is not able to give an accurate preoperative grading of glioma and early assessment of the therapy effectiveness(3). MR Diffusion-weighted imaging (DWI) with quantitative apparent diffusion coefficient (ADC) can detect the random of water molecules driven by thermal energy. The ADC values would be expected to be useful in brain tumor assessment because variations in water mobility can be found within tumors for various reasons (e.g., necrosis, variations in cellularity) and adjacent to tumors (e.g., peritumoral edema), it can provides information which not readily available from conventional MR imaging(3, 4).

DWI have been applied in assess gliomas characterization, preoperative diagnosis and early assessment of the effectiveness of therapy(5, 6). ADC values have been used for predict the grade of gliomas(6). Conventional DWI in biological tissue is most frequently quantified using a mono-exponential model. However, mono-exponential model DWI signal decay do not accord with the characterization of the brain and brain tumors, and its have been shown to be multi-exponential (7) when b-values ≥3000 s/mm2, Maier, S. E et al (7) introduced the bi-exponential model, which may be a better way to describe the multiple exponential signal attenuation. Van Zijl et al(8)showed that complete separation of the intra- and extracellular spaces in cell cultures was workable by means of DW spectroscopy. However, the study of Niendorf et al(9) indicated that the water populations determined in vivo by localized DW spectroscopy and the extra- and intracellular compartments is not straightforward consistency. Meantime, Bennett, K. M et al (10) indicated that the bi-exponential model is probably also an over underestimation of reality, and it is more idealized to assume more than two proton pools with different diffusion coefficients in intravoxel(10). In addition, completely studies have shown that the data not supported the assumptions of fast and slow compartments represent extra- and intracellular water pools, respectively (11) .

To describe the behavior of the number of intravoxel proton pools with different diffusion coefficients in biological tissue, Bennett et al(10, 12) proposed the use of stretched-exponential model. The form of stretched-exponential model is:

$$S(b)/S_0 = \exp\{-(b \times DDC)^{\alpha}\} \quad (1)$$

Where α is the stretching parameter, which relates to intravoxel water diffusion heterogeneity, and is limited to values between 0 and 1. The DDC is the distributed diffusion coefficient, representing mean intravoxel diffusion rates .The value of α is near 1 indicates high homogeneity in apparent diffusion, by examination of Eq. (1), scilicet a highly mono-exponential attenuation curve. Conversely, lower values ofα shown multi-exponential behavior caused by the addition of multiple separable proton pools within the voxel, thus indicates high intravoxel diffusion heterogeneity (10, 12). Bennett et al (10, 12) defined αas a heterogeneity index. It is shown that a numerically high α index (i.e. near to 1) represents low degree of diffusion heterogeneity (i.e. high intravoxel diffusion homogeneity) approximate mono-exponential attenuation. Conversely, a low α index (i.e. near to 0) represents a high degree of diffusion heterogeneity shown as multi-exponential attenuation. DWI data can be obtained by fitting stretched-exponential model, then, α and DDC maps can be acquired. α and DDC have been used for evaluation the heterogeneity and average diffusion rate of high-grade gliomas(13), respectively. The two parameters potentially offer new method for evaluating brain tumors. Since high-grade gliomas are histologically more heterogeneous than low-grade gliomas, meantime, there are differences of cell density in different grade of glioma (14). Therefore, the purpose of this study was to determine the potential differential diagnostic value of intravoxel heterogeneity imaging and average diffusion rate for gliomas.

Materials and methods

Clinical data This study was approved by the institutional review board of Tongji Hospital (Wuhan, China) and written informed consent was obtained from their family members of all patients. Fifty-nine patients with cerebral astrocytomas (WHO grades II: N=20, WHO grades III: N=15, WHO grade IV: N=24; 42 men, 17 women, mean age 43.8 years ,range 6~77 years) proved by pathological fndings were recruited from Tongji Hospital from May 2010 to October 2011. One patient with grade-I glioma was excluded because the sample size was too small. All patients underwent traditional mono-exponential model DWI and multi-b stretched- exponential model DWI of the brain, before any treatment was started.

MR imaging All patients were examined with a 3.0 T MR scanner (Signa HDx, GE Medical system Milwaukee, WI) using an eight-channel head coil. Multi-b DWI was performed using a spin-echo (SE) echo-planar imaging (EPI) sequence, with the following parameters: repetition time/echo time of 3000/17.2ms, slice thickness/gap of 5/1.5mm, image acquisition in the axial plane, number of slices of 20, field of view of 240× 240 mm, acquisition matrix of 128×128, NEX=2, b-values of 0,1000, 2000 and 3000 s/mm^2, number of imaging of 1 (for b-value of 0 s/mm^2), and 3 (for b-values of 1000, 2000 and 3000 s/mm^2), spectral presaturation inversion recovery fat suppression, total scan time of 4 min and 57s. Traditional mono-exponential DWI with b value of 1000 s/mm^2 was obtained for comparison. In addition, sagittal T1-weighted images were acquired to locate the prescribed positions of the anterior and posterior commissures. Conventional axial T1WI, T2WI and post-gadolinium T1WI were performed to determine the solid regions of tumors.

Image analysis All image processing and analysis was performed on GE Advantage Workstation 4.4. Whole-brain ADC maps were created using the images acquired at b values of 0 and 1000 s/mm2. Subsequently, whole-brain α and DDC maps created by the stretched-exponential model ,which fitted to signal intensities of images obtained at b-values of 0, 1000, 2000, and 3000 s/mm^2 using a nonlinear least squares routine(10, 12, 13). Noise thresholds were set to exclude the voxels that fitting with low signal-to-noise ratio. Freehand regions of interest (ROIs) were placed in the tumor, repeated measure three times, and obtain the mean value. The ROIs of ADC and DDC were located in the solid regions of tumors, cystic cavity, calcification, hemorrhage, cerebrospinal fluid were excluded in order to minimize partial volume effects between tumor and above factors. However, the ROIs of α were placed in whole tumor to evaluate the total heterogeneity of the tumors. ROIs of tumor were contoured on post-gadolinium T1-weighted images, T2-FLAIR images and diffusion-weighted images by the same researcher. The ROIs size of ADC and DDC are similar, and located in the same slice. α, DDC, ADC of tumor were automatically calculated, after the ROIs were determined.

Statistical analysis Differences of ADC and DCC between groups of grade II, III and IV gliomas were analyzed with One-way ANOVA, respectively.αvalues between groups of grade II, III and IV gliomas were analyzed with One-way ANOVA. Correlation between tumor ADC and DDC was assessed using Spearman's correlation coefficient. P-values$<$0.05 were considered statistically significant. Statistical analyses were executed

using software (SPSS for Windows, version 17.0; SPSS, Chicago, Ill).

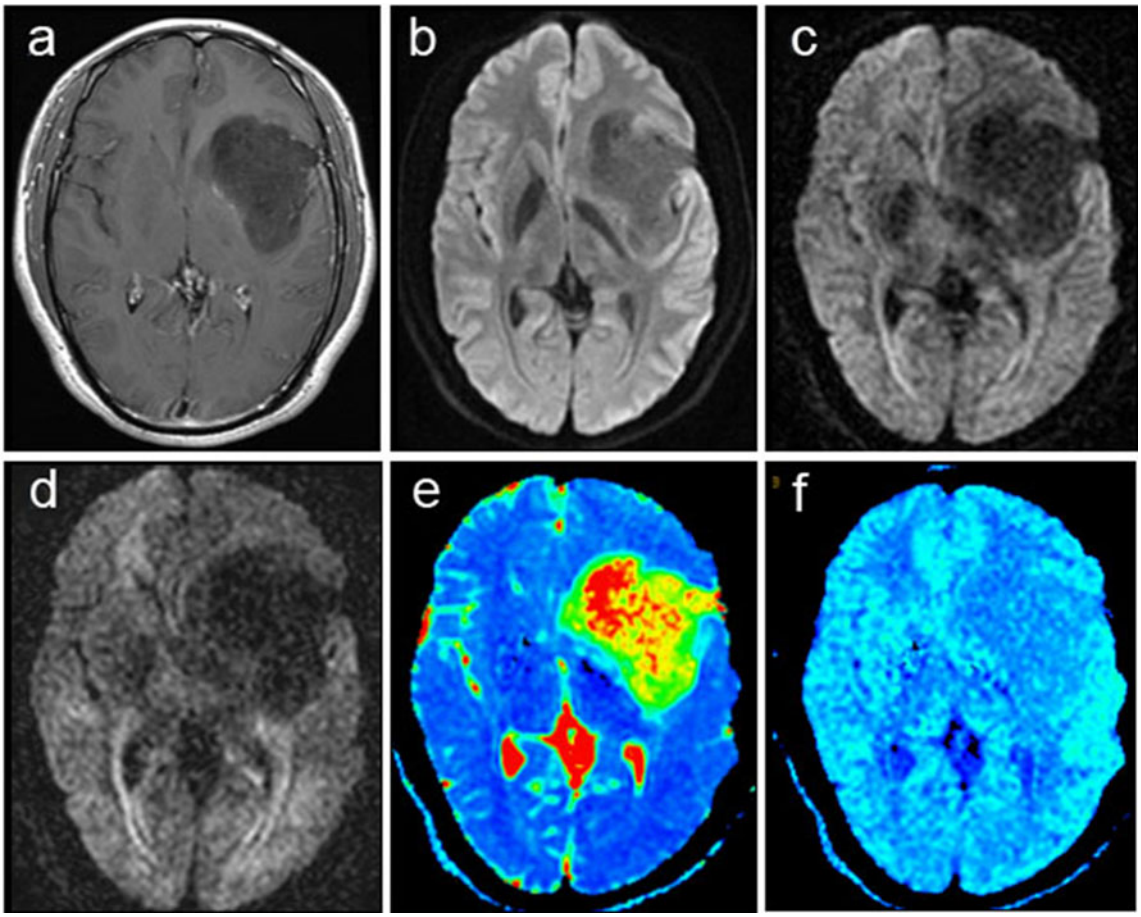

Fig. 1 A 32-year-old male with grade II glioma in the left insula and basal nuclei. Axial post-gadolinium T1-weighted image (a), diffusion-weighted images at b-values of 1000 s/mm^2 (b), 2000 s/mm^2 (c), and 3000 s/mm^2 (d), DDC(e) and α(f)maps show the tumor . This tumor had a mean DDC of 1.87×10^{-3}mm^2/s and a mean value of 0.699. Note the good contrast between the tumor and the surrounding brain tissue on the DDC and α map (e, f)

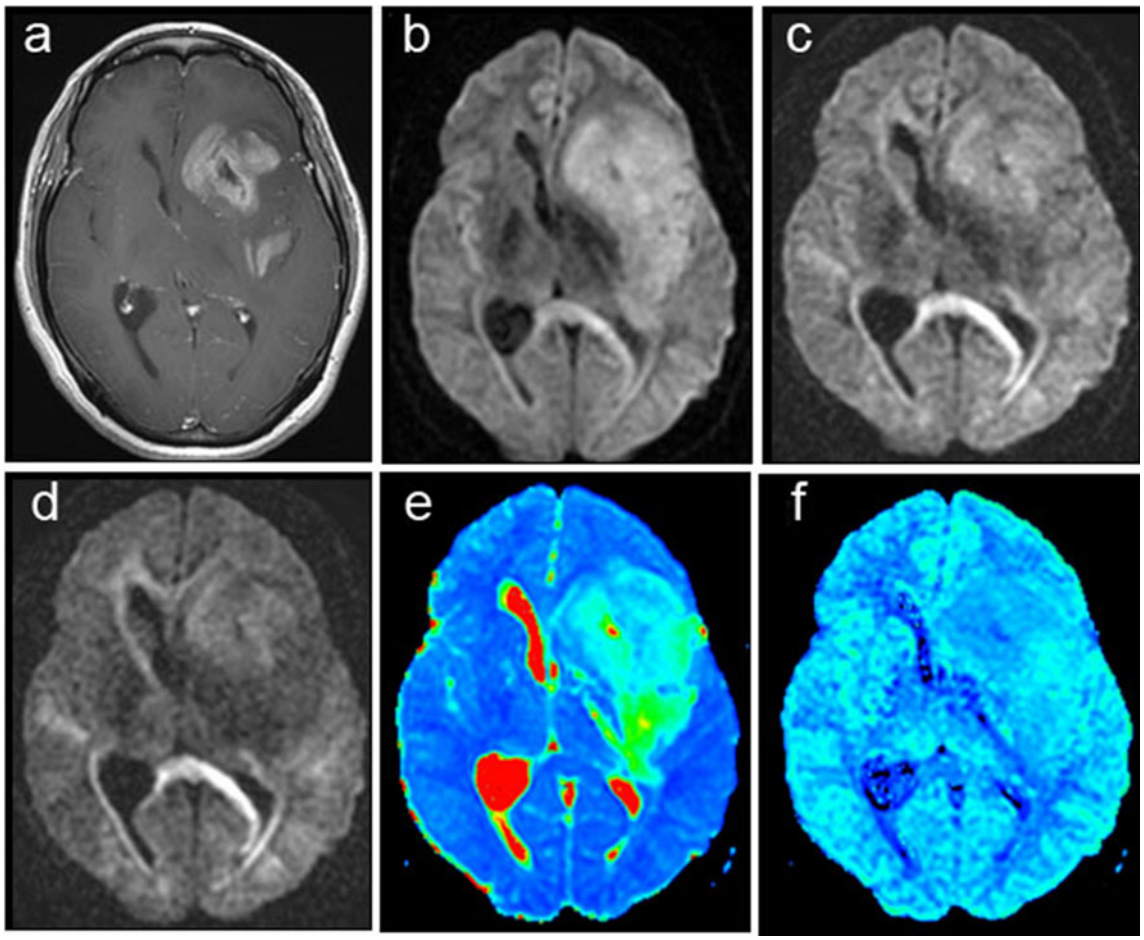

Fig. 2 A 32-year-old female with a glioma (WHO grade III) in the left insula, frontal lobe ,and basal nuclei. Axial post-gadolinium T1-weighted image (a), diffusion-weighted images at b-values of 1000 s/mm^2 (b), 2000 s/mm^2 (c), and 3000 s/mm^2 (d), DDC(e) and α(f)maps show the tumor. This tumor had a mean DDC of 1.11×10^{-3}mm2/s and a mean α value of 0.608. Note the good contrast between the tumor and the surrounding brain tissue on the DDC and α map

Resuts Mean DDC in the group of grade II, III, and IV was $1.40\pm0.36\times10^{-3}$, $0.91\pm0.28\times10^{-3}$, $0.72\pm0.12\times10^{-3}$mm^2/s, respectively. Moreover, DDC had significant difference between any two groups(P <0.05),and much more higher in

grade II group than those in grade III, and IV group. Mean α in the group of grade II, III, and IV was 0.71± 0.06, 0.65±0.05, 0.64±0.07, respectively. There was a significant difference in α between grade II group and III or IV group($P < 0.05$) and no significant difference between grade III and IV group. Mean ADC in the group of grade II, III, and IV was $1.49\pm0.31\times10^{-3}$, $1.01\pm0.23\times10^{-3}$, $0.91\pm0.17\times10^{-3}mm^2/s$, respectively. There was a significant difference in ADC between grade II and III or IV group ($P<0.05$) and no significant difference between grade III and IV group. Figures 1~3 showed representative examples of$\alpha$and DDC maps of grade II, III, and IV glioma. Statistical analysis demonstrated a threshold value of $1.033\times10^{-3}mm^2/s$ for DDC to provide sensitivity and specificity of 92.6%, and 95.0%, respectively, in differentiating low-grade from high-grade gliomas. An ADC value of $1.05\times10^{-3}mm^2/s$ was defined as a threshold below which tumors were classified as high-grade gliomas and a sensitivity and specificity of 92.3% and 92.9% respectively, were obtained.

As presented in Figure 4, there is a strongly positive correlation between DDC and ADC in the solid part of tumors (Spearman correlation coefficient, $R=0.8493$; $P< 0.001$). The agreement of tumor ADC and DDC was dependent on the grade of gliomas, with a good agreement at the grade II and III (low ADC/DDC), and a poor agreement at the grade IV (high ADC/DDC).

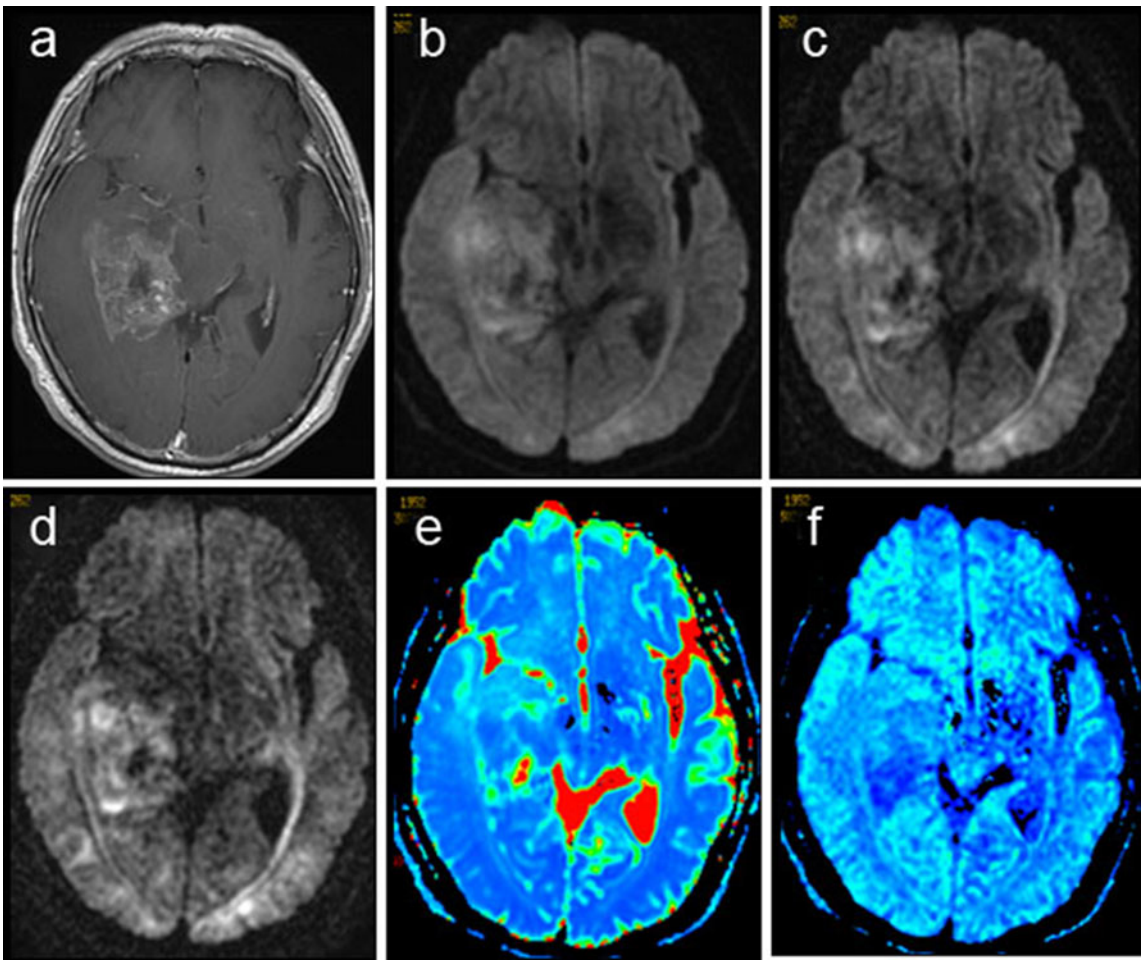

Fig. 3 A 56-year-old male with a glioma (WHO grade IV) in the right temporal lobe. Axial post-gadolinium T1-weighted image (a), diffusion-weighted images at b-values of 1000 s/mm^2 (b), 2000 s/mm^2 (c), and 3000 s/mm2 (d), DDC(e) and α(f)maps show the tumor . This tumor had a mean DDC of 0.65×10-3mm^2/s and a mean α value of 0.505. Note the poor contrast between the tumor and the surrounding brain tissue on the DDC and α map

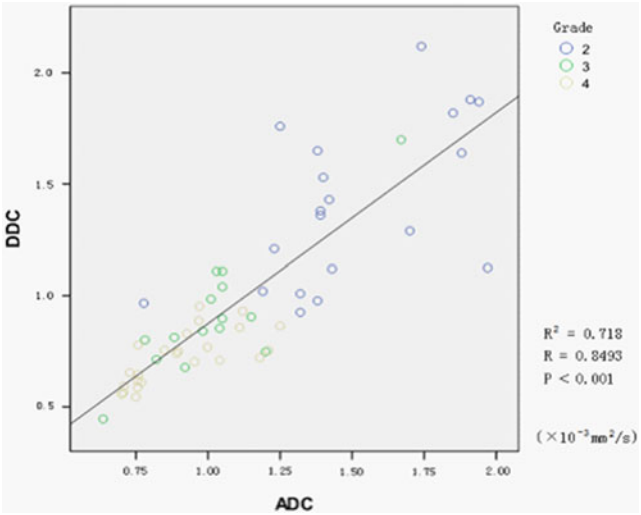

Fig. 4 Scatter plot with the solid regions of tumor DDC against ADC, correlation between ADC and DDC was strongly positive (R^2=0.718, R=0.8493; P<0.001). However, notice that the plotted data more scatter at grade II, meaning overall poor agreement between ADC and DDC. Nevertheless, note that agreement between ADC and DDC is dependent on the grade of gliomas, with a good agreement at the grade III and IV (low ADC/DDC), and a poor agreement at the grade II (high ADC/DDC)

Discussion

DWI has been applied to assess the tumor cellularity non-invasively since ADC is inversely proportional to the cellular density(15), which may help to know well about tumor characteristics. DWI and ADC have been useful for predicting the grade of glioma(6), evaluating the effectiveness of treatment, and the survival analysis(5, 16). In this study, we found that ADC of grade II gliomas was significantly higher than those of grade III and IV, but no significant difference between grade III and IV gliomas, in short, ADC only can differentiate high-grade from low-grade glioma, which is consistent with the results of previous studies(6).

Our study suggests DDC be an imaging biomarker to determine the grade of gliomas. The results demonstrated that DDC had significant difference between any two groups of grade II, III and IV glomas, was much more higher in grade II than those in grade III, and IV group, and there is a strongly positive correlation between DDC and ADC in the solid part of tumors. All these findings can be explained by the fact that tumor cell density increased with the grade (14), and negatively correlated with tumor diffusion coefficient (15). In the meantime,DDC has more higher sensitivty and specificity in identifying low-grade and high-grade gliomas than ADC, and can differentiate grade III from IV, while ADC can not. It is known that there is similar pathologic characteristics between grade III and IV gliomas(14), complex structures (necrosis, densely cell, plenty microvessel, haemorrhage), thus the diffusion is complex and propinquity. However, the conventional mono-exponential ADC (in the brain usually b =1000 s/mm^2) is still the most prevalent method applied in clinical practice to assess the diffusion (17). But in highly heterogeneous tissue, such as high-grade glioma(grade III and IV), the ADC only an approximation of the distribution of diffusion rates in a voxel(10, 12, 13). The DDC has the capabilities and units of a standard diffusion coefficient and can be thought of as the composite of individual ADC weighted by the volume fraction of water in each part of the continuous distribution of ADC (10, 12). Therefore, DDC can provide more complete and accurate depiction of tissue water diffusion in the presence of multi-exponential decay.

The purpose of accurate grading of the glioma was a requisite for best strategy for treating planning, including surgery, radiotherapy, chemotherapy and gene therapy (18). It is easy to differentiate the grade of the enhanced lesions, but it is difficult to grading the non-enhancing lesions by conventional MRI. Especially, it is important to correctly confirm if tumor involvement in the non-enhancing region of peritumoral edema, but this is still an unsolved diagnostic problem (3). Catalaa et al (19) showed that the combination of anatomic MR, perfusion and diffusion weighted imaging and spectroscopy has provided limited value to differentiate if tumor infiltrated to the non-enhancing region. In our study, some cases the DDC map suggested tumor extent larger than the T2WI, the region of peritumoral showed the same color as tumor region in the DDC map. Therefore, we assume the DDC can provide important information to determinate whether tumor involves in the non-enhancing region of peritumoral edema.

In this study, we found that mean α values of human gliomas of grade IV or III group were significantly lower than grade II group, In short, mean αvalues of high-grade gliomas (grades III, IV) were significantly lower than low-grade gliomas (grades II). This finding can be explained by the fact that high-grade gliomas are usually associated with considerable histological heterogeneity(13, 20); high-grade gliomas have the characteristic of the high degree of cellular pleomorphism (i.e. high variability in the size and shape of cells and cellular nuclei), the presence of intravoxel microscopic cystic/necrotic foci, and intravoxel heterogeneity in vascular structures, may lead to the existence of a high number of different compartments with different proton pools relative to low-grade gliomas. Thomas C. Kwee et al (13)showed that mean $\alpha$of high-grade gliomas was

significantly lower than that of contralateral areas, which indicated there was more degree heterogeneity in high-grade gliomas.

The α representing intravoxel water diffusion heterogeneity (12, 13), our study showed that grade of histological was correlated to intravoxel diffusion heterogeneity, therefore, it may provide some information in preoperative, including tumor grade, extent, which can guide biopsy, manage treatment planning. Bennett et al. (21) showed that meanαvalues of peritumoral brain tissue were significantly lower than in the normal white matter, and fluorescence microscopy had confirmed the tumor cells infiltration in the peritumor region. However, there was no changes on conventional MRI in the peritumor region. Thomas C. Kwee et al(13)found that intravoxel diffusion heterogeneity imaging may assess tumor extent, and supported by the other MR sequences. However, a further pathological study is required to test this hypothesis.

Currently, many methods have been applied to evaluate the effectiveness of gliomas treatment (22). DWI and ADC is a prevalent method to assess the response to therapy in glioma patients (23). Since DDC can provide more accurate depiction of tissue water diffusion than ADC, and has higher sensitivity and specificity to determine the glioma grade than ADC does. Therefore, DDC will be a promising method to assess the response to treatment,

A limitation of the present study is that only grade II ~IV gliomas were investigated, and it is still unclear whether there any significant differences between grade I and grade II~IV gliomas. Despite this limitation, DDC is significantly different between grade II, III and IV, and DDC has strongly positive correlation with ADC in the solid part of tumors. Mean αvalues of high-grade gliomas (grades III, IV) were significantly lower than low-grade gliomas (grades II). These results provided the basis for several important potential clinical applications of mean intravoxel diffusion rates and diffusion heterogeneity.

In conclusion, the multi-b stretched exponential model DWI provides a more accurate estimate in the preoperative grading of gliomas than the traditional mono-exponential model DWI. DDC can be a new imaging marker to differentiate the grade of gliomas and may be used to evaluate the effectiveness of therapy.

References:

1. Daumas-Duport C, Scheithauer B, O'Fallon J, Kelly P (1988) Grading of astrocytomas. A simple and reproducible method. Cancer 62:2152-2165
2. Rees J (2003) Advances in magnetic resonance imaging of brain tumours. Curr Opin Neurol16:643-650
3. Provenzale JM, Mukundan S, Barboriak DP (2006) Diffusion-weighted and perfusion MR imaging for brain tumor characterization and assessment of treatment response. Radiology 239:632-649
4. Sotak CH (2004) Nuclear magnetic resonance (NMR) measurement of the apparent diffusion coefficient (ADC) of tissue water and its relationship to cell volume changes in pathological states. Neurochem Int 45:569-582
5. Stegman LD, Rehemtulla A, Hamstra DA, Rice DJ, Jonas SJ, Stout KL, Chenevert TL, Ross BD (2000) Diffusion MRI detects early events in the response of a glioma model to the yeast cytosine deaminase gene therapy strategy. Gene Ther 7:1005-1010
6. Bulakbasi N, Guvenc I, Onguru O, Erdogan E, Tayfun C, Ucoz T (2004) The added value of the apparent diffusion coefficient calculation to magnetic resonance imaging in the differentiation and grading of malignant brain tumors. J Comput Assist Tomogr 28:735-746
7. Maier SE, Bogner P, Bajzik G, Mamata H, Mamata Y, Repa I, Jolesz F, Mulkern RV (2001) Normal brain and brain tumor: multicomponent apparent diffusion coefficient line scan imaging. Radiology 219:842-849
8. Van Zijl PC, Moonen CT, Faustino P, Pekar J, Kaplan O, Cohen JS (1991) Complete separation of intracellular and extracellular information in NMR spectra of perfused cells by diffusion-weighted spectroscopy. Proc Natl Acad Sci U S A 88:3228-3232
9. Niendorf T, Dijkhuizen RM, Norris DG, van Lookeren CM, Nicolay K (1996) Biexponential diffusion attenuation in various states of brain tissue: implications for diffusion-weighted imaging. Magn Reson Med 36:847-857
10. Bennett KM, Schmainda KM, Bennett RT, Rowe DB, Lu H, Hyde JS (2003) Characterization of continuously distributed cortical water diffusion rates with a stretched-exponential model. Magn Reson Med 50:727-734
11. Lee JH, Springer CJ (2003) Effects of equilibrium exchange on diffusion-weighted NMR signals: the diffusigraphic "shutter-speed". Magn Reson Med 49:450-458
12. Bennett KM, Hyde JS, Schmainda KM (2006) Water diffusion heterogeneity index in the human brain is insensitive to the orientation of applied magnetic field gradients. Magn Reson Med 56:235-239
13. Kwee TC, Galban CJ, Tsien C, Junck L, Sundgren PC, Ivancevic MK, Johnson TD, Meyer CR, Rehemtulla A, Ross BD, Chenevert TL (2010) Intravoxel water diffusion heterogeneity imaging of human high-grade gliomas. NMR Biomed 23:179-187
14. Daumas-Duport C (1992) Histological grading of gliomas. Curr Opin Neurol Neurosurg 5:924-931
15. Sugahara T, Korogi Y, Kochi M, Ikushima I, Shigematu Y, Hirai T, Okvda T, Liang LX, Ge YL, Komohara Y,

Ushio Y, Takahashi M (1999) Usefulness of diffusion-weighted MRI with echo-planar technique in the evaluation of cellularity in gliomas. J Magn Reson Imaging 9:53-60
16. Oh J, Henry RG, Pirzkall A, Li XJ, Catalaa I, Chang SS, Dillon WP, Nelson SJ (2004) Survival analysis in patients with glioblastoma multiforme: predictive value of choline-to-N-acetylaspartate index, apparent diffusion coefficient, and relative cerebral blood volume. J Magn Reson Imaging 19:546-554
17. Schaefer PW (2001) Applications of DWI in clinical neurology. J Neurol Sci 186:S25-S35
18. Reardon DA, Rich JN, Friedman HS, Bigner DD (2006) Recent advances in the treatment of malignant astrocytoma. J Clin Oncol 24:1253-1265
19. Catalaa I, Henry R, Dillon WP, Graves EE, Mcknight TR,Lu Y,Vigneron DB,Nelson SJ (2006) Perfusion, diffusion and spectroscopy values in newly diagnosed cerebral gliomas. NMR Biomed 19:463-475
20. Louis DN, Ohgaki H, Wiestler OD, Cavenee WK, Burger PC, Jouret A,Scheithauer BW, Kleihues P (2007) The 2007 WHO classification of tumours of the central nervous system. Acta Neuropathol 114:97-109
21. Bennett KM, Hyde JS, Rand SD, Bennett R, Krouwer HGJ, Rebro KJ, Schmainda KM (2004) Intravoxel distribution of DWI decay rates reveals C6 glioma invasion in rat brain. Magn Reson Med 52:994-1004
22. Dhermain FG, Hau P, Lanfermann H, Jacobs AH, van den Bent MJ (2010) Advanced MRI and PET imaging for assessment of treatment response in patients with gliomas. Lancet Neuro l9:906-920
23. Murakami R, Sugahara T, Nakamura H, Hirai T, Kitajima M, Hayashida Y, Baba YJ, Oya N, Kuratsu J, Yamashita Y (2007) Malignant supratentorial astrocytoma treated with postoperative radiation therapy: prognostic value of pretreatment quantitative diffusion-weighted MR imaging. Radiology 243:493-499

AR-007

Efficient generation of neural precursors from rat adipose- derived stem cells

Yu Zhang, Sui-qiang Zhu, Na Liu, Ying-xin Tang, Ping Zhang, Er-fang Yang, Yong-ming Liu, Hou-jie Ni, Zhou-ping Tang

Department of Neurology, Tongji hospital, Tongji Medical College, Huazhong university of science and technology, Wuhan, Hubei, China

Yu Zhang and Sui-qiang Zhu contributed equally to this work

Correspondence to Zhou-ping Tang (ddjtzp@163.com)

Tel: +86-13971616328

Abstract

Recent studies have shown that adipose- derived stem cells (ADSCs) can be differentiated into neurosphere-like clumps(neural precursors) , but the efficient conversion of ADSCs into neural precursors(NPs) is not mentioned. In our study, we demonstrate the derivation of highly enriched populations of NPs from rat ADSCs. Rat ADSCs were cultured in serum-free neurobasal medium with the addition of 20 ng/ml epidermal growth factor, 20 ng/ml fibroblast growth factor-2, 2% B27, either on uncoated culture flasks or on coated culture flasks. While on uncoated culture flasks, rat ADSCs can be differentiated into neural precursors efficiently. These cells grow in neurosphere-like structures, express high levels of neural stem cells markers (Nestin). However, on coated culture flasks, only a small number of NPs were formed. In the abscence of growth factors, ADSCs-derived NPs can be differentiated into neuronal and glial phenotypes, express neuron and astroglia markers (NeuN, GFAP). Upon differentiation, the expression of Nestin becomes downregulated. Our results demonstrate that the presence of ADSCs-derived NPs is highly enriched only in absence of any attachment factor. ADSCs-derived NPs have potential for autologous cell transplantation therapy for neurological disorders in the future.

Keywords adipose derived stem cells · neural precursors · neural differentiation

Introduction

Neural stem cells or neural precursors are grown in free floating aggregates termed ‘neurospheres’ (NSs)[1]. In the past two decades, researchers have isolated NSs successfully from brain, bone marrows,spinal cord and many other tissues and organs.However, the harvest of brain, bone marrow, spinal cord is an invasive and painful procedure. Neuronal stem cells (NSCs) are multipotent stem cells which can differentiate into three major central nervous system (CNS) cell types: neurons, astrocytes, and oligodendrocytes, with the properties of indefinite growth and division and pluripotency [2]

In recent years, stem cell research is expanding, and researchers have identified stem cells within most body organs; these are referred to as adult stem cells[3]. As

adult stem cells, mesenchymal stem cells (MSCs) don't have the tumorigenic potential because of their embryonic correlatives and in the meantime, possess other specific characteristics such as their almost null immunogenicity. Moreover, mesenchymal stem cells seem to be immunosuppressive in vitro. MSCs are described as MHC II negative cells and what's more, lacking costimulatory molecules such as CD40, CD80 and CD86, which make allogenic transplantation without immunosuppression possible [4].

A significant amount of recent interest has focused on adipose derived stem cells(ADSCs). adipose tissue has been identified as an alternative source of pluripotent mesenchymal stem cells[5], the large number of evidence demonstrated that under appropriate conditions , adipose derived stem cells not only differentiated into mesenchymal lineages but also into endodermal and ectodermal cell lineages in vitro, including osteoblasts, chondrocytes, adipocytes , myocytes, neural cells and so on, which can be used for repair of mesodermal or mesenchymal-derived tissues [6]. Recently, ADSCs are regarded as one of the most promising adult stem cells, ADSCs can be used for regenerative medicine because they can be harvested safely by liposuction, and a large number of cells can be anticipated. The immunomodulatory properties of ADSCs were associated with soluble cytokines and reduce graft-versus-host disease efficiently. Transplantation of ADSCs can improve the neurological functions in some animal experimental of neurological disorders [7].

Several studies have already show that adipose tissue contains a large amount of cells that are capable of exhibiting several morphologic, excitotoxic and characteristics of neuronal and glial tissues. Adipose derived stem cells can express select properties of neuronal and glial cells. In the past two decades, neurospheres were harvested by a culture method, which was originally developed as a culture method of isolating spheres of neural stem cells from the embryonic and adult brain[8] It is already known that adult neurogenesis occurs within the specific local environment called "niche", which provides supportive and instructive signals for the development of adult neural progenitors[9]. In the study, neural progenitors (NPs) were formed by culturing rat ADSCs in serum-free neurobasal medium with the addition of 20 ng/ml epidermal growth factor, 20 ng/ml fibroblast growth factor-2, 2% B27, either on uncoated culture flasks or on coated culture flasks. While on uncoated culture flasks, we can get highly enriched populations of proliferating NPs from rat ADSCs, however, on coated culture flasks, rat ADSCs can only generate a small number of NPs. Those spheres are morphologically very similar to neuronal stem cell-derived neurospheres, and express marker such as nestin, which expressed in neural tissues and what's more, those spheres are capable of differentiating into neurons and neuroglia in vitro.

Indeed most patients possess excess fat depots that can be harvested without invasive and painful procedure, adipose tissue will be regard as the ideal large-scale source for scientific research on the clinical application of neural progenitors. ADSCs-derived NPs is an appropriate agent for cell therapy in the future.

Results *Morphology and Flow cytometry for characterization of adipose-derived stem cells*

After 7 days under DMEM-F12/10% FBS culture conditions, most cells adhere to the tissue culture dishes assuming a fibroblast-like phenotype: large, flat and spindle shaped. (Fig 1 A). Passages 2 ADSCs retain multilineage differentiation capability undergoing adipogenesis in vitro(Fig 1 B). To explore the phenotypic characteristics of ADSCs , flow cytometry using primary antibodies against surface epitopes were performed. The flow cytometry results indicate that ADSCs are negative for the hemaopoietic marker CD45. They do express the cell-surface epitopes CD106(29.88%),CD34 (10.69%),CD44(91.5%),but the expression of CD34 is low. (Fig 1 C)

Culture conditions for conversion of rat ADSCs into NPs

Under uncoated culture flasks conditions, ADSCs-derived NPs were cultured in neurobasal medium supplemented with B27, bFGF, and EGF for 3days. The neurosphere-like cellular aggregates were clearly observed on the first day (Fig 2 A),The number and the size of the spheres became increasingly larger within the next 2 days (Fig 2, B and C). On the fourth day neurospheres were passaged , the spheres were mechanically dissociated and centrifuged for 10 min at 1000 rpm, resuspended in the new neurosphere medium ,the spheroids were newly formed after culturing again for about there days(Fig 2 D), suggesting self renewal of the ADSCs-derived neurospheres.

Under coated culture flasks, before the neurospheres formation, ADSCs adhere to the culture flasks assuming a fibroblast-like phenotype (Fig 2 E). after 5 days in neurosphere medium , there is a small number of spheres which generating from the fibroblast-like ADSCs, however, the spheres were still adhere to the culture flasks.(Fig 2 F). And for about another 10 days, the free-floating spheres were formed(Fig 2 G),but the number of the spheres is very limited. Sometimes, when

cultured in coated culture flasks, none of spheres were formed.

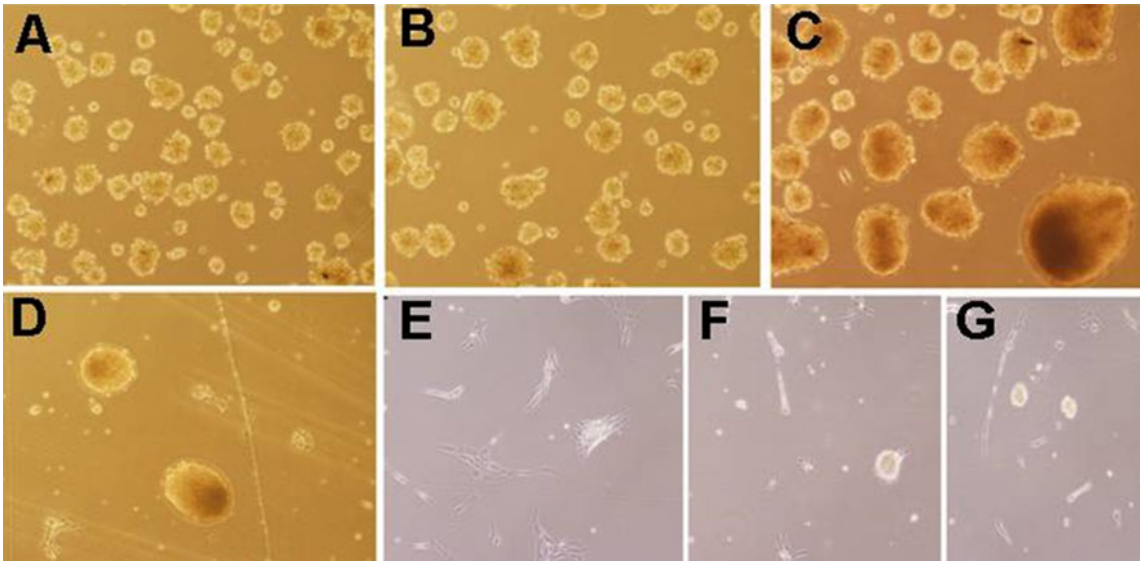

Fig. 1 Culture-expanded ADSCs demonstrate the spindle-shaped fibroblastic morphology. Phase contrast at 100 X magnification (A). Adipocytes containing lipid droplets detected by oil Red O staining, Phase contrast at 400 X magnification(B). Flow cytometry histograms of ADSCs: ADSCs express CD106, CD44, CD34, and are negative for CD45. a,b,c were examined as controls(C)

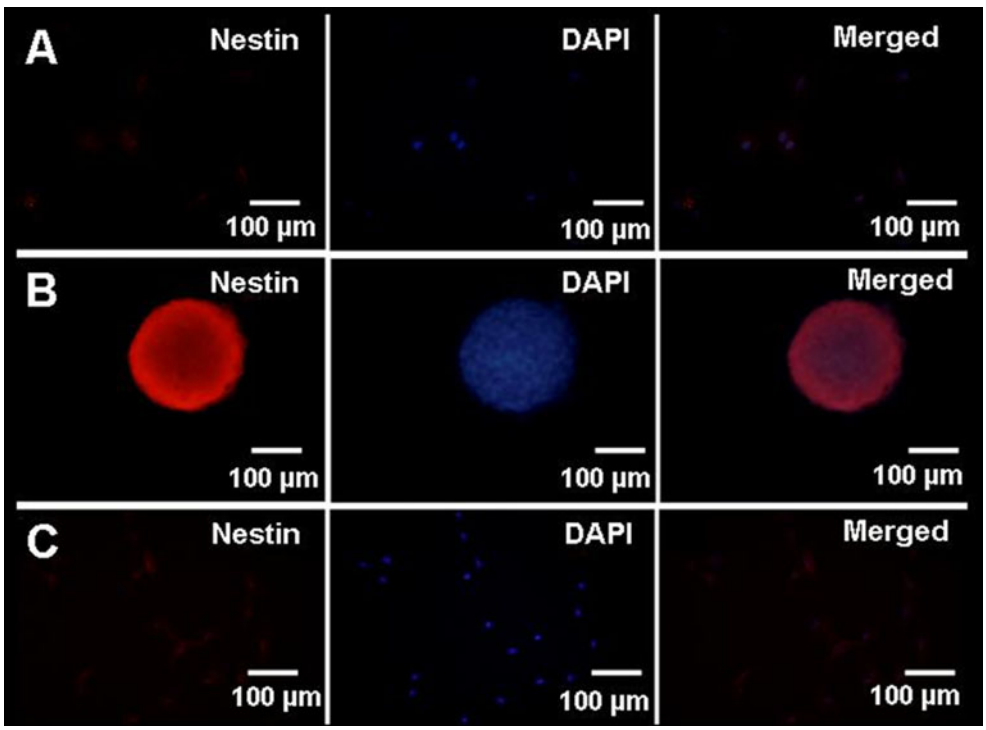

Fig. 2 Neurosphere formation of adipose-derived stem cells cultured in neurosphere medium under uncoated culture flasks: after cultured in neurosphere medium for 1 day(A), 2days(B) ,3 days(C). When neurospheres were passaged, the spheroids were newly formed(D). While under coated culture flasks: ADSCs firstly adhere to the culture flasks(E), after 5 days in neurosphere medium, only a little spheres formed, but still adhere to the culture flasks(F), after about 15 days in neurosphere medium, free-floating spheres were formed.(G). All Phase contrast at 100 X magnification

Comparison of the expression of nestin in ADSCs, ADSCs-derived NPs, and the differentiation of ADSCs-derived NPs
Nestin is an intermediate filament protein expressed by neural stem or progenitor cells. [31] passage3 rat ADSCs express low levels of the neuronal progenitor marker (nestin) (Fig 3 A). ADSCs-derived NPs show high levels of nestin (Fig 3 B), after ADSCs-derived NPs differentiated into neurogenic cell phenotypes, the expresssion of nestin down-regulated(Fig 3 C). It is known that nestin is mainly expressed in dividing cells during the early stages of development in the central nervous system(10)

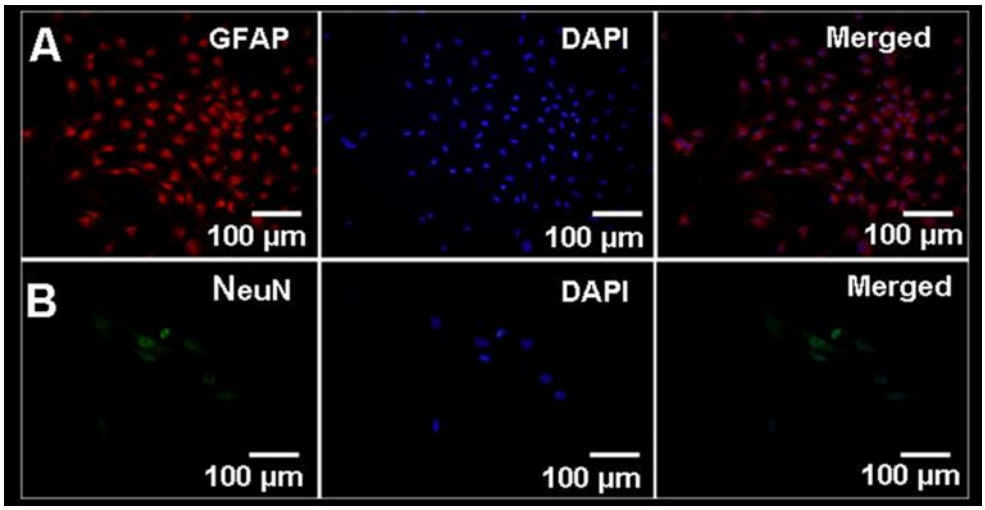

Fig. 3 The expression of nestin: ADSCs, Phase contrast at 100 X magnification(A), ADSCs-derived NPs, Phase contrast at 400 X magnification(B), the differentiation of ADSCs-derived NPs, Phase contrast at 100 X magnification (C). Nuclei are labeled with DAPI

Neuronal and Glial differentiation of ADSCs-derived NPs
The glial fibrillary acidic protein (GFAP) is a structural element of astrocytes[32], Neuronal nuclear antigen (NeuN) is a marker of intermediate and mature neuronal nuclei[33]. ADSCs-derived NPs were induced neural differentiation by culturing on the PLL-coated culture flasks for 14 days in neurobasal medium supplemented with B27, and 1% FBS, without growth factor. Neurospheres attached to the bottom of the culture flasks and extended extensive cell processes. The expression of GFAP (Fig 4 C) and NeuN (Fig 4 D) were detected by immunoflurocence staing.
Fig 4: In vitro differentiation of ADSCs-derived NPs into neuronal and astroglial cell types: Upon differentiation, Neurospheres attach to the bottom of the culture flasks: 3 days(A), by day 14, nearly all neurospheres attached to the flasks and protrude cell processes(B), Phase contrast at 100X magnification . Express the astroglia and neuron markers: GFAP, Phase contrast at 200X magnification (C). NeuN, Phase contrast at 400X magnification (D). Nuclei are labeled with DAPI.

Discussion

Some studies have already shown the criteria to identify mesenchymal stem cells (MSCs). First MSC must adhere to plastic in standard culture conditions. Second,≥ 95% of the MSCs express CD105, CD73 and CD90, and these cells lack expression (≤/2% positive) of CD45, CD34, CD14 or CD11b, CD79a or CD19 and HLA class II. Third, the cells must be able to differentiate to osteoblasts, adipocytes and chondroblasts under standard in vitro differentiating conditions [10].
ADSCs is one of the pluripotent mesenchymal stem cells. In our study, ADSCs can be differentiated into adipogenic, and neurogenic lineages, which demonstrating the multipotency of ADSCs. Flow cytometry analysis demonstrated that ADSCs express CD44, CD106 and low levels of CD34, but do not express the hematopoietic stem cell marker CD45. Although CD34, is recognized as hematopoietic stem cell marker, which is expressed in early passages of ADSCs, and lost in later passages gradually[11].In our study, second passage ADSCs were used for flow cytometry analysis, the expression of CD34 is low. Immunoflurocence staing indicates ADSCs express low levels of the neuronal progenitor marker (nestin)
ADSCs were cultured on uncoated culture flasks in serum-free medium supplement with EGF,FGF-2,B27, Our study indicates that only in absence of any attachment factor, ADSCs-derived NPs can generate a large amount. Unfortunatelly, the reason is not clear. The phenotype of ADSCs-derived NPs is similar to that of neural progenitor cells derived from fetal forebrain. In addition, those spheres express high levels of neuronal progenitor marker(Nestin) . When ADSCs-derived NPs are transferred onto an adherent

surface and cultured in absence of growth factor , they attach and extend neural processes, what's more, can express neuron and astroglia markers(NeuN,GFAP). Unfortunately, we have not yet characterized these neurons (generated from ADSCs- derived NPs) electrophysiologically. Nestin is expressed in dividing cells during the early stages of development in the central nervous system. Upon differentiation, nestin becomes down-regulated(36). While, ADSCs express low levels of the neuronal progenitor marker nestin, which is similar to other stem and progenitor cells.

The conversion of ADSCs into NPs, previously called "transdifferentiation". In recent years, the mechanism for transdifferentiation of MSCs is unclear, but some studies indicate it may result from the induction of neurotrophic factors (NTFs), NTFs are connected with neuroblast proliferation, neural development, and maturation.

Human neurological disorders are mostly caused by a loss of neurons and glial cells in the spinal cord or brain. In recent years, there are few effective therapy for many central nervous system diseases, such as ischemic injury, degenerative disorders .Recently, Cell based therapies are emerging as innovative approaches for the treatment of such disorders [12] Neuronal cell transplantation include fetal neuronal stem cells is a promising option. But the sources of adult neuronal stem cell are limited. It is known to us that neurogenesis is occurred in limited regions of the adult brain. In the past several years, researchers have harvested neural precursors from embryonic stem cells, spinal cord and fetal brain, but the ethical and clinical issues is rising, such as the requirement for immune suppression. Currently, the use of adult human stem cells as a realistic cell therapy for the diseased nervous system is rising. The more attention has been focused at alternative sources of neuronal stem cells, such as the mesenchymal lineages ADSCs-derived NPs offer a more clinically feasible source than brain-derived neural stem cells.

Acknowledgments This work was supported by the National Natural Science Foundation of China(30570628 & 30770751&81171089)

References:

1. F.H. Gage (2000) Mammalian neural stem cells. Science 287:1433–1439
2. Weiss S, Reynolds BA, Vescovi AL, Morshead C, Craig CG, van der Kooy D (1996) Is there a neural stem cell in the mammalian forebrain? Trends Neurosci 19:387–393
3. Simons BD, Clevers H (2011) Strategies for homeostatic stem cell self-renewal in adult tissues. Cell 145 (6):851-862
4. Griffin, M.D., Ritter, T., Mahon, B.P. (2010) Immunological aspects of allogeneic mesenchymal stem cell therapies. Hum. Gene Ther 21(12):1641-1655
5. P.A. Zuk, M. Zuh, H. Mizuno, J. Huang, J.W. Futrell, A.J. Katz, P. Benhaim, H.P. Lorenz, M.H. Hedrick (2001) Multilineage cells from human adipose tissue: implications for cell-based therapies. Tissue Eng 7(2):211-228
6. Pettersson, P., Van, R., Karlsson, M., and Bjoentorp, P (1985) Adipocyte precursor cells in obese and non-obese humans. Metabolism 34(9):808-812
7. N. M. Vieira, V. Brandalise, M. Zatz (2010) Isolation, Characterization, and Differentiation Potential of Canine Adipose-Derived Stem Cells. Cell Transplantation 19:279-289
8. Jang S, Cho HH, Jeong HS (2010) Functional neural differentiation of human adipose tissue-derived stem cells using bFGF and forskolin. BMC Cell Biol 11:25
9. Ana Paula Franco Lambert, João Antônio Pêgas Henriques (2009) Differentiation of human adipose-derived adult stem cells into neuronal tissue: Does it work? Differentiation 77(3):221-228
10. Chi GF, Kim MR, Kim DW, Jiang MH, Son Y (2010) Schwann cells differentiated from spheroid-forming cells of rat subcutaneous fat tissue myelinate axons in the spinal cord injural. Exp Neurol 222(2):304-317
11. Morrens J, Van Den Broeck W, Kempermann G (2012) Glial cells in adult neurogenesis. Glia 60(2):159-174
12. Jiang Y, Jahagirdar BN, Reinhardt RL et al (2002) Pluripotency of mesenchymal stem cells derived from adult marrow. Nature 418:41-49

AR-008

Induced formation and maturation of acetylcholine receptor clusters in a defined 3D bio-artificial muscle

Lin Wang1,2,3, Janet Shansky4, Herman Vandenburgh4,5

Medical Research Center, Union Hospital, Tongji Medical College, Huazhong University of Science and Technology, Wuhan, China1
Laboratory for Regenerative Medicine and Tissue Engineering, Union Hospital, Tongji Medical College, Huazhong University of Science and Technology, Wuhan, China2
Department of Molecular Pharmacology, Physiology and Biotechnology, Brown University, Providence, Rhode Island, USA3
Department of Pathology and Laboratory Medicine, Miriam Hospital, Providence, Rhode Island, USA4
Department of Pathology and Laboratory Medicine, Brown University, Providence, Rhode Island, USA5

Abstract
Dysfunction of neuromuscular junction (NMJ) is involved in a wide range of muscular diseases. The development of neuromuscular junction (NMJ) through which skeletal muscle is

innervated requires the functional modulation of AchR clustering on myofibers. However, studies on AchR clustering in vitro are mostly done on monolayer muscle cell culture, which lacks a three-dimensional structure, a prominent limitation of the 2D system. To enable a better understanding of the structure-function correlation underlying skeletal muscle innervation, a muscle system with a well-defined geometry mimicking the in vivo muscular setting is needed. Here, we report a 3D bio-artificial muscle (BAM) bioengineered from GFP-transduced C3H murine myoblasts as a novel in vitro tissue-based model for muscle innervation studies. Our cell biological and molecular analysis showed that this BAM is structurally similar to in vivo muscle tissue and can reach the perinatal differentiation stage, higher than does 2D culture. Effective clustering and morphlogical maturation of AchRs on BAMs induced by agrin and laminin indicates the functional activity and plasticity of this BAM system toward innervation. Taken together, our results show that the BAM provides a favorable 3D environment that at least partially recapitulates real physiological skeletal muscle with regard to innervation. With a convenience of fabrication and manipulation, this 3D in vitro system offers a novel model for studying mechanisms underlying skeletal muscle innervation and testing therapeutic strategies for relevant nervous and muscular diseases.

Keywords: Neuromuscular junction (NMJ), Nicotinic acetylcholine receptor (AchR), Bio-artificial muscle (BAM), Skeletal muscle, Agrin, Laminin

Introduction

Native skeletal muscle is innervated and controlled by motor neurons through the neuromuscular junction (NMJ), a synapse where motor neuron axons form presynaptic apparatus releasing acetylcholine, a neurotransmitter, to activate acetylcholine receptors (AchR) on the postsynaptic side resided on the muscle cell membrane [1-3]. During NMJ development, AchRs are densely clustered on the postsynaptic side of the future neuromuscular junction before the nerve contacts the skeletal muscle at this NMJ [1, 2, 4].

A growing number of studies have suggested that defects in the structure, differentiation and function of NMJ are a key pathological alteration involved in a wide range of diseases, such as age related muscle wasting [5-7], congenital myasthenic syndromes [8, 9] and myasthenia gravis (an autoimmune syndrome) [10]. Impaired NMJ can lead to muscle weakness, fatigue and even muscle loss. Furthermore, diseased skeletal muscle often contains large areas of fibrotic tissue lacking innervation, which could result in further functional deterioration, such as atrophy. Thus, the modulation of innervation through NMJ in muscle tissue can be a critical approach for developing therapeutic strategies for these neuromuscular disorders.

Skeletal muscle innervation requires clustering of mature AchRs on the post-synaptic side, which provides a functional and structural foundation for developing NMJ through which neurons innervate myofibers [4]. Previous studies on in vitro NMJ development and innervation are mostly based on 2D culture systems [11-13]. Here, we propose that a tissue-engineered BAM can be used as a 3D in vitro system to study NMJ formation and muscle innnervation. The advantages of tissue-based in vitro systems reside in that cells organized into 3D structures are often more representative of in vivo tissues than 2D monolayer culture systems [14], allowing investigations of biomedical processes at the functional tissue level [15]. Moreover, like 2D monolayer culture, this 3D system retains the convenience of manipulating the system variables, dissecting the mechanisms or pathways and analyzing results [16].

In this study, skeletal muscle myoblasts were tissue-engineered into a miniature 3D bio-artificial muscle (BAM) [17]. The BAM developed aligned and well-organized myofibers resembling in vivo muscle tissue. The gene expression profiling of myosin heavy chain (MHC) isoforms showed that the muscle cells within the BAM were differentiated approximately to the perinatal stage. The BAM exhibits the ability to effectively cluster AchRs and improve maturation of AchR clusters in response to agrin, a nerve-derived protein [3, 18], and laminin, a major basal lamina component that plays an important role in NMJ development [19, 20], respectively. Our results suggest that this BAM partially resembles real muscle tissue topologically and molecularly. The BAM maintains physiological capabilities toward innervation. This simplified 3D system can be used to investigate innervation and NMJ development, and for developing treatment for muscle related diseases. The mechanistic insight gained through this 3D BAM system may be a more faithful reflection of in vivo muscle tissue.

Materials and Methods

Myoblast Tissue Culture

The GFP-transduced skeletal myoblasts, as previously described [21, 22], were maintained in primary mouse myoblast growth medium (PMMGM) (20 % fetal bovine serum (Gibco, Grand Island, New York), 1:1 DMEM (Gibco): FGM (Lonza, Gaithersburg, Maryland), 1 % ITS+1 (Sigma, St. Louis, Missouri) and 1 % penicillin-streptomycin) in collagen-coated tissue culture dishes. FGM contained 2 μg/ml insulin and 400 ng/ml human fibroblast growth factor (FGF). When near confluent, the cells were trypsinized with 0.5 mg/ml trypsin, pelleted by centrifugation, resuspended in PMMGM, and harvested for bio-artificial muscle (BAM) tissue engineering.

Preparation of BAMs

BAMs were prepared as previously described [17]. Briefly, 0.2 million GFP-transduced primary mouse myoblast (PMMGFP) cells were trypsinized and suspended in 120 μl fibrin gel made by mixing 0.5 mg/ml fibrinogen and 1U/ml thrombin (both purchased from Tisseel, Baxter Health Care, Westlake Village, California) and cast in silicone rubber molds [17]. The cell-gel mixture was allowed to sit for 30 mins at 37 °C and was then overlayed gently with 150 μl growth medium per well. The cell-gel mixture gelled rapidly within

48 hours post casting. BAMs were formed and kept under tension between two silicone posts. The passive forces in the contracted fibrin gel allow the myoblasts become aligned to the long axis of the BAMs. BAMs were maintained in growth medium for the first 2 days, and then switched to differentiation medium (1:1 FGM: DMEM, 10 % horse serum and 1 % penicillin-streptomycin supplemented with aprotinin) for 14 days. Medium was changed daily. BAMs were treated with 1 μg/ml Cytosine Arabinoside (Ara C) from the third day for 11 days to eliminate undifferentiated proliferating cells.

Treatment of BAMs with Agrin

On the 14th day after casting BAMs, 6 μl 1U/ml mouse agrin (generously provided by Dr. Justin Fallon, Brown University) was added into 150 μl differentiation medium plus aprotinin and incubated with BAMs overnight.

Treatment of BAMs with Laminin

The BAMs were fabricated from 0.2 million PMMGFP suspended in 120 μl fibrin gel supplemented with laminin (10 nM, 25 nM and 50 nM) (BD Bioscience, San Jose,California). BAMs were cast into the molds and incubated as described above but with Ara C treatment from the third day to the fifth day only.

Quantitative PCR

Total RNA was extracted from BAM samples at Day 6 and myoblasts cultured in petri dishes, respectively, with a RiboPure kit (Ambion, Austin, Texas). The expression of myosin heavy chain (MHC) isoforms was investigated using Taqman gene expression assays (Applied Biosystems, Foster City, California). The following myosin heavy chain transcripts were investigated: embryonic (Myh3, Mm01332463_m1), perinatal (Myh8, Mm01329512_m1), adult fast IIa (Myh2, Mm00454991_m1), adult fast IIb (Myh4, Mm01332518_m1) and adult fast IId (Myh1, Mm01332489_m1) with mouse GAPDH as an endogenous control. BAM and cell samples were tested in triplicate on a 7500 Fast Real-Time PCR system (Applied Biosystems) using Taqman one-step RT-PCR master mix (Applied Biosystems). Data was analyzed with Sequence Detection Software v1.3.1 (Applied Biosystems).

Confocal Microscopy

After 14 days of incubation, the BAM samples were fixed in 2 % formaldehyde for 20 mins at room temperature, rinsed with phosphate buffered saline (PBS) for 5 mins, then BAMs were stained with Alexa 594-bungarotoxin (Invitrogen, Grand Island, New York) for 45 mins and rinsed with PBS twice. Confocal images were captured with a Leica confocal microscope (TCS SP2 AOBS) (Leica Microsystems,Wetzlar, Germany). 10 random fields were recorded for each BAM sample. The average number of AchR clusters on muscle fibers per 104 μm2 GFP positive area were quantified using Metamorph software.

Statistical Analysis

All results are expressed as mean±SD. T-test was performed using Sigma Stat software (Systat Software, San Jose, California).

Results

BAMs were successfully fabricated in vitro

We prepared a tissue-engineered 3-dimensional bio-artificial muscle (BAM) as described previously [17]. This BAM was formed and maintained between two parallel flexible silicone posts (Fig. 1A) (see details in Materials and Methods). Muscle cells within the BAMs were self-organized into aligned myofibers and stably expressed GFP protein from a construct transduced into the isolated C3H skeletal muscle myoblasts [17] (Fig. 1B and C).

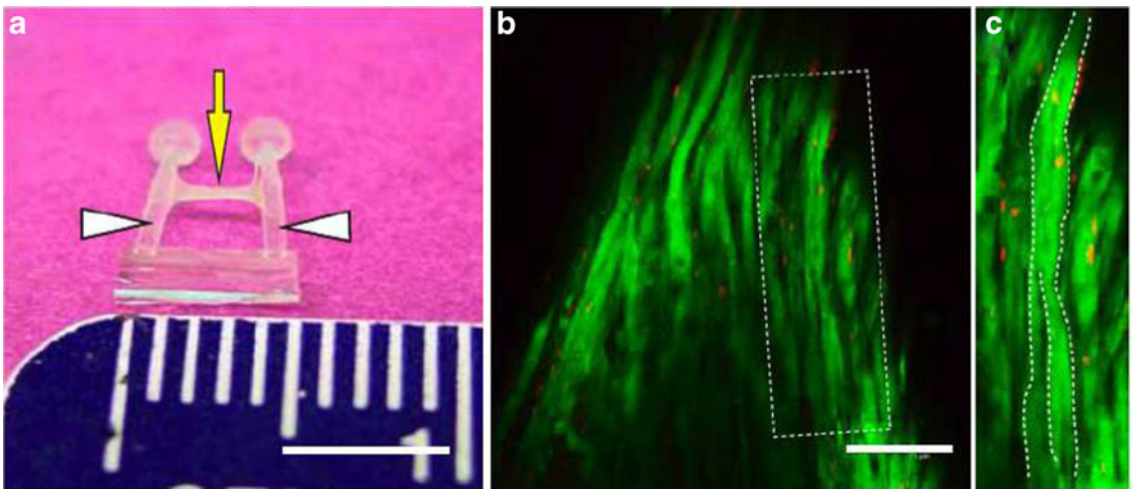

Fig. 1 An in vitro prepared BAM. (A) The BAM (indicated by a yellow arrow) is grown between two flexible silicone posts (indicated by white arrowheads). Scale bar: 5 mm. (B) The confocal image of the BAM after being treated with agrin. Muscle fibers express GFP (green) and form AchR clusters (red) stained with Alexa 594-bungarotoxin. (C) The enlarged image of the

dash-lined rectangular region in B. The representative parallel myofibers are outlined by white dash lines. Scale bar: 75 μm.

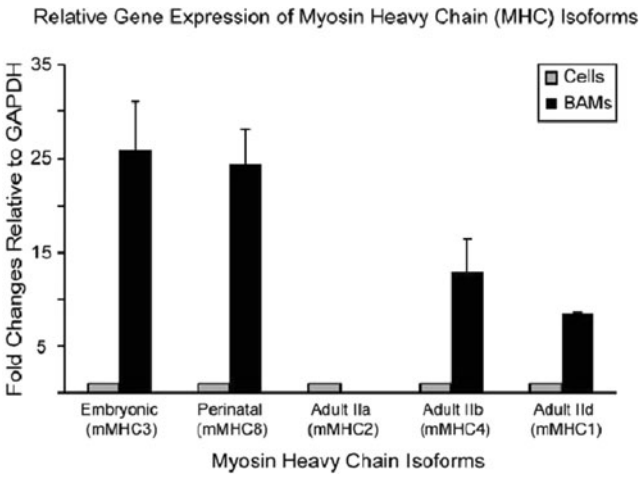

Fig. 2 Relative expression of MHC isoforms in BAMs at Day 6 post casting and in 2D cultured cells. Expression levels of these isoforms were quantified by QPCR as the fold changes (mean±SD) relative to GAPDH (n=3 for each group).

Skeletal muscle myoblasts underwent differentiation within 3D BAMs.

Myosin heavy chain (MHC) isoforms are expressed in a developmentally regulated manner in skeletal muscle [23, 24]. For embryonic and perinatal stages, MHC3 and MHC8 are expressed, respectively. Three isoforms, MHC1 (adult fast IId), 2 (adult fast IIa) and 4 (adult fast IIb) are expressed at the adult stage. The maturation degree of BAMs can be estimated by examining the types and levels of MHC isoforms expressed. Quantitative PCR was employed to profile relative expression levels of these isoforms in BAMs, and myoblasts cultured in a monolayer in petri dishes. Compared to 2D cultured cells that expressed all MHC isoforms at the relatively low level, the cells from the BAMs harvested at Day 6 post casting highly expressed four of the five isoforms measured (Fig. 2). Among these four types, the expression of the embryonic and perinatal isoforms (MHC3 and 8) was significantly higher than that of two other adult isoforms (MHC1 and MHC4), suggesting that muscle cells within BAMs can differentiate to the level comparable to the perinatal skeletal muscles under the culture condition.

Agrin effectively induces the formation of AchR clusters on BAMs

During synaptogenesis, agrin, a nerve-derived protein, acts to activate muscle-specific kinase (MuSK), thereby promoting AchR clustering [3, 18]. To test whether BAMs are capable of forming AchR clusters in response to agrin, BAMs were incubated with agrin overnight (see details in Materials and Methods). Compared with non-treated BAMs, the number of AchR clusters in the BAMs treated with agrin was increased 7.3 fold from 0.8 to 5.8 AchR clusters per 104 um2 GFP positive area ($p<0.005$) (Fig. 3 A-E).

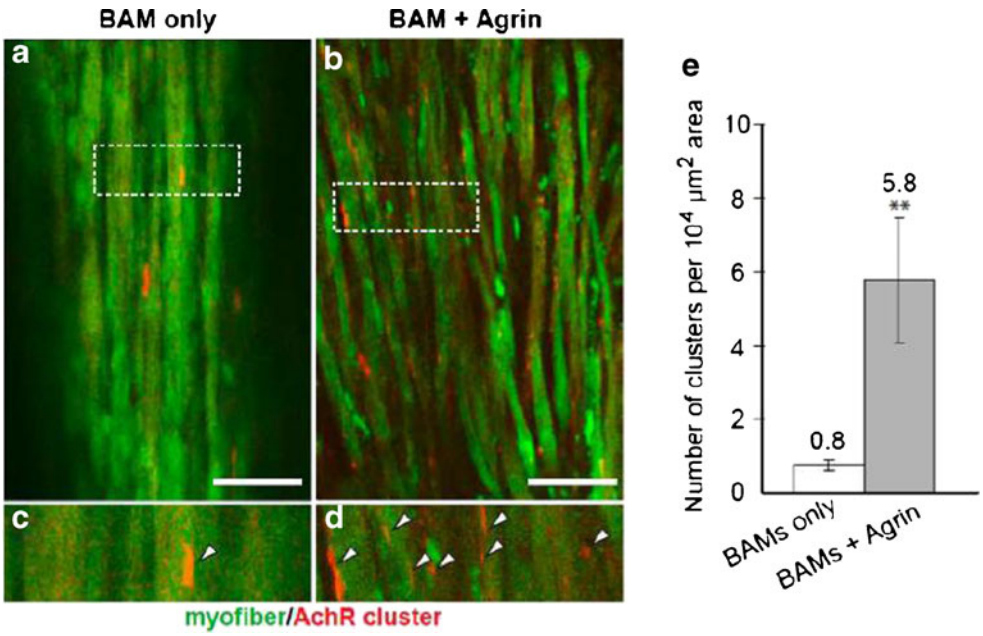

Fig. 3 Agrin increases the number of AchR clusters on BAMs. Myofibers (green) in BAMs express GFP and AchR clusters (red) stained with Alexa 594-bungarotoxin. (A) AchR clusters are formed on the myofibers in the control BAM. (B) Compared to the control, more AchR clusters are formed on the muscle cells in the BAM treated with agrin.

(C and D) The enlarged images of the dash-lined rectangular regions in A and B. AchR clusters are indicated by white arrowheads. (E) The quantification of the density of AchR clusters (mean±SD) is shown ($p<0.005$, n=4 samples for each group, 10 random fields analyzed for each sample). Scale bar: 75 μm.

Laminin promotes the morphological maturation of AchR clusters on BAMs

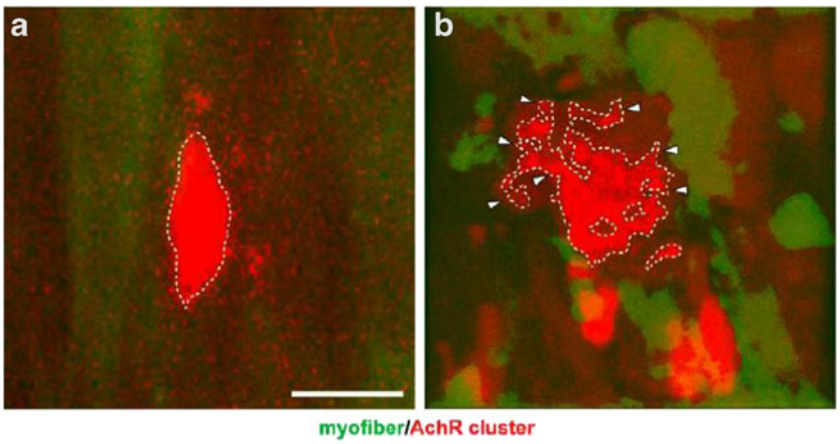

Fig. 4 Morphology of induced AchR clusters. Myofibers are green and AchR clusters are stained in red. (A) Agrin induces the formation of an AchR cluster in an oval plaque shape (outlined by a dash line) lacking branches. (B) Laminin at the concentration of 50 nM induces the aggregation of AchR clusters in a pretzel shape (outlined by a dash line) with multiple branches (indicated by white arrowheads), a morphological indicator for the maturation of AchR clusters.

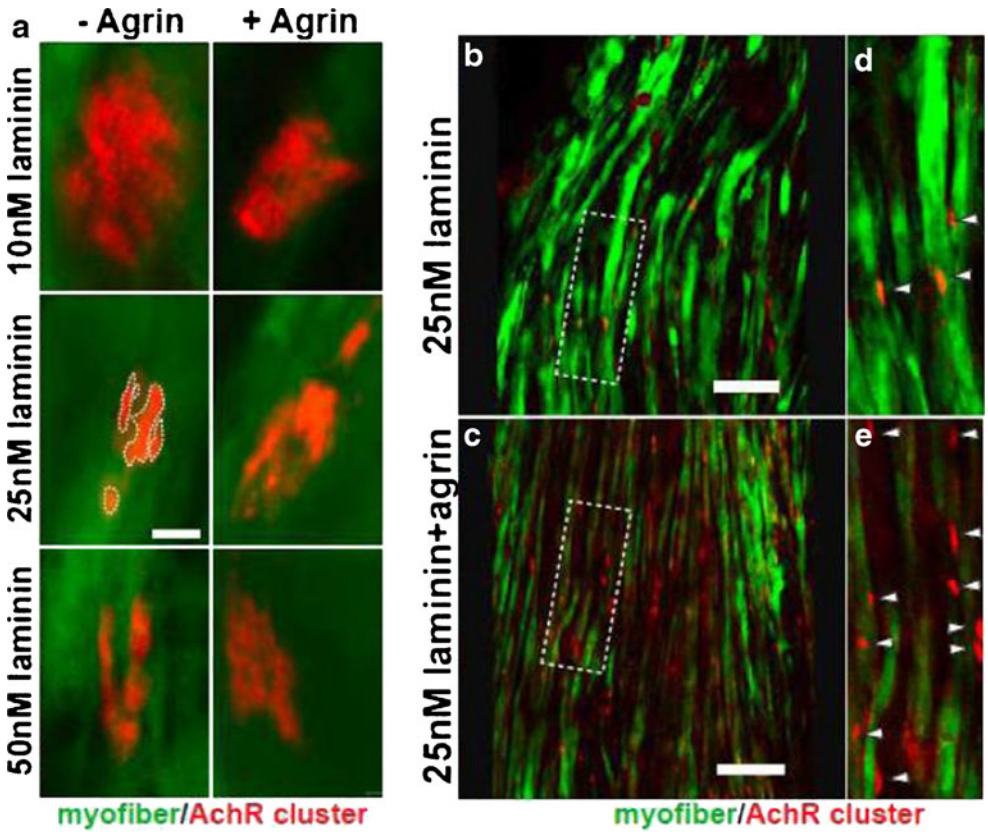

Fig. 5 Laminin promotes the morphological maturation of AchR clusters. Myofibers are green and AchR clusters are stained in red. (A) All three different concentrations (10 nM, 25 nM and 50 nM) of laminin induced a mature and pretzel-shaped aggregation of AchR clusters. Addition of agrin did not further increase the maturity of AchR clusters or the number of mature AchR clusters. Scale bar: 5 μm. (B) AchR clusters are formed on the myofibers of the BAM treated with 25 nM laminin. (C) More AchR clusters are formed on muscle cells of the BAM treated with 25 nM laminin and agrin. Scale bar for B and C: 75 μm. (D and E). The enlarged images of the dash-lined rectangular regions in A and B. AchR clusters are indicated by white arrowheads.

The mature AchR clusters often aggregate in a pretzel shape (Fig. 4B), offering morphological basis for functional innervation. Although agrin effectively increased the number of AchR clusters in the BAMs, agrin-induced AchR clusters were in an oval plaque shape, an early stage of AchR clustering (Fig. 4A). To examine whether 3D BAMs can generate mature AchR clusters in vitro under the induction of laminin, we incubated BAMs with laminin at three different concentrations, 10 nM, 25 nM and 50 nM. At all these concentrations, the pretzel-like aggregation of AchR clusters was observed (Fig. 5A), indicating that laminin promotes the maturation of AchR clusters, consistent with its known role [19]. Addition of agrin to laminin-treated BAM did not increase the number of mature (pretzel-shaped) AchR clusters and pretzel-shaped AchR clusters were not further matured morphologically (Fig. 5A). However, the total number of AchR clusters (immature) was increased when adding agrin to the laminin treatment (Fig. 5B-E), consistent with agrin's role in inducing effective formation of AchR clusters. Thus, in the 3D BAMs, laminin but not agrin promotes the appearance of morphologically mature AchR clusters.

Discussion

The proper clustering of AchR, an essential step leading to the neuromuscular junction (NMJ) formation, provides the morphological basis for skeletal muscle innervation [1, 3]. Much of our understanding about AchR, NMJ and muscle innervation comes from studies on conventional 2D culture lacking well-defined spatial structure and a mechanical setting that can limit the reliability and significance of studies. Thus, 3D in vitro models have been proposed to overcome the limitations of 2D culture for various fields, for example, stem cells [25] and cancer research [26]. To determine whether a 3D skeletal muscle system in vitro can be used for skeletal muscle innervation, we fabricated a BAM where myoblasts were tissue-engineered into 3D muscle tissue in the hope of mimicking the real physiological skeletal muscle.

We characterized BAMs in terms of MHC gene expression in that myosin is a major component of the contractile apparatus of muscle and its isoforms are expressed in a tissue-specific and developmentally regulated manner in skeletal muscle [23, 24]. The BAMs prepared under our experimental condition can differentiate to the level similar to the muscle at the perinatal stage. This result indicates that the BAMs more closely resemble in vivo muscle tissue than do monolayer cultured muscle cells that exhibit almost no differentiation. The higher differentiation state may be associated with greater functional capabilities. These BAMs have been shown to contract and generate force when stimulated [17], suggesting the BAM system is functionally close to in vivo muscles. The muscle cells/ myofibers in BAMs may have the potential to reach a more advanced development stage if BAM culture conditions can be optimized to allow further differentiation.

Functional NMJ requires the topological maturation of the postsynaptic apparatus from an oval plaque of AchR clusters into a complex postnatal topology characterized by a pretzel-shaped and branched morphology [27]. Although the artificial muscle lacks mature AchR clusters that are essential for innervation, the BAM is capable of responding to agrin, a nerve-derived protein, markedly and effectively forming a large number of AchR clusters. However, the agrin-stimulated receptor clusters are morphologically immature, showing an oval plaque shape. Laminin has been reported to induce maturation of AchR clusters in monolayer cell culture [19, 20]. We found that the addition of laminin to BAM fabrication significantly induces the pretzel-shaped aggregation of AchR clusters, an advanced structure. Thus, laminin-mediated maturation of AchR clusters confers a topological advantage on the BAMs for NJM development.

Together with proper protein induction, the formation and maturation of AchR clusters, a key step toward innervation, can be readily modulated in a nerve-independent defined 3D bio-artificial muscle model. Given this morphological plasticity and functional activity, the BAMs would be a suitable tissue-based in vitro model for studies on skeletal muscle innervation. Our study here serves as an example where tissue engineering and neurobiology are integrated into one single system for the study of the molecules affecting skeletal muscle innervations. This system can also be widely applied for identifying other proteins/ factors that might improve AchR formation and maturation, and studying single or cumulative effects of different molecules on muscles at the tissue level. The understanding of cross-talk between proteins/ growth factors and the neuromuscular systems may provide potential targets to advance skeletal muscle innervations and contribute to development of new potential therapeutic approaches for treatment of neuromuscular dysfunctions, especially with the recent ability to form functional NMJs in vitro between human skeletal muscle fibers and human stem cell-derived motoneurons [28].

Acknowledgement
We are grateful to Dr. Justin Fallon for providing mouse agrin. This research was supported by NIH grants R41 AR053386 and R43 AG029705. The authors confirm that no competing financial interests exist and there has been no financial support for this research could have influenced its outcome.

References:

1. Sanes J RJ W Lichtman. (2001) Induction, assembly, maturation and maintenance of a postsynaptic apparatus. Nat Rev Neurosci 11: 791-805.
2. Hall Z WJ R Sanes. (1993) Synaptic structure and development: the neuromuscular junction. Cell 99-121.
3. Sanes J RJ W Lichtman. (1999) Development of the vertebrate neuromuscular junction. Annu Rev Neurosci 389-442.
4. Ferraro E, F Molinari L Berghella. Molecular control of neuromuscular junction development. J Cachexia Sarcopenia Muscle 1: 13-23.
5. Shigemoto K, S Kubo, S Mori, S Yamada, T Akiyoshi T Miyazaki. Muscle weakness and neuromuscular junctions in aging and disease. Geriatr Gerontol Int S137-147.
6. Jang Y CH Van Remmen. Age-associated alterations of the neuromuscular junction. Exp Gerontol 2-3: 193-198.
7. Balice-Gordon R J. (1997) Age-related changes in neuromuscular innervation. Muscle Nerve Suppl S83-87.
8. Engel a GS M Sine. (2005) Current understanding of congenital myasthenic syndromes. Curr Opin Pharmacol 3: 308-321.
9. Nogajski JH, M C Kiernan, R a Ouvrier P I Andrews. (2009) Congenital myasthenic syndromes. J Clin Neurosci 1: 1-11.
10. Conti-Fine B M, M Milani HJ Kaminski. (2006) Myasthenia gravis: past, present, and future. J Clin Invest 11: 2843-2854.
11. Arnold a S, M Christe C Handschin. A functional motor unit in the culture dish: co-culture of spinal cord explants and muscle cells. J Vis Exp 62.
12. Anderson M JM W Cohen. (1977) Nerve-induced and spontaneous redistribution of acetylcholine receptors on cultured muscle cells. J Physiol 3: 757-773.
13. Bernareggi A, E Luin, E Formaggio, G Fumagalli P Lorenzon. Novel role for prepatterned nicotinic acetylcholine receptors during myogenesis. Muscle Nerve 1: 112-121.
14. Nelson C MM J Bissell. (2006) Of extracellular matrix, scaffolds, and signaling: tissue architecture regulates development, homeostasis, and cancer. Annu Rev Cell Dev Biol 287-309.
15. Vandenburgh H, J Shansky, F Benesch-Lee, K Skelly, JM Spinazzola, Y Saponjian B S Tseng. (2009) Automated drug screening with contractile muscle tissue engineered from dystrophic myoblasts. FASEB J 10: 3325-3334.
16. Mueller-Klieser W. (1997) Three-dimensional cell cultures: from molecular mechanisms to clinical applications. Am J Physiol 4 Pt 1: C1109-1123.
17. Vandenburgh H, J Shansky, F Benesch-Lee, V Barbata, J Reid, L Thorrez, R Valentini G Crawford. (2008) Drug-screening platform based on the contractility of tissue-engineered muscle. Muscle Nerve 4: 438-447.
18. Bowe M AJ R Fallon. (1995) The role of agrin in synapse formation. Annu Rev Neurosci 443-462.
19. Kummer TT, T Misgeld, JW Lichtman J R Sanes. (2004) Nerve-independent formation of a topologically complex postsynaptic apparatus. J Cell Biol 7: 1077-1087.
20. Nishimune H, G Valdez, G Jarad, C L Moulson, U Muller, JH Miner J R Sanes. (2008) Laminins promote postsynaptic maturation by an autocrine mechanism at the neuromuscular junction. J Cell Biol 6: 1201-1215.
21. Thorrez L, H Vandenburgh, N Callewaert, N Mertens, J Shansky, L Wang, J Arnout, D Collen, M Chuah T Vandendriessche. (2006) Angiogenesis enhances factor IX delivery and persistence from retrievable human bioengineered muscle implants. Mol Ther 3: 442-451.
22. Vandenburgh H, J Shansky, M Del Tatto J Chromiak. (1999) Organogenesis of skeletal muscle in tissue culture. Methods Mol Med 217-225.
23. Mahdavi V, S Izumo B Nadal-Ginard. (1987) Developmental and hormonal regulation of sarcomeric myosin heavy chain gene family. Circ Res 6: 804-814.
24. Wydro R M, HT Nguyen, R M Gubits B Nadalginard. (1983) Characterization of Sarcomeric Myosin Heavy-Chain Genes. Journal of Biological Chemistry 1: 670-678.
25. Lund a W, B Yener, J P Stegemann G E Plopper. (2009) The natural and engineered 3D microenvironment as a regulatory cue during stem cell fate determination. Tissue Eng Part B Rev 3: 371-380.
26. Nyga A, U Cheema M Loizidou. 3D tumour models: novel in vitro approaches to cancer studies. J Cell Commun Signal 3: 239-248.
27. Mazhar SR Herbst. The formation of complex acetylcholine receptor clusters requires MuSK kinase activity and structural information from the MuSK extracellular domain. Mol Cell Neurosci 4: 475-486.
28. Guo X, M Gonzalez, M Stancescu, HH Vandenburgh J J Hickman. Neuromuscular junction formation between human stem cell-derived motoneurons and human skeletal muscle in a defined system. Biomaterials 36: 9602-9611.